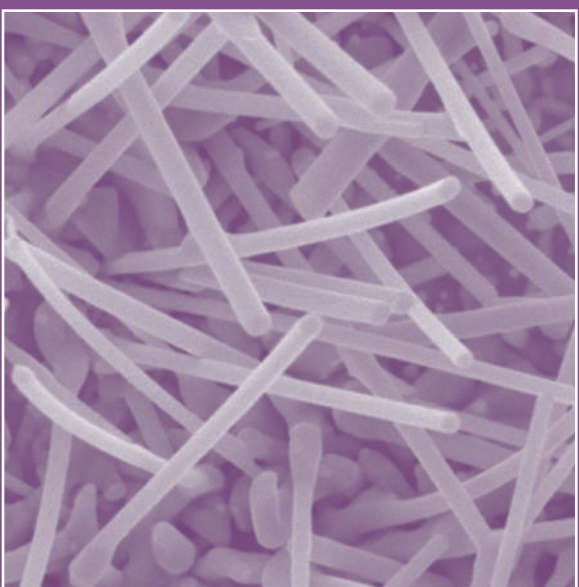
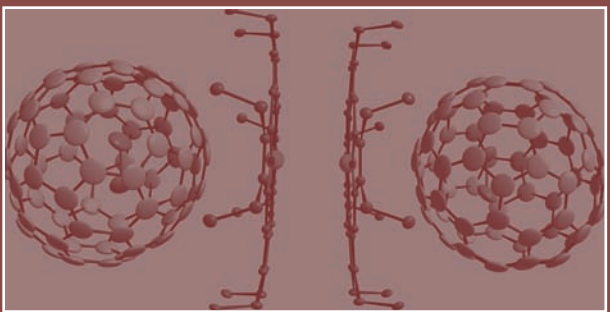
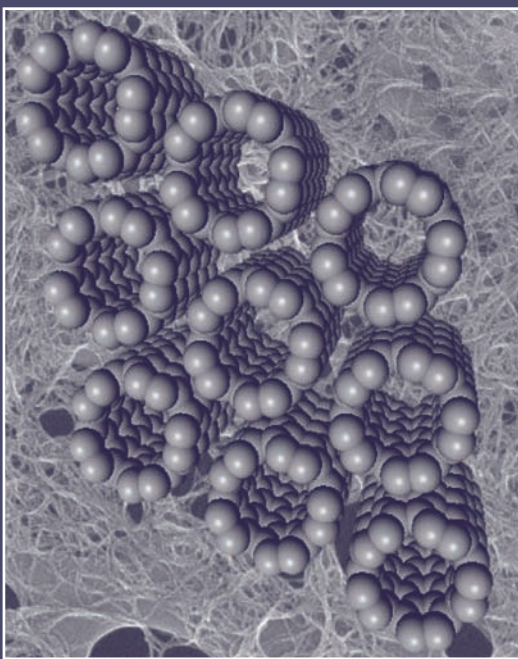
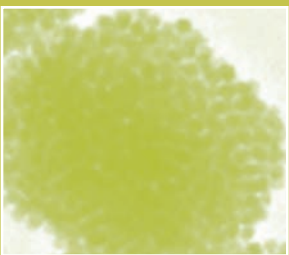


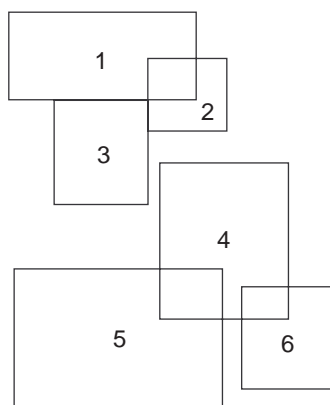
National
Synchrotron
Light
Source

Activity Report 2005



BNL 75555

National Synchrotron Light Source Activity Report 2005



Cover Images

1. from Science Highlight: "The Structure of $Ba@C_{74}$," page 2-38
2. from Science Highlight: "Mediator-Template Assembly of Nanoparticles," page 2-76
3. from Science Highlight: "Physical Properties and 20 K Synchrotron X-ray Charge Density of a Magnetic Metal Organic Framework Structure, $Mn_3(C_8O_4H_4)_3(C_5H_{11}ON)_2$," page 2-30
4. from Feature Highlight: "Nanotubes in a New Light," page 2-12
5. from Science Highlight: "Zinc Oxide Nanowires Grown by Vapor-Phase Transport Using Selected Metal Catalysts: A Comparative Study," page 2-22
6. from Feature Highlight: "Hunting the RNA Slicer," page 2-8

Disclaimer

This report was prepared as an account of work sponsored by an agency of the United States Government. Neither the United States Government nor any agency thereof, nor any of their employees, nor any of their contractors, subcontractors, or their employees, makes any warranty, express or implied, or assumes any legal liability or responsibility for the accuracy, completeness, or usefulness of any information, apparatus, product, or process disclosed, or represents that its use would not infringe privately owned rights. Reference herein to any specific commercial product, process, or service by trade name, trademark, manufacturer, or otherwise, does not necessarily constitute or imply its endorsement, recommendation, or favoring by the United States Government or any agency, contractor, or subcontractor thereof. The views and opinions of authors express herein do not necessarily state or reflect those of the United States Government or any agency, contractor, or subcontractor thereof.

NATIONAL SYNCHROTRON LIGHT SOURCE 2005 ACTIVITY REPORT

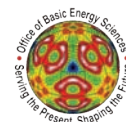
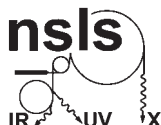
Lisa M. Miller
managing editor

Laura Y. Mgrdichian
science editor

Nancye A. Wright & Stephen A. Giordano
design & layout

The National Synchrotron Light Source Department is supported by the
Office of Basic Energy Sciences, United States Department of Energy, Washington, D.C.

Brookhaven National Laboratory, Brookhaven Science Associates, Inc., Upton, New York 11973
Under contract no. DE-AC02-98CH10886



Introduction

Introduction by the Chairman	1-3
Users' Executive Committee Report	1-5

Science Highlights

Introduction.....	2-3
Table of Contents	2-4
Feature Highlights	2-8
Chemical Science.....	2-22
Condensed Matter Physics	2-36
Geology and Environmental Science	2-46
Life Science.....	2-56
Materials Science.....	2-70
Soft Condensed Matter and Biophysics	2-82

Year in Review

Short Course Participants Learn the Value of Synchrotron Light for Powder Diffraction	3-3
NSLS Engineer John Skaritka Wins BNL's Engineering Award	3-3
Unique Global Light Source Website Launched.....	3-4
X6A Workbench Provides Hands-On Training in Synchrotron Crystallography	3-4
BNLers Help Promote Community Interest in Science.....	3-5
Scientists Create, Study Methane Hydrates in "Ocean Floor" Lab	3-5
Ceria Nanoparticle Experiments at NSLS Promise Cleaner Fuel Future	3-6
What Do You Do At Work? Tom Seda: Bringing Bright Ideas to the Light Source	3-7
Brookhaven Town Honors Two BNL Scientists	3-8
EnviroSuite: Environmental Science at the NSLS.....	3-8
Crystallographers Bloom at RapiData 2005.....	3-9
CFN Site Dedication Draws Special Guests at the NSLS	3-10
Strain-Mapping Workshop Marked by Enthusiasm and Idea-Sharing	3-11
Four BNLers Win Environmental Stewardship Awards	3-12
NSLS Daughters and Sons are Forensic Scientists for a Day	3-12
Women in Science Career Day at BNL	3-13
BNL Workshop on Intense Coherent THz Pulses	3-13
A Passion for Synchrotron Science and its Future: News from the NSLS Users' Meeting	3-14
Nanomagnetism: Materials and Probe Workshop.....	3-17
Synchrotron Imaging of Biominerals Workshop	3-18
Cryogenic Specimen Automounters and the Future of Macromolecular Crystallography	3-20
Spectroscopic Studies of Nanoscaled Systems Workshop	3-21

Application of SAXS to Biological Structures Workshop	3-22
<i>In-Situ</i> Kinetic Analyses in Environmental and Chemical Systems Workshop	3-23
Tony Lenhard Receives the 2005 UEC Community Service Award	3-24
NSLS Physicist, Zhong Zhong, Awarded Tenure	3-25
Crystallization Workshop Gets Top Marks from Participants	3-25
BioCD-2005	3-26
Changes to NSLS User Access Policy	3-27
NSLS Scientists Recognized by the American Physical Society	3-27
Protein Rush at the NSLS	3-28
Highlights from the 2005 NSLS Summer Sunday	3-28
Meet the NSLS Summer Students of 2005	3-30
NSLS-II Gets CD-0!	3-31
Synchrotron Environmental Science III (SES) Meeting	3-31
The 2005 NSLS Barbeque Wraps up the Year	3-33
SBU Student Wins First Dr. Mow Shiah Lin Scholarship	3-34
New Grant for Catalysis Research at the NSLS	3-35
EXAFS Course: Theory, Experiments and Advanced Applications	3-35
Brookhaven Lab Breaks Ground for New Nanocenter	3-36
NSLS Users Recognized	3-37
COMPRES Sponsored Workshop on High Pressure Synchrotron IR Spectroscopy	3-38
The NSLS Remembers Bill Oosterhuis	3-39
BNL Establishes NSLS-II Project in Light Sources Directorate	3-40
NSLS Visitors and Tours in 2005	3-41
NSLS Workshops in 2005	3-43

NSLS Organization

Organization Chart	4-3
Advisory Committees	4-4

Facility Report

Accelerator Division Report	5-3
Operations and Engineering Division Report	5-5
User Science Division Report	5-9
User Administration Report	5-14
Safety Report	5-16
Building Administration Report	5-18

Facts and Figures

Beamline Guide.....	6-3
Linac and Booster Parameters.....	6-10
VUV Storage Ring Parameters	6-11
X-Ray Storage Ring Parameters.....	6-12
2005 Ring Performance and Usage.....	6-13

Publications

NSLS Users.....	7-4
NSLS Staff.....	7-29



Introduction

Chairman's Introduction

Steven Dierker

Chairman, National Synchrotron Light Source

In 2005, the NSLS proved itself, once again, to be a center of scientific excellence. This remarkable facility, commissioned in the early 1980s, is still attracting some of the world's best researchers in almost every scientific field, who produce more than seven hundred scientific papers every year using the NSLS.

The "Science Highlights" and "Feature Highlights" sections of this report are just a small sampling of the many, many impressive research projects conducted at the NSLS in 2005. For example, a user group synthesized and studied zinc-oxide nanowires, which have applications in many optical and electrical devices. Another user group studied how strontium and uranium are removed from high-level radioactive waste. And in another interesting study, users deciphered the basis for antibiotic resistance.

However, as always, the success of these projects depends on the performance of the facility. Again this year, the rings were in top form — reliability was 96 percent for the x-ray ring and 99 percent for the VUV-IR ring. Additionally, to keep the NSLS as productive as possible and to continue to attract users, many beamline upgrade projects were completed this year. One of the highlights of these upgrades is the new mini-gap undulator installed at beamline X25. This insertion device is providing a much brighter x-ray source for the program at X25.

In the always important area of safety, several noteworthy activities took place this year. In particular, NSLS staff made a major commitment to labeling and inspecting electrical equipment. And perhaps the best news is what didn't happen — there were no reportable occurrences related to environmental, safety, or health issues in 2005, and no injuries that resulted in restricted or lost time. We all owe thanks to the dedicated NSLS staff and users who have ensured that the NSLS remains a reliable, safe, up-to-date research facility.

As 2005 came to an end, I stepped down as NSLS Chairman in order to focus my primary efforts on NSLS-II, the world-leading third-generation synchrotron planned for construction at BNL. NSLS-II passed a critical milestone in 2005 with the approval by the Department of Energy of CD-0. BNL has established the NSLS-II Project Organization within the Light Sources Directorate to put in place the management systems and infrastructure necessary to execute this complex undertaking. I will serve as NSLS-II Project Director and also retain my position as Associate Laboratory Director for Light Sources, with the NSLS reporting to me.

Another exciting development is the planned establishment of the Joint Photon Sciences Institute (JPSI). JPSI will be devoted to cultivating and fostering collaborative, interdisciplinary R&D in areas of the physical sciences, engineering, and the life sciences that are united in employing synchrotron-based methods. JPSI will also develop new methods and applications that exploit the unique capabilities of NSLS-II and will serve as a gateway for NSLS-II users.

JPSI will be a partnership between the Department of Energy and New York State, and I am delighted that New York State Governor George Pataki has pledged \$30 million for the construction of the JPSI building.

Steve Dierker



The building will be located adjacent to NSLS-II and will contain offices, meeting rooms, and specialized laboratories. The operating expenses of JPSI and funding for its research programs will be provided by the federal government.

Until a permanent NSLS Director is selected, NSLS User Science Division Associate Chair Chi-Chang Kao will serve as the Interim NSLS Director. I couldn't be leaving the facility in more capable hands. Chi-Chang will lead NSLS staff and users this year in the development of a five-year strategic plan for the NSLS, scheduled for completion by the end of summer 2006. The plan will outline the course for the future operation and development of the NSLS, and will help ensure that the future of the NSLS remains as bright as its past.

Users' Executive Committee Report

Peter Stephens

Stony Brook University

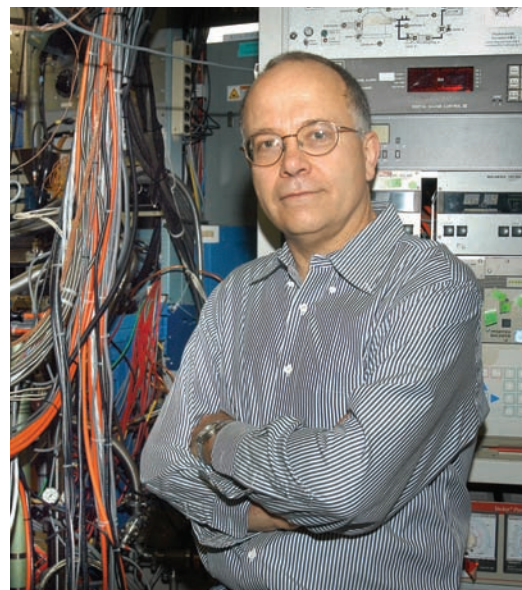
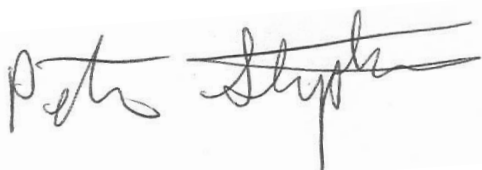
The NSLS is an environment of vital and exciting research, even as it continues in its third decade of operations. It is a strong testament to the staff of the NSLS that it operates so well. As users, we must not take their experience and ingenuity for granted. Keeping the NSLS at the top of its form in scientific productivity is a significant challenge.

In its previous (2001) review of the facility, the Office of Basic Energy Sciences (BES) of the DOE recommended that the NSLS staff should operate more beamlines for the benefit of general users, a policy that has been continuously implemented as resources permit. Early in 2005, the Science Advisory Committee was charged with the task of reviewing each beamline and advising the NSLS of which were being operated safely and effectively, and which required improvement or a significant change of management. It is gratifying to see that nearly all of the beamlines operating at that time were indeed found to be fulfilling their mission to serve the community of users.

This year, the DOE also released the preliminary results of an assessment of beamlines in all four BES synchrotron radiation facilities. I strongly recommend that everybody involved in research with synchrotron radiation take a look. It counts 179 beamlines throughout the system, 77 of which are at the NSLS. However, of 45 beamlines rated on various technical grounds as "best in class," only four are at the NSLS. This is partly a consequence of the small number of insertion device ports available on the NSLS storage rings, and partly a result of the fact that most NSLS beamlines are relatively old. That is not to say, however, that the NSLS and its user community are letting the cutting edge pass us by. Highlights include the new X29 undulator line for macromolecular crystallography and recently constructed instruments at the X21 wiggler for small-angle scattering and studies of in-situ materials preparation. A new undulator is being put in place for X25, and an undulator beamline dedicated to small-angle scattering, to be operated in conjunction with the Center for Functional Nanomaterials, is planned for the near future. Perhaps less immediately visible to users, but no less important, is the steady upgrade of storage-ring components, such as RF cavities, the meticulous analysis of faults by the Operations & Engineering Group, and actions such as the formation of an orbit task force to assess users' needs and meet them.

In the years from 1984 to 1993, the number of users coming to the NSLS rose essentially linearly, to somewhat more than 2000. Since 1993, that number has held essentially constant, while the number of users at all four DOE-operated synchrotron radiation sources has risen to nearly 8000. At the same time, we have seen the NSLS increasingly become a regional facility, with 62% of its users coming from the northeastern part of the country, compared, say, with 15% of Advanced Photon Source users coming from the northeast.

The above notwithstanding, the NSLS will continue to fill a critical need and play an indispensable role in American science for many years into the future. We continue to hold our own as a leading source of research productivity in many fields. But it is equally clear that the opportunity is upon us to push the envelope of science and technology beyond the capabilities of any existing synchrotron radiation source. This is the case for NSLS-II, a new machine with brightness beyond any synchrotron source in existence or planned, essentially to the theoretical limits of storage ring performance. Along with research that can be performed at



other facilities, NSLS-II will indeed be a national facility, as the original NSLS once was, with capabilities unequalled elsewhere in the world.

Defining the scientific needs and opportunities of what will be the world's brightest storage ring for synchrotron radiation is an enormous job. For this, we gratefully acknowledge years of effort by many people: countless current synchrotron radiation users and members of the NSLS user science division, who organized and participated in workshops in 2003; the NSLS Accelerator and Operations & Engineering divisions, who have been pushing (so far, theoretically) the limits of storage ring brightness; and especially NSLS-II Project Director Steve Dierker and BES Associate Director Pat Dehmer, who have advanced and refined the case within DOE. Earlier this year, these efforts bore fruit with the signing of Critical Decision Zero (CD-0) for NSLS-II by the DOE. This signifies that the DOE acknowledges the need for the facility, and is receptive to a proposal for a specific plan and design. As I write these words, the President's budget for fiscal year 2007 has just been announced, with substantial resources committed to the NSLS-II project. This promises to be an exciting time for all of us associated with the NSLS.

It has been a stimulating year for the NSLS, and for the Users' Executive Committee. I am grateful for the hard work and thoughtful suggestions of the other members of the UEC and its special interest groups, and to all of you who have communicated your needs and interests to our representatives in the federal government. But I especially salute your most important achievement, safely doing excellent science at the NSLS!



Science Highlights

Science at the NSLS

Laura Mgrdichian
NSLS Science Writer

Another year has passed, and the NSLS is still a thriving, rich, and productive scientific facility. Who would have thought 23 years ago, when the VUV ring produced its first beams of light, that the year 2005 would see the NSLS so vibrant? It really is remarkable.

As the NSLS science writer, I've had a great view of this continuing success. In order to choose which research projects I'll write about, in the form of "feature highlight" stories, or which ones will become scientist-written "science highlights," I am exposed to nearly 800 published papers throughout the year — all the result of NSLS experiments.

Sifting through these papers, typically about 40 at a time, is always humbling. It really drives home the amount of science that goes on here. Perhaps more importantly, it makes me appreciate the hard work and dedication of the scientists that come to the NSLS. This is why choosing which research papers will receive special attention is such a difficult task.



So what are these scientists studying, analyzing, probing? Almost every type of material you can think of. As you look through this year's feature and science highlight stories, that diversity becomes apparent. For example, if you haven't heard of a "tryptophan zipper" or a "fluoropolymer," here's where you can read about them. Interested in environmental cleanup or nanomaterials? Several studies took place this year that you might just want to take a look at.

In short, the following pages make it clear that the NSLS, for lack of a better phrase, goes on. However, I cannot say the same thing for myself. This will be my last Activity Report letter, as I will soon be leaving the NSLS. Since I have this platform, I want to say that's it's been a privilege to do this job. My sincere thanks and best wishes to all the NSLS users and staff members that I've worked with — I will miss you!

Laura Mgrdichian

SCIENCE HIGHLIGHTS

Feature Highlights

Hunting the RNA "Slicer"	2-8
Floating Films on Liquid Mercury.....	2-9
A Catalyst Uncovered.....	2-10
Nematodes: Nature's Tiny Lead Filters?	2-11
Nanotubes in a New Light	2-12
The Role of Titanium in Hydrogen Storage.....	2-14
Yale Scientists "See" Basis of Antibiotic Resistance	2-15
NSLS Vortex-Tube Study is a Win for Safety.....	2-16
Studying the Effects of Acid Mine Drainage	2-17
A New Structural View of Organic Electronic Devices	2-18
Scientists Describe New Way to Peer Inside Bacteria	2-19
Removing Uranium From Contaminated Steel Surfaces	2-20
Filling "Nanocontainers" with Liquid.....	2-21

Chemical Science

Zinc Oxide Nanowires Grown by Vapor-Phase Transport Using Selected Metal Catalysts: A Comparative Study	2-22
Z. Zhu, T.-L. Chen, Y. Gu, J. Warren, and R.M. Osgood, Jr.	
Chain Length Dependence of the Conformational Order in Self-Assembled Dialkylammonium Monolayers on Mica Studied with Soft X-ray Absorption.....	2-24
G. Hähner, M. Zwahlen, and W. Caseri	
A Step Closer to Understanding Immobilized Organo- and Bio-Molecular Complexes on Solid Surfaces	2-26
S.-J. Xiao, S. Brunner, and M. Wieland	
Preparation and Comparison of Supported Gold Nanocatalysts on Anatase, Brookite, Rutile, and P25 Polymorphs of TiO ₂ for Catalytic Oxidation of CO.....	2-28
W. Yan, B. Chen, S.M. Mahurin, V. Schwartz, D.R. Mullins, A.R. Lupini, S.J. Pennycook, S. Dai, and S.H. Overbury	
Physical Properties and 20 K Synchrotron X-ray Charge Density of a Magnetic Metal Organic Framework Structure, Mn ₃ (C ₈ O ₄ H ₄) ₃ (C ₅ H ₁₁ ON) ₂	2-30
R.D. Poulsen, A. Bentien, M. Chevalier, and B.B. Iversen	
Structure Sensitivity in Methanol Oxidation over Model Rhenium Oxide Catalysts	2-32
A.S.Y. Chan, W. Chen, H. Wang, J.E. Rowe, and T.E. Madey	
Activation Energies for Oxygen Reduction on Platinum Alloys: Theory and Experiment.....	2-34
A.B. Anderson, J. Roques, S. Mukerjee, V.S. Murthi, N.M. Markovic, and V. Stamenkovic	

Condensed Matter Physics

Robust TaN _x Diffusion Barrier for Cu Interconnect Technology with Sub-Nanometer Thickness by Metal Organic Plasma-Enhanced Atomic Layer Deposition.....	2-36
H. Kim, C. Detavenier, O. van der Straten, S.M. Rossnagel, A.J. Kellock, and D.-G. Park	
The Structure of Ba@C ₇₄	2-38
A. Reich, M. Panthöfer, H. Modrow, U. Wedig, and M. Jansen	
The Electron-Boson Spectral Function $\alpha^2F(\omega)$ of High-T _c Superconductors	2-40
S.V. Dordevic, C.C. Homes, J.J. Tu, T. Valla, M. Strongin, P.D. Johnson, G.D. Gu and D.N. Basov	
Microscopic Origin of Polarity in Quasi-Amorphous BaTiO ₃	2-42
A.I. Frenkel, Y. Feldman, V. Lyahovitskaya, E. Wachtel, and I. Lubomirsky	
High Pressure Study of Structural Phase Transitions and Superconductivity in La _{1.48} Nd _{0.4} Sr _{0.12} CuO ₄	2-44
M.K. Crawford, R.L. Harlow, S. Deemyad, V. Tissen, J.S. Schilling, E.M. McCarron, S.W. Tozer, D.E. Cox, N. Ichikawa, S. Uchida, and Q. Huang	

Geology and Environmental Science

Arsenic Leachability in Water-Treatment Adsorbents	2-46
C. Jing, S. Liu, M. Patel, and X. Meng	
Mechanisms of Strontium and Uranium Removal from Radioactive Waste Simulant Solutions by the Sorbent Monosodium Titanate	2-48
M.C. Duff, D.B. Hunter, D.T. Hobbs, S.D. Fink, Z. Dai, and J.P. Bradley	
Immobilization Processes in Soils Contaminated with Several Heavy Metals.....	2-50
A. Voegelin and R. Kretzschmar	
NaMgF ₃ Perovskite Under Pressure: Octahedral Tilting Evolution and Phase Transition.....	2-52
H. Liu, J. Chen, J. Hu, C.D. Martin, D.J. Weidner, D. Häusermann, H.-k. Mao	
Methylmercury Binding Sites in Humic Substances: An X-ray Absorption Study.....	2-54
S.-j. Yoon, L.M. Diener, P.R. Bloom, E.A. Nater, and W.F. Bleam	

Life Science

Disulfide Trapped Structure of a Repair Enzyme Interrogating Undamaged DNA Sheds Light on Damaged DNA Recognition.....	2-56
A. Banerjee, W. Yang, M. Karplus, and G.L. Verdine	
Structural and Biochemical Studies Identify SABP2 as a Methylsalicylate Esterase and Further Implicate it in Plant Innate Immunity	2-58
F. Forouhar, Y. Yang, D. Kumar, Y. Chen, E. Fridman, S.W. Park, Y. Chiang, T.B. Acton, G.T. Montelione, E. Pichersky, D.F. Klessig, and L. Tong	

Evolution of Xylem Lignification and Hydrogel Transport Regulation.....	2-60
C.K. Boyce, M.A. Zwieniecki, G.D. Cody, C. Jacobsen, S. Wirick, A.H. Knoll, and N.M. Holbrook	
A Hairpin Turn in a HIV-Gag-Derived Peptide Bound to HLA-DR1 Orients Peptide Residues Outside the Binding Groove for T Cell Recognition.....	2-62
Z. Zavala-Ruiz, I. Strug, B.D. Walter, P.J. Norris, and L.J. Stern	
A New Addition to the Folding Repertory: An Engineered Five-Stranded Tryptophan Zipper.....	2-64
J. Liu and M. Lu	
Crystal Structures of Nitroalkane Oxidase: High Resolution Data Collection Strategy for Crystals with a Very Long Unit Cell Edge.....	2-66
A. Nagpal, M.P. Valley, P.F. Fitzpatrick, and A.M. Orville	
Shape Selective RNA Recognition by CysteinyI-tRNA Synthetase.....	2-68
S.I. Hauenstein, C.-M. Zhang, Y.-M. Hou, and J.J. Perona	

Materials Science

Effect of Interfacial Bonds on Morphological Instability of Slightly Lattice Mismatched Epitaxial Thin Films.....	2-70
J.H. Li, D.W. Stokes, O. Caha, S.L. Ammu, J. Bai, K.E. Bassler, and S.C. Moss	
Perovskite Thin Films Under Strain.....	2-72
F. He, B.O. Wells, and S.M. Shapiro	
Epitaxial Tilting of GaN Grown on Vicinal Surfaces of Sapphire.....	2-74
X.R. Huang, J. Bai, M. Dudley, R.D. Dupuis, and U. Chowdhury	
Mediator-Template Assembly of Nanoparticles.....	2-76
M.M. Maye, I.-S. Lim, J. Luo, Z. Rab, D. Rabinovich, T. Liu, and C.-J. Zhong	
Time-Resolved Morphology Development of Tri-axial Reinforced Epoxy Montmorillonites Nanocomposites in Uni-Axial Magnetic Fields.....	2-78
H. Koerner, E. Hampton, D. Dean, Z. Turgut, L. Drummy, P. Mirau, and R. Vaia	
Resonant X-ray Scattering from a Magnetic Multilayer Reflection Grating.....	2-80
L.-A. Michez, C.H. Marrows, P. Steadman, B.J. Hickey, D.A. Arena, J. Dvorak, H.-L. Zhang, D.G. Bucknall, and S. Langridge	

Soft Condensed Matter and Biophysics

Crystallization and Melting Behavior of Poly(ϵ -caprolactone) Under Physical Confinement.....	2-82
R.-M. Ho, Y.-W. Chiang, C.-C. Lin, and B.-H. Huang	
Jamming and Crystallization of Polymeric Micelles.....	2-84
T. Nicolai, F. Lafèche, and A. Gibaud	

Characterization of Ionomer Compatibilized Blend Morphology Using Synchrotron Small-Angle X-ray Scattering	2-86
G.C. Gemeinhardt and R.B. Moore	
Control of Surface Properties Using Fluorinated Polymer Brushes Produced by Surface-Initiated Controlled Radical Polymerization.....	2-88
L. Andruzzi, A. Hexemer, X. Li, C.K. Ober, E.J. Kramer, G. Galli, E. Chiellini, and D. Fischer	

Hunting the RNA “Slicer”

NSLS users may have found a key player in RNA interference

As the result of work done at the NSLS, scientists from Cold Spring Harbor Laboratory have very likely determined the identity of a sought-after protein that is vital to RNA interference (RNAi). RNAi is fundamental cellular process intimately involved in the development and virus-fighting ability of all organisms, as well as gene expression — how genes produce certain cell features. The researchers' result, the crystal structure of the protein, will significantly impact the field of biology by helping to illuminate the details of these mechanisms.

Before the protein was identified, biologists only knew that there should be a protein, dubbed the “Slicer,” that performed a critical role in RNAi. It received this nickname for the function the scientists suspected it carried out: slicing, or cleaving, strands of messenger RNA into pieces, much like a pair of molecular “scissors.” Messenger RNA is the type of RNA that decodes the information contained in DNA (i.e. genes) and carries it out of the cell nucleus, where it is used to synthesize proteins. The Slicer is one component of a large multi-protein structure, called the RNA-induced silencing complex (RISC), that “interferes” with messenger RNA’s mission.

This research team is the first to discover very convincing evidence that a certain protein is, in fact, the Slicer. The protein is known as Argonaute. It is discussed in the group’s research paper on the work, which appears in the September 4, 2004 edition of *Science*.



Authors (from left) Leemor Joshua-Tor, Gregory J. Hannon, Ji-Joon Song, and Stephanie K. Smith

“The crystal structure of Argonaute contained a clue that led us to identify it as the Slicer,” said Leemor Joshua-Tor, a structural biologist and the study’s lead researcher. “We observed that an important structural feature on Argonaute was very similar to that of another enzyme already known to cleave RNA.”

The group found that Argonaute is composed of a large crescent-shaped base and a smaller globular region that sits over it, tethered by a thin stalk-like region. The crescent has its own sub-structure, made up of three distinct parts, or “domains” — a center domain and two outer ones.

Based on these features, Joshua-Tor and her colleagues postulated how Argonaute might act as the Slicer. In their scenario, a strand of “small interfering” RNA (siRNA), which is a short type of RNA created earlier in the interference process, binds to Argonaute and guides it to a complementary strand of messenger RNA. The siRNA positions the messenger RNA in the groove created by Argonaute’s crescent and globular segments. Once in place, the crescent’s “PIWI” domain cleaves the messenger RNA, leaving the siRNA intact.

“This is an important result, but many questions still remain,” said Joshua-Tor. “For example, we still do not know how Argonaute proteins participate in developmental processes.”



A schematic depiction of the model for siRNA-guided messenger RNA cleavage. The siRNA (yellow) binds with its 3' end in the cleft in the globular domain (red). The 5' end is predicted to bind near the other end of the cleft. The messenger RNA strand (brown) comes in between the crescent’s N-terminal (blue) and globular domains and out between the globular domain and the crescent’s middle domain (purple).

Gene silencing during RNAi (the act of blocking gene expression) may sound destructive, but the process can prevent messenger RNA from carrying out the orders of potentially malicious genes — genes for defects, for example. RNAi also appears to play an important role in normal organ function. Currently, biologists are experimenting with ways to silence specific genes for medical purposes.

Joshua-Tor and her colleagues, including student researcher Ji-Joon Song, collected data at NSLS beamline X25 and later used the data to determine Argonaute’s structure. Using protein crystallography, they directed a beam of x-rays at a crystal of Argonaute protein and used a detector to collect the x-rays as they scattered away from the atoms in the crystal. The researchers then analyzed this pattern, which is unique to Argonaute, to create a three-dimensional model of the protein.

This research was funded by Cold Spring Harbor Laboratory. Ji-Joon Song is a Bristol-Myers Squibb fellow.

For more information, see: J.J. Song, S.K. Smith, G.J. Hannon, and L. Joshua-Tor, “Crystal Structure of Argonaute and its Implications for RISC Slicer Activity,” *Science*, **305**, 1434-1437 (2004).

— Laura Mgrdichian

Floating Films on Liquid Mercury

New results may lead to advances in nanotechnology, molecular electronics

Scientists from Brookhaven National Laboratory, Bar-Ilan University, and Harvard University have grown ultrathin films of organic chain molecules on the surface of liquid mercury and discovered that the molecules form ordered structures. Similar to sixty years ago when fundamental studies of silicon paved the way to the semiconductor-electronics age, these results help to build a foundation for the development of tiny circuits built using organic molecules — called molecular electronics — a field believed to be the future of many electronic applications.

The scientists are participating in an ongoing program at Brookhaven to grow ultrathin organic films on solid and liquid surfaces. They are most interested in films that have controllable properties at a thickness of just a few nanometers, or billionths of a meter, so that they can engineer technologies based on these properties. In addition to being useful for molecular electronics development, ultrathin organic films are becoming increasingly important for many other emerging technologies, such as flexible electronic displays and advanced biotechnological materials that can, for example, mimic the function of cell membranes.

“We decided to use liquid mercury as a surface, instead of a solid,” said Brookhaven physicist Benjamin Ocko, the lead author of the study, reported in the January 14, 2005 edition of *Physical Review Letters*. “Liquid surfaces are disordered, hence they do not impose a structure of their own on the film. This makes them important testing grounds for organic thin film growth.”

The researchers filled a small tray with a layer of liquid mercury and deposited a controlled amount of the organic molecules, called alkyl-thiol, onto its surface. “We chose alkyl-thiol because one end of each molecule is terminated by a sulfur atom that bonds strongly to metal surfaces,” explained Henning Kraack, a physicist from Bar-Ilan who participated in the study. “Thiol molecules have been studied extensively on gold surfaces, but the exact nature of the sulfur-gold bond has remained controversial. One of our main goals was to determine the nature of the bond between a similar pair: sulfur and mercury.”

At NSLS beamline X22, the scientists measured how x-rays scattered off the film from different angles using a unique instrument they developed that tilts the x-rays downward onto the liquid mercury surface. The scientists repeated this procedure several times, adding more alkyl-thiol each time to follow how the structure of the film evolved as the density of molecules increased.

The scientists discovered that three distinct scattering patterns emerged as the alkyl-thiol density was increased on the mercury surface, with each pattern corresponding to a different degree of molecular order. At the lowest density, the molecules lay flat on the mercury's surface. At an intermediate density, the molecules tilt so that the sulfur end is in contact with the mercury. Finally, at the highest density, the molecules stand up straight.

The x-ray analysis of the lying-down phase showed that the alkyl-thiol molecules are disordered, pointing in all different directions. However, the standing-up and tilted phases are very ordered, with the molecules arranged in crystalline patterns, despite the disordered liquid nature of the underlying mercury. Additionally, the tilted phase contains an unusual structural feature: The alkyl-thiol chain portions and sulfur atoms line up differently so that the chains form one pattern while the sulfur atoms form another.

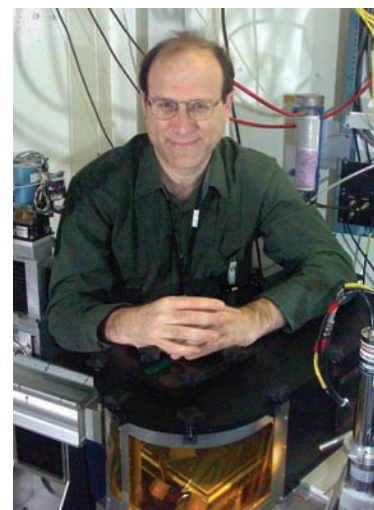
“The x-ray analysis indicates that the sulfur atoms from two neighboring chains chemically bond to one underlying mercury atom,” explained Ocko. “In the tilted phase, the sulfur-mercury bonds exhibit crystalline order. These bonds also form in the standing-up phase, but, surprisingly, they appear disordered.”

“These specific structural and chemical details are necessary for understanding the electronic properties of the film, which is necessary for determining how to use them in new technologies,” he said.

In upcoming research, Ocko and his colleagues plan to study the structure of molecular layers sandwiched between two conducting surfaces, a configuration directly relevant to molecular electronics. This work was funded by the Office of Basic Energy Sciences within the U.S. Department of Energy's Office of Science and the U.S.-Israel Binational Science Foundation.

For more information, see: B. Ocko, H. Kraack, P. Pershan, E. Sloutskin, L. Tamam, and M. Deutsch, “Crystalline Phases of Alkyl-Thiol Monolayers on Liquid Mercury,” *Phys. Rev. Lett.*, **94**, 017802 (2005).

— Laura Mgrdichian



Benjamin Ocko

A Catalyst Uncovered

To many, the phrase “synthetic organic chemistry” probably sounds a bit dull. But this scientific field — the making, or “synthesizing,” of carbon-based (i.e. organic) chemical compounds — has produced many, many products that we use every day. Examples include medicines, fuel, pesticides, paper, and even fabric for clothing. These breakthroughs are the results of many specific, intricate studies into how molecular reactions work.

One such study was recently completed at the National Synchrotron Light Source. Led by chemist Simon Bare, a user scientist from the corporation UOP LLC, the group used x-rays to investigate a new, safe catalyst for an important type of reaction called Baeyer-Villiger (B-V) oxidation. Their results, reported in the September 21, 2005 edition of the *Journal of the American Chemical Society*, add a link to the long chain of discovery that leads, eventually, to better consumer and industrial products.

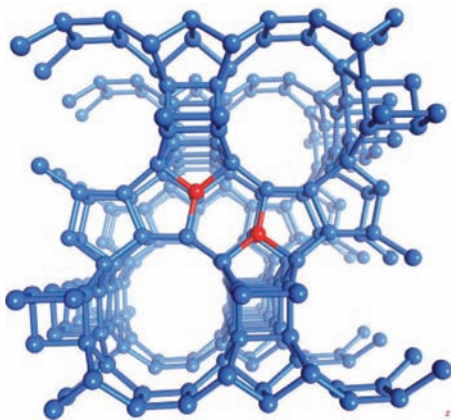


Authors (from left) Wharton Sinkler, Frank Modica, Laszlo Nemeth, Simon Bare, John Low. (Not pictured) Shelly Kelly, Susanna Valencia, and Avelino Corma

“Baeyer-Villiger oxidation is an important reaction in synthetic organic chemistry,” said Bare. “Our aim is to make the reaction more stable and efficient by producing a better catalyst.”

The B-V reaction involves transforming “ketones” – a class of organic solvents – into “esters,” a type of compound formed by reacting an alcohol with an acid. Typically, this transformation is catalyzed by a group of acids called peracids, but these compounds are inherently unstable and require caution when used in large amounts. In contrast, the catalyst Bare’s group is studying is a silicon-based mineral compound known as Sn- β -zeolite. In previous work, they showed Sn- β -zeolite to be an efficient, safe catalyst for B-V oxidation. Now, they have evidence that helps to explain, at the molecular level, *why* the catalyst is so successful.

Their results show that the effectiveness of Sn- β -zeolite as a catalyst depends on the “Sn” portion of the mineral — that is, the tin (Sn) atoms that are dispersed within the mineral’s crystal structure. By shining x-rays at a Sn- β -zeolite crystal sample, they discovered that the tin atoms are not randomly placed within the crystal, but instead are found at regular, specific locations.



A representation of the Sn- β -zeolite structure as derived from the x-ray data Bare and his group collected. The red areas mark one possible Sn-atom pair.

“We believe that the uniform distribution of tin atoms produces sites in the mineral with uniform catalytic activity, which, in total, leads to the excellent overall behavior of the catalyst,” said Bare. “However, we are still not sure why the Sn atoms are positioned so evenly in the crystal.”

In future work, Bare’s group will try to resolve this issue. In the meantime, they hope that this study illustrates that it is possible to synthesize catalysts with uniformly spaced reactivity sites. As long as those sites are easily accessible to the compounds taking part in the reaction, this approach has the potential to produce many effective, efficient catalysts.

This study was supported by the U.S. Department of Energy, the Frederick Seitz Materials Research Laboratory at the University of Illinois at Urbana-Champaign, the National Institute of Standards and Technology, and UOP LLC.

For more information, see: S.R. Bare, S.D. Kelly, W. Sinkler, J.J. Low, F.S. Modica, S. Valencia, A. Corma, and L.T. Nemeth, “Uniform Catalytic Site in Sn- β -Zeolite Determined Using X-ray Absorption Fine Structure,” *J. Am. Chem. Soc.*, **127**(37), 12924-12932 (2005).

— Laura Mgrdichian

Nematodes: Nature's Tiny Lead Filters?

A study performed at the National Synchrotron Light Source has revealed evidence that members of a family of tiny soil-dwelling roundworms, called nematodes, may naturally help lower soluble-lead levels in metal-contaminated soils.

Researchers from the University of Georgia and the University of Chicago exposed the worms to lead in solution and used x-rays to “see” how the metal distributed within their bodies. They found that the lead concentrated in the nematodes’ pharynx regions, or throats, in the form of a solid crystalline material — pyromorphite, a lead-containing mineral. The results are described in the August 1, 2005 edition of *Environmental Science & Technology*.

“The nematodes seem to ‘trap’ the lead, somehow converting it into crystalline pyromorphite. We think this is the first report of this occurring,” said the study’s lead researcher, Brian Jackson, an environmental scientist now at the Center for Environmental Health Sciences at Dartmouth College, formerly with the University of Georgia’s Savannah River Ecology Laboratory.

The results also suggest that the nematodes took in the lead via ingestion using the same mechanism they use to feed. This may explain the high concentration of lead in the pharynx.

A nematode is typically less than one millimeter in length with a pharynx of only 10 – 20 micrometers, or millionths of a meter, in diameter. To characterize the distribution of lead within the organism Jackson and his group used a synchrotron x-ray “microprobe,” a tool that can produce very narrow, intense beams of x-rays. The group then used a technique called x-ray fluorescence (XRF) to create an image of the distribution of lead within the worm (areas of high lead concentration in the nematodes are bright and low concentrations are darker).

In XRF, a beam of high-energy x-rays is aimed at a sample, which absorbs the rays and almost instantly re-emits them. The emitted x-rays have varying energies depending on the types of atoms in the sample. Lead atoms, for example, emit x-rays with a different energy than any other element. Scientists use a device called a spectrometer to analyze the emitted rays and determine which elements, and approximately how much of each, are present in the sample or in parts of the sample.

Once the team identified areas of high lead content in the nematodes, they then used another research method, called x-ray diffraction, to identify the lead-rich areas of the worm as pyromorphite. In this technique, x-rays passing through the mineral emerge in a pattern as a result of diffracting through the closely spaced lattice of atoms in the crystal. Each crystalline solid has a characteristic x-ray diffraction pattern, much like a unique “fingerprint.”

The researchers also tested the nematodes’ response to copper and found that, unlike the lead, the copper did not localize in a specific area. Instead, it dispersed evenly within the worms.

“Given the high numbers of nematodes in soil, their ability to convert lead in pyromorphite may help detoxify lead in contaminated soils and mediate lead in non-contaminated soils,” said Jackson.

He continued, “In the future, we will look to see if lead in these invertebrates becomes absorbed by predators or, because pyromorphite is so insoluble, if the lead could pass through the digestive system of a predator unchanged.”

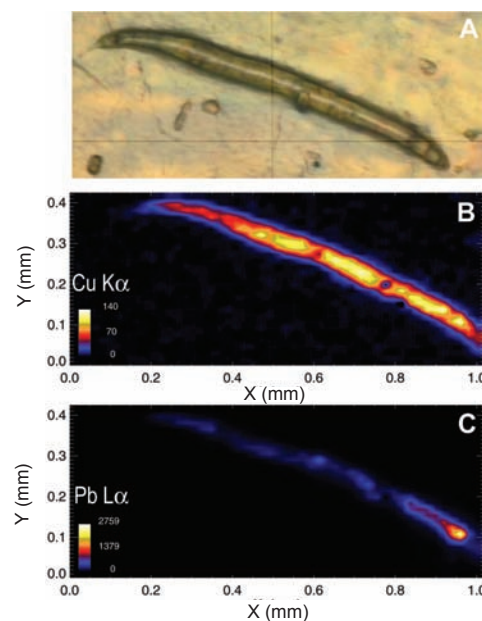
This study was supported by the Office of Biological and Environmental Research within the U.S. Department of Energy’s Office of Science via a Financial Assistance Award to the University of Georgia Research Foundation.

*For more information, see: B.P. Jackson, P.L. Williams, A. Lanzirotti, and P.M. Bertsch, "Evidence for Biogenic Pyromorphite Formation by the Nematode *Caenorhabditis elegans*," *Environ. Sci. Technol.*, **39**(15), 5620-5625 (2005).*

— Laura Mgrdichian



Brian Jackson



Optical (A) and XRF (B and C) images of a nematode exposed to both copper (B) and lead (C).

Nanotubes in a New Light

Using x-rays to investigate order and function in nanotube systems

Nanotubes are cylindrical molecules just a few nanometers (billionths of a meter) in diameter. However, their potential for new technologies is vast. They are extraordinarily strong, conduct electricity well, and can even emit light, properties suitable for many applications, from flat-panel television displays to building materials. But nanotubes must be extensively studied before they can be used in industrial applications.

A collaboration of scientists has pioneered a novel way of using x-rays to study arrays of nanotubes. In ongoing research, they have determined the degree of order contained in certain nanotube systems — that is, to what extent they form organized patterns — and have investigated the structural and chemical properties of others.

The team includes Mahalingam Balasubramanian, Brookhaven National Laboratory (BNL); Sarbajit Banerjee, Stony Brook University (SBU); Tirandai Hemraj-Benny, SBU; Daniel Fischer, National Institute of Standards and Technology (NIST); Weiqiang Han, BNL; James Misewich, BNL; Sharadha Sambasivan, NIST; and Stanislaus Wong, BNL and SBU.

The group is investigating two types of carbon nanotubes: single-walled nanotubes (SWNTs), consisting of a single cylinder, and multi-walled nanotubes (MWNTs), which resemble cylinders concentrically nested together. They have also completed a study of boron nitride nanotubes, which are equally intriguing.

A New Approach

Nanotubes are being studied across the globe, and the technique used in this case has been used for years to study various materials. Now, the technique has been applied to nanotubes, with excellent results.

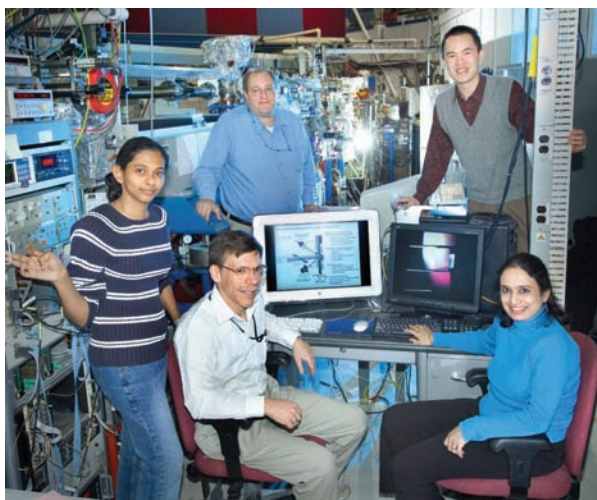
The technique is called “near-edge x-ray absorption fine structure,” or NEXAFS. In NEXAFS analysis, a nanotube sample is bombarded by a beam of low-energy x-ray “photons,” or particles of light. The photons are absorbed by each carbon atom’s “core” electrons — those closest to the nucleus - giving them an energy boost. As a result, they jump to an orbit further away from the nucleus. When this occurs across many, many atoms, scientists can record the sample’s absorption “spectrum,” which measures its absorption behavior.

At beamline U7A (owned by NIST and The Dow Chemical Company), the researchers aimed the x-rays at each sample from several angles, producing several spectra for each array. By analyzing the spectra, they uncovered information about the nanotubes’ electronic and physical structures.

“The beauty of using NEXAFS to study nanotubes is that it is able to provide us with detailed information that is truly complementary to what can be obtained using other techniques,” said Fischer.

Your Order, Please

In the May 5, 2005 issue of the *Journal of Physical Chemistry*, the group describes how they used NEXAFS to determine the degree of order in very thin films of single-walled nanotubes, known as “buckypaper,” and a MWNT film grown on a surface of platinum. They compared their results to two “control” groups: graphite, a highly ordered form of carbon, and SWNT and MWNT powders, which have essentially no order.



Authors (from left) Tirandai Hemraj-Benny, Dan Fischer, Jim Misewich, Stanislaus Wong, and Sharadha Sambasivan

The group found that the buckypaper spectra are similar to graphite’s. For both, the spectra change when the x-rays graze the sample rather than strike head-on. This property — the tendency of a material to react differently to outside fields depending on the direction the field is applied — is called “anisotropy.” It is very useful to study, since high anisotropy often implies a high degree of order. Conversely, a material shows “isotropy” when its reaction to an outside field is the always the same. Nanotube powders, containing nanotubes in all possible orientations, display isotropy.

The buckypaper displayed anisotropy, but not as extensively as graphite — approximately 87 percent of the nanotubes were on their sides. The MWNT film was also quite anisotropic, behaving as if most of the nanotubes were standing upright.

“These results are encouraging because they indicate that two com-

mon nanotube systems already contain a fair degree of order,” said Wong. “We plan to continue studying MWNT and SWNT films. Our hope is to find a way to produce a nanotube array with order comparable to graphite.”

A Matter of Function

“Functionalizing” a set of nanotubes is a process that allows scientists to manipulate the tubes into ordered arrays with specific properties. One way to do this is “ozonolysis” — reacting the nanotubes with ozone, a form of oxygen gas. This produces tiny holes into the nanotubes’ walls and creates various oxygenated compounds along their surfaces, which serve as tethering points for a variety of other compounds.

Ozonolysis can also cleanse the nanotubes or produce reactions that “unhinge” the nanotubes’ half-sphere end caps, leaving the tubes open to a variety of interesting “stuffings.” Filling the tubes with metal atoms, for example, could boost their ability to conduct electricity.

But studying the specific electronic structure of the nanotubes, as well as the chemical make-up and ordering of the oxygen-carbon compounds, which are called functional groups, has been difficult. Most techniques are unable to simultaneously yield both types of information. The team showed that NEXAFS is an important complement to these other methods.

For example, their article in the September 20, 2004 issue of *ChemPhysChem*, focuses on MWNTs exposed to ozone. NEXAFS showed that the ozone treatment cleared the nanotubes of “amorphous” carbon — carbon atoms not incorporated into the ordered structure of the nanotubes themselves — opened the end caps, and produced functional groups along the nanotubes.

A Nanotube by Another Name

The word “nanotube” is very often preceded by the word “carbon,” but nanotubes made of other materials can be equally — or even more — interesting. One such material is boron nitride.

Boron nitride nanotubes are also tremendously strong. But they possess some superior properties, such as flexibility without compromising strength and the ability to withstand very high temperatures. Like carbon nanotubes, they are being investigated for a wide array of potential applications.

In the March 21, 2005 issue of the journal *Physical Chemistry Chemical Physics*, the team describes how they used NEXAFS to gain valuable structural information about a sample of boron nitride nanotubes. Their results show that the nanotubes in their sample have atomic structures that mimic a type of carbon nanotube with hexagonally bonded carbon atoms (like a rolled-up sheet of chicken-wire fence). NEXAFS also revealed that the boron nitride nanotubes have few defects and are highly crystalline, perhaps even more so than carbon nanotubes.

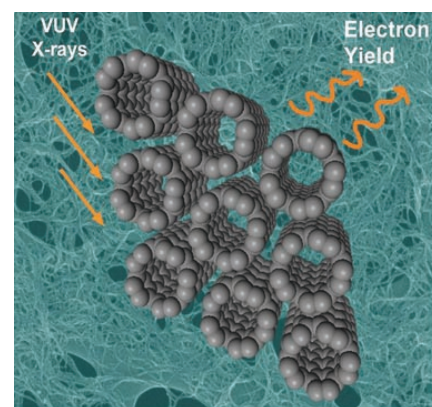
For more information, see:

S. Banerjee, T. Hemraj-Benny, S. Sambasivan, D.A. Fischer, J.A. Misewich, and S.S. Wong, “Near-Edge X-ray Absorption Fine Structure Investigations of Order in Carbon Nanotube-Based Systems,” *J. Phys. Chem. B*, **109**(17), 8489-8495 (2005).

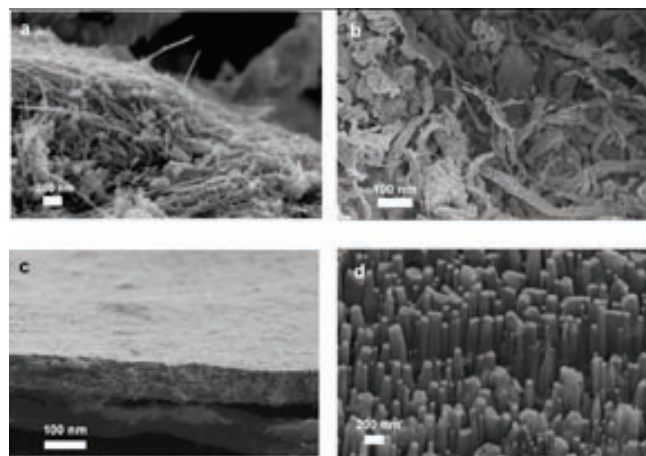
S. Banerjee, T. Hemraj-Benny, M. Balasubramanian, D.A. Fischer, J.A. Misewich, and S.S. Wong, “Surface Chemistry and Structure of Purified, Ozonized, Multiwalled Carbon Nanotubes Probed by NEXAFS and Vibrational Spectroscopies,” *ChemPhysChem*, **5**(9), 1416-1422, (2004).

T. Hemraj-Benny, S. Banerjee, S. Sambasivan, D.A. Fischer, W. Han, J.A. Misewich, and S.S. Wong, “Investigating the Structure of Boron Nitride Nanotubes by Near-Edge X-ray Absorption Fine Structure (NEXAFS) Spectroscopy,” *Phys. Chem. Chem. Phys.*, **7**(6), 1103-1106 (2005).

— Laura Mgrdichian



A rendering of carbon nanotubes being studied using NEXAFS. Light comes in (left) and electrons are emitted (right).



Scanning electron microscope images of (a) MWNT powder, (b) SWNT powder, (c) SWNT buckypaper, and (d) aligned MWNTs.

The Role of Titanium in Hydrogen Storage

As part of ongoing research to make hydrogen a mainstream source of clean, renewable energy, scientists from the U.S. Department of Energy's Brookhaven National Laboratory have determined how titanium atoms help hydrogen atoms attach to an aluminum surface. Their study isolates the role of titanium, which is used as a catalyst in the crucial first step to trap hydrogen within a particular class of hydrogen-storage materials. The work may also help identify and develop similar hydrogen-storage systems.



James Muckerman



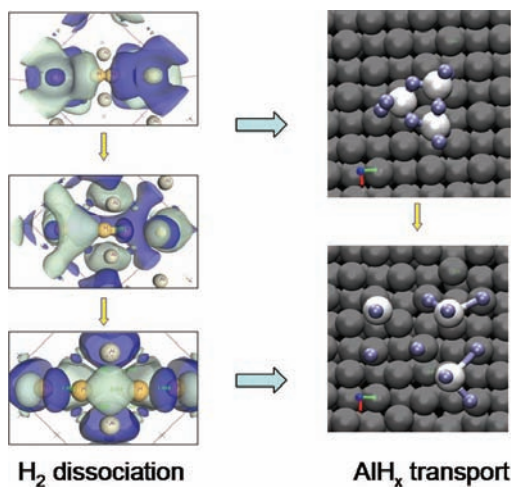
Santanu Chaudhuri

Brookhaven chemist Santanu Chaudhuri presented this research at the 230th National Meeting of the American Chemical Society in Washington, D.C. on August 28, 2005.

To be a mainstream source of fuel, hydrogen must be stored safely and efficiently. Conventional high-pressure storage tanks can be dangerous and are too big and heavy for certain applications, such as hydrogen-based fuel cells in automobiles. Hydrogen-storage materials, however, incorporate hydrogen safely and compactly, and temporarily hold large quantities of it that can be recovered easily under safe, controlled conditions.

“A hydrogen-storage material must be able to store hydrogen quickly under ‘normal’ conditions — that is, without very high temperatures and pressures,” said Chaudhuri. “In tiny amounts, an appropriate catalyst, such as titanium, can speed up the reaction and make the hydrogen-storage process suitable for practical applications. Our study has helped us better understand the role of these catalysts.”

Through this research, Chaudhuri and his collaborator, Brookhaven chemist James Muckerman, hope to improve the performance of sodium alanate, a hydrogen-storage material composed of sodium and aluminum hydride. Sodium alanate, known as a “complex metal hydride,” expels hydrogen gas (the fuel) and aluminum when heated, leaving a mixture of sodium hydride and metallic aluminum. But because neither aluminum nor sodium hydride absorb hydrogen well, putting the hydrogen back in — to reform sodium alanate and allow reuse of the material — becomes difficult.



Molecular orbital rearrangements (left) during the dissociation and subsequent absorption of a hydrogen molecule (H_2) onto an aluminum surface. This process is facilitated by a tiny amount of titanium that is present in the aluminum phase of depleted sodium alanate (the hydrogen-storage material under study). Then, small, mobile molecular clusters of aluminum hydride (AlH_x) transport the hydrogen and aluminum to sodium hydride (right), where the sodium alanate is reformed.

“We found that aluminum absorbs significantly more hydrogen — and does so more quickly and at lower temperatures — when a small number of titanium atoms are incorporated into its surface,” Chaudhuri said.

Chaudhuri and Muckerman created a computer model that provides a plausible mechanism of the reaction. Their model agrees with an experimental x-ray absorption study of sodium alanate, performed at the National Synchrotron Light Source.

Chaudhuri and Muckerman's collaborators at Brookhaven used x-rays to “see” and thus calculate how the titanium atoms subtly changed the atomic-level structure of the aluminum, resulting in a more hydrogen-absorbent surface. Results from these two studies agree on the role of titanium atoms on an aluminum surface and mechanisms of subsequent steps in hydrogen capture.

In the future, Chaudhuri and Muckerman's group plans to study the subsequent steps in the sodium alanate hydrogen-storage process, in which aluminum and hydrogen react with sodium hydride to reform the starting material.

This research was funded by the Office of Basic Energy Sciences within the U.S. Department of Energy's Office of Science.

— Laura Mgrdichian

Yale Scientists “See” Basis of Antibiotic Resistance

Using x-ray crystallography, researchers at Yale have “seen” the structural basis for antibiotic resistance to common pathogenic bacteria, facilitating design of a new class of antibiotic drugs, according to an article in the April, 2005 issue of *Cell*.

In recent years, common disease-causing bacteria have increasingly become resistant to antibiotics, such as erythromycin and azithromycin. Although the macrolide antibiotics in this group are structurally different, all work by inhibiting the protein synthesis of bacteria, but not of humans. They bind tightly to an RNA site on the bacterial ribosomes, the cellular machinery that makes protein, but not to the human ribosomes. Bacteria can become resistant to antibiotics in several different ways. When bacteria mutate to become resistant to one of these antibiotics, they usually are resistant to all antibiotics in the group.

Studies led by Sterling Professors Thomas A. Steitz and Peter B. Moore in the Departments of Molecular Biophysics and Biochemistry, and Chemistry at Yale University illuminate one of the ways that bacteria can become resistant to macrolide antibiotics.



Authors (from left) Daqi Tu, Peter B. Moore, Thomas A. Steitz, and Gregor Blaha

“A major health concern of antibiotic resistance is that two million people every year get infections in hospital facilities and 90,000 per year die from them,” said Steitz. “Macrolide-resistant *Staphylococcus aureus* is the most common of these infections.”

Some of the clinically important bacteria are resistant because of mutation of a single nucleotide base, from an A to a G, in the site where macrolide antibiotics bind to the ribosome. The Yale group was able to “see” structural alterations when antibiotics were bound to ribosomes with different sensitivity to the drugs because of mutation. They can now explain why that mutation has the effect that it does. “The mutant G has an amino group that pokes into the center of the macrolide ring, causing it to back off the ribosome by an Angstrom or so,” said Steitz. The change of that one base in the ribosomal RNA reduced the ability of the antibiotic to bind by a factor of 10,000.

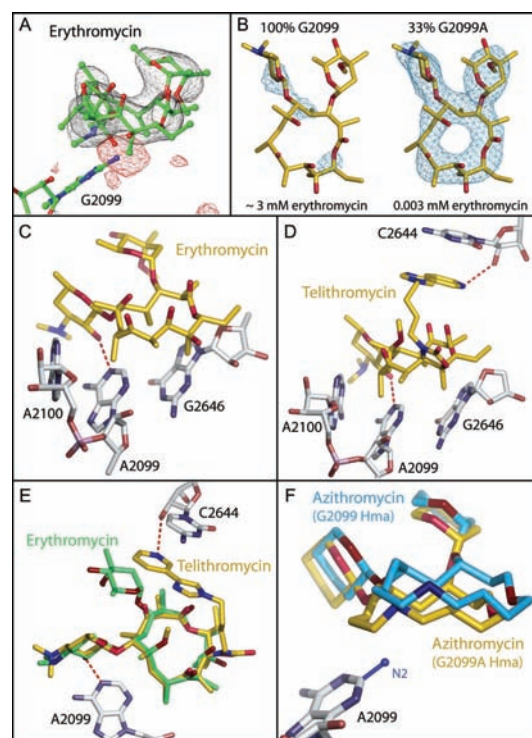
Mutation of this type happens naturally, but rarely — only one in 100,000 to one in 10,000,000 bacterial mutations will cause this kind of resistance. However, each bacterium can divide as often as every 20 minutes, allowing one with a resistant mutation to rapidly cause a dangerous infection.

Daqi Tu, a student, and Gregor Blaha, a postdoctoral fellow in molecular biophysics and biochemistry and associate of the Howard Hughes Medical Institute, are co-authors on the study. Funding for this research was obtained from the National Institutes of Health and the Agouron Institute.

For more information, see: D. Tu, G. Blaha, P.B. Moore, and T.A. Steitz, “Structures of MLS_BK Antibiotics Bound to Mutated Large Ribosomal Subunits Provide a Structural Explanation for Resistance,” *Cell*, **121**(2), 257-270 (2005).

— Janet Rettig Emanuel, Yale University

Interactions of macrolides with G2099A large ribosomal subunits. (A) A (Fo(mutant + drug) – Fo(wild type – drug)) difference map calculated using wild-type phases shows positive 4σ density (black) for erythromycin, and a negative 4σ peak (red) at N2 of G2099. (B) No convincing difference density is observed when erythromycin is soaked into wild type *H. marismortui* 50S crystal with ~ 3 mM concentration (left), but when it is soaked into 50S crystals containing 33% G2099A mutants, clear density is observed when the drug concentration is 3 μ M (right). (C) Erythromycin binds in the hydrophobic pocket formed by residue A2100 (A2059), A2099 (A2058) and G2646 (C2611), with its desosamine nitrogen hydrogen bonded to A2099N1. (D) Telithromycin binds in the hydrophobic pocket formed by residue A2100, A2099 and G2646 the way erythromycin does, with its alkyl-aryl extension making an additional stacking interaction with the base of C2644 (U2609), and a hydrogen bond to the 2’OH of C2644 (U2609). (E) The lactone rings of erythromycin and telithromycin bound to Hma ribosomes are perfectly superimposable. (F) Comparison of azithromycin bound to G2099 (blue) and G2099A (yellow) ribosomes. The N2 of a G was modeled onto residue A2099. The two structures were aligned by least squares superimposition of ribosomal RNA phosphorus atoms.



NSLS Vortex-Tube Study is a Win for Safety

During machining at the NSLS, a vortex-tube device that directs chilled air to cool the cutting tool is often utilized because it reduces the amount of fluid coolant that needs to be used. This makes it more environmentally friendly than other cooling methods — always a good thing. But the *safety* of vortex tubes — whether they make a machine operator more or less safe — has been in debate.

Recently, however, the debate was put to rest by NSLS engineer Ed Haas, technical supervisor Bob Scheuerer, and machinist Ed Losee, who designed and completed a series of tests to determine if vortex tubes enhance or diminish safety during machining. Their work is summarized in an article, which they co-wrote, that published in September 2005 trade journal *Modern Machine Shop*.



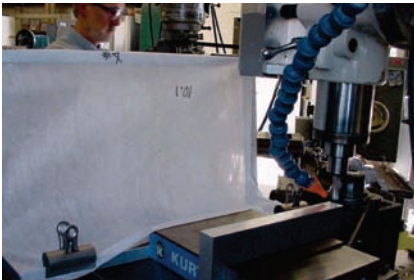
Authors (from left) Ed Haas, Ed Losee, and Bob Scheuerer

Said Haas, “At Brookhaven, uncertainty when it comes to safety is considered not acceptable. We wanted to settle this safety issue using objective tests.”

The issue of vortex-tube safety lies in the fact that the chilled air flow produced by the vortex tube may increase the amount of high-speed metal chips that are directed toward the machine tool operator. Therefore, one way to gauge the safety or lack of safety of a vortex tube is to measure (by weight) the quantity of those chips. To help make this measurement, Haas, Scheuerer, and Losee designed a “chip catcher” — cloth clamped to a metal frame — which they placed on a milling machine.

Under identical conditions, using nine identical chip catchers, the men ran nine trials using a one-inch-thick piece of aluminum: three trials with no coolant whatsoever, three with a vortex tube, and three using coolant spray. After each run, Haas, Scheuerer, and Losee weighed the chips caught by the chip catcher (the chips from the last three runs were rinsed and dried to remove the liquid coolant, before they were weighed).

The results? Compared to the no-coolant and spray-coolant runs, which produced nearly the same volume of chips compared to each other, the vortex-tube runs resulted in more than 60 percent fewer chips directed toward the machine operator.



Vortex tube and chip catcher test set-up



Chips collected by chip-catcher using vortex tube during machining



Chips collected by chip-catcher during dry machining

“We concluded that using a vortex tube does in fact enhance the safety of the operator compared to cases in which no coolant or spray coolant is used,” said Haas. “This is particularly true if guarding or shielding is used behind the machine tool so that chips cannot travel toward any other personnel in the area. Clean-up would then be easier since dry chips would then accumulate against the shield.”

In the future, Haas, Scheuerer, and Losee may consider performing additional vortex-tube safety tests using other conditions, such as denser materials and higher cutter speeds.

For more information, see: E. Haas, R. Scheuerer, and E. Losee, “Vortex Tube Machining Improves Safety While Reducing Environmental Waste,” *Mod. Mach. Shop.*, 78, 54 (2005).

— Laura Mgrdichian

Studying the Effects of Acid Mine Drainage

New information from a study performed at the NSLS may one day help to mitigate the contamination caused by acid mine drainage, in which the breakdown of minerals in mines causes harmful materials to leach into waters and soils.

NSLS user scientists from Princeton University used infrared light and x-rays to study the interactions between two main components of acid mine drainage: two different positively charged iron ions, known as iron(II) and iron(III), and a negative sulfate ion (a sulfur-oxygen molecule). These substances are typically produced by the weathering of pyrite, a common mine ore.

"Acid mine drainage contaminates surface waters, groundwater, and soils in many locations around the world," said geoscientist Juraj Majzlan, the paper's lead author, now a faculty member at Albert-Ludwig-University of Freiburg (this work was performed when he was at Princeton).

"We studied how iron and sulfate interact in solution, such as how they combine to form various iron-sulfate compounds," he explained. "This is important, since the presence of iron-sulfate compounds affects the solubility of other harmful substances in water contaminated by acid mine drainage, such as trace metals and other ions, which contribute to its toxicity."

The work is published in the January 1, 2005 edition of *Environmental Science & Technology*.

Majzlan and Princeton geoscientist Satish C.B. Myneni, the paper's co-author, prepared two types of solutions, the first type containing sulfate and iron(II) and the second containing sulfate and iron(III). These solutions simulate the concentrations found in contaminated water. For each type, they prepared samples with varying concentrations of iron(II) and iron(III). They studied the solutions using infrared and x-ray "spectroscopy," a technique that measures how the light is absorbed by the solution. The absorption behavior of the solution provides scientists with structural and compositional information, such as the types of atomic clusters, known as complexes, that form within it.

Majzlan and Myneni focused on the sulfate ion, using it as an indicator. That is, they studied how the sulfate was altered in the presence of iron(II) or iron(III) and, based on any changes, inferred how it had interacted with the iron.

The researchers found that sulfate and iron(II) either interacted very weakly or did not form any complexes at all. However, they measured a significant distortion of the sulfate ion in the presence of iron(III). Upon further study, they determined that sulfate and iron(III) formed molecular complexes strongly bound together by hydrogen atoms.

This system serves as a model for acid-polluted waters. The sulfate-iron(III) complexes are small-scale versions of the mineral precipitates — solid materials that crystallize out of a liquid — that appear in acid-mine drainage. Based on the particular complexes that form in the sulfate-iron(III) solutions, the scientists can predict which precipitates are most likely to occur in acid mine drainage. One day, this information may assist in devising clean-up strategies for water contaminated by acid mine drainage.

This study was supported by the National Science Foundation and a Hess Fellowship from the Princeton University Geosciences Department.

For more information, see: J. Majzlan and S.C.B. Myneni, "Speciation of Iron and Sulfate in Acid Waters: Aqueous Clusters to Mineral Precipitates," *Environ. Sci. Technol.*, **39**(1), 188-194 (2005).

— Laura Mgrdichian



Juraj Majzlan



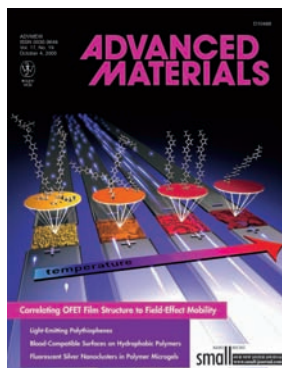
Satish Myneni



Examples of water contaminated by acid mine drainage.

A New Structural View of Organic Electronic Devices

Although still in the qualifying rounds, U.S. researchers are helping manufacturers win the race to develop low-cost ways to commercialize a multitude of products based on inexpensive organic electronic materials — from large solar-power arrays to electronic newspapers that can be bent and folded.



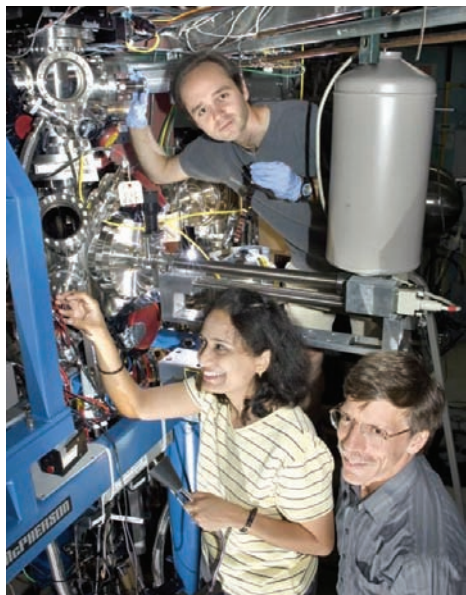
The group's research is showcased on the cover of the October 4, 2005, edition of *Advanced Materials*.

In the October 4, 2005 issue of *Advanced Materials*, researchers from the National Institute of Standards and Technology (NIST) and the University of California at Berkeley report success in using a non-destructive measurement method to detail three structural properties crucial to making reliable electronic devices with thin films of the carbon-rich (organic) semiconductors. The new capability could help industry clear hurdles responsible for high manufacturing development costs that stand in the way of widespread commercial application of the materials.

With the technique called near-edge x-ray absorption fine-structure spectroscopy, or NEXAFS, the team tracked chemical reactions, molecular reordering and defect formation over a range of processing temperatures.

They then evaluated how process-induced changes in thin-film composition and structure affected the movement of charge carriers (either electrons or electron "holes") in organic field effect transistors, devices basic to electronic circuits. With NEXAFS measurements taken over the range from room temperature to 300 degrees Celsius, the team monitored the conversion of a precursor chemical to an oligothiophene, an organic semiconductor. The molecular organization and composition achieved at 250 degrees Celsius yielded the highest levels of charge carrier movement and, consequently, maximum electric-current flow.

As chemical conversion progressed, the researchers calculated how the molecules arranged themselves on top of an electrical insulator. Top transistor performance corresponded to a vertical alignment of molecules. In addition, they used NEXAFS to determine the angles of chemical bonds and to assess the thickness and uniformity of film coverage, also critical to performance.



NIST researchers (clockwise from top) Dean DeLongchamp, Daniel Fischer, and Sharadha Sambasivan.

NEXAFS has the potential to be the "ideal measurement platform for systematic investigation" of organic electronic materials, says lead investigator Dean DeLongchamp, a NIST materials scientist. "A straightforward means of correlating chemical and physical structure to the electronic performance of organic semiconductor films is a much-needed tool."

The research was conducted at beamline U7A, the NIST/Dow Chemical materials characterization facility at the National Synchrotron Light Source. Funding providers included the U.S. Department of Energy, Defense Advanced Research Projects Agency, and the Microelectronics Advanced Research Corporation.

Article originally published at http://www.msrl.nist.gov/OE_Highlight.htm.

For more information, see: D.M. DeLongchamp, S. Sambasivan, D.A. Fischer, E.K. Lin, P. Chang, A.R. Murphy, J.M.J. Frechet, and V. Subramanian, "Direct Correlation of Organic Semiconductor Film Structure to Field-Effect Mobility," *Adv. Mater.*, **17(19)**, 2340-2344 (2005).

— Mark Bello, NIST Media Contact

Scientists Describe New Way to Peer Inside Bacteria

X-rays yield pictures and chemical clues that may help trace contaminants, thwart terrorists

As part of the search for better ways to track and clean up soil contaminants, scientists at the U.S. Department of Energy's Brookhaven National Laboratory and Stony Brook University have developed a new way to "image" the internal chemistry of bacteria. The technique will allow scientists to "see" at the molecular level how soil-dwelling microbes interact with various pollutants. The method might also help scientists better understand and prevent bacterial diseases, or find ways to detect or disable bacteria used in a terror attack.

"The more we learn about soil microbe chemistry, the better we'll be able to predict the movement of contaminants in the environment," said Brookhaven microbiologist Jeffrey Gillow. "What we learn might also suggest new ways to harness microorganisms to immobilize things like heavy metals and radioactive contaminants," he said. Gillow gave a talk on the new method at the 230th National Meeting of the American Chemical Society in Washington, D.C. on August 28, 2005.

Called x-ray spectromicroscopy, the method uses the extremely bright x-rays available at Brookhaven's National Synchrotron Light Source (NSLS) -- but not just to take pictures. At the NSLS, the scientists can actually "tune" the energy level of the beam to measure subtle differences in the energy absorbed by different forms of carbon. This carbon absorption spectrum, or "fingerprint," reveals detailed biochemical information about what is inside and around the bacterial cells — and can even detect the formation of bacterial spores at an early stage invisible to other methods.

"We are starting to learn a lot more about the molecular chemistry of these bacteria," said Gillow. "The goal is to understand better how they interact with metals and radionuclides."

The technique may also reveal details about the process of bacterial spore formation. This could be important to environmental cleanup because spore-forming microbes often live in contaminated environments. It might also offer new targets for the detection of weaponized bacteria (by finding spores at an early stage), or help thwart disease or a terrorist attack by finding ways to prevent the spores from germinating into active, infective bacterial cells.

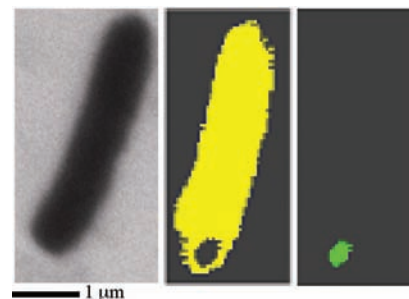
With this technique, Gillow added, samples can be studied wet or dry, without staining, sectioning, or any other intervention such as those used in electron and fluorescence microscopy.

This work is a collaborative effort of the Center for Environmental Molecular Science, which consists of scientists from Stony Brook University and Brookhaven Lab, and the University of Guelph in Canada. The work was funded by the U.S. National Science Foundation and the Office of Biological and Environmental Research within the U.S. Department of Energy's Office of Science.

— Karen McNulty Walsh



Researchers (from left, top) Sue Wirick, Bjorg Larson, and Jeffrey Gillow



A single cell of *Clostridium* sp. (a strictly-anaerobic, soil-dwelling bacterium) as imaged by scanning transmission x-ray spectromicroscopy (left). By analyzing the x-ray absorption spectrum, scientists can pick up subtle biochemical differences between the bulk of the cell body (yellow) and a tiny spore (green) forming inside. This early stage of spore formation would be invisible to other imaging techniques.

Removing Uranium From Contaminated Steel Surfaces

2000 DOE student intern who assisted in research is among authors of published paper

Scientists from BNL's Environmental Sciences Department and Stony Brook University (SBU) Environmental & Molecular Sciences, have developed a simple, safe method of removing uranium from contaminated metallic surfaces using citric acid formulations so that the materials can be recycled or disposed of as low-level radioactive or nonradioactive waste. This research, published in the July 1, 2005 issue of *Environmental Science and Technology*, is funded by the Environmental Management Science Program of the Environmental Remediation Sciences Division, Office of Biological & Environmental Research of DOE's Office of Science.

Decontamination of radionuclides from metallic and other surfaces contaminated by radiological incidents is a major environmental challenge. A.J. Francis, assisted by Cleveland Dodge, BNL, and by SBU's Gary Halada, developed an innovative and improved process for decontaminating metal surfaces and other materials. Another team member named among the authors was BNL 2000 summer intern Jason McDonald, currently pursuing his Ph.D. at Louisiana State University. Material Science Department, both affiliated with the Center for The research team developed an environmentally friendly green-chemistry process that uses all naturally occurring materials — citric acid, common soil bacteria, and sunlight.



Discussing their uranium decontamination research conducted at BNL's National Synchrotron Light Source are scientists: (from left) A.J. Francis, BNL; Gary Halada, Stony Brook University; and Cleveland Dodge, BNL. Also participating in this research was Jason McDonald (not shown). McDonald worked with the research team at BNL in summer 2000 through a DOE summer internship program administered by BNL's Office of Educational Programs and is currently working on his Ph.D. in agronomy and environmental management at Louisiana State University, Baton Rouge.

Present methods of removing uranium from contaminated metal surfaces include sand blasting, chemical extraction, and electrochemical dissolution. These methods generate secondary waste streams, creating additional disposal problems. "In the event of a radiological incident, such as a 'dirty bomb,' this technology can be used to clean up contaminated materials," Francis said. "It will also treat the secondary waste generated from the treatment process, resulting in waste minimization. It is a comprehensive process."

For more information, see: A.J. Francis, C.J. Dodge, J.A. McDonald, and G.P. Halada, "Decontamination of Uranium-Contaminated Steel Surfaces by Hydroxycarboxylic Acid with Uranium Recovery," Environ. Sci. Technol., 39, 5015-5021 (2005).

— Kay Cordtz

BEAMLINE X18A

Funding

National Science Foundation; Instrumentation (Columbia and Brookhaven National Laboratory) by the U.S. Department of Energy

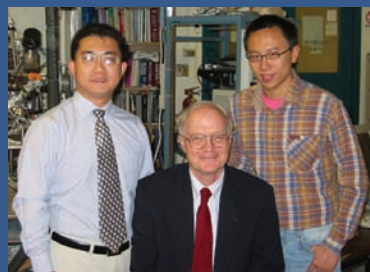
Publication

Z.M. Zhu, T. Chen, Y. Gu, J. Warren, and R.M. Osgood, Jr., "Zinc-Oxide Nanowires Grown by Vapor-Phase Transport Using Selected Metal Catalysts: A Comparative Study," *Chem. Mater.*, **17**, 4227 (2005).

For More Information

Richard Osgood, Applied Physics Department, Columbia University

Email: osgood@columbia.edu



Authors (from left) Zuoming Zhu, Richard M. Osgood, Jr., and Tsung-Liang Chen

Zinc Oxide Nanowires Grown by Vapor-Phase Transport Using Selected Metal Catalysts: A Comparative Study

Z. Zhu¹, T.-L. Chen², Y. Gu¹, J. Warren³, and R.M. Osgood, Jr.^{1,2,3}

¹Department of Applied Physics and Applied Mathematics and ²Department of Electrical Engineering, Columbia University; ³Center for Functional Nanomaterials, Brookhaven National Laboratory

The search for new methods of synthesizing nanomaterials is a key goal of the national nanoscience initiative. Our research involves a comparative study of metal-surface-catalyzed growth of ZnO nanowires using four different metal catalysts and using substrates of differing materials and differing crystal orientations. We have employed multiple materials diagnostic techniques to compare the material, structural, and optical properties of nanowires grown using these different surface systems. In particular, we have found that the growth modes of nanowires are dependent on the choice of surface catalysts, e.g. for the Fe thin-film catalysts, the growth of ZnO nanowires may occur via a vapor-solid process, while, for the case of Au, Ag, and Ni catalysts, the vapor-liquid-solid process usually dominates the wire growth.

Nanowire growth has been investigated as a route to low-dimensional crystal structures. These nanostructures have potential applications in a variety of optical- and electronic-devices, such as lasers or light-emitting diodes. While the growth of these wires has been achieved under a wide variety of conditions, including liquid and vapor growth, one of the most reliable and well-studied approaches uses vapor-phase transport of the constituents coupled with surface catalysis of the nucleation and growth steps. Prof. Peidong Yang and his collaborators at Lawrence Berkeley National Laboratory have described an excellent example of this approach for the growth of ZnO nanowires. In this method, small surface-bound droplets of Au are formed on a solid substrate surface, such as Si(100), by heating a thin Au film and depositing it on the Si surface. These droplets served as alloying sites for the condensation of Zn vapor from a nearby solid-ZnO source. Single-crystal ZnO nanowires then grew from the supersaturated AuZn alloy, in the presence of constant trace amounts of oxygen (**Figure 1**). The orientation of the wires was thought to be governed by registration on the substrate crystalline lattice.

The success of this method in growing nanoobjects caused us to ask a series of questions: Can other catalysts be used? How general is the technique? What exactly controls the properties of the nanowires? Answering such questions is difficult because both the catalyst and substrate play important roles in determining the properties and the structure of the nanowires. In addition, the attainment of good nanowire material properties, such as good crystallinity and low impurity concentration, plays an important role in the practicality of various nanowire applications in electronics and optics.

Thus, we have employed multiple materials diagnostics, including x-ray diffraction, to compare the material, structural, and optical properties of the nanowires grown using these different surface systems. In particular, our research shows that the growth modes of nanowires depends on the exact metal surface catalysts used. Thus, for Fe or Ni thin-film catalysts, the growth of ZnO nanowires apparently proceeds via a vapor-solid process, while, for the case of Au, Ag, and sometimes Ni catalysts, the vapor-liquid-solid process appears

to dominate the wire growth. These differences are apparent in the high-resolution SEMs taken at the BNL Center for Functional Nanomaterials (CFN); see **Figure 2**. Further, as shown in **Figure 3**, our study shows that the degree of nanowire alignment on the substrates is a function of both the substrate lattice matching with the lattice of the nanowires, as well as the growth mode and its role in affecting the substrate-interfacial properties.

From a more general point of view, our investigation shows that the use of different catalysts provides versatility in the growth of one-dimensional ZnO nanostructures with different ranges of parameters such as diameters, areal densities, and aspect ratios. In particular, our studies suggest that, compared to noble-metal catalysts, the rate of growth using transition-metal catalysts is relatively faster and therefore typically yields thicker wires with a higher aspect ratio. However, this high growth rate is achieved at the expense of inducing more oxygen vacancies. These differences in growth properties would be expected to affect other properties of the wires, such as their electrical transport and surface chemistry. Exploring these aspects is of interest for practical applications of ZnO and other metal-oxide nanowires in nanodevices and chemical sensors.

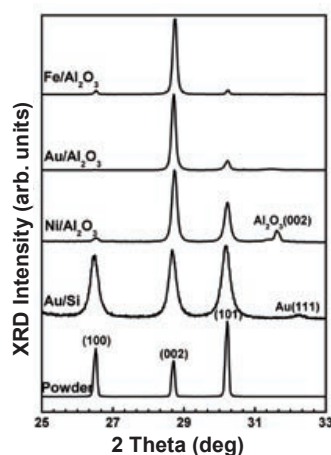


Figure 3. A series of XRD spectra for ZnO nanowires synthesized using several different metal catalysts. The spectra were recorded at angles covering three major characteristic XRD diffraction peaks of the wurtzite ZnO.

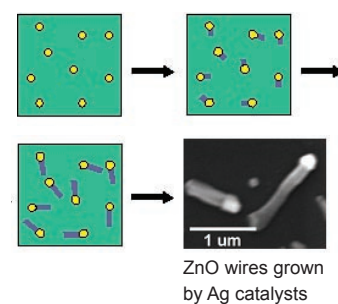


Figure 1. Illustration of the vapor-phase-transport process for ZnO nanowire growth.

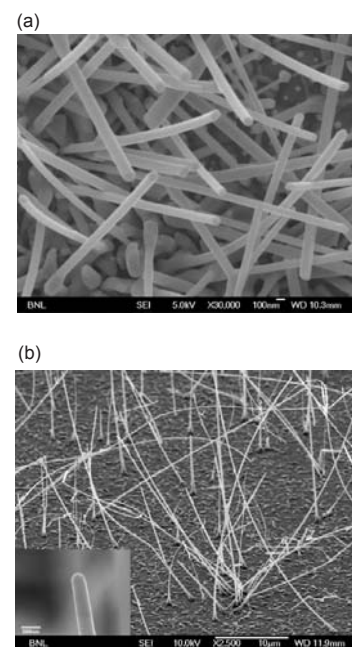


Figure 2. A FE-SEM image of ZnO nanowires grown on (a) a Si(111) substrate with Au as the catalyst; the predominant growth direction is 30° to the surface; (b) an a-plane (110) sapphire substrate with Fe as the catalyst; the predominant growth direction is at the surface normal. (Pictures taken at the BNL/CFN).

BEAMLINE U1A

Funding

Swiss National Science Foundation;
Deutsche Forschungsgemeinschaft; U.S.
Department of Energy

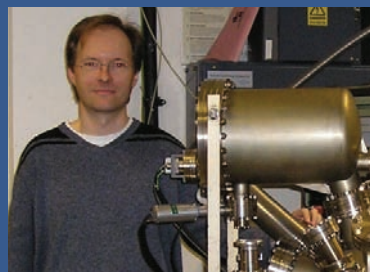
Publication

G. Hähner, M. Zwahlen, and W. Caseri,
"Chain Length Dependence of the
Conformational Order in Self-Assembled
Dialkylammonium Monolayers on Mica
Studied with Soft X-ray Absorption,"
Langmuir, **21**, 1424-1427 (2005).

For More Information

Georg Hähner, *EaStCHEM* School of
Chemistry, University of St Andrews

Email: gh23@st-and.ac.uk



Georg Hähner

Chain Length Dependence of the Conformational Order in Self-Assembled Dialkylammonium Monolayers on Mica Studied with Soft X-ray Absorption

G. Hähner¹, M. Zwahlen^{1,2}, and W. Caseri²

¹EaStCHEM School of Chemistry, University of St Andrews, UK; ²Department of Materials, ETH-Hönggerberg, Switzerland

Self-assembled alkyl chain-based monolayers on mica are important for industrial and technological processes because they can be used to organically modify inorganic substrates. The conformational structure and orientational order of the films determine how the modified substrate interacts with the environment and also determines the chemical character and stability of its surface. Using near-edge x-ray absorption fine structure (NEXAFS) spectroscopy, we have systematically studied the conformational order in ion-exchanged dialkylammonium monolayers adsorbed on mica and how that order depends on the length of the alkyl chains. We found that the absolute number of gauche defects in the films increases with decreasing chain length.

Organic monolayer coatings can be employed to modify the surface properties of inorganic materials. The molecular order and orientation of the films are important parameters, since they determine the homogeneity, stability, and chemical properties of the modified surface. Films on mica have attracted less attention than the more widely studied thiol-gold system, despite their importance to industrial and technological processes. For alkane thiols on gold, it is known that the number of "gauche" conformations in the film — that is, conformational defects — depends on the temperature. But for alkyl chains with more than 11 carbon atoms, that number is rather independent of the chain length. Results from the thiol-gold system, however, cannot simply be transferred to films on mica, since the bonding mechanism and molecular arrangements are different. In the case of ion-exchanged films on mica, the packing density in the resulting film is determined by the surface cation density of the layered silicate surface.

We prepared films of dialkylammonium cations (2C_n) with n=8-18 carbon atoms per chain on mica substrates and characterized them with NEXAFS. **Figure 1** shows spectra recorded at the carbon 1s edge at grazing and normal photon incidence (left). On the right hand side, we show the corresponding difference spectra between grazing and normal incidence.

The high anisotropy of the C-H (labeled 3) and C-C related signals (labeled 4) indicates a high degree of conformational order of the alkyl chains.

The observed anisotropy can be converted into an (average) number of gauche defects per molecule. Note that each molecule contains two alkyl chains. **Table 1** summarizes these numbers for the molecular ions investigated.

Interestingly, the absolute number of defects in these films increases with decreasing chain length. This is in contrast to the thiol-gold system. **Figure 2** illustrates this result schematically.

Dialkylammonium species films with 12 or more methylene units per chain

show a significantly high degree of molecular orientation. The higher number of gauche defects found for shorter chains can be attributed to a decreasing van der Waals interaction between neighboring molecules in connection with an overall coverage of about 80%.

The employment of long alkyl chains for well ordered monolayers appears to be more important for films on mica prepared by ion-exchange compared to alkanethiols on gold. This is due to the lower overall coverage and packing density of the films on mica, which leaves more molecules exposed to uncovered regions and leads to weaker intermolecular interactions, resulting in a strong increase in the number of gauche defects for shorter alkyl chains. In order to prepare densely packed and highly ordered monomolecular films on mica, quaternary dialkyldimethylammonium ions with 16 or more carbon atoms should be employed.

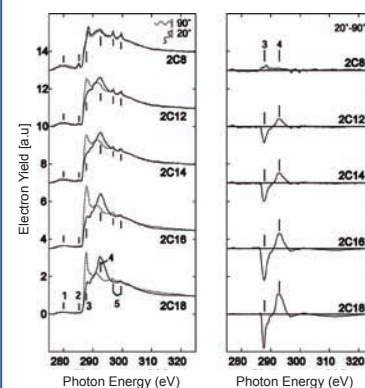


Figure 1. NEXAFS C 1s spectra of dialkyldimethylammonium films with various chain lengths adsorbed on mica recorded at normal (dashed line) and grazing (solid line) photon incidence. On the right hand side the corresponding difference spectra are shown.

	C-H	C-C
2C18	5.4(3.2)	8.3(2.5)
2C16	7.4(2.2)	11.2(1.6)
2C14	13.2(2.8)	15.4(1.4)
2C12	13.2(1.2)	15.4(1.2)
2C8	-	15.4(0.8)

Table 1. Number of gauche defects per molecule. The numbers in brackets denote the error limits.

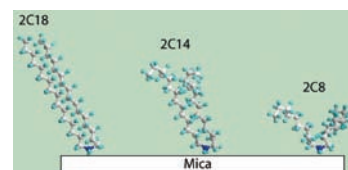


Figure 2. Schematic of the average molecular order for dialkyldimethylammonium ions of different chain length adsorbed onto mica.

Beamline U1A

Funding

Swiss Priority Program on Materials (PPM)

Publication

S.-J. Xiao, S. Brunner, and M. Wieland, "Reactions of Surface Amines with Heterobifunctional Cross-Linkers Bearing Both Succinimidyl Ester and Maleimide for Grafting Biomolecules," *J. Phys. Chem. B*, **108**, 16508-16517 (2004).

For More Information

Shou-Jun Xiao, State Key Laboratory of Coordination Chemistry, Nanjing University, P.R. China

Email: sjxiao@nju.edu.cn

A Step Closer to Understanding Immobilized Organo- and Bio-Molecular Complexes on Solid Surfaces

S.-J. Xiao¹, S. Brunner², and M. Wieland¹

¹Laboratory for Surface Science and Technology, Swiss Federal Institute of Technology, Switzerland; ²EMPA (Swiss Federal Laboratories for Materials Testing and Research), Materials Science and Technology, Switzerland

Organic reactions on plane metal surfaces are of much interest for applications in biosensors, biomaterials, and biochips. However, the details of the reactions are not easy to characterize because surface-sensitive technologies cannot fully determine molecular structures, and collecting enough grafted materials for sufficient bulk analyses is tremendously difficult. In this study, a well-known amine-reactive cross-linking reaction for biomolecular conjugation occurs on an amine-pendant self-assembled monolayer on gold. The infrared reflection absorption spectroscopy (IRRAS) of that reaction and other analogous reactions produces significantly different spectra. With the help of x-ray photoelectron spectroscopy (XPS) and near-edge x-ray absorption fine structure spectroscopy (NEXAFS), we deduced that a so-called side reaction, accompanying the main reaction, occurred in this case. Furthermore, a peptide bearing both a free amino and a free thiol group was immobilized as two configurations on the surface, either one-end or two-end fixed.

Self-assembled monolayers (SAMs) on metal surfaces such as gold, silicon, and titanium have been the subject of intense investigations over the past 20 years. The driving force for these endeavors is the goal of combining micro- and nano-electronics with biotechnology. Unlike in a bulk reaction, however, where the pure product from organic reactions can be separated and definitely identified by well-established analysis methods such as nuclear magnetic resonance (NMR), elemental analysis, and x-ray single crystal diffraction, the molecular structure of a surface product on a plane metal surface can only be deduced from surface-sensitive analysis techniques, such as IRRAS, XPS, NEXAFS, and time-of-flight secondary ion mass spectroscopy (TOF-SIMS). But each of these methods provides partial information only. Therefore, an integrated analysis and logical interpretation of the results from these surface-sensitive techniques is necessary.

We investigated a well known cross-linking reaction on gold surfaces as a method for biomolecular immobilization, i.e. fixing biological molecules onto a substrate (**Scheme 1**). The reaction includes three steps: 1) the activation of the inert gold surface via the self-assembly an amino-terminated species, cystamine, which contains both a disulfide and two end-amines; 2) the subsequent surface reaction of the primary amines with hetero-bifunctional cross-linkers bearing both an amine-reactive species, succinimidyl ester (NHS), and a thiol-reactive species, maleimide; and finally 3) the covalent attachment of biomolecules onto the surface.

In step 2, we found that a surface derived from N-succinimidyl-6-maleimidyl-hexanoate (SMH) presented a specific IRRAS spectrum, where four bands were observed in the carbonyl stretching region (1700-1900 cm⁻¹), while only one band around 1710 cm⁻¹ was observed for its analogous surfaces (**Figure 1**). It is widely believed that the reaction occurs between amine and NHS, eliminating NHS as the leaving group and producing a maleimide-terminated surface. In this case, due to the asymmetric stretching mode of maleimide,



Authors (from left) Shou-Jun Xiao, Samuel Brunner, and Marco Wieland

the infrared spectra should exhibit one strong band around 1710 cm^{-1} . What caused the other three bands? We first thought that either a side reaction or an orientation of maleimide might account for them. Since NEXAFS studies for the orientation of functional groups are well understood by our colleagues, G. Hähner and D. Brovelli from the Laboratory of Surface Science and Technology at the Swiss Federal Institute of Technology in Switzerland, they collected the NEXAFS data at beamline U1A on our behalf. The results (**Figure 2**) confirmed the existence of the double bond ($\text{C}=\text{C}$) of maleimide and the random orientation of $\text{C}=\text{C}$ and $\text{C}=\text{O}$. This measurement helped us to identify the real culprit, a side reaction of amine with maleimide, and thus the resulted terminal NHS groups, for the anomalous IRRAS spectrum. Further, we cross-proved our deduction with another experiment: the synthesis of the expected surface product, N,N'-bis(maleimidylhexanoyl)cystamine (BMHC), in which BMHC self-assembles on gold surfaces. The IRRAS spectrum of BMHC only presents one strong band around 1710 cm^{-1} , corresponding to the maleimide-terminated surfaces, but is different than the spectrum for the SMH-derived surface that contains NHS.

Finally, a cell-adhesive peptide bearing both a free amino and a free thiol group was grafted to two functionalized surfaces, a singular maleimidyl-pendant (BMHC-derived) surface and a two-linker (SMH-derived maleimide and NHS) modified surface, respectively. The first reaction produced an amino-terminated peptide structure via a thioether linkage; the latter produced a bridging peptide structure via both amide and thioether linkages. The above conclusions are carefully deduced from IRRAS measurements, and additionally supported by XPS, NEXAFS, and TOF-SIMS.

The different configurations of biomolecules on solid surfaces will have a significant impact on the development of applications in biomaterials, biosensors, and biochips. The geometry and topology of the attached biomolecules affect surface charges, hydrophobic and hydrophilic properties, molecular orientations, and native conformations. In turn, these surface properties determine the molecules' biological activity and function.

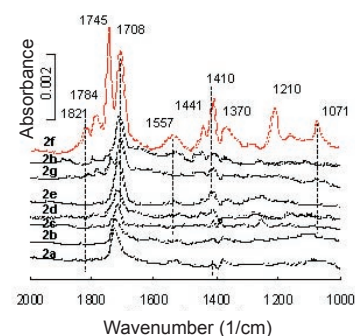


Figure 1. IRRAS spectra of a series of linker-functionalized surfaces, where the side-reaction-resulted curve 2f (surface 2 in Scheme 1) on the top is significantly different from its analogs (2a-g, 2h).

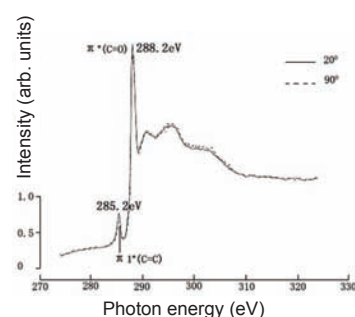
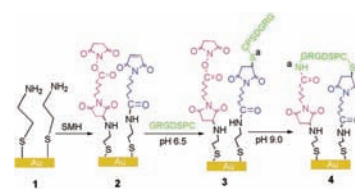


Figure 2. NEXAFS spectra of surface 2 in Scheme 1 at the C 1s edge recorded for two angles of incidence. The overlapping of two lines between grazing (20°) and normal (90°) angles indicates the random orientation of maleimidyl groups.



Scheme 1. Sketch of the subsequent surface reactions. 1) cystamine SAMs, 2) a side-reaction-resulted two-linker (maleimide and NHS)-terminated surface from SMH, 3) a one-end fixed peptide, and 4) a two-end fixed peptide. The linkage atoms S and N (marked a) are highlighted from amino acids Cys and Gly, respectively, but the peptide sequence H-Gly-Arg-Gly-Asp-Ser-Pro-Cys-OH (GRGDSPC) is still kept. SMH is N-succinimidyl-6-maleimidylhexanoate.

BEAMLINE X18B

Funding

U.S. Department of Energy, Office of Basic Energy Sciences

Publication

W.F. Yan, B. Chen, S.M. Mahurin, V. Schwartz, D.R. Mullins, A.R. Lupini, S.J. Pennycook, S. Dai, and S.H. Overbury, "Preparation and Comparison of Supported Gold Nanocatalysts on Anatase, Brookite, Rutile, and P25 Polymorphs of TiO₂ for Catalytic Oxidation of CO." *J. Phys. Chem. B*, **109**, 10676-10685 (2005).

For More Information

Sheng Dai, Surface Sciences Division, Oak Ridge National Laboratory

Email: dais@ornl.gov

Preparation and Comparison of Supported Gold Nanocatalysts on Anatase, Brookite, Rutile, and P25 Polymorphs of TiO₂ for Catalytic Oxidation of CO

W. Yan¹, B. Chen¹, S.M. Mahurin¹, V. Schwartz¹, D.R. Mullins¹, A.R. Lupini², S.J. Pennycook², S. Dai¹, and S.H. Overbury¹

¹Chemical Sciences Division and ²Condensed Matter Physics Division, Oak Ridge National Laboratory

Scientists working at the Oak Ridge National Laboratory have prepared and characterized gold nanocatalysts supported on anatase, rutile, and brookite, which are polymorphs of titanium dioxide (TiO₂). The objective of this investigation was to probe the effect of different catalyst supports on the gold's catalytic activities. All catalysts in the study were exposed to an identical sequence of treatment and measurement. The as-synthesized catalysts exhibited high activity rates with concomitant Au reduction upon exposure to the CO-containing reactant stream. The reduction of cationic gold species was verified by x-ray absorption near-edge spectroscopy (XANES), suggesting what the dominant contribution of the reduced gold species to the observed catalytic activity could be. The deactivation of the catalysts was observed following a treatment sequence at temperatures up to 573 K. The brookite-supported gold catalyst sustains the highest catalytic activity after all treatments. Both x-ray diffraction (XRD) and transmission electron microscope (TEM) results indicate that, following the reaction and pretreatment sequences, the gold particles supported by the brookite are smaller than those on the other supports.

In the late 1980s and the early 1990s, Haruta and coworkers (*J. Catal.* 1989, 115, 301) discovered that gold particles deposited on titanium dioxide exhibited a surprisingly high catalytic activity for low-temperature CO oxidation. This discovery has prompted worldwide research into the applications of gold catalysts in a number of industrially important reactions. The unique catalytic properties of gold nanoparticles have been correlated to many factors and structural parameters. Among them, the type of oxide support used plays a key role in controlling the catalytic activities of gold nanoparticles. The titanium-oxide support used originally by Haruta and coworkers consists of a polymorphic mixture (P25) of anatase and rutile. To more deeply understand the reaction mechanism associated with gold nanoparticles, it is useful to study the support effect induced by allotropic forms. Titanium dioxide is a good candidate because it exists in three different allotropic forms: anatase, brookite, and rutile.

The main objective of our study was to prepare and test Au catalysts supported on three polymorphs of TiO₂, as well as on P25. EXAFS and XANES were employed along with other spectroscopic techniques for probing structural properties associated with the above systems. Our results indicated that when other experimental factors are kept constant, the catalytic activity is not much affected by the variation of the TiO₂ phases. However, the stability of the Au nanoparticles varies with the specific support structure. We demonstrated that the brookite-supported Au catalyst is the most stable catalytic system.

Scanning transmission electron microscopy (STEM) analyses on the most active samples show predominantly 0.5 – 2 nm-sized gold particles on the TiO₂ surface. On rutile and anatase these ultra-small gold nanoparticles are susceptible to aggregation under reaction conditions. Both the XRD and STEM techniques can be used to follow the size variation of gold nanoparticles. In



Sheng Dai (photo courtesy of ORNL)

contrast to the gold catalysts supported on anatase and rutile, the brookite-supported gold catalyst is much more stable. No gold XRD peaks were observed even after extended exposure to catalytic reaction conditions, suggesting that Au nanoparticles are stable on the brookite support under reaction conditions. The Z-contrast microscopy results were obtained on the brookite-supported samples at three different stages: 1) as-synthesized, 2) after reduction at 423 K, and 3) after calcination at 573 K. The micrographs in each of these stages are shown in **Figure 1**. The Au nanoparticles are visible in the as-synthesized state as very small, apparently thin rafts with sizes of 0.5 to 2 nm (**Figure 1a**). Little is changed following a mild treatment at 423 K (**Figure 1b**). The lattice fringes of the needle-like TiO₂ crystallite are readily visible in both micrographs. After calcination at 573 K, these small rafts were not observed and Au particles were few or absent in several micrographs obtained by using the highest magnification. The micrograph in **Figure 1c** shows a single Au particle that is 2 – 3 nm in size and exhibits fringes, suggesting that it is a faceted 3-D particle. At a lower magnification, many particles in the range of 1 – 10 nm are visible, and still lower magnification reveals many particles in the range of 30 – 70 nm.

XANES was used to extract information about the oxidation state of the Au species during the pre-treatment steps used in each of the sequences. Typical XANES spectra are shown for the Au-rutile surface in **Figure 2**. The pre-edge of the Au L_{III} absorption edges exhibits a sharp peak for the as-synthesized state, indicating that it is highly oxidized, probably mostly in the Au³⁺ state. This peak is slowly diminished by exposure to the reaction mixture of 1% CO/air at room temperature (**Figure 2**). This result demonstrates that reaction conditions at room temperature bring about the partial reduction of the Au, even though excess oxygen is present. Heating in Ar causes an additional decrease of the peak, indicating that some auto reduction is possible due to heating. Finally, reduction at 423 K causes a complete loss of the peak and leaves a spectrum that, except for slightly less pronounced oscillations, closely matches that of an Au foil. Additional treatments in hydrogen and in oxygen were performed up to 573 K and subsequent spectra were run in the CO/air mixture. These treatments did not further alter the general shape of the spectrum or bring about any growth of the peak at the Au edge. Therefore, no re-oxidation occurs as a result of these treatments or exposure to reaction conditions.

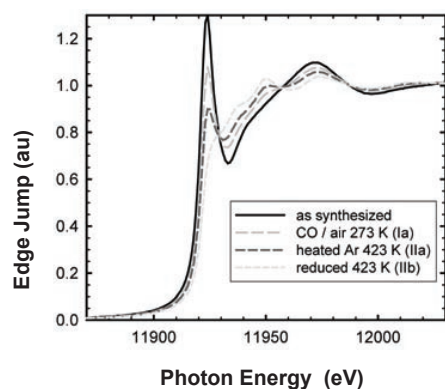


Figure 2. Au XANES spectra of the 14 wt% Au-rutile sample recorded in the as-synthesized state, b) after exposing to the reaction mixture of 1% CO/air for 50 minutes, c) after heating to 473 K in Ar for 30 minutes, and d) after reducing for 30 minutes in 4% H₂/He. Spectra were collected using a fluorescence detector.

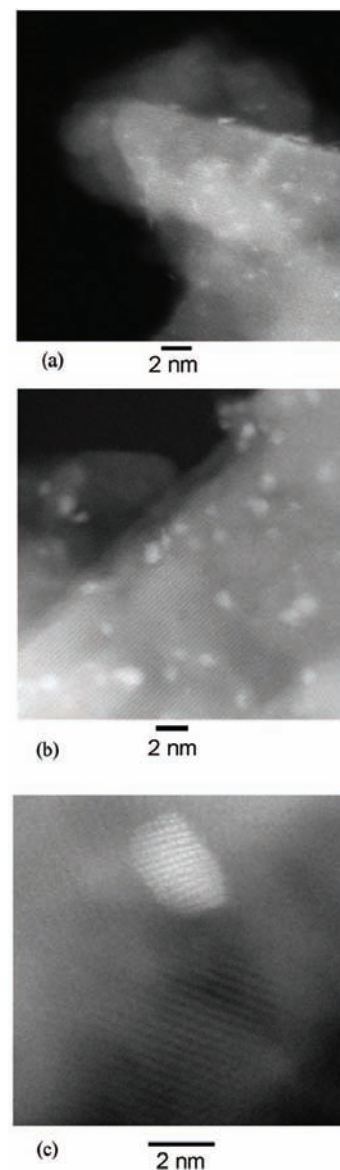


Figure 1. The HRTEM micrograph of Au on brookite gold catalysts recorded in (a) the as-synthesized state, (b) following mild reduction at 423K, and (c) following calcination at 573 K. Micrographs in (a) and (b) are obtained at 2×10^7 magnification and (c) is obtained at 5×10^7 magnification.

BEAMLINE X3A1

Funding

The Danish Research Councils (Dansync)

Publication

R.D. Poulsen, A. Bentien, M. Chevalier, and B.B. Iversen, "Synthesis, Physical Properties, Multitemperature Crystal Structure, and 20 K Synchrotron X-ray Charge Density of a Magnetic Metal Organic Framework Structure, $\text{Mn}_3(\text{C}_8\text{O}_4\text{H}_4)_3(\text{C}_5\text{H}_{11}\text{ON})_2$," *J. Am. Chem. Soc.*, **127**(25), 9156-9166 (2005).

For More Information

Bo Brummerstedt Iversen, Department of Chemistry, University of Aarhus, Denmark

Email: bo@chem.au.dk

Physical Properties and 20 K Synchrotron X-ray Charge Density of a Magnetic Metal Organic Framework Structure, $\text{Mn}_3(\text{C}_8\text{O}_4\text{H}_4)_3(\text{C}_5\text{H}_{11}\text{ON})_2$

R.D. Poulsen, A. Bentien, M. Chevalier, and B.B. Iversen

Department of Chemistry, University of Aarhus, Denmark

Interest in metal organic frameworks (MOFs) has exploded recently due to the potential gas-storage applications of these nanoporous materials. Here we present an investigation of a new magnetic MOF, $\text{Mn}_3(\text{C}_8\text{O}_4\text{H}_4)_3(\text{C}_5\text{H}_{11}\text{ON})_2$, performed using a combination of physical properties measurements and x-ray charge density modeling. We found that the structure has an anti-ferromagnetic ordering at ~4 K. The electron density, determined from multipole modelling of 20 K single-crystal synchrotron x-ray diffraction data, provides a microscopic understanding of the macroscopic magnetic properties. Furthermore, it allows for a detailed analysis of the chemical bonding as well as the calculation of derived properties, such as the electrostatic potential.

Experimental determination of electron densities (EDs) demands x-ray diffraction data of high quality. In order to reduce systematic errors in the data, such as extinction and absorption, x-ray diffraction experiments are preferably carried out on very small crystal samples. Extinction and absorption effects are also reduced if high-energy radiation is used. Thus, synchrotron radiation is highly advantageous in accurate x-ray charge density studies. Proper description of thermal motion requires high-resolution data, and this necessitates the use of helium cryostats. Very low temperature experiments have the added benefit of drastically reducing thermal diffuse scattering (TDS) effects. If accurate data have been measured, the ED can be modeled using the multipole method. A Bader topological analysis of the ED provides a characterisation of the chemical bonding.

The structure of $\text{Mn}_3(\text{C}_8\text{O}_4\text{H}_4)_3(\text{C}_5\text{H}_{11}\text{ON})_2$, **1**, consists of 1D chains of carboxylate-bridged manganese atoms, which are interconnected by the organic benzene-1,4-dicarboxylate linker ($\text{C}_8\text{H}_4\text{O}_4$, BDC), forming rhombic cavities. A multitemperature structural characterization reveals a possible phase transition between 100 K and 20 K due to ordering of the diethylformamide molecules, ($\text{C}_5\text{H}_{11}\text{ON}$, DEF), bonded directly to the 1D chain and located in the rhombic cavities (**Figure 1**). The synthesis, physical property characterisation, and synchrotron x-ray charge density of a similar 1D manganese chain metal organic framework structure, $\text{Mn}_2(\text{C}_8\text{O}_4\text{H}_4)_2(\text{C}_3\text{H}_7\text{ON})_2$, **2**, have been reported previously¹. As for the structure of **1**, this framework also consists of rhombic cavities spanned by the BDC linker, which interconnect the 1D manganese chains. However, contrary to **1**, the magnetic susceptibility and heat-capacity measurements revealed no magnetic ordering down to 2 K.

The topological analysis of the EDs of **1** and **2** reveal that no direct Mn-Mn bonds are present. The magnetic ordering in **1** is due to super-exchange via oxygen bridges between the Mn atoms within the 1D chain, whereas the lack of ordering in **2** is the result of one bridge being an entire carboxylate group (**Figure 1**). The 3D ordering in **1** is due to the alignment of the BDC π -systems at low temperature. The analysis of the magnetic susceptibility and heat-



Authors (from left) Rasmus D. Poulsen, Bo B. Iversen, Anders Bentien, and Marie Chevalier

capacity data suggest Mn^{2+} ions for both **1** and **2**. However, the ED analyses reveal very different Mn centers in **1** and **2**. Orbital populations and a topological analysis show that both Mn atoms of **1** are almost neutral with a substantial anisotropy of the d-orbitals, whereas the Mn atoms of **2** are spherical, high-spin Mn^{2+} ions. The oxygen ligands have similar atomic properties in **1** and **2**, and the difference between the Mn charges is due to a reversed polarity of the carbon atoms (slightly positive in **1**, slightly negative in **2**).

It is somewhat surprising that two structurally similar MOFs have quite different chemical-bonding and atomic properties. The differences can be directly observed in the electrostatic potentials (**Figure 2**) calculated from the experimental EDs. For **1** the potential is fairly uniform, whereas the potential for **2** shows both negative and positive regions. Whether these observations can be correlated with the gas-absorption properties is not yet known, but future ED studies of similar MOFs will be of considerable interest.

¹R.D. Poulsen, A. Bentien, T. Graber, and B.B. Iversen, *Acta Crystallogr. Sect. A*, **60**, 382-389 (2004).

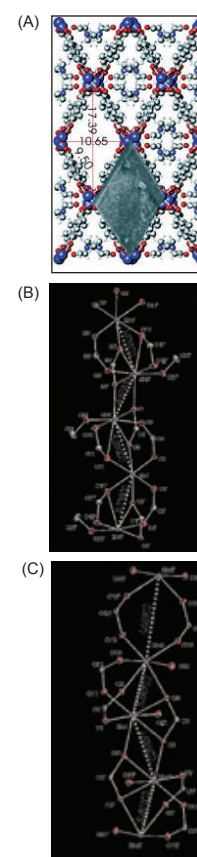


Figure 1. (A) A view of the crystal structure along the a-axis. In one of the nanopores an electron microscope image of a single crystal specimen is overlaid. Approximate pore dimensions are given in Å. (B) The 1D manganese chain of **1**. (C) The Mn-chain in **2**. The Mn-chain runs approximately along the a-axis. Thermal ellipsoids are drawn at 50% level, and in all figures the axes directions are shown with arrows.

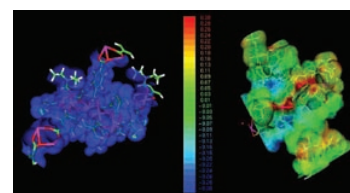


Figure 2. The electrostatic potentials of **1** and **2**, calculated from the experimental electron density and plotted on density isosurfaces of $0.01 \text{ e}/\text{\AA}^3$. The potentials are drawn with the same color coding, which ranges from $-0.3 \text{ e}/\text{\AA}$ (blue) to $0.3 \text{ e}/\text{\AA}$ (red).

Beamline U4A

Funding

U.S. Department of Energy, Office of Basic Energy Sciences; U. S. Army Research Office

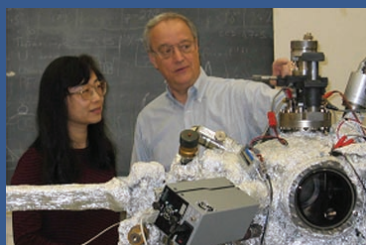
Publication

A.S.Y. Chan, W. Chen, H. Wang, J.E. Rowe, and T.E. Madey, "Methanol Reactions over Oxygen-Modified Re Surfaces: Influence of Surface Structure and Oxidation," *J. Phys. Chem. B* **108**, 14643-14651 (2004).

For More Information

Theodore E. Madey, Department of Physics and Astronomy, Rutgers University

Email: madey@physics.rutgers.edu



Authors (clockwise from top left) Hao Wang, Ally Chan, Theodore Madey, and Wenhua Chen

Structure Sensitivity in Methanol Oxidation over Model Rhenium Oxide Catalysts

A.S.Y. Chan¹, W. Chen¹, H. Wang¹, J.E. Rowe², and T.E. Madey¹

¹Rutgers, The State University of New Jersey; ²University of North Carolina, Chapel Hill

The catalytic oxidation of methanol into products that serve as primary reagents for organic synthesis, such as formaldehyde, is a leading process in the chemical industry. Metal oxide catalysts are conventionally used in methanol oxidation, but understanding the active phases in these catalysts is challenging since they usually have a wide range of geometric structures and oxide compositions. Using soft x-rays produced at the National Synchrotron Light Source, scientists at Rutgers University and the University of North Carolina have shown a direct correlation between the presence of rhenium oxides in low oxidation states and catalyst deactivation. Disordered oxygen phases are revealed to enhance catalytic activity and the formation of these phases is affected by catalyst structure.

How active a catalyst is depends strongly on its morphology and surface structure. Most industrial catalysts contain an active component, typically nanometer-scale particles of transition metals and oxides, which are dispersed on a high-area support made of a relatively inert oxide. In these composite materials, catalyst particles of varying sizes expose a number of different structural planes, each with its own contribution to the overall catalytic activity. Because the complex structures of a real catalyst often hinder the development of rational connections to its performance, studies on model catalysts with well-defined structures allow scientists to establish more precise structure–activity relationships in catalysis.

We prepared model rhenium (Re) oxide catalysts with different morphologies, atomic-scale structures, and oxidation states, since Re oxides are demonstrated to be selective catalysts for methanol oxidation reactions. Using soft x-ray photoelectron spectroscopy (SXPS) at NSLS beamline U4A, we characterized the chemical states of Re atoms and cations on the surfaces of the model catalysts. The energy range of soft x-rays at beamline U4A matches the binding energies of Re states well, which allows us to probe the surface region of the model catalysts — where chemical reactions take place — with ultrahigh sensitivity and resolution. We also tested the chemical reactivity of these model catalysts towards methanol by applying temperature programmed reaction spectroscopy.

We chose the atomically rough Re (12 $\bar{3}$ 1) surface, shown in **Figure 1**, because it easily converts to different structures when treated with oxygen. When covered with oxygen at room temperature, this surface retains its planar form. When heated in small quantities of oxygen, however, Re (12 $\bar{3}$ 1) undergoes massive structural rearrangements to build nanosized 'hill-and-valley' facets that cover the entire surface. These tiny facets have (11 $\bar{2}$ 1) and (01 $\bar{1}$ 0) surface structures, each of which is much smoother on the atomic scale than the planar (12 $\bar{3}$ 1) surface. SXPS data show that both planar and faceted Re remain covered with an oxygen layer, such that Re atoms at the surface are bonded to 1-, 2-, and 3-oxygen neighbors. But the planar surface has a broader distribution of these Re–O bonds, indicating more disorder in this oxygen overlayer compared to the faceted surface. On both surfaces, a small amount of oxygen

also reacts with the metal to form an oxide, ReO.

To increase oxide formation, Re (12 $\bar{3}$ 1) is exposed to a high overpressure of oxygen at an elevated temperature. This produces a thin oxide film on the facets composed of Re cations in low oxidation states, mainly ReO and Re₂O₃ (**Figure 1**). So, we can prepare oxygen-covered rhenium surfaces with different planar and faceted structures, as well as rhenium oxide films, in order to investigate how surface structure and oxide composition affect the activity of methanol oxidation catalysis.

Methanol reacts on the planar and faceted surfaces to yield the oxidation products, formaldehyde and carbon monoxide, as shown in **Figure 2**. A competing reaction to methanol oxidation is non-selective decomposition of methanol to its constituent atoms. Notably, the faceted surface is much less active towards methanol conversion, and a portion of methanol leaves the surface unreacted. In contrast, the thin oxide film exhibits virtually no activity for methanol reaction.

Our studies indicate that rhenium oxides in low oxidation states are completely inert towards methanol, and that surface structure plays a key role in enhancing the activity of oxide catalysts towards oxidation reactions. These findings were made possible by using soft x-ray photoelectron spectroscopy to characterize the catalytically active states on the model catalysts.

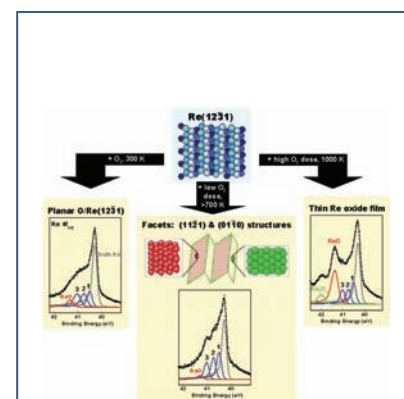


Figure 1. (Top) Surface structure of atomically rough Re (12 $\bar{3}$ 1). (Bottom) High resolution soft x-ray photoelectron spectra (SXPS) of the planar and faceted oxygen-covered Re surfaces, and of the thin Re oxide film, formed by different oxygen treatments to the Re (12 $\bar{3}$ 1) surface.

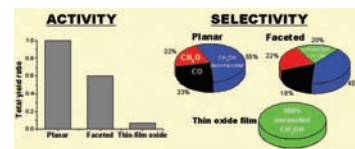


Figure 2. Methanol conversion activity and product selectivity from the model Re oxide catalysts.

BEAMLINE X11A

Funding

U.S. Department of Energy; UTC Fuel Cells; Army Research Office

Publication

A.B. Anderson, J. Roques, S. Mukerjee, V.S. Murthi, N.M. Markovic, and V. Stamenkovic, "Activation Energy for Oxygen Reduction on Platinum Alloys: Theory and Experiment," *J. Phys. Chem. B*, **109**, 1198 (2005).

For More Information

Alfred B. Anderson, Chemistry Department, Case Western Reserve University

Email: aba@po.cwru.edu

Activation Energies for Oxygen Reduction on Platinum Alloys: Theory and Experiment

A.B. Anderson¹, J. Roques¹, S. Mukerjee², V.S. Murthi², N.M. Markovic³, and V. Stamenkovic³

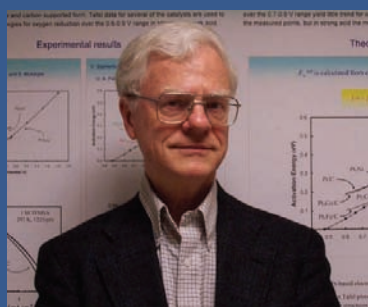
¹Chemistry Department, Case Western Reserve University; ²Chemistry Department, Northeastern University; ³Materials Science Division, Lawrence Berkeley National Laboratory, University of California

We present a quantum chemical and experimental analysis of the electrode-potential dependencies of activation energies for the first step in oxygen reduction over platinum and platinum-alloy catalysts in both polycrystalline and carbon-supported form. Tafel data for several of the catalysts are used to predict potential-dependent activation energies for oxygen reduction over the 0.6-0.9 V range in acid. Comparisons with the theoretical curve show good agreement above 0.8 V, suggesting a fairly constant pre-exponential factor. Arrhenius determinations of activation energies over the 0.7-0.9 V range for strong acid trend with the potential, as predicted by theory. These combined results provide strong support that, during the four-electron reduction of O₂ to H₂O on fuel-cell platinum cathodes, the first electron-transfer step has the highest activation energy.

Determining the compositions and structures of electrocatalyst surfaces and the mechanisms and kinetic parameters of reactions occurring on them are goals at the frontier of the field of electrochemistry. In this study, we found that measured kinetic results for oxygen reduction on unsupported polycrystalline platinum and platinum alloy (Pt₃M) electrodes and on carbon-supported nanoclusters are quite similar. The similarity is justified theoretically with a simple local reaction center model for the first reduction step, which involves just two Pt atoms.

For the unsupported electrodes studied by the Lawrence Berkeley National Laboratory (LBL) group, surface compositions were determined using low-energy ion-scattering (LEIS) spectroscopy. The group found that the annealed electrodes were covered with a Pt skin. Supported nanoclusters studied by the Northeastern University group were characterized using x-ray diffraction (XDS), x-ray absorption near edge fine structure (XANES), and extended x-ray absorption fine structure (EXAFS) spectroscopies at beamline X11A. That group determined, respectively, nanocatalyst particle sizes, atomic ratio, and atom-coordination and nearest-neighbor distances. They found that the particles have average sizes of 2.5 nm for Pt/C, 3.6 nm for PtCo/C, and 3.9 nm for PtFe/C. The XANES and EXAFS results were consistent with Pt₃M alloy composition and the presence of a Pt skin on their surfaces.

Rotating disc electrodes were used to ensure accurate current density measurements at the chosen electrode potentials, and the temperature dependencies yielded Arrhenius activation energies. For all the unsupported polycrystalline electrodes (Pt, sputtered Pt₃Ni and Pt₃Co, and annealed Pt₃Co), activation energies centered on 0.24 eV ± 0.025 eV and did not demonstrate a dependence on potential, the results being the same as earlier studies of supported nanoparticles at LBL. In its measurements of supported nanoclusters, the Northeastern group was able to reduce the uncertainties in activation energies to about 0.02 eV for Pt/C and 0.005 eV for PtCo/C. For PtFe/C the uncertainties were the same as in the LBL measurements. The Northeastern activation energies for Pt/C and PtCo/C displayed the same trend as the theoretically



Alfred Anderson

predicted electrode potential values, as shown in **Figure 1**. The theoretical values determined using the local reaction center model electron transfer theory developed at Case Western Reserve University (Case) are systematically about 0.1 eV smaller than the Arrhenius values, for unknown reasons.

We then took the Arrhenius/Tafel expression

$$\log[i(U)] = \log(A) - E_a(U)/(2.3026RT)$$

where i is the kinetic current density, A is the preexponential factor, U is the potential, and E_a is the activation energy, and determined the A values by fitting one of the experimental E_a values. With the A values, we used the above equation to calculate activation energies, as shown in **Figure 2**. The trends in E_a vs. U over the 0.8 V – 0.95 V range are in good agreement with the trend predicted at Case.

The overall agreement between the theoretical predictions and the measured current densities suggest that (i) the first electroreduction step, forming adsorbed OOH, is the rate-limiting step; and (ii) the active catalyst sites for the various catalyst systems are similar, and the presence of alloying atoms adjacent to the active site does not dramatically affect the activation energy. The ability to calculate qualitative apparent activation energies as functions of electrode potential from the Tafel plot data suggests that the surface density of active sites may remain fairly constant over the 0.8 to 0.95 V range on each of the catalysts.

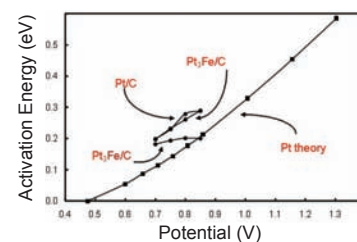


Figure 1. Experimental activation energies at different electrode potentials (SHE) for carbon-supported Pt, Pt₃Co, and Pt₃Fe in 1M CF₃SO₃H.

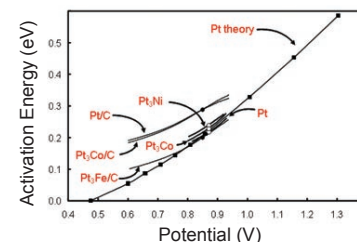


Figure 2. Calculated activation energies at different electrode potentials (SHE) determined from Tafel plots data. Open circles are for unsupported electrodes at LBL and filled circles are for supported nanoparticles at Northeastern.

BEAMLINE X20C

Funding

IBM Research; U.S. Department of Energy

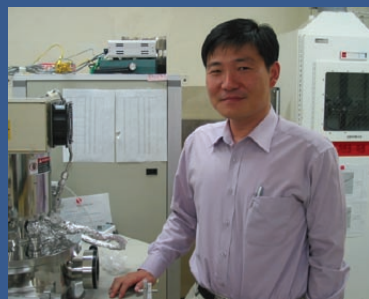
Publication

H. Kim, C. Detavernier, O. van der Straten, S.M. Rossnagel, A.J. Kellock, and D.-G. Park, "Robust TaN_x Diffusion Barrier for Cu Interconnect Technology with Sub-Nanometer Thickness by Metal Organic Plasma-Enhanced Atomic Layer Deposition," *J. Appl. Phys.*, **98**, 14308 (2005).

For More Information

Hyungjun Kim, Dept. of Materials Science and Engineering, Pohang University of Science and Technology, Rep. of Korea

Email: hyungjun@postech.ac.kr



Hyungjun Kim

Robust TaN_x Diffusion Barrier for Cu Interconnect Technology with Sub-Nanometer Thickness by Metal Organic Plasma-Enhanced Atomic Layer Deposition

H. Kim¹, C. Detavernier², O. van der Straten², S.M. Rossnagel², A.J. Kellock³, and D.-G. Park⁴

¹Department of Materials Science and Technology, Pohang University of Science and Technology, South Korea; ²IBM T.J. Watson Research Center; ³IBM Almaden Research Center; ⁴IBM Microelectronics Division

TaN_x diffusion barriers with good barrier properties at sub-nanometer thickness were deposited by plasma-enhanced atomic layer deposition (PE-ALD) from pentakis(dimethylamino)Ta. A hydrogen and/or nitrogen plasma was used as the reactant, producing TaN_x thin films with different nitrogen content. The film properties, including the carbon and oxygen impurity content, were affected by the nitrogen flow during this process. The film, deposited using the hydrogen-only plasma, forms nanocrystalline grains while an amorphous structure was obtained by using the nitrogen plasma. The diffusion-barrier properties of deposited TaN films, as for Cu interconnects, have been studied using thermal stress tests based upon synchrotron x-ray diffraction. The results indicate that the PE-ALD TaN films are good diffusion barriers even at thicknesses as small as 0.6 nm. Better diffusion barrier properties were obtained for films with higher nitrogen content. Based on a diffusion kinetics analysis, the nanocrystalline microstructure of the films was responsible for the better diffusion barrier properties compared to polycrystalline PE-ALD TaN films deposited from TaCl₅.

Among the key materials used for today's semiconductor processing, thin films of inert, refractory materials are expected to be used continuously in Cu interconnect applications, such as diffusion barriers and seed and adhesion layers, as well as for potential front-end applications, such as contacts or gate metalization. With the scaling down of these devices, atomic layer deposition (ALD) has been spotlighted due to its ability to produce highly conformal films. The use of a metal organic (MO) precursor for diffusion-barrier ALD has the benefit of producing a chlorine-free diffusion barrier. However, the diffusion-barrier properties of MO-based ALD TaN layers for Cu interconnects were not studied systematically.

In this study, we have developed a metal organic PE-ALD method for depositing TaN thin films from pentakis(dimethylamino)Ta (PDMAT) using nitrogen and hydrogen plasmas as the reactants. A solid PDMAT (powder) source contained in a glass tube was used as a metal precursor. Atomic hydrogen and activated N₂ were generated by a quartz tube connected to the sample chamber via a gate valve, and hydrogen and nitrogen gases were supplied via a leak valve. For Cu diffusion-barrier measurements, a 200 nm Cu layer (created via physical vapor deposition (PVD)) was deposited on top of the PE-ALD TaN layer, without breaking the vacuum, using a UHV (ultra high vacuum) sputtering system with a power level of 1 kW (dc). A SiO₂ buffer layer placed between the poly-Si layer and Si (100) substrate was used on the other samples to electrically isolate the Si(100) substrate during the sheet-resistance analysis.

Copper diffusion-barrier failure was studied using three different in situ techniques, including synchrotron x-ray diffraction (XRD), optical scattering, and sheet resistance measurements, conducted simultaneously, while the samples were annealed at a temperature ramp rate of 3 °C/s from 100 to 1000 °C in a He environment. The analysis was completed at National Synchrotron Light Source beamline X20C.

Figure 1 shows the synchrotron XRD contour map for MO PE-ALD TaN films of three different thicknesses — 3 nm, 0.6 nm, and 0.3 nm — that were all grown with hydrogen plasma. For the 3 nm thick film, the Cu 111 peak begins to disappear at about 750 °C, indicating the good diffusion-barrier property of the MO PE-ALD TaN film. Even after decreasing the thickness to 0.6 nm, the Cu 111 peak begins to disappear at temperatures higher than 700 °C. Thus, the thermal diffusion-barrier properties of MO PE-ALD TaN films are excellent even at sub-nanometer thicknesses. Only for film thicknesses smaller than 0.3 nm, where the film is only a couple of monolayers thick, does the Cu silicide formation occur at a temperature below 500 °C. Even for this ultra-thin film, however, most of the Cu layer stays intact, judging from the observation that the Cu 111 peak intensity remains high up to 720 °C. Thus, we can conclude that the formation of silicide occurs locally (where the TaN film is not formed evenly). The barrier-failure temperatures for MO PE-ALD TaN layers, obtained from Figure 1, are represented in **Figure 2**. The barrier-failure temperatures increase with increasing thickness. For comparison, the previously reported barrier-failure temperatures for PE-ALD TaN films from TaCl₅ and a hydrogen and nitrogen mixture with stoichiometric composition, which were analyzed using exactly the same conditions, are also shown. From the microstructure analysis, done via XRD and transmission electron microscopy (TEM), the good diffusion barrier property of MO PE-ALD TaN is due to the amorphous microstructure of the film. In this sense, PE-ALD films with engineered microstructures and compositions are very promising barriers in the near-future integration of Cu interconnect technology.

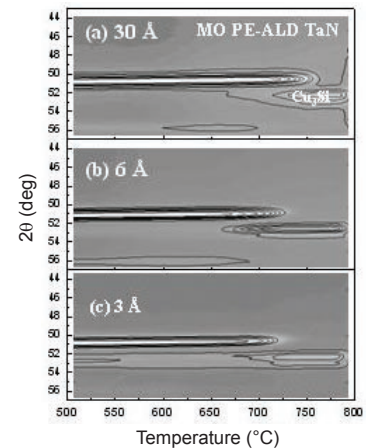


Figure 1. Synchrotron x-ray diffraction analysis as a function of annealing temperature for a 200 nm PVD Cu/ MO PE-ALD TaN/poly-Si test structure with TaN thicknesses of (a) 3 nm, (b) 0.6 nm, and (c) 0.3 nm. The samples were annealed at 3 °C/s from 100 to 1000 °C in forming gas.

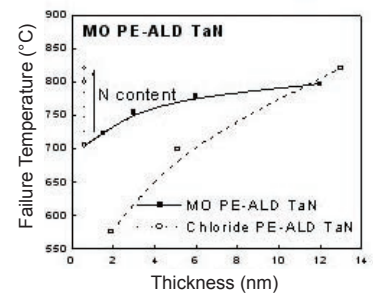


Figure 2. Barrier-failure temperatures determined using synchrotron x-ray diffraction analysis for MO PE-ALD TaN (black squares) and chloride PE-ALD Ta (open circles). Also shown are the failure temperatures of 0.5 nm MO PE-ALD TaN_x deposited at different nitrogen plasma conditions (open squares).

BEAMLINE X3A1

Funding

Max Planck Society (Germany)

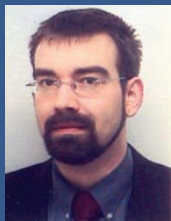
Publication

A. Reich, M. Panthöfer, H. Modrow, U. Wedig, and M. Jansen, "The Structure of $Ba@C_{74}$," *J. Am. Chem. Soc.*, **126** (44), 14428-14434 (2004).

For More Information

Martin Jansen, Max Planck Institute for Solid State Research, Germany

Email: M.Jansen@fkf.mpg.de



(Authors left to right) (top) Martin Jansen, Andreas Reich, (middle) Hartwig Modrow, Martin Panthöfer, and (bottom) Ulrich Wedig

The Structure of $Ba@C_{74}$

A. Reich¹, M. Panthöfer¹, H. Modrow², U. Wedig¹, and M. Jansen¹

¹Max Planck Institute for Solid State Research, Germany; ² Institute of Physics of the University of Bonn, Germany

For the first time, the structure of a monometallofullerene has been analyzed using single-crystal synchrotron diffraction on microcrystals of $Ba@C_{74}\cdot Co(OEP)\cdot 2C_6H_6$ (where $Co(OEP)$ is cobalt(II)-octaethylporphyrin) at 100 K. This monometallofullerene exhibits a high degree of localization of its endohedral metal ion, with just two split positions for barium and two orientations for the C_{74} cage. The crystal structure consists of complex units $(Ba@C_{74})[Co(OEP)]_2(Ba@C_{74})$ arranged in a distorted, primitive hexagonal packing. Despite the disorder still present, we have derived a consistent and conclusive structure model for the title compound by employing a combination of x-ray diffraction, x-ray absorption near-edge structure (XANES) spectroscopy, and quantum chemical calculations.

Since the discovery of fullerenes, information about the molecular and electronic structure of this new family of carbon allotropes, which include "endohedral" metallofullerenes (those with metal atoms inside the fullerene cage) and fullerene compounds, has been essential for understanding their physical and chemical properties. To acquire such information, the availability of precise crystal structure data is a crucial prerequisite.

In ongoing research efforts, we have developed a method that allows a high-yield synthesis of small and mid-sized endohedral fullerenes consisting of divalent metals that follow $M@C_m$ (where $m = 60, 70, 72, 74, 76$; $M = Ca, Sr, Ba, Eu$). In this method, we inductively heat graphite and the corresponding metal inside a radiofrequency field to temperatures of up to 3000 K (**Figure 1**), and then isolate individual species from the raw soot extracts using multi-step high-performance liquid chromatography (HPLC).

By employing micro-crystal synchrotron diffraction techniques, computational chemistry, and XANES spectroscopy in a synergetic manner, we were able to determine the structure of $Ba@C_{74}$ as a co-crystallizate with Co-octaethylporphyrin ($Co(OEP)$) and C_6H_6 (benzene). The crystal structure of $Ba@C_{74}\cdot Co(OEP)\cdot 2C_6H_6$ consists of complex units $(Ba@C_{74})[Co(OEP)]_2(Ba@C_{74})$ exhibiting a back-to-back orientation of two $Co(OEP)$ molecules, each coordinating one $Ba@C_{74}$ molecule (**Figure 2**). The overall structure may be regarded as a distorted, primitive hexagonal packing of these complex units. Yet, the fullerene substructure is disordered, with two orientations for the C_{74} cage and two positions for the barium atom. Thus, four different barium-to- C_{74} coordination schemes have to be discussed. Out of those, two are similar to those found from the results of the quantum-chemical investigations. Yet, the shortest Ba-C distances do not correspond to the central 6:6 bond of a pyracylene unit located at one of the three pockets of the cloverleaf-shaped C_{74} molecule, but to its vicinity.

As stated above, computational investigations on $Ba@C_{74}$ show that the local minimum structure of $Ba@C_{74}$ corresponds to a three-fold degenerate arrangement with barium located in one of the three pockets of C_{74} , coordinating to the central 6:6 pyracylene bond. Remarkably, the molecular structure of the neutral C_{74} cage in $Ba@C_{74}$ differs only slightly from the molecular structure

of a C_{74}^{2-} dianion (both determined using the density-functional theory in local-density approximation). Those differences are highly localized in the central 6:6 bond of the pyracylene units.

This discrepancy between the results of the experimental and the computational investigations is clearly due to the intermolecular interactions present in the co-crystallizate. On one hand, those $Co(OEP)-Ba@C_{74}$ configurations that result in a large contact surface between the two molecules allow attractive $\pi-\pi$ and dispersion interactions. On the other hand, configurations where the pyracylene unit at the pocket of $Ba@C_{74}$ is pointed towards the Co-atom of the $Co(OEP)$ molecule allow stabilization via multipole-multipole interactions. The competition between these two different intermolecular interactions triggers the orientational disorder of the C_{74} cage. Furthermore, molecular dynamics simulations reveal a nearly flat potential hypersurface around the local minima positions within the pocket of the cloverleaf-shaped molecule. This suggests an easy displacement of the Ba atom near a minimum that is produced by a direct interaction between the Ba^{2+} cation and the $Co(OEP)$ molecule. Thus, the positional disorder of the barium atom is a consequence of the orientational disorder of the C_{74} cage, which is due to the competition of $\pi-\pi$ and electrostatic interactions.



Figure 1. The radio-frequency furnace for endohedral fullerene synthesis in action.

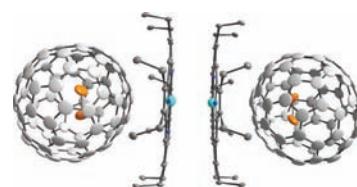


Figure 2. A $(Ba@C_{74})[Co(OEP)]_2(Ba@C_{74})$ unit in $Ba@C_{74} \cdot Co(OEP) \cdot 2C_6H_6$ (for clarity, only one fullerene orientation is given).

BEAMLINES U10A, U13UB**Funding**

U.S. Department of Energy

Publication

S.V. Dordevic *et al.*, "Extracting the Electron-Boson Spectral Function $\alpha^2F(\omega)$ from Infrared and Photoemission Data using Inverse Theory", *Phys. Rev. B*, **71**, 104529 (2005).

For More Information

Sasa V. Dordevic, Department of Physics,
The University of Akron

Email: sasha@physics.uakron.edu



Sasa Dordevic

The Electron-Boson Spectral Function $\alpha^2F(\omega)$ of High- T_c Superconductors

S.V. Dordevic¹, C.C. Homes¹, J.J. Tu¹, T. Valla¹, M. Strongin¹, P.D. Johnson¹, G.D. Gu¹, and D.N. Basov²

¹Department of Physics, Brookhaven National Laboratory; ²Department of Physics, University of California, San Diego

We have developed and implemented a new numerical procedure for extracting electron-boson spectral functions from infrared (IR) and angle-resolved photoemission spectroscopy (ARPES) data. The new method is based on inverse theory and has numerous advantages over previously employed procedures. Using this new method we have calculated the electron-boson spectral functions of high-critical-temperature (high- T_c) cuprates, from both IR and ARPES data obtained at the NSLS. The spectral functions have a characteristic shape, dominated by a pronounced peak at low energies and a significant contribution at higher energies.

The nature of the collective boson mode responsible for superconductivity in the cuprate family of high-critical-temperature (high- T_c) superconductors is currently the center of great controversy in the field. Two opposing views have been battling for supremacy. The older scenario, dating back to the early 90s, argues for spin-fluctuations as the pairing glue for high- T_c superconductivity. More recently, phonons have been put forward as possible mediators for superconductivity in the cuprates.

The physical quantity that characterizes coupling between charge carriers and collective bosonic modes is a so-called Eliashberg electron-boson spectral function $\alpha^2F(\omega)$. It is one of the most important characteristics of a boson-exchange superconductor. This function can be obtained from tunneling, photoemission (ARPES), or infrared (IR) spectroscopy. However, the process of obtaining $\alpha^2F(\omega)$ is nontrivial because $\alpha^2F(\omega)$ is convoluted in the experimental data. For example, in the IR case the celebrated Allen result relates $\alpha^2F(\omega)$ to the experimentally accessible quasiparticle scattering rate $1/\tau(\omega)$ through an integral relation:

$$\frac{1}{\tau(\omega)} = \frac{2\pi}{\omega} \int_0^{\infty} (\omega - \Omega) \alpha^2F(\Omega) d\Omega. \quad (\text{Equation 1})$$

We have recently developed a new numerical procedure for extracting $\alpha^2F(\omega)$ based on a mathematical procedure called inverse theory. The method uses a so-called singular value decomposition (SVD) of matrices and has numerous advantages over previously employed procedures. For example, the inversion can be performed not only at $T = 0$ K but also at higher temperatures, the effect of the superconducting energy gap can be taken into account, and the numerical error can be controlled. Using this new procedure we have re-analyzed our IR and ARPES data on several families of cuprate data, part of which were obtained on NSLS beamlines U10A and U13UB.

Figure 1 displays inversion calculations on IR data at 10 K for underdoped $\text{YBa}_2\text{Cu}_3\text{O}_{6.6}$ (YBCO) with $T_c = 59$ K. The right panels show scattering-rate data (green lines) and the left panels present the calculated spectral function $\alpha^2F(\omega)$ (blue lines). The right panels also show the scattering rate $1/\tau_{\text{cal}}(\omega)$ (red lines) calculated from the corresponding spectral function on the left. Different panels display inversion results with different levels of smoothing, i.e.

different levels of error. The spectral function has a characteristic shape, with a pronounced peak in the far-IR followed by a strong dip and a significant contribution at higher frequencies. The peak is believed to originate from the coupling of charge carriers to the so-called (π, π) -resonance observed in neutron-scattering experiments. More recently, phonons have been advocated as an alternative explanation.

Similar numerical procedures can also be applied to ARPES. **Figure 2** displays inversion calculations of ARPES data of optimally doped $\text{Bi}_2\text{Sr}_2\text{CaCu}_2\text{O}_{8+\delta}$ (BSCCO) with $T_c = 92$ K obtained at beamline U13UB. The top panels display data in the normal state (above T_c), whereas the bottom panels display the data in the superconducting state. The right panels are measured quasiparticle dispersions (red dots) and the left panels are calculated $\alpha^2F(\omega)$ values. The right panels also show calculated spectral functions (green lines).

The importance of this new numerical procedure goes beyond high- T_c superconductors, IR, and ARPES. Similar numerical procedures can be applied to conventional superconductors, as well as to other experimental methods whose data can be described by an integral equation similar to **Equation 1**.

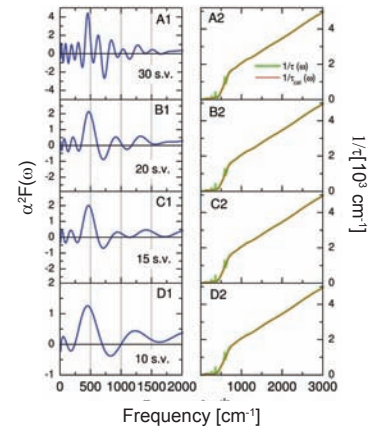


Figure 1. Spectral function $\alpha^2F(\omega)$ for underdoped $\text{YBa}_2\text{Cu}_3\text{O}_{6.6}$ with $T_c = 59$ K. The left panels show $\alpha^2F(\omega)$ and the right panels show the experimental $1/\tau(\omega)$ along with $1/\tau_{\text{cal}}(\omega)$ calculated from the corresponding spectral function on the left. The level of smoothing is easily controlled by the new inversion procedure.

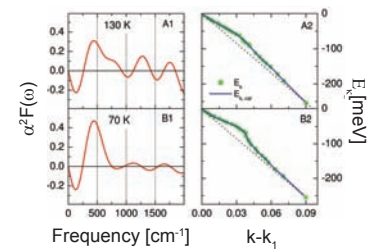


Figure 2. The spectral function $\alpha^2F(\omega)$ of optimally doped BSCCO with $T_c = 92$ K, extracted from ARPES data. The left panels show $\alpha^2F(\omega)$ spectra and the right panels show the ARPES quasiparticle dispersion E_k (green circles) and calculated dispersion $E_{k,\text{cal}}$ (blue lines).

BEAMLINE X16C

Funding

U.S. Department of Energy; Israel Science Foundation; U.S.-Israel Binational Science Foundation

Publication

A.I. Frenkel, *et al.*, "Microscopic Origin of Polarity in Quasi-Amorphous BaTiO₃," *Phys. Rev. B*, **71**, 024116 (2005).

For More Information

Anatoly I. Frenkel, Physics Department, Yeshiva University

Email: Anatoly.Frenkel@yu.edu



Anatoly Frenkel

Microscopic Origin of Polarity in Quasi-Amorphous BaTiO₃

A.I. Frenkel¹, Y. Feldman², V. Lyahovitskaya², E. Wachtel², and I. Lubomirsky²

¹Yeshiva University; ²Weizmann Institute of Science

The recent demonstration of pyroelectricity in quasi-amorphous thin films of BaTiO₃ introduced a new type of material: non-crystalline polar ionic solids. To elucidate the origin of polarity in this system we investigated its local bonding environment using the x-ray absorption near-edge structure (XANES) and extended x-ray absorption fine structure (EXAFS) techniques. We found that the local bonding unit of TiO₆ octahedra is identical in amorphous (as-deposited, non-polar), quasi-amorphous (non-crystalline, polar), and crystalline (highly polar) BaTiO₃. The TiO₆ octahedra are distorted due to the off-center displacement of the Ti ion; therefore, these octahedra have a local dipole moment. This implies that the macroscopic dipole moment in the quasi-amorphous films is the result of the partial alignment (<5%) of the TiO₆ octahedra.

A group from the Weizmann Institute of Science, led by Igor Lubomirsky, recently synthesized a new type of amorphous ionic solid that is polar but lacks long-range order. Radio frequency magnetron-sputtered BaTiO₃ thin films (100-180 nm) on Si (100) are pulled through a temperature gradient with a peak temperature of 600 °C. The resulting non-crystalline but pyroelectric and, therefore, polar phase was named "quasi-amorphous," in contrast to the as-deposited amorphous phase that is neither pyroelectric nor piezoelectric and, therefore, non-polar. A collaboration between Yeshiva University's Anatoly Frenkel and Lubomirsky's group investigated the origin of polarity in this new type of material. Another objective of their investigation was to find out whether the local dipoles responsible for the polarity of the quasi-amorphous BaTiO₃ had already existed in the as-deposited films, or if they were formed during the temperature-gradient step.

Ti K-edge XANES and EXAFS were the techniques of choice due to their sensitivities to the short-range ordering around Ti atoms. In addition to the as-deposited and quasi-amorphous films, we also studied the partially crystallized films prepared by isothermally annealing the as-deposited films. The XANES data features the peak A located at 4967 eV, the region corresponding to the 1s-3d transition, which is dipole-forbidden in the atom by the $\Delta L = 1$ selection rule (**Figure 1**). In order to contribute significantly to XANES data in this range of energies, the final state of the photoelectron must have some p-like character in the solid, via a hybridization of the Ti 3d and O 2p orbitals and the concomitant displacement of the Ti atom away from the TiO₆ octahedra's center of inversion symmetry. Both the height and position of the pre-edge feature, A, are directly related to the degree of p-d mixing and, therefore, to the coordination geometry and oxidation state of Ti. The majority of Ti atoms were found to be in an octahedral environment in all samples (**Figure 2**). This result was independently confirmed by the EXAFS data (the first shell signals in all the data were identical), which implies that the local environment of the Ti⁴⁺ ion did not undergo detectable changes during the transformation of the amorphous (non-polar) phase into the quasi-amorphous (polar) phase (**Figure 3**) and that it was octahedral in both cases.

As shown by Krayzman et al, the area under the peak A is a measure of the displacement (d) of the Ti ion from the center of the TiO₆ octahedron: $A \sim d^2$.

The strength of the local dipole moment is proportional to d and can therefore be measured in the XANES experiment. We obtained the values of d in all samples and found that they exceeded that of bulk BaTiO_3 (0.23 Å), the amorphous and quasi-amorphous samples being the most distorted (0.45 Å).

Preservation of the local bonding unit in amorphous BaTiO_3 implies that the formation of the macroscopic dipole moment (polarity) in the quasi-amorphous material occurs via the partial alignment of the TiO_6 octahedra in the temperature gradient. The degree of alignment, estimated from the magnitude of the pyroelectric effect, is below 5%, which indicates that even a relatively small deviation from the random orientation of local dipoles may lead to macroscopic dipole moments, comparable to those observed in pyroelectric crystals. This was confirmed experimentally by polarized XANES measurements in quasi-amorphous films oriented at different angles with respect to the incident x-ray beam. The anisotropy of Ti-atom displacements in the in- and out-of-film plane directions was found to be less than 5%.

The origin of polarity in quasi-amorphous BaTiO_3 is caused by 1) the existence of large off-center displacements of the Ti atoms within relatively stable TiO_6 local bonding units; 2) their weak orientational order, generated by the gradient of mechanical strain produced in the temperature gradient; and 3) the electric field resulting from the concomitant flexoelectric effect. Therefore, the quasi-amorphous films can be viewed as being analogous to a poorly aligned nematic liquid crystal. These results imply that, under similar conditions, it may be possible to align and/or manipulate polar local bonding units (for instance, in TiO_4 , TiO_6 , NbO_4 , NbO_6 , or VO_6) to create other quasi-amorphous materials, which will similarly possess an unusual combination of properties, such as polarity in the absence of crystallinity.

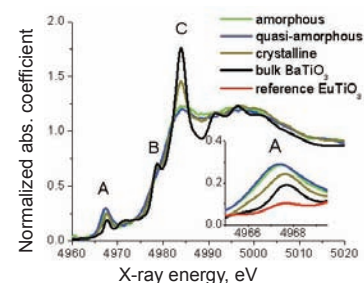


Figure 1. XANES spectra of as-deposited amorphous, quasi-amorphous, and crystalline films. The data for bulk BaTiO_3 and a sample of EuTiO_3 are given for comparison. The feature A (insert) is affected by the size of Ti displacements that range from small and dynamic (as in cubic EuTiO_3) to large and static (as in BaTiO_3).

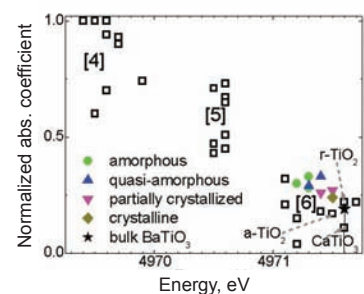


Figure 2. Intensities and positions of XANES feature A in four-, five-, and six-fold coordinated Ti in different reference compounds (hollow squares) and in our BaTiO_3 films (color symbols).

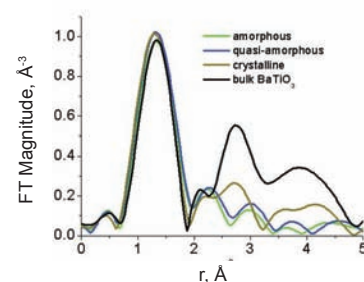


Figure 3. EXAFS data in r -space of the amorphous, quasi-amorphous, crystalline, and bulk BaTiO_3 samples.

BEAMLINE X7A**Funding**

National Science Foundation; U.S. Department of Energy Division of Materials Sciences & Division of Chemical Sciences

Publication

M.K. Crawford, R.L. Harlow, S. Deemyad, V. Tissen, J.S. Schilling, E.M. McCarron, S.W. Tozer, D.E. Cox, N. Ichikawa, S. Uchida, and Q. Huang, "High-Pressure Study of Structural Phase Transitions and Superconductivity in $\text{La}_{1.48}\text{Nd}_{0.4}\text{Sr}_{0.12}\text{CuO}_4$," *Phys. Rev. B*, **71**, 104513 (2005).

For More Information

Michael K. Crawford, Central Research and Development, DuPont Company

Email: michael.k.crawford@usa.dupont.com



Authors (from left) Richard Harlow and Michael Crawford

High Pressure Study of Structural Phase Transitions and Superconductivity in $\text{La}_{1.48}\text{Nd}_{0.4}\text{Sr}_{0.12}\text{CuO}_4$

M.K. Crawford¹, R.L. Harlow¹, S. Deemyad², V. Tissen², J.S. Schilling², E.M. McCarron¹, S.W. Tozer³, D.E. Cox⁴, N. Ichikawa⁵, S. Uchida⁵, and Q. Huang⁶

¹DuPont Co.; ²Washington University; ³National High Magnetic Field Laboratory; ⁴Brookhaven National Laboratory; ⁵University of Tokyo, Japan; ⁶National Institute of Standards & Technology Center for Neutron Research

We have determined the crystal structures and superconducting transition temperatures of $\text{La}_{1.48}\text{Nd}_{0.4}\text{Sr}_{0.12}\text{CuO}_4$ under nearly hydrostatic pressures in diamond anvil cells to 5.0 GPa and 19.0 GPa, respectively. Synchrotron x-ray powder diffraction measurements were used to establish the material's pressure-temperature structural phase diagram. Under pressure the superconducting transition temperature (T_c) increases rapidly from $T_c \approx 3$ K to a maximum value of 22 K at 5 GPa, a pressure slightly greater than required to stabilize the undistorted I4/mmm structure in the superconducting state.

Superconductivity is among the most remarkable physical phenomena discovered during the 20th century. Although the famous Bardeen-Cooper-Schrieffer theory of superconductivity can explain most experimental observations for conventional superconductors, the high-temperature superconducting cuprates have yet to be completely understood in a similar way.

Perhaps the simplest superconducting cuprates are based upon the parent compound lanthanum cuprate (La_2CuO_4), whose structure is shown in **Figure 1**. This material, when doped with increasing amounts of alkaline-earth ions such as Sr^{2+} (i.e. $\text{La}_{2-x}\text{Sr}_x\text{CuO}_4$), transforms from a Mott insulator to a metal, and then superconducts with a critical temperature (T_c) as high as 38 K when $x = 0.15$. Lanthanum cuprates for which some of the La^{3+} is replaced with both Sr^{2+} and Nd^{3+} (i.e. $\text{La}_{2-x-y}\text{Nd}_y\text{Sr}_x\text{CuO}_4$) exhibit structural phase transitions involving tilts of the CuO_6 octahedra (**Figure 1**) that strongly suppress T_c . The suppression of T_c is most pronounced when the Sr^{2+} doping, x , is 1/8. These structural phase transitions are sensitive to external parameters such as pressure and temperature, and thus it is interesting to observe the effect of applied pressure at various temperatures upon the structure (and superconductivity) of these materials. Here we describe a set of x-ray powder diffraction experiments conducted for that purpose at beamline X7A.

The x-ray powder sample of composition $\text{La}_{1.48}\text{Nd}_{0.4}\text{Sr}_{0.12}\text{CuO}_4$ was immersed in a 4:1 ethanol:methanol mixture within a Merrill-Bassett diamond anvil cell that was then mounted in a displac closed-cycle refrigerator. A position-sensitive detector was used to detect the scattered x-rays of wavelength near 0.7 Å (energy of about 17 keV). Pressures were measured using laser-excited fluorescence from small ruby chips placed inside the diamond anvil cells, as well as by measurements of the lattice parameters of small quantities of NaCl or CaF_2 also included in the cells.

In **Figure 2** we show two typical x-ray diffraction patterns, obtained at pressures of 2.2 and 4.2 GPa, for a sample of composition $\text{La}_{1.48}\text{Nd}_{0.4}\text{Sr}_{0.12}\text{CuO}_4$. In **Figure 3** we show the structural phase diagram for this material (based upon the x-ray data), compared with the superconducting transition temperature, as a function of pressure. At ambient pressure this material has a low superconducting $T_c \approx 3$ K associated with the low-temperature tetragonal (LTT) structure and the special Sr^{2+} concentration of $x = 1/8$. Under pressure the LTT phase is first

replaced by the low-temperature orthorhombic LTO2 phase, then at pressures above 4.0 GPa the high-temperature tetragonal (HTT) structure remains stable to $T = 10$ K. The superconducting transition temperature increases dramatically under pressure and reaches a maximum value of $T_c = 22$ K near 5.0 GPa, coincident with the appearance of the undistorted HTT phase.

The results we describe here have implications for the presence of charge ordering in cuprates. The LTT structure of $\text{La}_{1.48}\text{Nd}_{0.4}\text{Sr}_{0.12}\text{CuO}_4$ was the first cuprate shown to exhibit *static* one-dimensional charge and spin stripes (in experiments performed at the High Flux Beam Reactor at Brookhaven National Laboratory by Tranquada, Axe, and coworkers). This observation provided an explanation for the previously known suppression of superconductivity in this material at 1/8 doping: *commensurate one-dimensional static charge and spin stripes compete with superconductivity*. Pressure is a convenient way to change the structure at constant chemical composition, and it is clear from our results that superconductivity is strongly enhanced by suppressing the structural phase transitions in $\text{La}_{1.48}\text{Nd}_{0.4}\text{Sr}_{0.12}\text{CuO}_4$. This observation suggests that the static charge and spin order is also eliminated by pressure. However, recent scanning tunneling microscope studies of other tetragonal cuprates in which the copper-oxygen planes are flat, as they are in the HTT structure of $\text{La}_{1.48}\text{Nd}_{0.4}\text{Sr}_{0.12}\text{CuO}_4$, have shown the presence of *two-dimensional* charge order. One way to reconcile these observations is to assume that the charge and spin order are one-dimensional in the LTT and LTO2 structures, but become two-dimensional in the HTT and LTO1 structures, with the latter situation more favorable toward superconductivity. This scenario would be consistent with the accumulating evidence for both one-dimensional and two-dimensional charge and spin order in the cuprates. Our results explicitly illustrate the impact of subtle changes of crystal structure upon superconductivity, and by implication upon charge and spin order, in these fascinating materials.

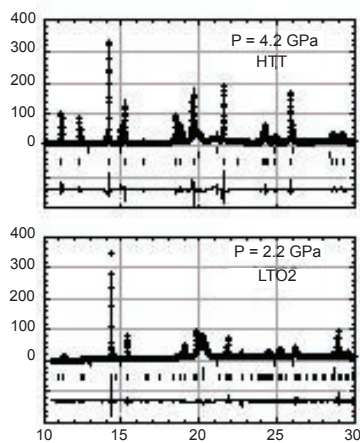


Figure 2. The x-ray powder diffraction patterns and results of General Structure Analysis Structure refinements for $\text{La}_{1.48}\text{Nd}_{0.4}\text{Sr}_{0.12}\text{CuO}_4$ at pressures of 4.2 GPa (top frame) or 2.2 GPa (bottom frame), at a temperature of 10 K. In the upper trace for each frame the crosses are the data, and the solid line is the calculated pattern; the lowest trace is the residual. The vertical tick marks are located at the positions of (top) NaCl included in the diamond anvil cell as an internal manometer, (middle) Fe due to the diamond anvil cell gasket, and (bottom) $\text{La}_{1.48}\text{Nd}_{0.4}\text{Sr}_{0.12}\text{CuO}_4$.

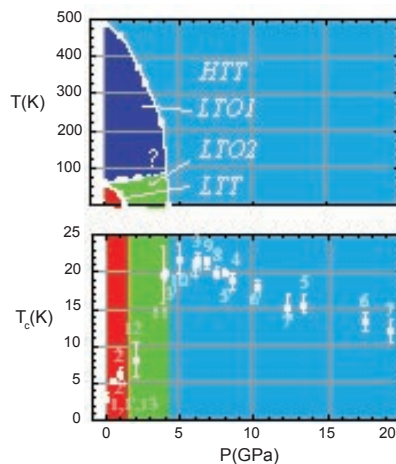


Figure 3. (Top) Pressure-temperature phase diagram for $\text{La}_{1.48}\text{Nd}_{0.4}\text{Sr}_{0.12}\text{CuO}_4$ determined by high-pressure x-ray powder diffraction. (Bottom) Superconducting transition temperature (T_c) versus pressure (P) for $\text{La}_{1.48}\text{Nd}_{0.4}\text{Sr}_{0.12}\text{CuO}_4$. In both frames the LTT phase region is shown in red, the LTO2 region in green, the LTO1 region in dark blue, and the HTT region in light blue.

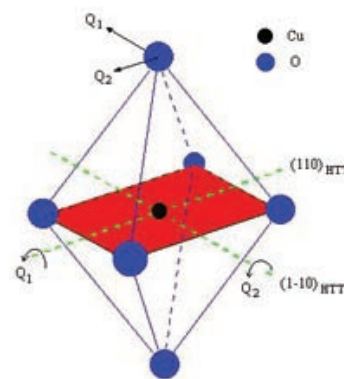
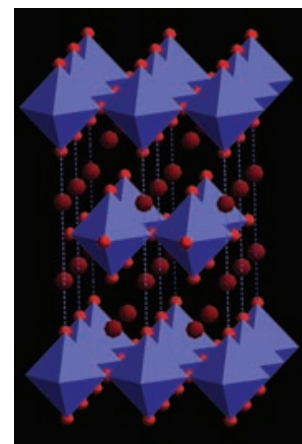


Figure 1. (Top) The crystal structure of La_2CuO_4 , showing the two-dimensional layers of corner-sharing CuO_6 octahedra (blue), the oxygen atoms (light red), and the La atoms (dark red). (Bottom) A schematic view of a single CuO_6 octahedron illustrating the relative orientations of the (110) and (1-10) axes of the HTT structure, for which $|Q_1| = |Q_2| = 0$. The LTO1 structure is obtained by a single rotation of magnitude $|Q_1|$ or $|Q_2|$ about either of these axes (yielding one of the two orthorhombic twin structures). The LTO2 structure is obtained by rotations of magnitude $|Q_1|$ and $|Q_2|$ about both axes (where $|Q_1| \neq |Q_2|$). The LTT structure has rotations of equal magnitude about both axes, $|Q_1| = |Q_2| \neq 0$.

BEAMLINE X19A**Funding**

New Jersey Department of Environmental Protection

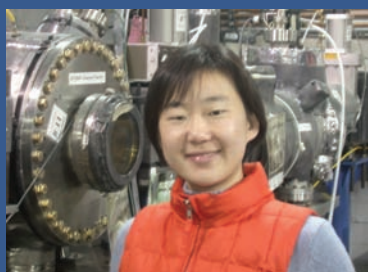
Publication

C. Jing, S. Liu, M. Patel, and X. Meng, "Arsenic Leachability in Water Treatment Adsorbents," *Environ. Sci. and Tech.*, **39**, 5481-5487 (2005).

For More Information

Chuanyong Jing, Center for Environmental Systems, Stevens Institute of Technology

Email: cjing@stevens.edu



Authors (from top) Chuanyong Jing and Suqin Liu

Arsenic Leachability in Water-Treatment Adsorbents

C. Jing¹, S. Liu¹, M. Patel^{1,2}, and X. Meng¹

¹Center for Environmental Systems, Stevens Institute of Technology; ²New Jersey Department of Environmental Protection

At NSLS beamline X19A, we used extended x-ray absorption fine structure (EXAFS) spectroscopy and leaching tests to investigate arsenic (As) leachability in spent water-treatment adsorbents. The EXAFS results indicate that arsenic forms inner-sphere bidentate binuclear surface complexes on the adsorbents, which include granular ferric hydroxide, granular ferric oxide, titanium dioxide, activated alumina, and modified activated alumina. This study improved the understanding of arsenic bonding structures on adsorptive media surfaces and As leaching behavior for different adsorbents.

The U.S. Environmental Protection Agency (EPA) has adopted an arsenic maximum contaminant level (MCL) of 10 µg/L, which will be enforceable as of January 23, 2006. This more stringent arsenic drinking water standard requires the installation of new water-treatment systems and the upgrading of existing ones. Filtering arsenic in water using adsorbents is especially suitable for small community systems and individual homes because the filters do not require much effort to operate. Recently, more effective adsorbent media have been developed and used for arsenic removal. As a result of the enhanced removal efficiency, large amounts of spent media with elevated arsenic content will be generated. Accurately determining the leachability of arsenic in this waste is crucial for both economic concerns and the evaluation of environmental impacts.

In this study, EXAFS spectroscopy at NSLS beamline X19A was employed to determine the arsenic local coordination environment of spent adsorbent media. Spent adsorbents were collected from five pilot-scale filters that were tested for their ability to remove arsenic from groundwater in New Jersey. The spent media included granular ferric hydroxide (GFH), granular ferric oxide (GFO), titanium dioxide (TiO₂), activated alumina (AA), and modified activated alumina (MAA).

The As leachability, determined with the Toxicity Characteristic Leaching Procedure (TCLP), was below 180 µg/L for all spent media. The leachate As concentration in the California Waste Extraction Test (WET) was more than 10 times higher than that in the TCLP, and reached as high as 6650 µg/L in the spent GFH sample. The EXAFS analysis shows that the first and strongest peak in the Fourier transform (FT) curve was contributed by four oxygen atoms at an average As-O distance of 1.69 Å for all five media samples (**Figure 1**). The constant As-O interatomic distance was independent of the media to which the As(V) was adsorbed. The second shell atom (distance) was Fe (3.32 Å), Fe (3.28 Å), Ti (3.27 Å), Al (3.14 Å), and Al (3.13 Å) for GFO, GFH, TiO₂, AA, and MAA, respectively. The EXAFS results show that arsenic formed bidentate binuclear inner-sphere complexes on the surfaces of these five spent adsorbents. This stable structure can be used to explain the high affinity of arsenic for the adsorbent surfaces. The difference in the leachate As concentrations determined with WET and TCLP could be attributed to different acids used in the leaching solutions. An aggressive chelating agent, such as the citric acid used in the WET process, could form soluble complexes with

the adsorbent and release the arsenic. This is especially important for the GFH, which failed in the WET. A moderate organic acid, such as the acetic acid used in the TCLP, could only extract arsenic at a low concentration, less than $180 \mu\text{g L}^{-1}$. However, this kind of organic acid is a relatively stable degradation product of organic matter and is widely available in landfill leachate. Thus, the co-disposal of arsenic containing wastes with municipal solid waste (MSW) may have a potential risk of arsenic re-contamination.

The correlation of the percentage of As leached with the percentage of the adsorbent dissolved for the media is shown in **Figure 2**. The amount of As released was positively related to the amount of adsorbent dissolved in the leachate, which suggests that adsorbent dissolution may be the main mechanism of enhanced As release in the WET.

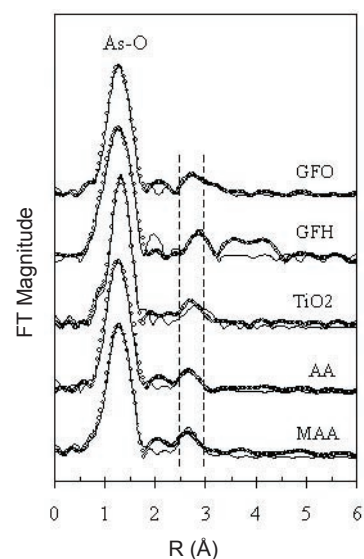


Figure 1. The observed (dotted line) and model calculated (solid line) As K-edge FT EXAFS spectra resulting in a radial distance structure for the spent media. The peak positions are uncorrected for phase shift. Arsenic formed binuclear bidentate surface complexes on the media surface.

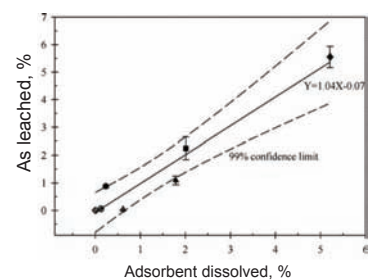


Figure 2. Correlation of percentage As leached and adsorbent dissolution in GFH (\blacklozenge , \blacklozenge), GFO (\bullet , \circ), AA (\blacksquare , \square), and MAA (\blacktriangle , \triangle) for the WET (close) and TCLP (open), respectively. The solid line is the regression and the dashed lines are 99% confidence limits.

BEAMLINES X23A2, X26A

Funding

U.S. Department of Energy

Publication

M.C. Duff, D.B. Hunter, D. T. Hobbs, S.D. Fink, Z. Dai, and J.P. Bradley, "Mechanisms of Strontium and Uranium Removal from High-Level Radioactive Waste Simulant Solutions by the Sorbent Monosodium Titanate," *Environ. Sci. Technol.*, **38**, 5201-5207 (2004).

For More Information

Martine C. Duff, Savannah River National Laboratory

Email: Martine.Duff@srs.gov



Authors (from top) Douglas B. Hunter and Martine C. Duff

Mechanisms of Strontium and Uranium Removal from Radioactive Waste Simulant Solutions by the Sorbent Monosodium Titanate

M.C. Duff¹, D.B. Hunter¹, D.T. Hobbs¹, S.D. Fink¹, Z. Dai², and J.P. Bradley²

¹Savannah River National Laboratory; ²Lawrence Livermore National Laboratory

High-Level Radioactive Waste (HLW) is the priority problem for the U.S. Department of Energy's Environmental Management Program. Current HLW treatment processes at the Savannah River Site (Aiken, SC) include the use of monosodium titanate (MST, similar to $\text{NaTi}_2\text{O}_5 \cdot x\text{H}_2\text{O}$) to concentrate radioactive strontium (Sr) and actinides. Mechanistic information about radionuclide uptake will provide us with insight into the reliability of MST treatments. We characterized the morphology of MST and the chemistry of sorbed Sr^{2+} and uranium [U(VI)] on MST with x-ray based spectroscopic and electron microscopic techniques. Sorbed Sr^{2+} exhibited specific adsorption as partially-hydrated species, whereas sorbed U exhibited site-specific adsorption as monomeric and dimeric U(VI)-carbonate complexes. These differences in site specificity and mechanism may account for the difficulties associated with predicting MST loading and removal kinetics.

High-Level Waste (HLW) is the radioactive waste associated with the dissolution of spent nuclear fuel rods for the recovery of weapons-grade material. At the Savannah River Site (SRS) nearly 130 million liters of HLW await disposal. This waste is highly alkaline and rich in Na^+ , NO_3^- , and NO_2^- . Waste treatment involves concentrating the radionuclides (which consists of mainly ^{90}Sr and the actinides, such as uranium, plutonium, and neptunium) from the waste, and then vitrifying the waste concentrate. Titanate solids, such as monosodium titanate (MST), are chemically stable in high pH solutions, making MST an ideal candidate material for waste treatment.

Our x-ray diffraction studies with MST indicate it is highly amorphous, and scanning electron microscopy reveals that it contains spherical (snowball-like) particles with a typical size range of 5 to 12 μm . Our high-resolution transmission electron microscopy analyses indicate that MST has two prominent morphological populations of titanate material, the first being a very fine fibrous nanocrystalline surficial material, and the second being an amorphous glass-like material (data not shown).

We conducted synchrotron-based x-ray absorption fine structure (XAFS) analyses with Sr- and U-loaded MST that was made by exposing a MST suspension to dissolved Sr and U(VI) (individually) in a HLW simulant solution. Our findings indicate that the sorbed Sr^{2+} and UO_2^{2+} (the uranyl ion) exhibit inner sphere (specific adsorption) sorption behavior with the MST, as opposed to other mechanistic behaviors, such as precipitation, outer sphere adsorption, or structural incorporation with the amorphous MST material (see generalized mechanisms delineated in **Figure 1A-D**).

Our chi XAFS data for the Sr- and U-loaded MST are shown in **Figures 2A and 2B**. The XAFS analyses indicate that the local environment of Sr^{2+} on the MST is partially hydrated (for example, see the spectral comparison with dissolved $\text{SrCl}_{2(s)}$ in **Figure 2A**). However, the XAFS data for the outer shells of the added Sr^{2+} indicate that titanium (Ti) atoms are present at two radial dis-

tances. We conclude that the Sr^{2+} is sorbed as a partially hydrated species that is specifically adsorbed on the MST surface — indicating that specific adsorption is the likely Sr uptake mechanism (as described in **Figure 1C**).

Model fits of the U XAFS data indicate that the sorbed U(VI) has an outer shell environment that is consistent with specifically adsorbed U(VI) carbonato species. The data also indicate that at low U(VI) surface loadings, there is specific adsorption of monomeric U(VI) carbonato species at the MST surface (as shown in **Figure 3A**). At high U(VI) surface loadings, however, there is dimerization of sorbed U(VI) carbonato species at the MST surface (as shown in **Figure 3B**).

These studies that characterized the uptake of U and Sr on MST show that there is a strong interaction between MST and the target solution species. This study improves our understanding of this highly amorphous MST material.

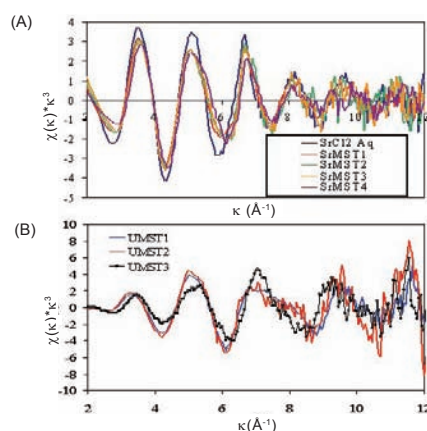


Figure 2. Chi data for (A) Sr (K edge) in the Sr-loaded MST samples and (B) for U (L_3 edge) in the U(VI)-loaded MST samples.

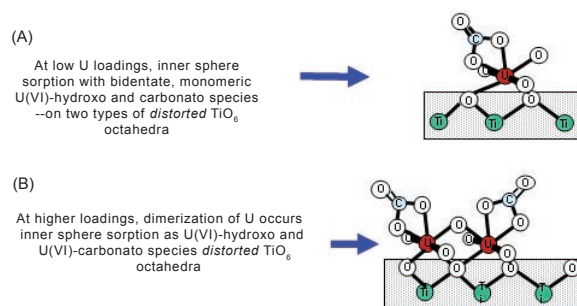


Figure 3. Atom scale pictorial representations of sorbed U(VI) carbonato species on MST at (A) low and (B) high U loadings.

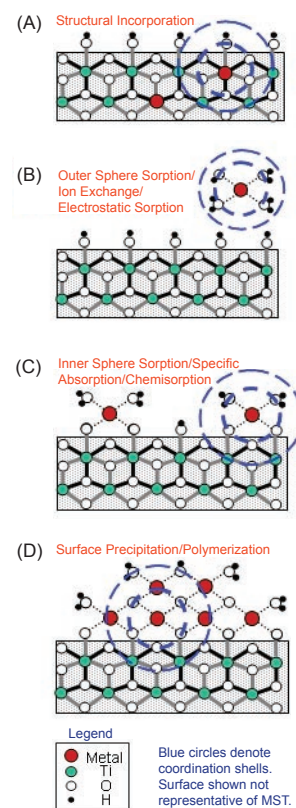


Figure 1. Mechanisms by which metals can interact with a solids shown relative to the type of information that can be obtained with XAFS (such as local structural atom identification, radial distances, and coordination number). (A) Structural incorporation with MST, where the addition of the metal to the MST-containing solution facilitates precipitation and uptake of metals. In this example, the structural environment appears much like the bulk material that is crystallizing. (B) Outer sphere sorption, where the local environment of the sorbed species resembles that of a truly hydrated metal species. (C) Inner sphere sorption of the added metal by MST, where a large amount of Ti would be visible in the XAFS data. This is in contrast to outer sphere sorption, where no Ti would exist in the outer shell of the Sr or U XAFS data. (D) Precipitation/polymerization of added metal at or away from the MST surface, where little Ti (from the MST) is observed relative to the outer shell metals that was present in the XAFS data.

BEAMLINE X11A**Funding**

Swiss Federal Institute of Technology
Research Grant

Publication

A. Voegelin and R. Kretzschmar, "Formation and Dissolution of Single and Mixed Zn and Ni Precipitates in Soil: Evidence from Column Experiments and Extended X-ray Absorption Fine Structure Spectroscopy," *Environ. Sci. and Tech.*, **39**, 5311-5318 (2005).

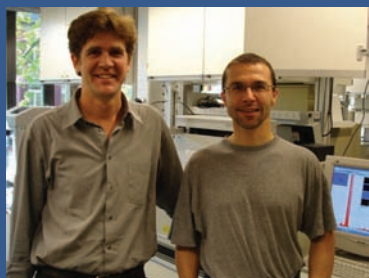
For More Information

Andreas Voegelin, Soil Chemistry Group,
Department of Environmental Sciences,
Swiss Federal Institute of Technology
(ETH) Zurich, Switzerland

Email: voegelin@env.ethz.ch

Ruben Kretzschmar, Professor of Soil
Chemistry, Department of Environmental
Sciences, Swiss Federal Institute of Tech-
nology (ETH) Zurich, Switzerland

Email: kretzschmar@env.ethz.ch



Authors (from left) Ruben Kretzschmar and Andreas Voegelin

Immobilization Processes in Soils Contaminated with Several Heavy Metals

A. Voegelin and R. Kretzschmar

Department of Environmental Sciences, Swiss Federal Institute of Technology, Zurich, Switzerland

Contaminated soils are often polluted with a mixture of heavy metals. Little is currently known about the effects of these cocktails on the immobilizing role of heavy-metal precipitates in contaminated soils. For the case of Zn-Ni, we found that more Zn than Ni was retained in a soil leached with heavy-metal containing solutions and that the amounts did not vary whether the metals were present alone or together. Synchrotron spectroscopy showed that Zn and Ni formed individual precipitates when present alone and a single mixed precipitate when present together. This mixed precipitate dissolves much faster than the pure Ni precipitate, indicating a mobilizing effect of Zn on Ni in the case of a combined contamination. Our results demonstrate that the interactions of different metals need to be considered when assessing the relevance of heavy-metal precipitation reactions in contaminated soils.

Contamination of soils with heavy metals can cause a reduction in crop yield or a contamination of underlying groundwater. The formation of heavy-metal bearing minerals in soils may attenuate those adverse effects and has been therefore extensively studied in recent years. However, soils are often contaminated by several heavy metals and little is still known about the effects to be expected in such cases. We therefore systematically investigated the formation and dissolution of nickel (Ni) and zinc (Zn) precipitates in soil in the presence of only one or both of these metals. Heavy-metal precipitates in soils are weakly crystalline and occur at low concentrations. Synchrotron-based x-ray absorption spectroscopy is a unique method for obtaining direct molecular-scale information on the binding of metals in those systems. Taking advantage of these possibilities, we employed a combined approach of controlled laboratory column studies and extended x-ray absorption fine structure (EXAFS) spectroscopy to investigate the interaction of Ni with Zn in a natural soil.

A neutral soil was packed into a chromatographic column and leached over a long period of time with solutions containing low concentrations of Zn and/or Ni that are realistic for actual environmental systems. We found that about twice as much Zn than Ni was retained in the soil when reacted with either Zn or Ni. Interestingly, the same amounts of Zn and Ni were retained in the soil when present together in solution. While this finding might suggest that Zn and Ni acted independently, a different picture was obtained from EXAFS spectroscopy.

Figure 1 shows (A) EXAFS spectra of the reacted soil samples, (B) their Fourier transforms, and (C) the structure of a layered double hydroxide (LDH) type phase (see also caption). Following a fingerprinting approach, i.e. comparing the experimental spectra (A) to those of known reference minerals, we concluded that Ni and Zn were incorporated into LDH-type minerals in all studied cases. Considering the mixed-metal experiment, the question to be answered by EXAFS spectroscopy was whether Zn and Ni would precipitate into a mixed ZnNi-LDH or form individual precipitates as in the single-metal experiments. We therefore analyzed the Fourier transforms of the EXAFS spectra (see panel B), in which peaks at an increasing distance from the central atom of

interest (Ni or Zn) correspond to different shells of neighboring atoms. While the first peak results from the six oxygens of the hydroxyl groups surrounding Zn or Ni in the octahedra, the second peak results from the next nearest Zn or Ni neighbors in the octahedral sheet (see panel C). For the experiments with either Zn or Ni, we find that the distance between neighboring Zn atoms is significantly larger than between neighboring Ni atoms, due to the larger ionic radius of Zn^{2+} than Ni^{2+} . In the mixed-metal experiment, we would find the same distance if the metals had precipitated into individual phases. However, the analysis of the Fourier transforms of the mixed-metal sample clearly shows that the distances for Zn and Ni converge. Zn and Ni therefore seem to have precipitated into a single mixed ZnNi-LDH.

Formation of such a mixed NiZn-LDH has a significant impact on the immobilization of Ni or Zn in soil. Leaching the metal-enriched soils with acidified water at pH 3.0, we found that the Zn-LDH dissolved much more rapidly (within minutes) than the Ni-LDH (within days). The mixed NiZn-LDH in the mixed-metal system dissolved almost as fast as the pure Zn-LDH, and considerably faster than the pure Ni-LDH. Thus, the presence of Ni only had a minimal immobilizing effect on Zn, while the presence of Zn in turn led to the incorporation of Ni in a substantially less acid-resistant phase.

Our results show that heavy metals present in mixtures may behave significantly different than if present alone. Further research on this issue is warranted to improve our understanding of heavy metals in contaminated environmental systems. While sorption and extraction studies provide macroscopic information on the interactions of different types of heavy metals in soils, synchrotron-based spectroscopy is required to obtain complementary molecular-scale information on the effective reaction mechanisms.

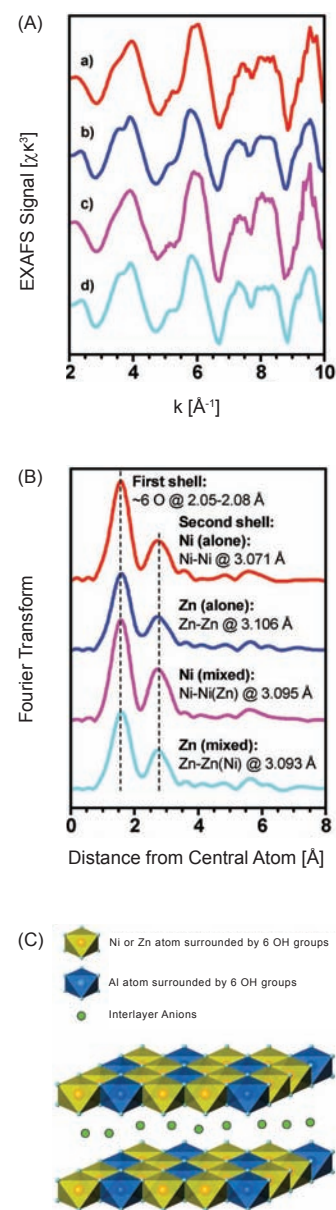


Figure 1. (A) EXAFS spectra of a) Ni in soil reacted with Ni, b) Zn in soil reacted with Zn, c) Ni and d) Zn in soil reacted with Ni and Zn. (B) Fourier transforms of EXAFS spectra shown in the left panel, indicating the position of different atomic shells around the central atom. (C) Structure of layered double hydroxide (LDH), which is composed of divalent (Zn or Ni) and trivalent (Al) cations (double) that are coordinated by six OH groups (hydroxide), forming octahedral sheets in a layered arrangement.

BEAMLINE X17C

Funding

National Science Foundation; U.S. Department of Energy; U.S. Department of Defense

Publication

H.-Z. Liu, J. Chen, J. Hu, C.D. Martin, D.J. Weidner, D. Häusermann, and H.-K. Mao, "Octahedral Tilting Evolution and Phase Transition in Orthorhombic NaMgF_3 Perovskite Under Pressure," *Geophys. Res. Lett.*, **32**, L04304 (2005).

For More Information

Dr. Haozhe Liu, HPCAT, Advanced Photon Source, Argonne National Laboratory

Email: hliu@hpcat.aps.anl.gov



Authors (from top) Jingzhu Hu, Haozhe Liu, and Jiu-hua Chen

NaMgF_3 Perovskite Under Pressure: Octahedral Tilting Evolution and Phase Transition

H. Liu¹, J. Chen², J. Hu¹, C.D. Martin², D.J. Weidner², D. Häusermann¹, H.-k. Mao¹

¹High Pressure Collaborative Access Team, Carnegie Institution of Washington, Advanced Photon Source, Argonne National Laboratory; ²Mineral Physics Institute, Stony Brook University

A high-pressure test of an analog for a common deep-Earth mineral may allow researchers to estimate the physical properties of materials in the planet's lower mantle. We induced pressures greater than 16 gigapascals (GPa), more than 160,000 times the normal atmospheric pressure on the Earth's surface, on a perovskite material with a similar makeup as the ubiquitous deep-mantle perovskite MgSiO_3 and analyzed the change in its physical makeup under the stress. We observed slight changes to its chemical bonds beginning at 6 GPa and a compression that destroyed the perovskite crystal structure at pressures approaching 20 GPa.

Geophysical interest in the perovskite family of materials dates from the 1960s when geologist A.E. Ringwood proposed that the Earth's lower mantle is dominated by iron-bearing MgSiO_3 perovskite. A fundamental understanding of the behavior of selected representatives of the perovskite family of structures to high-pressure/high-temperature conditions is valuable for establishing possible behaviors of this family in general. We have chosen to study NaMgF_3 perovskite (neighborite) as it has gained significant attention as an analogue material of MgSiO_3 perovskite since O'Keefe et al pointed out their structural similarity in 1970s. Neighborite is isoelectronic with MgSiO_3 , and they are isostructural, possessing the same type of distortion from the ideal cubic perovskite structure to crystallize in space group $Pbnm$.

We used a diamond anvil cell high-pressure device and synchrotron x-ray micro-diffraction to *in situ* study the crystalline change of the sample under high-pressure conditions. A series of experiments were carried out using various pressure-transmitting media, the focusing beam size and grain size of the sample (at NSLS beamline X17C and the High Pressure Collaborative Access Team facility at the Advanced Photon Source) to optimize the quality of our diffraction data. The structural evolution of NaMgF_3 under high pressure, therefore, could be analyzed from the Rietveld refinement of the high-quality x-ray diffraction patterns. The atomic positions could be obtained under high pressure; for example, **Figure 1** demonstrates the crystalline structure of neighborite under 10.1 GPa when helium was used as the pressure medium.

The centrosymmetrically distorted orthorhombic perovskite with space group $Pbnm$ is distorted by two independent octahedral tilting angles θ and ϕ , where θ is an anti-phase tilt and ϕ is an in-phase tilt. It can also be conceived as the tilting Φ about the threefold $\langle 111 \rangle_{pc}$ axes of the regular octahedra (see **Figure 2** insert). The octahedral tilting of the NaMgF_3 perovskite could be quantitatively derived from the cell parameters (macro-approach) as well as from the positional parameters of atoms (micro-approach), as shown in **Figure 2**. The overall trends of the octahedral tilting angles, i.e. increasing with increasing pressure, are similar for both the macro and micro approaches. The volumetric compression was dominated by the shortening of the octahedral Mg-F bond at the beginning of compression below 6 GPa. In the 6-12 GPa pressure range, the contribution from the octahedral tilting matches that of the bond length

compression. This is followed by an increasing contribution from the octahedral tilting above 12 GPa.

The octahedral tilting, increasing with pressure, finally destroys the perovskite structure. An experiment was carried out using silicone oil as the pressure medium, which could generate more shear stress to accelerate the phase transition. We observed a phase transition at about 19.4 GPa, and the patterns above this pressure can no longer be indexed by the *Pbnm* perovskite structure, but can be indexed with the layering-type post-perovskite structural model with space group *Cmcm*. This distinct material created under these extremely high-pressure conditions should be further studied to establish its properties. Such research could help scientists better understand the mechanisms of perovskite, including the temperatures and pressures required for it to stabilize near the Earth's core.

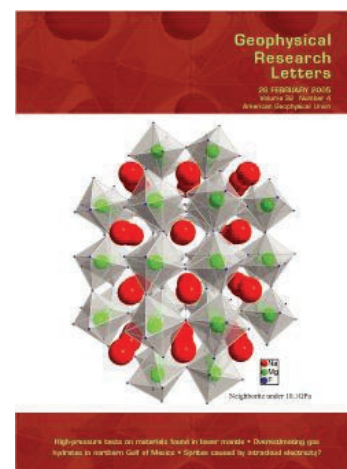


Figure 1. The crystalline structure of NaMgF_3 under pressure of 10.1 GPa, was featured on the cover of Geophysical Research Letters.

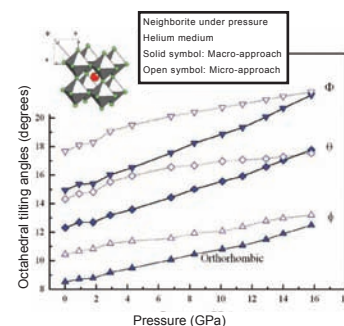


Figure 2. Pressure evolution of the octahedral tilting angles of NaMgF_3 perovskite as derived from lattice parameters (macro-approach), and atomic positions (micro-approach) plotted as solid and open symbols, respectively. Insertion shows the octahedral tilting angles referred to an ideal cubic *Pmm* perovskite.

BEAMLINES X10C, X11A, X19A**Funding**

U.S. Department of Agriculture; U.S. Department of Energy

Publication

S. Yoon, L.M. Diener, P.R. Bloom, E.D. Nater, and W.F. Bleam, "X-ray Absorption Studies of CH_3Hg^+ -Binding Sites in Humic Substances," *Geochim. et Cosmochim. Acta*, **69**, 1111-1121 (2005).

For More Information

Soh-joong Yoon, Department of Crop and Soil Sciences, Pennsylvania State University

Email: syoon@psu.edu



Authors (from top) Soh-joong Yoon, Paul Bloom, and William Bleam

Methylmercury Binding Sites in Humic Substances: An X-ray Absorption Study

S.-j. Yoon¹, L.M. Diener¹, P.R. Bloom², E.A. Nater², and W.F. Bleam¹

¹Department of Soil Science, University of Wisconsin; ²Department of Soil, Water, and Climate, University of Minnesota

Methylmercury, a highly toxic and bioaccumulative form of mercury, is known to have a strong affinity for binding to organic matter in soil, sedimentary, and aquatic environments. The objective of our study was to determine the dominant ligands that bind to the methylmercury cation (CH_3Hg^+) in humic acids (complex organic compound mixtures) by evaluating several CH_3Hg^+ -ligand complexation models. Mercury L_{III} -edge extended x-ray absorption fine structure (EXAFS) results show that CH_3Hg^+ preferentially binds to thiol ligands (-SH), also known as sulfhydryl. After saturating reactive thiol ligands, the remaining CH_3Hg^+ binds to carboxyl ligands rather than to amine or reduced-sulfur ligands other than thiol.

In organisms, such as fish, the dominant form of accumulated mercury is the organometallic methylmercury cation CH_3Hg^+ , rather than the inorganic cation Hg^{2+} . Scientists have reported that the biotic and abiotic methylation of inorganic mercury is affected by natural organic matter. Humic substances, for example, either stimulate mercury methylation, acting as methyl donors for Hg^{2+} , or suppress it by forming complexes with Hg^{2+} . Examining the nature of organic and inorganic mercury complexes with natural organic matter is important for understanding the biogeochemical cycle of mercury as well as the fate of mercury in the environment.

Both Hg^{2+} and CH_3Hg^+ have strong affinities for organic matter in terrestrial and aquatic environments, with CH_3Hg^+ having a lower affinity than Hg^{2+} . The principle of hard and soft acids and bases (the HSAB principle) predicts the strong affinity of reduced-sulfur ligands for Hg^{2+} and CH_3Hg^+ . Previous mercury L_{III} -edge extended x-ray absorption fine structure (EXAFS) studies show that humic sulfur ligands bind both Hg^{2+} and CH_3Hg^+ . Scientists, however, have reported that only a small fraction of reduced sulfur in humic substances binds to CH_3Hg^+ , with oxygen or nitrogen binding to the remaining CH_3Hg^+ . They speculated that CH_3Hg^+ -binding sulfur ligands were, most likely, thiol and possibly sulfide, disulfide, and hydrogen disulfide groups. In this study, we determined the major CH_3Hg^+ -binding humic ligands using mercury L_{III} -edge EXAFS. Our spectra were obtained at NSLS beamlines X11A and X10C.

We examined several CH_3Hg^+ -ligand models as potential CH_3Hg^+ -binding structures in humic acids: thiol (-SH), sulfide (-S-), disulfide (-SS-), hydrogen polysulfide (-SSH or -SSSH), carboxyl (-COOH), and amine (- NH_2). We examined carboxyl and amine ligands, although they are hard Lewis ligands, because CH_3Hg^+ -amine complexes exhibit relatively high complexation constants, and carboxyl is the most abundant ligand in humic acids.

We equilibrated two different humic-acid solutions (soil and aquatic) at CH_3Hg^+ -to-reduced-sulfur ratios ranging from 0.3 to 1.5, quantifying the reduced-sulfur (e.g., thiol, sulfide, and hydrogen polysulfide) content using sulfur K-edge x-ray absorption near edge structure (XANES) spectroscopy at beamline X19A.

Our results show that thiol is the dominant CH_3Hg^+ complexing ligand among the reduced sulfur ligands (**Figure 1**). We did not observe EXAFS evidence of CH_3Hg^+ complexation to sulfide, disulfide, or hydrogen disulfide ligands in any of our samples. CH_3Hg^+ complexation by carboxyl ligands (**Figure 2**) becomes significant after CH_3Hg^+ saturates the available thiol ligands. Carboxyl ligands, rather than amine, eclipse thiol ligands as the CH_3Hg^+ -to-reduced-sulfur ratio approaches and then exceeds 1. We also found evidence for proximately coordinated heavy atoms in a sample where the CH_3Hg^+ -to-reduced-sulfur ratio slightly exceeded 1. The heavy-atom backscattering behavior agrees the best with that of mercury or, possibly, other atoms with similar atomic numbers.

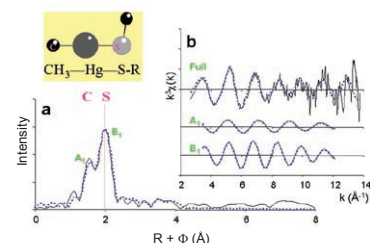


Figure 1. Experimental (solid lines) and least-squares fitted (dotted lines) Hg L_{III} -edge EXAFS of CH_3Hg^+ -humic thiol complex (aquatic humic acid; CH_3Hg^+ to reduced sulfur ratio, 0.3, pH 5): (a) radial structure function and (b) EXAFS scattering curves (full scattering curve and Fourier-filtered scattering curves of peak A_1 and peak B_1).

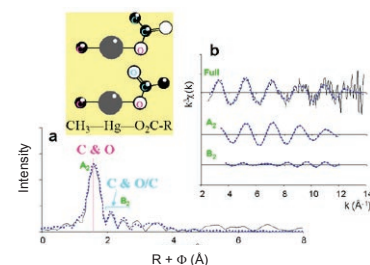


Figure 2. Experimental (solid lines) and least-squares fitted (dotted lines) Hg L_{III} -edge EXAFS of CH_3Hg^+ -humic carboxyl complex (soil humic acid; CH_3Hg^+ to reduced sulfur ratio, 1.3, pH 4): (a) radial structure function and (b) EXAFS scattering curves (full scattering curve and Fourier-filtered scattering curves of peak A_2 and scattering region B_2).

BEAMLINE X4A

Funding

National Institutes of Health

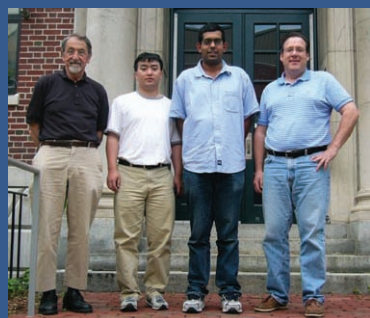
Publication

A. Banerjee, W. Yang, M. Karplus, and G.L. Verdine, "Structure of a Repair Enzyme Interrogating Undamaged DNA Elucidates Recognition of Damaged DNA," *Nature*, **434**, 612-618 (2005).

For More Information

Gregory L. Verdine, Department of Chemistry, Harvard University

Email: verdine@chemistry.harvard.edu



Authors (from left) Martin Karplus, Wei Yang, Anirban Banerjee, and Gregory L. Verdine

Disulfide Trapped Structure of a Repair Enzyme Interrogating Undamaged DNA Sheds Light on Damaged DNA Recognition

A. Banerjee¹, W. Yang¹, M. Karplus^{1,3}, and G.L. Verdine^{1,2}

¹Departments of Chemistry and Chemical Biology and ²Molecular and Cellular Biology, Harvard University;

³L'Institut de Science et d'Ingénierie Supramoléculaires (ISIS), Université Louis Pasteur, France

The integrity of the genome is constantly threatened in living cells by spontaneous alterations in the chemical structure of DNA that are caused by endogenous and exogenous agents. DNA repair pathways counteract these modifications and restore DNA to its undamaged state. Enzymes known as DNA glycosylases initiate the process, called base excision repair (BER), by locating a damaged nucleobase in the genome and then excising it from double-stranded (duplex) DNA. But how DNA glycosylases discriminate between very few damage sites amongst a huge amount of normal DNA is not well understood. We have used an efficient trapping strategy to capture a human repair protein, called 8-oxoguanine DNA glycosylase I (hOGG1), in the act of interrogating normal DNA for damage. By combining the structures of the protein-DNA complexes with free-energy calculations, we have gained novel insights into the mechanism by which hOGG1 is able to discriminate between normal and damaged DNA, and is able to prevent aberrant cleavage of normal DNA.

In humans, the DNA glycosylase hOGG1 is responsible for recognizing and removing 8-oxoguanine (oxoG), which is an oxidized form of the DNA base guanine (G) (**Figure 1c**). In general, DNA glycosylases bind at the site of the damaged base (lesion base), bend the duplex DNA considerably, and flip the lesion out in an active site pocket so that excision may occur (**Figure 2, left**). To understand how hOGG1 discriminates between the substrate oxoG and its normal counterpart G, which differ by only two atoms, it is imperative to obtain a three-dimensional structure of hOGG1 bound to undamaged DNA and compare it with existing oxoG-bound structures. The challenge lies in obtaining a homogeneous complex of hOGG1 with undamaged DNA in solution in the absence of a damaged base in the DNA to fix the "binding register." This problem was solved using the "disulfide crosslinking" technique (**Figure 3a**) that we have developed, which stabilizes protein-DNA complexes that would otherwise be transient. We use existing structural and/or biochemical data to decipher sites in which the protein and the DNA are in close proximity. The residue on the protein is then mutated to the amino acid cysteine and a disulfide-bearing tether is introduced on the DNA.

In the case of hOGG1, we reasoned that if the normal base G is extruded from the DNA helix — even transiently — we should be able to implant a disulfide bond between a tether emanating from G's partner base, cytosine (also called estranged C), and Asn149 (the amino acid asparagine, which is mutated to cysteine). Asn149 is one of the residues involved in recognizing the estranged C when the duplex DNA is invaded by hOGG1 in the complex with oxoG-containing DNA (**Figure 3b,c**).

The structure of the crosslinked complex of hOGG1 with undamaged DNA containing a G (G-complex) (**Figure 2, right**) resembled the structure of hOGG1 with oxoG-containing DNA (oxoG-complex) (**Figure 2, left**) that was solved earlier in our lab. However, the G residue, in spite of being extruded from duplex DNA, is rejected from entering the active site and lies at an alternative extrahelical site (exo-site). This explains how hOGG1 is able to scan long lengths of DNA without

accidentally excising normal bases. A superposition of the DNA molecules in the two structures reveals that large rotations about three backbone bonds in the DNA are enough to shift the G from the exo-site into the active site, leading us to propose that the G-complex is probably analogous to a late-stage intermediate in the base-extrusion pathway of oxoG. Contacts between the phosphate backbone of the DNA and the protein are almost identical on the 3' side of the oxoG/G. On the 5' side, however, the sole DNA contact (mediated by histidine, His270) is dislodged in the G-complex, leading to an over-twisted and considerably different conformation of the DNA on that side (**Figure 1a**).

Free-energy calculations using the G-complex and the oxoG-complex of hOGG1 help reveal how hOGG1 discriminates between oxoG and G. Computational work indicates that Lys249 (lysine), which participates in the excision reaction, forms a salt bridge with a conserved cysteine residue at the active site. Further analysis shows, quite unexpectedly, that the favorable electrostatic interaction of the salt-bridge dipole with oxoG and the unfavorable interaction with G (**Figure 1b**) is a major factor contributing to hOGG1's discrimination between G and oxoG. Although G is denied entry into the active site, computational data suggested that analogs of G (with a C-H replacing a nitrogen atom, N7) should be stabilized in the active site. We solved the structures of hOGG1 crosslinked to DNA containing analogs of guanine (**Figure 1c**). Indeed, the analogs were inserted into the active site at exactly the same place as oxoG.

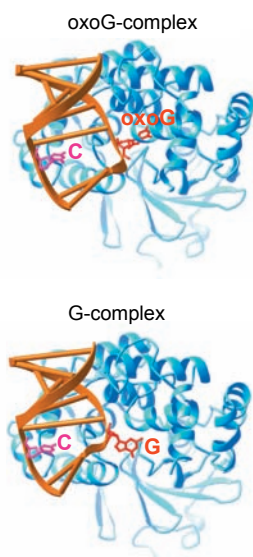


Figure 2. A comparison of the overall structures of the trapped complexes obtained with oxoG-containing (top) or G-containing (bottom) DNA. Both protein and DNA are represented as backbone ribbon traces, with the protein in cyan and the DNA in gold. The estranged C (magenta) and oxoG or G (red) are rendered in ball-and-stick representations. Note that oxoG is bound in the lesion-recognition pocket, while the G is bound at the alternative extrahelical site.

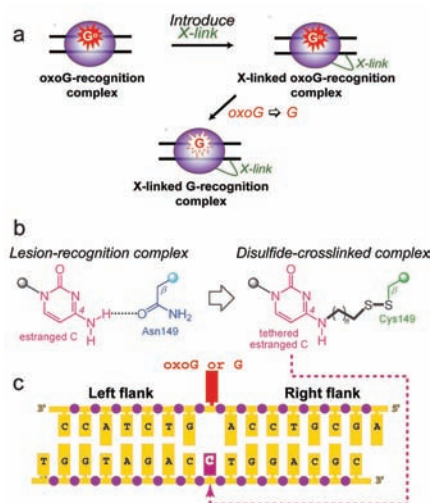


Figure 3. An overview of the strategy for obtaining a complex with G-containing DNA. (a) Based on the structure of the recognition complex, crosslinking sites are chosen first. The crosslinking strategy is validated by inspecting the structure of the crosslinked complex with oxoG-containing DNA and ensuring the absence of crosslinking-induced structural perturbations. Finally, oxoG in the DNA is replaced by G to obtain a crosslinked complex. (b) Details of the crosslinking strategy used in this case. The Asn149 contact with the estranged C was replaced with a disulfide crosslink by introducing a Cys149 point mutation and synthetically modifying DNA by introducing a tether with a disulfide linkage on the exocyclic amine. Note that introducing the tether does not perturb the Watson-Crick edge of the C as evident from existing structural information on similarly tethered DNA duplex. (c) The sequence of the DNA duplex. The crosslinking site is on the complementary strand of the oxoG/G-containing strand.

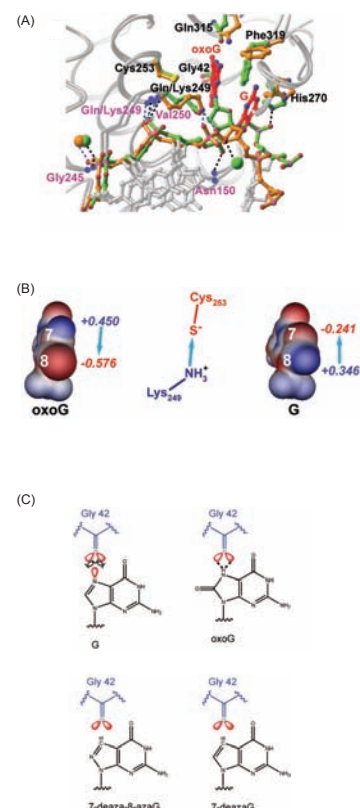


Figure 1. (a) Superposition of the oxoG-complex with the G-complex in the region around the protein/DNA interface. The overlay uses the protein backbone only (gray) for superposition, with the DNA backbone of the oxoG-complex in green and the G-complex in gold. Spheres are Ca^{2+} ions. The residues that interact with DNA through the backbone amid nitrogen atoms are denoted in magenta, and those that interact through side-chains are shown in black. Dotted lines are hydrogen bonds. (b) The electrostatic potential difference (from computational data) between oxoG and G. Regions of positive charge are in blue and negative regions are in red. Dipoles are in cyan, with Mulliken charges indicated. (c) A structural representation of the expected interactions between the main-chain carbonyl Gly42 and nucleobases examined in this study. Whereas oxoG is known to hydrogen-bond with Gly42, the lone pair of electrons on G produces a repulsive interaction with the lone pairs on Gly42. 7-deazaG and 7-deaza-8-aza-G are analogs of G.

BEAMLINE X4A

Funding

National Institutes of Health; National Science Foundation

Publication

F. Forouhar, Y. Yang, D. Kumar, Y. Chen, E. Fridman, S.W. Park, Y. Chiang, T.B. Acton, G.T. Montelione, E. Pichersky, D.F. Klessig, and L. Tong, "Structural and Biochemical Studies Identify Tobacco SABP2 as a Methylsalicylate Esterase and Implicate it in Plant Innate Immunity," *Proc. Natl. Acad. Sci. USA*, **102**, 1773-1778 (2005).

For More Information

Liang Tong, Department of Biological Sciences, Northeast Structural Genomics Consortium, Columbia University

Email: tong@como.bio.columbia.edu



Authors (from top left) Yang Chen, and Farhad Forouhar; Dharendra Kumar and Daniel Klessig; Yue Yang and Eyad Fridman

Structural and Biochemical Studies Identify SABP2 as a Methylsalicylate Esterase and Further Implicate it in Plant Innate Immunity

F. Forouhar¹, Y. Yang², D. Kumar³, Y. Chen¹, E. Fridman², S.W. Park³, Y. Chiang⁴, T.B. Acton⁴, G.T. Montelione⁴, E. Pichersky², D.F. Klessig³, and L. Tong¹

¹Department of Biological Sciences, Northeast Structural Genomics Consortium, Columbia University; ²Department of Molecular, Cellular, and Developmental Biology, University of Michigan; ³Boyce Thompson Institute for Plant Research; ⁴Center for Advanced Biotechnology and Medicine, Department of Molecular Biology and Biochemistry, Northeast Structural Genomics Consortium, Rutgers University, and Department of Biochemistry, Robert Wood Johnson Medical School

Salicylic acid (SA) is a critical signaling compound for the activation of plant defense responses against pathogen infections. SA binding protein 2 (SABP2) displays a high binding affinity for SA and plays a crucial role in the activation of systemic acquired resistance (SAR) — the triggering of defenses in uninfected parts of the plant — to pathogens. As a project of the Northeast Structural Genomics Consortium, we have determined the crystal structures of SABP2, alone and in complex with SA. SA is bound in the active site and is completely shielded from the solvent. Our biochemical studies reveal, for the first time, that SABP2 has strong esterase activity with methylsalicylate (MeSA) as the substrate, and that SA is a potent product-inhibitor of this catalysis. Our results suggest that SABP2 may be required to convert MeSA to SA as part of the signal transduction pathways that activate SAR.

Salicylic acid (SA) is a critical signaling compound for the activation of plant defense responses both at the site of infection and, systemically, in distal tissues such as leaves. For example, plants that are SA deficient fail to develop systemic acquired resistance (SAR) (the activation of defenses in uninfected parts of the plant), do not express pathogenesis-related (*PR*) genes in the uninoculated leaves, and display an enhanced susceptibility to pathogens. We recently identified and characterized a high-affinity SA-binding protein (SABP), termed SABP2, from tobacco. Silencing *SABP2* expression via RNA interference suppresses the plant's local resistance to Tobacco Mosaic Virus and SA-induced *PR-1* gene expression, and blocks the development of SAR.

To understand the biochemical and biological functions of SABP2, we have determined its structure in the absence and presence of SA at up to 2.1 Å resolution. The active site of SABP2 is located at the interface between the "core" and the "cap" domains of the enzyme, with the "catalytic triad" of amino acids — Ser81, His238, and Asp210 (**Figure 1A**). SA is bound in the active site, where it is completely shielded from the solvent and shows intimate polar and van der Waals contacts with the enzyme (**Figure 1B**). This provides a molecular explanation for the high affinity of SABP2 for SA.

We next demonstrated that SABP2 has esterase activity with methylsalicylate (MeSA), a methyl ester of SA, as the substrate (**Figure 2A**) and that SA is a potent product-inhibitor of this activity (**Figure 2B**). While SABP2 displays esterase activity with MeSA and the methylated derivatives of two plant hormones — methyl jasmonate (MeJA) and methyl indole acetic acid (MeIAA) — when they are present at high concentrations, it is highly specific for MeSA (among the substrates tested) at more physiologically relevant concentrations (**Figure 2A**).

To understand how SABP2 can catalyze the hydrolysis of MeSA, we modeled

this substrate into the SABP2 active site based on the structure of the complex obtained with SA (**Figure 1C**), which is the product of the reaction. By assuming a different torsion angle, the side chain of Ser81 can become hydrogen-bonded to the side chain of His238, completing the catalytic triad (**Figure 1C**). In addition, the side-chain hydroxyl is placed directly over the carboxyl carbon of MeSA, in a perfect position for initiating the nucleophilic attack. The model also shows that the active site is only large enough to accommodate the phenyl ring of MeSA, therefore explaining the poor activity of SABP2 with the MeIAA and MeJA substrates (**Figure 2A**).

These results, together with the genetic and physiological experiments previously reported for SABP2, suggest that MeSA may have an important role in SAR that is distinct from the role of SA. Since MeSA is more hydrophobic than SA and can thereby cross membranes more readily, it is possible that both short- and long-distance transmission of SA synthesized at the site of infection requires converting it first to MeSA. Our studies suggest that the role of SABP2 in plant host defense may be the hydrolysis of biologically inactive MeSA into active SA in the target cells. The potent inhibition of SABP2 by the product of the reaction, SA, may further help fine-tune intracellular SA levels. The presence of homologous proteins with MeSA esterase activity in other plant species suggests that MeSA may be a component of the plant innate immune response in general.

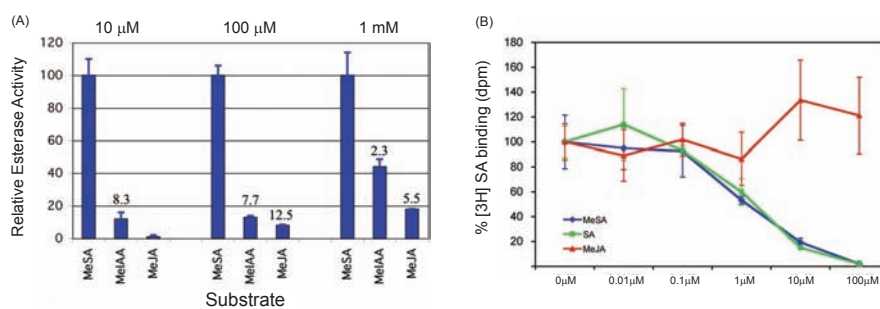


Figure 2. Comparisons of methyl esterase activities and binding affinities of SABP2. **(A)** Relative methyl esterase activity of SABP2 with MeSA, MeIAA, and MeJA substrates at three different concentrations (10 μM , 100 μM , and 1 mM). The activity with MeSA at each of the substrate concentrations was set at 100%. **(B)** SABP2 binds MeSA but not MeJA. MeSA (blue) competes with [^3H]SA for binding to SABP2 with the same potency as SA (green), whereas MeJA (red) does not compete for binding.

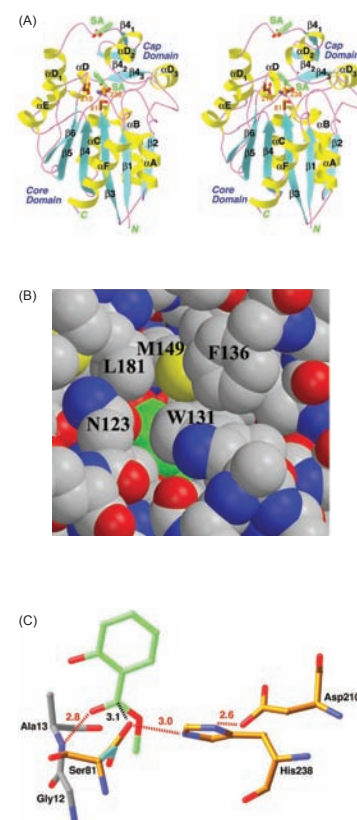


Figure 1. Structure of SABP2 in complex with SA. **(A)** Stereoview of the SABP2 monomer in complex with SA. SA (in green for carbon atoms) is located in the active site. **(B)** Active site of SABP2 in complex with SA, showing that the SA molecule (in green for carbon atoms) is shielded from the solvent in the active site. **(C)** Model of the binding mode of the MeSA substrate (green) to SABP2. The side chain of the catalytic Ser81 residue assumes a different conformation for catalysis (cyan and gold in complex with SA and MeSA, respectively). The hydrogen bonds are indicated in dashed lines in red, and the distance between Ser81 and the MeSA carboxylate carbon is indicated in black.

BEAMLINE X1A**Funding**

NASA Astrobiology Institute; National Science Foundation; Andrew W. Mellon Foundation; U.S. Department of Agriculture; U.S. Department of Energy

Publication

C.K. Boyce, M.A. Zwieniecki, G.D. Cody, C. Jacobsen, S. Wirick, A.H. Knoll, and N.M. Holbrook, "Evolution of Xylem Lignification and Hydrogel Transport Regulation," *Proc. Natl. Acad. Sci. USA*, **101**,17555-17558 (2004).

For More Information

Kevin Boyce, Department of Geophysical Sciences, University of Chicago

Email: ckboyce@uchicago.edu

Evolution of Xylem Lignification and Hydrogel Transport Regulation

C.K. Boyce¹, M.A. Zwieniecki², G.D. Cody³, C. Jacobsen⁴, S. Wirick⁴, A.H. Knoll⁵, and N.M. Holbrook⁵

¹Department of Geophysical Sciences, University of Chicago; ²Arnold Arboretum of Harvard University;

³Geophysical Laboratory, Carnegie Institution of Washington; ⁴Department of Physics, Stony Brook University;

⁵Department of Organismic & Evolutionary Biology, Harvard University

We have mapped the micron-scale distribution of cell-wall compounds in water-conducting cells with x-ray microscopy and shown that it varies across vascular plants. We have also shown that the extent to which water-transport properties can be modified by changes in the ionic content of transported water correlates with wall chemistry, which is consistent with the proposed wall-chemistry-based mechanism for this hydraulic response. Thus, the distribution of two key cell-wall compounds — hydrophilic polysaccharides and hydrophobic lignin — can likely affect the hydraulic and mechanical properties of cell walls. The evolutionary diversification of vascular cell types may reflect biochemical innovations evolved to fulfill opposing transport and structural support functions.

All land plants have primary cell walls that are largely made of polysaccharides, such as cellulose and pectin. The water-conducting cells of vascular plants also have complexly sculpted secondary wall thickenings that reinforce the primary walls and are impregnated with the polyphenolic polymer lignin. These vascular cells, comprising the xylem tissue, are typically responsible both for water transport and structural support in the plant — wood is an example.

Vascular cells are dead at maturity and can only physiologically interact with the rest of the organism through their cell walls. The distribution of hydrophilic polysaccharides and hydrophobic lignin within individual cell-wall layers may greatly influence the cells' structural and transport properties. For example, lignin would be optimally placed in the primary wall and middle lamella layer between adjacent cells in order to maximize the cell adhesion necessary for structural support, but such placement may interfere with aspects of hydraulic function as discussed below. Despite the functional importance of cell walls, details of their composition are difficult to observe due to the submicron scale of cell-wall layering. X-ray microscopy at the NSLS has allowed us to document the detailed distribution of wall polymers and demonstrate that sites of lignin deposition within cell walls vary substantially across vascular plants (**Figure 1**).

It was previously discovered that the resistance properties of xylem can be reversibly modified by altering the ionic concentration of the water being transported. The mechanism proposed for this was that the pectin in the middle lamella layer acts as a hydrogel and reversibly contracts and expands due to the binding and release of ions from solution, thereby altering the size of the pores through which water travels from one xylem cell to the next. We hypothesized that the lignification of the middle lamella, which provides structural support, would disrupt this capacity to modify the xylem's transport-resistance properties. We then demonstrated that, in fact, patterns of lignin deposition and resistance properties are strongly correlated (**Figures 1 and 2**).



Authors (from left) Kevin Boyce, Missy Holbrook, Maciej Zwieniecki, and George Cody

This work suggests that a number of important evolutionary trends in vascular cells that have been traditionally framed in terms of changes in cell shape and wall anatomy must also be considered in terms of the evolution of wall chemistry, including the diversification of vascular cell types. For example, the primitive condition in vascular plants is to have a single cell type (tracheids) responsible for both support and transport, but flowering plants have evolved morphologically distinct cell types specialized either for transport (vessels) or for support (fibers). This appears also to involve a divergence in patterns of lignin deposition. Vessels have a lignification pattern that might compromise structural support, but fibers that maintain an alternative lignification pattern are available to provide that support (**Figure 1**). It is likely that a number of such shifts in wall biochemistry may be documented through further studies of living and fossil plants.

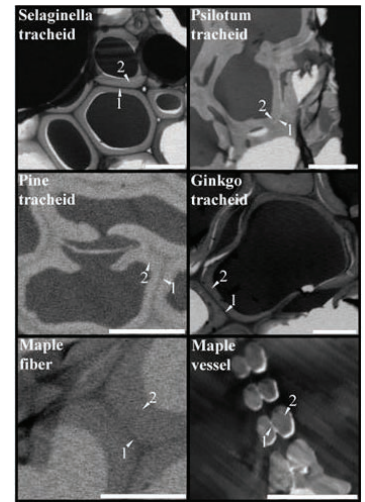


Figure 1. X-ray microscopy images of xylem cells, with darker shades indicating greater x-ray absorbance and lignin abundance. Images were taken at 285.2-286 eV absorption peak for aromatic carbon, which is most prevalent in lignin. All of the images depict cross-sections of xylem cells: water conducting tracheids and vessels, or non-conducting fibers specialized for support. Selaginella and Psilotum are basal vascular plants with a fern-grade organization. Maple is a flowering plant. Primary walls (1) and secondary walls (2) are labeled in each image. Nearly black or white areas found in cell lumens are epoxy or holes in the section. Scale bars are 6 microns.

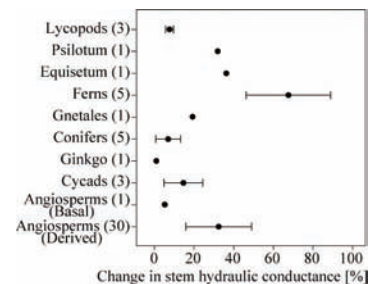


Figure 2. Percent increase of stem hydraulic conductance (mean \pm standard deviation) measured with 20 mMol KCl solution over conductance determined with deionized water. Numbers in parentheses reflect the number of different species used in the analysis.

BEAMLINE X12B

Funding

National Institutes of Health; Doris Duke Charitable Foundation

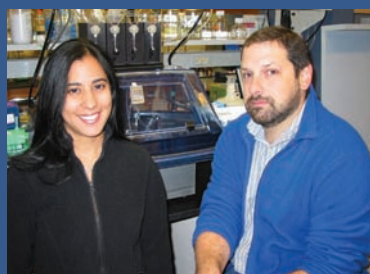
Publication

Z. Zavala-Ruiz, I. Strug, I., B.D. Walker, P.J. Norris, and L.J. Stern, "A Hairpin Turn in a Class II MHC-Bound Peptide Orients Residues Outside the Binding Groove for T Cell Recognition," *Proc. Natl. Acad. Sci. USA*, **101**(36),13279-84 (2004).

For More Information

Lawrence J. Stern, Ph.D., Department of Pathology, University of Massachusetts Medical School

Email: Lawrence.Stern@umassmed.edu



Authors (from left) Zarixia Zavala-Ruiz and Lawrence J. Stern

A Hairpin Turn in a HIV-Gag-Derived Peptide Bound to HLA-DR1 Orients Peptide Residues Outside the Binding Groove for T Cell Recognition

Z. Zavala-Ruiz¹, I. Strug², B.D. Walter³, P.J. Norris^{3,4}, and L.J. Stern²

¹Department of Chemistry, Massachusetts Institute of Technology; ²Department of Pathology, University of Massachusetts Medical School; ³Partners AIDS Research Center and Infectious Disease Unit, Massachusetts General Hospital and Harvard Medical School; ⁴Blood Systems Research Institute

T-cell receptors (TCRs) recognize peptide antigens bound to class II Major Histocompatibility Complex (MHC) proteins — molecules that transport and present the antigens to the T-cells, thus activating the immune system response. The receptors contact the antigen residues within or immediately flanking the seven-to-nine-residue sequence accommodated by the MHC-peptide binding groove. We identified a HIV-Gag-specific T-cell clone that requires an unusually long peptide for activation. The crystal structure of the HIV-gag peptide bound to an MHC protein known as HLA-DR1 shows that the peptide binds in an unexpected conformation, with its C-terminal region making a hairpin turn that bends back over the groove. The residues at the C-terminus are critical for T-cell recognition, and disrupting the hairpin cancels the immune response. The results suggest a new mode of MHC-peptide-TCR interaction.

Major Histocompatibility Complex (MHC) proteins are heterodimeric cell surface proteins that present antigens to T-cells, triggering the cell-mediated immune system. Peptides isolated from class II MHCs found in antigen-presenting cells are usually 15-20 residues long. Approximately one-third of the total peptide surface (the central region of the peptide) is accessible to solvent, which is necessary for recognition by the T-cell receptors (TCRs). Typically, TCRs specifically recognize a stretch of approximately nine residues.

We investigated the binding of peptides to class II MHC molecules using x-ray crystallography. The structures show that peptides bind in a polyproline type-II conformation with several conserved binding pockets within the overall MHC peptide-binding groove. Generally, the pockets accommodate the side chains of peptide residues at the P1, P4, P6, and P9 positions, with smaller pockets or shelves for the P3 and P7 residues. In the canonical conformation, the side chains of residues at the P-1, P2, P5, and P8 locations are solvent-accessible and point toward the TCRs. Mutagenesis studies of many MHC-TCR pairs, in addition to the two available MHC-peptide-TCR crystal structures, show that the TCRs contact the MHC-bound peptide in the region circumscribed by MHC-peptide contacts at the P-1, P2, P3, P5, and P8 positions.

A T-cell clone isolated from an individual acutely infected with HIV-1 recognizes a peptide antigen derived from the HIV-Gag protein bound to the human class II MHC protein HLA-DR1. This clone requires an unusually long version of the peptide for activation.

The crystal structure of HLA-DR1 in complex with the unusually long Gag-derived peptide, Gag[PP16], shows that the peptide binds in an unexpected bent conformation, forming a hairpin turn that orients the C-terminal region above the remainder of the peptide. An alignment of HLA-DR1-Gag[PP16] with other crystal structures of HLA-DR complexes for which clear electron density can be seen beyond the P10 peptide residue is shown in **Figure 1**. On each of the

other HLA-DR complex structures, the peptide extends straight out of the binding site.

To determine the importance of the C-terminal region in T-cell activation and to confirm the physiological relevance of the hairpin observed in the crystal structure, we performed alanine scanning mutagenesis. Each Gag[PP16] peptide residue was changed independently to alanine and standard MHC-peptide binding assays and T-cell activation experiments were conducted. In the MHC-peptide binding assay, we saw some significant reductions in binding affinity upon alanine substitution of Val(P1) and Met(P4) and Ser(P9). These effects are consistent with the binding frame observed in the crystal structure. In the T-cell activation assay, alanine substitutions of Glu(P-1), Ile(P2), Phe(P5) and Thr(P13) completely abolished T-cell activation. The side chains located at positions P-1, P2, and P5 are solvent-exposed and therefore accessible for recognition by the TCRs (**Figure 2**). Substitution of Gly(P11) to proline, which cannot be accommodated in the hairpin, also abolished T-cell activation.

In conclusion, our study shows that peptides can bind to MHC II in previously unobserved conformations in which residues outside the binding groove can bend back and become accessible for TCR recognition. This provides evidence for a new mode for MHC-peptide-TCR interaction.

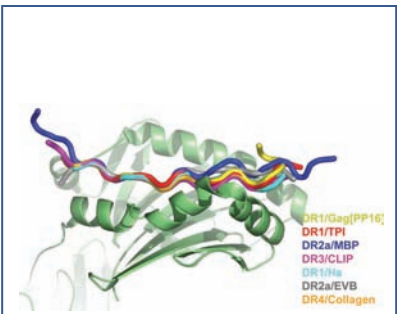


Figure 1. Alignment of HLA-DR crystal structure exhibiting ordered peptide density beyond the P10 residue. Complexes were aligned by least-squares fitting of $\alpha 1$ and $\beta 1$ domains of the MHC protein. Peptides are shown as α traces. DR1/TPI is red (PDB ID code 1KLU), DR2a/MBP is blue (PDB ID code 1FV1), DR3/CLIP is magenta (PDB ID code 1A6A), DR1/Ha is cyan (PDB ID code 1DLH), DR2a/EBV is gray (PDB ID code 1H15), and DR4/collagen is orange (PDB ID code 2SEB).

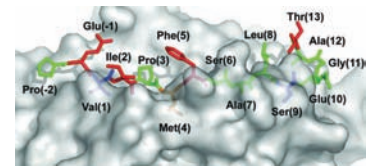


Figure 2. The Gag[PP16] hairpin turns orient important C-terminal residues in position to interact with the TCR. Side view of surface of HLA-DR1 with the Gag[PP16] peptide shown as a stick model. Peptide side chains essential for T-cell activation are red and those important for peptide binding to HLA-DR1 are blue. Met(P4) is in orange; it affects both MHC peptide binding and T-cell activation.

BEAMLINE X4A

Funding

National Institutes of Health and the Irma T. Hirschl Trust

Publication

J. Liu et al., "Atomic Structure of A Tryptophan-Zipper Pentamer," *Proc. Natl. Acad. Sci. USA*, **101**, 16156 (2004).

For More Information

Min Lu, Cornell University

Email: lu@mail.med.cornell.edu

A New Addition to the Folding Repertory: An Engineered Five-Stranded Tryptophan Zipper

J. Liu and M. Lu

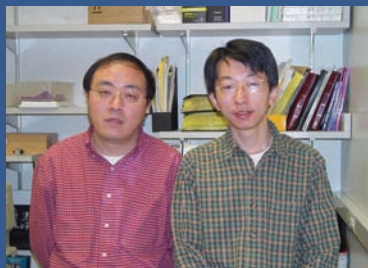
Cornell University

Coiled-coil motifs are ubiquitous mediators of specific protein-protein interactions through the formation of interlocking hydrophobic seams between α -helical chains. We engineered a "Trp-zipper" protein with tryptophan (Trp) residues at 14 first and fourth heptad positions. The protein forms a discrete, stable, α -helical pentamer in water at physiological pH. Its 1.45 Å crystal structure reveals a parallel, five-stranded coiled coil, a new type of "knobs-into-holes" packing interaction, and an unusual ~ 8 Å diameter axial channel lined with indole rings. The engineered Trp-zipper pentamer expands current views of coiled-coil assembly, molecular recognition, and protein engineering, and may serve as a soluble model for membrane ion channels.

Coiled coils are one of the most common motifs in protein-protein interactions and have been used as the basis for the design of helical bundles and many related structures. They consist of entwined alpha helices that form a hydrophobic seam based on nonpolar side chains located at the first (**a**) and fourth (**d**) positions in a characteristic seven-amino-acid sequence repeat, called a heptad. Despite their simple sequence pattern, coiled coils exhibit great diversity in the number and orientation of the chains involved. Proteins composed of two to twelve "strands" are known, and general principles for assembling dimers as well as higher-order structures, including hexamers and dodecamers, have been deduced.

About five years ago, we became interested in the *E. coli* lipoprotein (a protein-lipid molecule, denoted Lpp) that contains a three-stranded coiled-coil domain (Lpp-56) embedded between the outer cell membrane and the periplasmic peptidoglycan. Surprisingly, the crystal structure of this trimeric domain shows that the superhelical structure is not a uniform cylinder, but has a pinched-in region where three adjacent alanines (small hydrophobic amino acids) occupy the normally bulky nonpolar side chains at the **a** and **d** heptad positions. This unusual flexibility in the local helix geometry has not been seen in GCN4 leucine-zipper models, and led us to undertake a systematic analysis of the effect that the number and size of the side chains at the **a** and **d** positions might have on the structure and stability of the protein. Replacing *all* of the **a** and **d** residues with alanine, for example, completely unfolds the protein in solution, although the trimer is stable in crystals. This effect had not been reported before, to our knowledge: Intermolecular interactions in the crystal were sufficient to stabilize a coiled-coil trimer that could *not* fold in solution. Even when we cross-linked the chains covalently, the protein in solution remained monomeric. The monomer provided a useful model for defining the folding pathway in this system because we could identify a nascent helical sequence near the carboxyl terminus that unfolded as the temperature increased.

To explore the effects of helix geometry on coiled-coil formation, we engineered a Lpp-56 variant that contains exclusively Trp residues at the **a** and **d** positions (**Figure 1**). This Trp-zipper protein (denoted Trp-14) forms a stable pentameric coiled coil in solution. Its 1.45 Å crystal structure reveals a never-



Authors (from left) Min Lu and Jie Liu

seen-before interface between five parallel helices formed by interacting Trp residues. Only the residues at the **a** positions obey classical “knobs-into-holes” packing, while the **d** positions exhibit a more perpendicular stacking arrangement of the indole rings. This result suggests that the **a** and **d** layers in larger diameter helical barrels may unequally contribute to the stability of the structure. The Trp-14 structure also contains an irregular hydrophobic cavity (with a diameter of 8 Å) running along the long axis. This engineered Trp-zipper structure shows that we have not achieved a complete understanding of the principles of coiled-coil assembly. We are exploring additional variants of Lpp-56 that will help us to do so. Meanwhile, we note that the channel in Trp-14 may serve as a soluble model for membrane ion channels, and may help determine the thermodynamic effect of binding various ligands in such a channel.

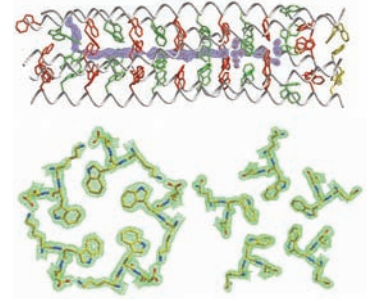


Figure 1. Crystal structure of Trp-14. The top panel shows a side view of the pentamer. The bottom panel shows the cross-section of the pentamer in the W18 (**a**, left) and W21 (**d**, right) layers. The view is from the amino terminus of the Trp-14 pentamer.

BEAMLINE X26C**Funding**

American Chemical Society Petroleum Research Fund; National Institutes of Health

Publication

A. Nagpal, M.P. Valley, P.F. Fitzpatrick, and A.M. Orville, "Crystallization and Preliminary Analysis of Active Nitroalkane Oxidase in Three Crystal Forms," *Acta Cryst.*, **D60**, 1456-1460 (2004).

For More Information

Allen M. Orville, School of Chemistry and Biochemistry, Georgia Institute of Technology

Email: allen.orville@chemistry.gatech.edu



Authors (from top) Akanksha Nagpal and Allen M. Orville

Crystal Structures of Nitroalkane Oxidase: High Resolution Data Collection Strategy for Crystals with a Very Long Unit Cell Edge

A. Nagpal¹, M.P. Valley², P.F. Fitzpatrick², and A.M. Orville¹

¹ School of Chemistry & Biochemistry, Georgia Institute of Technology; ² Department of Biochemistry & Biophysics, Texas A&M University

Nitroalkane oxidase (NAO) catalyzes the oxidation of neutral nitroalkanes to the corresponding aldehydes or ketones with the production of H₂O₂ and nitrite. Oxidized NAO readily crystallizes in a trigonal space group, diffracts to beyond 1.6 Å, but with a c unit-cell edge of 488 Å. These characteristics push data collection facilities to the limit. Using a combination of 2θ detector offsets, kappa geometry, and multiple data sets, a complete data set to 1.6 Å resolution has been achieved. To determine the structure we used crystals of a Se-Met enriched form of NAO, but trapped in a stable reaction intermediate complex (E^{red}-S). Although the orthorhombic unit cell of E^{red}-S* was smaller, it nevertheless required analysis of 52 Se sites with MAD phasing methods. The 2.2 Å structure of E^{red}-S* was then used to solve the structure of NAO in the large unit-cell crystal form.*

One of the research interests of the Orville lab is the structure/function analysis of enzymes that catalyze nitrite elimination from natural and "xenobiotic" nitrochemicals. Nitroaliphatic compounds are often produced by plants to inhibit the central metabolic enzymes of the TCA cycle in potential pathogens. Nitroalkane oxidase (NAO) is an FAD-dependent enzyme in fungus, which is induced by nitroalkanes and enables the microbe to obtain all its nitrogen from these types of compounds. Oxidized NAO crystallizes easily, which encouraged us to vigorously pursue the structure. However, the diffraction pattern observed with our in-house Cu K α x-rays was very streaky, even at the maximum crystal-to-film distance (**Figure 1**). In contrast, our first diffraction images obtained at X26C clearly indicated a different story. The NAO crystals diffracted to beyond 1.6 Å resolution in space group *P*3₂21, but with unit cell dimensions of *a* = *b* = 104 Å, *c* = 488 Å.

As of January 2005 only 158 x-ray structures (out of 29,040) deposited in the PDB contain a *c* axis unit cell edge greater than 450 Å. Moreover, only 16 of these structures were to at least 2.5 Å resolution. Thus, NAO would set the highest resolution record for a large unit cell, provided that high-resolution diffraction data could be collected, the phases could be solved, and the structure refined. We visited several beamlines at NSLS and APS to achieve these goals.

The observed x-ray diffraction pattern has a reciprocal relationship with the unit cell dimensions of the crystal in real space. Therefore, the resulting x-ray reflections for NAO crystals are very close together and appear as streaks with Cu K α x-rays. In order to resolve closely spaced reflections, the crystal-to-detector distance must be sufficiently large to allow the reflections to diverge from each other before they reach the detector. However, this also significantly decreases the maximum Bragg angle of reflection, so consequently the high-resolution data are not observed.

To collect the high-resolution data of NAO, several data sets were merged.

They were obtained with different detector vertical offsets (approximately equivalent to 2θ) and optimized kappa geometry to align the long cell axis approximately parallel to the crystal rotation axis. This strategy was first utilized at X26C to collect three data sets. The first two data sets used a vertical offset of 75 mm and a kappa of either 0° or 40° . The third data set was standard, employing no vertical or kappa offset. Merging these data sets yielded a 90% complete dataset to 2.5 Å resolution with $I/\sigma(I)$ of 8.3 in the highest resolution shell. We subsequently collected data at APS beamline 14-BMC (operated by BioCARS) using the strategy established at X26C and a 150 mm maximum vertical offset. The merged data is 93.5% complete to 2.07 Å resolution, including 80% completeness in the 2.07 Å resolution shell, but still only 60% complete to 1.6 Å resolution. Further high-resolution studies are ongoing at several synchrotron beamlines.

To solve the structure, we took advantage of the fact that during NAO turnover of nitroethane a N5-(2-nitrobutyl)-1,5-dihydro-FAD adduct (**Figure 2**) can be trapped at low temperature ($E^{\text{red}}\text{-S}^*$). This form of the enzyme crystallizes in a smaller, orthorhombic space group and contains one holoenzyme (α_4) per asymmetric unit. A Se-Met enriched form of $E^{\text{red}}\text{-S}^*$ was used for MAD data analysis (52 selenium sites) and solved to 2.2 Å resolution.

The larger unit cell for oxidized NAO contains $1\frac{1}{2}$ holoenzymes (six subunits) per asymmetric unit. The structure was solved by molecular replacement using $E^{\text{red}}\text{-S}^*$ as a search model. The structure of oxidized NAO has been refined to 2.07 Å resolution. We are currently analyzing our structures to characterize a subtle rearrangement of subunits associated with the conversion of oxidized NAO to $E^{\text{red}}\text{-S}^*$. The approximately 26° rotation for the subunits is unique to NAO, since analogous conformational changes are not observed in the acyl-CoA dehydrogenases, which are structural but not functional homologs of NAO.



Figure 1. The x-ray diffraction patterns obtained from crystals of oxidized NAO. The diffraction pattern on the left was obtained with Cu $K\alpha$ x-rays (1.54 Å), whereas the pattern on the right was collected with 1 Å synchrotron radiation. Synchrotron facilities provide a more intense, smaller, and focused x-ray beam. This enables longer crystal-to-film distances and the ability to resolve very closely spaced reflections from large unit cells.

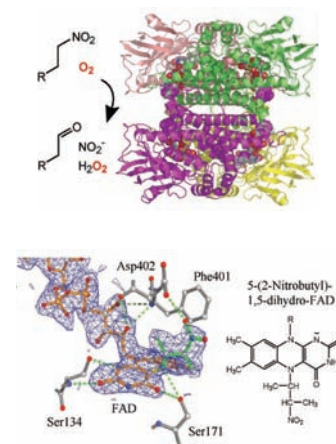


Figure 2. The structures of NAO and $E^{\text{red}}\text{-S}^*$ are homotetramers (top). The 2.2 Å resolution electron density for the N5-FAD adduct within the $E^{\text{red}}\text{-S}^*$ trapped intermediate (bottom) clearly indicates the presence of the 2-nitrobutyl moiety.

BEAMLINE X8C

Funding

National Institutes of Health

Publication

S. Hauenstein, C.M. Zhang, Y.-M. Hou, and J.J. Perona, "Shape Selective RNA Recognition by Cysteinyl-tRNA Synthetase," *Nat. Struct. Mol. Biol.*, **11**(11), 1134-1141 (2004).

For More Information

John Perona, Department of Chemistry and Biochemistry, University of California at Santa Barbara

Email: perona@chem.ucsb.edu

Shape Selective RNA Recognition by Cysteinyl-tRNA Synthetase

S.I. Hauenstein¹, C.-M. Zhang², Y.-M. Hou², and J.J. Perona¹

¹Department of Chemistry and Biochemistry, University of California at Santa Barbara; ²Department of Biochemistry and Molecular Pharmacology, Thomas Jefferson University

Cysteinyl-tRNA synthetase (CysRS) is the enzyme responsible for attaching cysteine (Cys) to the 3'-end of cysteine-specific transfer RNA (tRNA^{Cys}). The synthesis of Cys-tRNA^{Cys} is a crucial preliminary step required to incorporate cysteine into new proteins. We determined the three-dimensional structure of the complex formed between CysRS and tRNA^{Cys} at high resolution, revealing that the complex has an extensive enzyme-RNA recognition interface. An intricate network of hydrogen-bonding, steric, and electrostatic interactions was found at the inner-corner of the tRNA L-shape, near an unusual tertiary base-pair previously implicated in tRNA aminoacylation. Our combined mutational analysis of enzyme and tRNA groups showed that tRNA recognition by CysRS is shape-selective.

Aminoacyl-tRNA synthetases are the class of enzymes responsible for the covalent attachment of amino acids to the 3'-ends of cognate transfer RNA molecules (tRNAs) — the process known as aminoacylation. Cysteinyl-tRNA synthetase (CysRS) is the smallest monomeric tRNA synthetase in *E. coli*, and is an excellent model for exploring how the enzymes discriminate among a large number of structurally similar L-shaped tRNAs. Biochemical data has previously suggested that CysRS may rely on the distinctive globular shape of the tRNA^{Cys} core to recognize critical molecular elements, via a general mechanism known as "indirect readout." A striking feature of the tRNA^{Cys} core is the presence of a rare G15:G48 noncanonical tertiary base-pair. To provide the essential framework for interpreting this type of functional data, we crystallized *E. coli* CysRS bound to tRNA^{Cys} and determined the crystal structure to 2.3 Å resolution.

Our previously determined structure of the unbound CysRS revealed that it has an elongated shape. It features a Rossman fold catalytic domain, an inserted domain adjacent to the tRNA-acceptor end, a bridging stem-contact fold, and an α -helical bundle domain conserved among a subclass of other tRNA synthetases. While the relative orientations of these four domains are identical in CysRS bound to tRNA, a fifth domain — consisting of approximately 60 amino acids forming a mixed α/β fold — appears at the C-terminus of the helical domain, adjacent to the anticodon loop (**Figure 1**). This is a unique feature not previously observed in tRNA synthetases.

A significant fraction of the binding surface between CysRS and tRNA^{Cys} consists of interactions between the CysRS α -helical bundle domain and the tRNA's D and anticodon domains (which together form the vertical arm of the L-shape). The structure of the arm shows that there are no base-specific contacts at the key G15-G48 base-pair (where G is the nucleotide guanine). Instead, hydrogen bonds are made at a non-bridging phosphate oxygen atom located on the G15 and at the 2'OH on A14 (the nucleotide adenine) by the side-chains of Asn351 and Glu354 (the amino acids asparagine and glutamic acid, respectively) (**Figure 2**). In addition, a water-mediated hydrogen bond links G15 with the side chains of Asp348 (aspartic acid) and Lys12 (lysine), which form an adjacent salt-bridge.



Authors (from left) Scott Hauenstein and John Perona

To test how cysteinylolation relies on these sugar-phosphate backbone contacts at G15, we carried out a combined mutational analysis of the CysRS enzyme and tRNA in this region. The data revealed that variant enzymes mutated at Asn351 were no longer able to distinguish between tRNAs possessing the unusual G15-G48 pair and a canonical G15-C48 pair found in most tRNAs. Asn351 mutants are just six times more likely to prefer G15:G48 tRNA^{Cys}, compared with a 125-fold preference that native CysRS has for the wild-type tRNA. Together with the highly complementary sugar-phosphate backbone interactions observed in the structure, these data indicate that the Asn351-G15 phosphate contact mediates tRNA recognition by indirect readout.

Because the 3'-terminus of the tRNA is disordered in the crystals, we do not yet know how interactions with the sugar-phosphate backbone are transmitted to the enzyme active site. The extent to which tRNA selectivity may be coupled to a unique zinc ion-mediated mechanism for amino acid selection is also unresolved. We are currently performing crystallographic and enzymological experiments to address these questions.

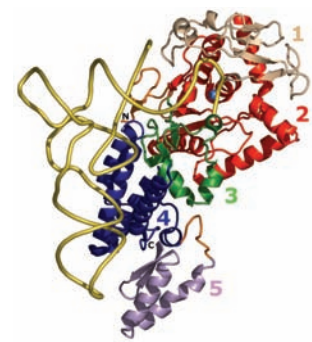


Figure 1. Ribbon representation of the *E. coli* CysRS-tRNA^{Cys} structure. The CP domain (1), Rossmann fold (2), SC fold (3), helical bundle domain (4), and AB domain (5) are colored tan, red, green, blue, and light purple, respectively. The tRNA molecule is shown as a gold tube and the active-site zinc ion as a blue sphere.

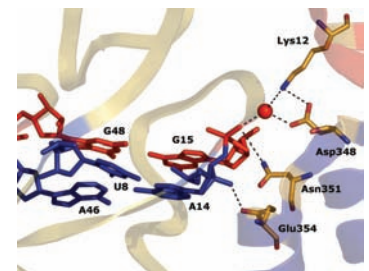


Figure 2. Indirect readout of the tertiary core. Asn351 makes a hydrogen bond with the phosphate of G15 in the G15-G48 Levitt pair (red). Glu354 makes secondary contact with the 2'OH group of A14 from the U8-A14-A46 pair (blue) stacked directly beneath the G15:G48 pair. A red sphere represents the water molecule involved in hydrogen bonding between the phosphate of G15 and Asp348/Lys12.

BEAMLINE X14A

Funding

National Science Foundation, Texas Center for Superconductivity and Advanced Materials at the University of Houston, Alfred P. Sloan Foundation

Publication

"Morphological Instability in InAs/GaSb Superlattices Due to Interfacial Bonds," *Phys. Rev. Lett.*, **95**, 96104-7 (2005).

For More Information

Donna Stokes and Jianhua Li, Department of Physics, University of Houston

Email: dwstokes@uh.edu; jl3@uh.edu



Authors (from left) Donna Stokes, Kevin Bassler, and Jianhua Li

Effect of Interfacial Bonds on Morphological Instability of Slightly Lattice Mismatched Epitaxial Thin Films

J.H. Li^{1,2}, D.W. Stokes¹, O. Caha¹, S.L. Ammu^{1,2}, J. Bai³, K.E. Bassler¹, and S.C. Moss^{1,2}

¹Department of Physics, University of Houston; ²Texas Center for Superconductivity and Advanced Materials, University of Houston; ³Oak Ridge National Laboratory

Using x-ray diffraction, we have investigated the strain and composition of InAs/GaSb superlattices grown on GaSb or InAs (001) substrates with InSb or GaAs interfacial bonds. An ordered InAs nanowire array is formed in the superlattice on GaSb (001) with InSb interfacial bonds, while the superlattice on InAs (001) with GaAs interfacial bonds remains planar. We have determined the composition and strain in both superlattices and found that the InAs layers are under compressive strain, rather than under the expected tensile strain or strain-free as we expected. We suggest that the strain state of the interfacial bonds is crucial for the morphological instability. This may provide a new channel in which to manipulate the self-assembling of nanowire structures.

The formation of self-organized semiconductor nanoscale structures, based on the morphological instability of strained films grown using molecular beam epitaxy, has been observed in many III-V systems. Instability occurs at some critical layer thickness, which is large for many III-V systems with a misfit of less than 1% (>150 Å), when the misfit strain energy is reduced more than the surface energy is increased. However, unusual instability phenomena have been observed in some non-common anion strained III-V single layers and heterostructures. For example, $\text{In}_{0.45}\text{Ga}_{0.55}\text{As}/\text{InP}$ (001) with a misfit of 0.5% demonstrates instability at an early stage of the growth. Similarly, InAs/GaSb (001) heterostructures have a misfit of 0.62%, but instability is observed at a thickness of a few monolayers.

In this work, two $(\text{InAs})_{13}/(\text{GaSb})_{13}$ superlattices, one with In-Sb interfacial bonds and one with Ga-As interfacial bonds, have been analyzed. Cross-sectional scanning tunneling microscope images showed that the sample with In-Sb interfacial bonds formed an array of nanowires, as shown in **Figure 1**. However, the sample with Ga-As interfacial bonds remained planar. **Figure 2(a)** shows the reciprocal space map around the GaSb (-224) substrate reciprocal lattice point for the nanowire sample. **Figures 2(b)** and **(c)** show line scans along the $Q_x||[-110]$ and $Q_z||[001]$ directions (indicated by the dashed lines in the map). The appearance of high-order two-dimensional satellites in these scans indicates the long-range ordering of the nanowire array. X-ray results from the planar superlattice sample (not shown) show one-dimensional satellites as expected.

Theoretical simulations of the x-ray results for the nanowire sample based on a structural model derived from **Figure 1** were performed considering the shape function of the nanowires — including the spacers, the scattering amplitude of a single nanowire, and the strain distribution in the nanowire array — through a direct solution of the equations of linear continuum elasticity. The simulations, also shown in **Figure 2**, yield that (1) the “InAs” nanowires were actually an $\text{InAs}_{0.88}\text{Sb}_{0.12}$ alloy due to Sb contamination and/or segregation, with a positive mismatch of +0.21%, and (2) the In-Sb interfacial bonds have a large positive mismatch of +6.28% with respect to the substrate.

For the planar sample, the x-ray rocking curve revealed that the "InAs" layers were also $\text{InAs}_{0.88}\text{Sb}_{0.12}$ alloy layers with a mismatch of +0.83%, which is much larger than that of the layers grown on the GaSb substrate. This sample is different because it contains Ga-As interfacial bonds, which experience a large negative mismatch of -6.69% with respect to the InAs substrate.

For the nanowire sample, the $\text{InAs}_{0.88}\text{Sb}_{0.12}$ and the InSb interfacial have a positive misfit. Thus, it is favorable for them to relax together. The strain energy is proportional to the layer thickness; therefore, the high misfit strain in the InSb interfacial reduces the critical layer thickness of $\text{InAs}_{0.88}\text{Sb}_{0.12}$, making it possible for instability to occur in just a few monolayers. For the planar sample, the $\text{InAs}_{0.88}\text{Sb}_{0.12}$ and the GaAs interfacial have opposite misfits. Relaxation of these two materials involves atomic displacements in opposite directions; therefore, it is unfavorable for them to relax together to form a planar sample. This suggests that it may be possible to manipulate the self-assembling of nanowire structures through the control of the strain relationship with respect to the substrate between the superlattice layers and interfacial bonds.

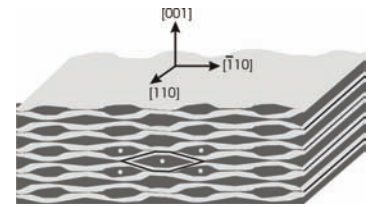


Figure 1. A reconstructed 3D structure of the nanowire array in the nanowire sample based on XSTM measurements. The dark areas are "InAs" and the bright areas are "GaSb." Enclosed in the solid lines is a nanowire model used in our simulation. The bright circles mark a super face-centered-rectangle unit cell that the nanowires form.

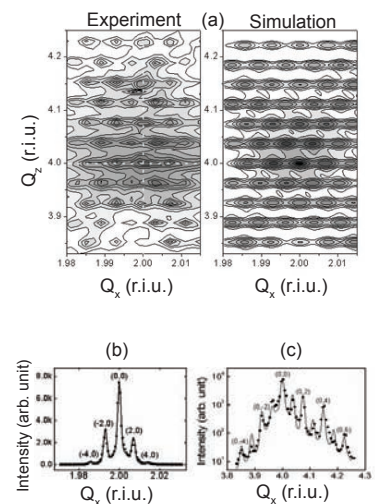


Figure 2. Experimental and simulated (a) x-ray reciprocal space map around (-224) reciprocal lattice point (b) $Q_x||[-110]$ scan (dots) corresponding to the dashed horizontal line in the map and (c) $Q_y||[001]$ scan (dots) corresponding to the dashed vertical line in the map. (m,n) indicates the lateral and vertical orders of the satellites.

BEAMLINES X22A, X22C

Funding

National Science Foundation; Cottrell Scholar Program of the Research Corporation; Division of Material Sciences, U.S. Department of Energy

Publication

F. He, B.O. Wells, and S.M. Shapiro, "Strain Phase Diagram and Domain Orientation in $SrTiO_3$ Thin Films," *Phys. Rev. Letts.*, **94**, 176101 (2005).

For More Information

Feizhou He, Canadian Light Source, University of Saskatchewan

Email: feizhou.he@lightsource.ca

Perovskite Thin Films Under Strain

F. He¹, B.O. Wells¹, and S.M. Shapiro²

¹Department of Physics, University of Connecticut; ²Department of Physics, Brookhaven National Laboratory

SrTiO₃ nanoscale films were studied as a model oxide film system. Highly strained films were grown on different substrates, resulting in either compressive or tensile strain. The measured strain-temperature phase diagram is qualitatively consistent with theory; however, the change in transition temperature is much larger than predicted. Further, the film is constrained because it is epitaxially clamped to the substrate, which causes the SrTiO₃ to be tetragonal at all temperatures. Therefore, the phase transition involves only a lowering of symmetry. This leads to the unique situation in which the low temperature phase under tensile strain has an orthorhombic Cmc space group but a tetragonal lattice, a situation not possible for bulk materials.

In epitaxial films only several nanometers thick, the film atoms tend to align with the underlying substrate atoms. If the lattice parameters of the film and substrate material are different, the film will be strained from its natural bulk atomic spacing. An important area of research in recent years has focused on understanding exactly why the properties of strained films differ from related bulk materials. An ultimate goal is to learn how to use these differences to enhance the performance of devices, or as a tool to probe the fundamental physics of materials with strong electron interactions.

The many fascinating properties of perovskite-related materials, such as ferroelectricity and high-temperature superconductivity, are particularly sensitive to strain. Our experiments used synchrotron x-ray scattering to investigate the structural phase transitions in very highly strained films of various perovskite-based film materials. Our main model system has been $SrTiO_3$, which has a well-known structural phase transition involving rotations of the internal TiO_6 octahedral, as shown in **Figure 1(a)**. In this case, the transition is from a high symmetry cubic phase at a high temperature to a lower symmetry tetragonal phase below the transition temperature. The structural phase transition in $SrTiO_3$ is monitored through the superlattice diffraction peaks associated with the low-temperature phase.

We produced $SrTiO_3$ films with different amounts and types (compressive or tensile) of strain by carefully growing them on different underlying crystals. Under compressive strain, the phase transitions in $SrTiO_3$ films go from a high-symmetry tetragonal structure to a low-symmetry tetragonal phase. Under tensile strain, the transition is from high-symmetry tetragonal to orthorhombic. The structural phase transition temperature T_s is enhanced under both compressive strain and tensile strain. The main difference between the two cases is that the orientation of the rotation axis is different for compressive strain and tensile strain, as illustrated in **Figure 1(b)**. A very similar effect happens to the spontaneous polarization in related ferroelectric films.

An interesting phenomenon in epitaxial films is that, although internally there are structural changes corresponding to the phase transitions, externally the dimensions of the unit cells do not change because of the strong bonding, or clamping, from the substrates. Therefore, the tetragonality of the unit cell,



Authors (from left) Barry Wells and Feizhou He

which is the secondary order parameter for bulk $SrTiO_3$, is no longer a good order parameter for phase transitions in films. The internal transitions without the external changes in the shapes of the unit cells create unique morphologies that are not possible in bulk materials. For example, the low-temperature phase in $SrTiO_3$ films under tensile strain has an orthorhombic space group ($Cmcm$) but a tetragonal lattice as a consequence of strain and substrate clamping.

The strain phase diagram based on our experimental data is compared with the theoretical calculations by Pertsev *et al*, shown in **Figure 2**. Many aspects of the strain-temperature phase diagram, such as the domain structures and the general trend of the phase boundary, are well described by current theory, though improvements are necessary to describe the magnitude of the increase in transition temperature.

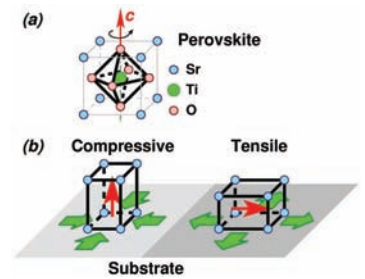


Figure 1. (a) Unit cell of $SrTiO_3$. The phase transition involves the rotation of internal TiO_6 octahedral. (b) The rotation axis of internal TiO_6 octahedral (red arrow) in $SrTiO_3$ oriented differently under compressive strain and tensile strain. The spontaneous polarizations in ferroelectric materials behave similarly.

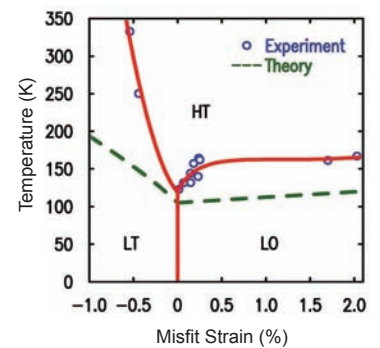


Figure 2. Strain-phase diagram for $SrTiO_3$ thin films. High-symmetry tetragonal, low-symmetry tetragonal, and orthorhombic phases are labeled HT, LT, and LO, respectively. For tensile strain, T_s increases rapidly over the small strain regime, then stabilizes at about 160–170 K for larger strain. Compressive strain induces a more dramatic effect. Only 0.5% compressive strain results in an increase in T_s of over 200 K versus the bulk value, nearing room temperature.

BEAMLINE X19C

Funding

Office of Naval Research; U.S. Department of Energy, Office of Basic Energy Sciences

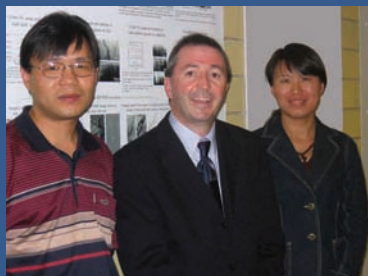
Publication

X.R. Huang, J. Bai, M. Dudley, R.D. Dupuis, and U. Chowdhury, "Epitaxial Tilting of GaN Grown on Vicinal Surfaces of Sapphire," *Appl. Phys. Lett.*, **86**, 211916 (2005).

For More Information

Michael Dudley, Department of Materials Science and Engineering, Stony Brook University

Email: mdudley@notes.cc.sunysb.edu



Authors (from left) Xian-Rong Huang, Michael Dudley, and Jie Bai

Epitaxial Tilting of GaN Grown on Vicinal Surfaces of Sapphire

X.R. Huang¹, J. Bai¹, M. Dudley¹, R.D. Dupuis², and U. Chowdhury²

¹Department of Materials Science and Engineering, Stony Brook University; ²School of Electrical and Computer Engineering, Georgia Institute of Technology

Using the synchrotron Laue method and high-resolution x-ray diffraction, we have revealed the epitaxial tilting effect of gallium nitride (GaN) films grown on vicinal (0001) surfaces of sapphire and their relationship to the offcut angles and the substrate surface steps. This effect is a consequence of the large out-of-plane lattice mismatch between GaN and sapphire, and can be explained by an extended Nagai theory. The large lattice tilts and their formation mechanism indicate that the substrate surface morphology is an important factor that affects the epitaxy process and the crystalline quality of GaN films grown via vicinal-surface epitaxy.

Although the growth of III-nitrides on sapphire (Al_2O_3) has been extensively investigated, little attention has been paid on the large c lattice mismatch ($\Delta c/c \approx 20\%$ for GaN/sapphire), particularly the case of vicinal surface epitaxy (VSE). We have recently demonstrated that GaN grown on a vicinal sapphire surface is generally tilted from the substrate (known as a Nagai tilt). For 1-bilayer steps of sapphire, shown in **Figure 1a**, the tilt α is related to the offcut angle ϕ by the relationship $\tan\alpha = -(\Delta c/c)\tan\phi \approx 0.2\tan\phi$ (<0). For step bunches, however, this principle may change. In **Figure 1c**, due to $3c \approx 2.5c_0$, the GaN lattices can be tilted in two directions with equal probabilities, $\tan\alpha \approx \pm 0.2\tan\phi$, leading to $\alpha \approx 0$ on average. For 4-bilayer steps, the GaN lattice is tilted toward the offcut direction by $\tan\alpha = [(4c-3c_0)/(4c)]\tan\phi \approx 0.1\tan\phi$ (>0). Similarly, the tilt for 5-bilayer steps is $\tan\alpha = [(5c-4c_0)/(5c)]\tan\phi \approx 0.04\tan\phi$ (>0).

The above principles have been explicitly verified by synchrotron Laue patterns and high-resolution x-ray diffraction performed on vicinal GaN/sapphire. GaN films 4 μm thick were grown using low-pressure metal organic chemical vapor deposition (MOCVD) in a temperature range of 1020-1080°C. **Figure 2** shows the back-reflection Laue patterns of three samples, where the displacement of the 0001 spot from O (white arrows) is caused by the offcut, and the displacement of the GaN 0001 spot from that of sapphire reflects the epilayer tilt, which is always parallel to the offcut direction \mathbf{n}_c . In **Figure 2a**, the measured tilt (negative) is in perfect agreement with the tilting model in **Figures 1a** and **1b**, indicating that on the small-offcut substrate the steps are dominantly 1- or 2-bilayer steps. For the 6.29°-off sample, the tilt shows that steps of various types coexist on the substrate surface, with 1- or 2-bilayer steps contributing to negative tilts and the other types reducing this tendency. The positive tilt of the 10.6°-off sample shows that 4- or 5-bilayer steps outweigh the other steps.

The tilting effect reveals a series of important mechanisms of GaN epitaxy that have been widely ignored in the past, including: 1) the sapphire surface morphology can greatly affect the epitaxy process and the crystalline quality of GaN films; 2) drastic step bunching and faceting of sapphire can occur during nitridation; 3) mismatch strains are dominantly relaxed by pure basal plane dislocations without out-of-plane Burgers vector components; and 4) the epilayer tilt-related shear stresses are believed to significantly affect the

growth kinetics and strain relaxation. In our latest work, we also found the tilting effect and the related mechanisms in GaN/SiC systems [X.R. Huang *et al.*, PRL **95**, 086101 (2005)] where, compared to flat-surface epitaxy, VSE shows explicit advantages for relaxing strains and improving epilayer quality.

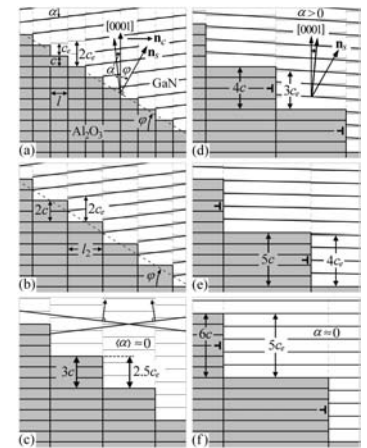


Figure 1. Epilayer tilts induced by steps of various heights in VSE of GaN on sapphire. n_s – substrate surface normal, n_c – offcut direction.

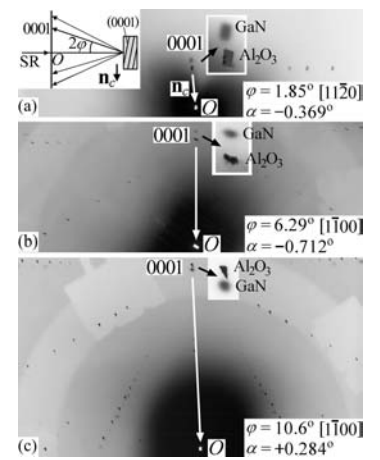


Figure 2. Laser-guided back-reflection synchrotron Laue patterns of vicinal GaN/Al₂O₃ samples showing the epitaxial tilts. The film-to-sample distance is 30 cm. Inset: a side view of the diffraction geometry.

BEAMLINE X10A

Funding

National Science Foundation

Publication

M.M. Maye, I.-S. Lim, J. Luo, Z. Rab, D. Rabinovich, T. Liu, and C.-J. Zhong, "Mediator-Template Assembly of Nanoparticles," *J. Am. Chem. Soc.*, **127**, 1519-1529 (2005).

For More Information

C.J. Zhong, Department of Chemistry, State University of New York at Binghamton

Email: cjzhong@binghamton.edu



Authors (from left) Lisa Cousineau, Li Han, Mathew Maye, Lingyan Wang, Qiang Rendeng, Nancy Kariuki, Mark Schadt, Yan Lin, Jin Luo, Stephanie Lim, Kaylie Young, Chuan-Jian Zhong (Group leader), Elizabeth Crew, Derrick Mott, Peter Njoki, and Xiangting Dong

Mediator-Template Assembly of Nanoparticles

M.M. Maye¹, I.-S. Lim¹, J. Luo¹, Z. Rab¹, D. Rabinovich², T. Liu³, and C.-J. Zhong¹

¹Department of Chemistry, State University of New York at Binghamton; ²Department of Chemistry, The University of North Carolina at Charlotte; ³Department of Chemistry, Lehigh University

The ability to construct size- and shape-controllable architectures using nanoparticles as building blocks is essential for exploring the properties of nanostructures. Our mediator-template strategy explores multidentate ligands as molecular mediators and surfactant-capped nanoparticles as templates in order to build size-controllable and monodispersed particle assemblies. Such assemblies display both soft and hard properties, depending on how they interact with their substrates. This duality could form the basis of a new strategy for manipulating nanoscale linkages, soldering nanoelectronics, and constructing nanosensor devices. The assemblies also allow for controlled disassembly and size regulation by a third molecular component, which could lead to developments in nanotechnological applications in controlled drug delivery.

Many areas of nanotechnology involve the use of nanoparticle-based materials in applications such as sensors, catalysis, and information storage. These applications require the ability to assemble nanoparticles into a structure with controllable size, shape, and interparticle spatial properties, resulting in unique nanoscale properties that can be effectively exploited. While a variety of assembly methods have been demonstrated, the ability to precisely control size, shape, and interparticle spatial properties is rarely reported due to the lack of molecular-level understanding of the interparticle interactions and reactivities.

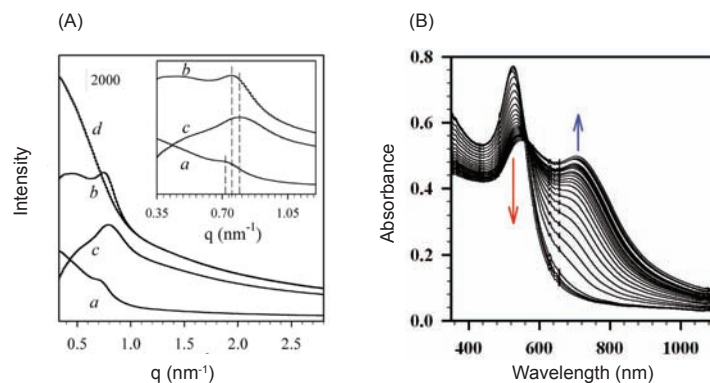
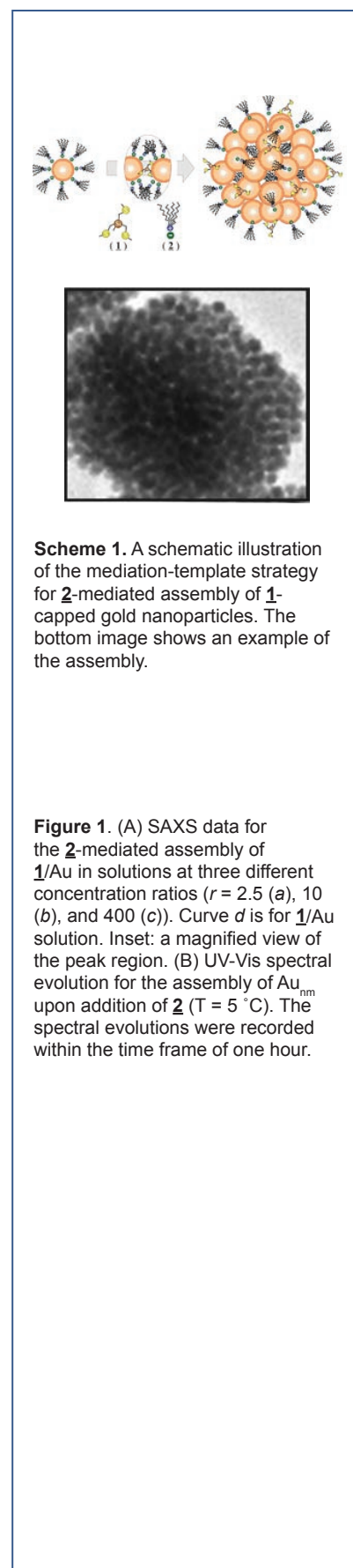
The key element of our assembly approach is a mediator-template strategy. The understanding of molecular driving forces exerted by molecular linkers or multidentate thioethers as mediators, as well as monolayer or surfactant capping molecules as templating agents, could lead to a general assembly strategy that would maximize our ability to control the structure's size, shape, and spatial properties. Consider, for example, a system in which multidentate thioethers, $\text{Me}_{4-n}\text{Si}(\text{CH}_2\text{SMe})_n$ (**2**), are used as mediators and tetraalkylammonium bromides, $[\text{CH}_3(\text{CH}_2)_m]_4\text{N}^+\text{Br}^-$ (**1**), are used as templating agents. **Scheme 1** illustrates the general concept of the **2**-mediated assembly of **1**-capped gold nanoparticles (**1**/Au). This mediator-template combination is simple and effective. The mediation force exploits the coordination reactivity between **2** and Au, which can be manipulated by the number of thioether groups on **2**. Simultaneously, the templating force resulting from the surfactant reactivity of **1** determines the geometry of the assembly, depending on the chain length and structure of **1**.

The average diameters of the spherical assembly (the TEM image in Scheme 1) are dependent on the relative ratios of mediators vs. templates. One important finding is from a small-angle x-ray scattering measurement that (**Figure 1A**) revealed a subtle decrease of the edge-to-edge distance with increasing mediator-to-template ratio, falling between the expected molecular lengths of **1** and **2**. Another important finding is from a spectrophotometric measurement of the surface plasmon resonance band (**Figure 1B**), which led to two important findings: that the mediator-template assembly of nanoparticles is an enthalpy-driven process, and that the enthalpy change (-1.3 kcal/mole) is close to the magnitude of the van der Waals interaction energy for alkyl chains. These

findings establish the important role played by the templating molecules in the mediate-template assembly.

The spherical assembly on mica does not wet the surface, and thus retains its shape. In contrast, the spherical assembly wets highly ordered pyrolytic graphite (HOPG), and thus the particles tend to spread over the surface. The interaction between the spherical assembly and HOPG must be relatively strong in view of the hydrophobic character of the HOPG surface and the hydrophobic character of **1**-capped Au nanoparticles and their assemblies.

The soft-hard nature of the nanoparticle assemblies and their interactions with contacting substrates could form the basis of a new strategy for manipulating nanoscale linkages, soldering nanoelectronics, and constructing nanosensor devices. Interestingly, the nanoparticle assemblies display interesting optical properties that are highly responsive to changes in assembly size, chemical environment, and molecular structures. The chemically responsive optical properties could find applications in devices such as sensors and biosensors. Such assemblies also allow for controlled disassembly and size regulation by a third molecular component, which could form the basis of nanotechnological applications in controlled drug delivery.



BEAMLINE X27C

Funding

Air Force Office of Scientific Research;
Air Force Research Laboratory and the
Materials and Manufacturing Directorate

Publication

H. Koerner, E. Hampton, D. Dean, Z.
Turgut, L. Drummy, P. Mirau, and R. Vaia,
"Generating Tri-axial Reinforced Epoxy
Montmorillonite Nanocomposites With Uni-
Axial Magnetic Fields," *Chem. Mater.*, **18**,
1990-1996 (2005).

For More Information

Richard A. Vaia, Air Force Research
Laboratory

Email: richard.vaia@wpafb.af.mil



Authors (from left) Richard Vaia, Peter
Mirau, Hilmar Koerner, and Larry
Drummy

Time-Resolved Morphology Development of Tri-axial Reinforced Epoxy Montmorillonite Nanocomposites in Uni-Axial Magnetic Fields

H. Koerner¹, E. Hampton², D. Dean², Z. Turgut³, L. Drummy⁴, P. Mirau⁴, and R. Vaia⁴

¹University of Dayton Research Institute; ²Tuskegee University; ³Zafer Turgut, UES Inc.; ⁴Air Force Research Laboratory, Materials and Manufacturing Directorate, Wright-Patterson Air Force Base

Numerous papers and patents have been published on polymeric nanocomposites. However, extensive research has not yielded nanocomposites with vastly improved properties, as was envisioned, but has instead mimicked the results of conventionally filled systems. This is mostly due to a poor nanoparticle-matrix interface and the lack of control over dispersion and orientation of nanofillers to an extent comparable to what has been accomplished in continuous-fiber reinforced composites. Utilizing the orthogonal magnetic susceptibility of Montmorillonite nanocomposites (MMTs) from different deposits with comparable Fe content (3.4%), we have generated a three-dimensional morphology composed of orthogonally aligned aluminosilicate layers from a mixture of Montmorillonites subjected to a uniaxial external magnetic field. Depending on the source, MMTs exhibit remnant magnetization arising from antiferro- and ferromagnetic impurities, and align with their layers parallel or perpendicular to the field. In-situ X-ray measurements show that within a few minutes an applied static magnetic field (1.2 or 11.7 Tesla) induces the stable alignment of an organically-modified MMT within an epoxy resin at room temperature. Structural relaxation is orders of magnitude slower. Overall, these studies demonstrate that a critical component of the chemistry in these nanofillers has been overlooked in the past. Remarkably minor compositional differences may allow researchers to explore many more possible techniques to address nanocomposite issues.

Real-time x-ray experiments were carried out at beamline X27C at the NSLS using a marCCD detector at a sample-to-detector distance of 82.5 cm. Two types of layered silicates, Southern Clay MMT modified with octadecylamine (SC18) and Nanocor I30.E (NC18), were dispersed in epoxy (an Epon 862 monomer) via sonication and high-shear mixing. After additional short mixing with a curing agent and subsequent degassing, the suspensions were deposited into x-ray capillaries for use in a 1.2-Tesla rare-earth permanent magnet.

The morphology response to the application of the magnetic field at room temperature ($\sim 27^\circ\text{C}$) was monitored in-situ by positioning the magnet such that the x-ray beam passed between the poles of the magnet and through the capillary. The capillaries were dropped into the magnetic field remotely via a solenoid switch and a paper clip attached to the top of the capillary. After alignment, the capillary was removed from the magnet and repositioned within the beam to examine the degree of randomization, or was fixed by a two-stage curing reaction (120 $^\circ\text{C}$ for 2 hours; 175 $^\circ\text{C}$ for two hours).

Figure 1 reveals that alignment of the 3 wt% SC18/NC18 mixture is 90% complete after 10 minutes in the 1.2-Tesla magnetic field at room temperature. **Figure 1a** shows a series of x-ray patterns at three-minute time intervals during the alignment process of that mixture. The final pattern was taken after a complete cure cycle and shows the partial exfoliation of the system, with the d-spacings of the galleries increasing from 3.7 nm to 12.5 nm. For this mixture, a two-dimensional contour plot of azimuthal scans at the d_{001} reflections

is shown in **Figure 1b**. This plot emphasizes the rapid formation of the four-point pattern, which reflects triaxial reinforcement by the OMM layers. A plot of the intensity of the d_{001} -layer diffraction at an azimuthal angle of 0 degrees (meridian) (**Figure 1c**) shows that steady-state alignment of the SC18/NC18 mixture (3wt% total) within the 1.2-Tesla magnetic is achieved after 15 minutes. This time scale is very similar to other OMMs and no indication of faster or slower orientation has been observed.

These experiments also show that once alignment has been achieved the sample does not quickly relax back to its random alignment, which is in agreement with rheology studies on similar systems. Alignment is possible in several solvents (Toluene, water) and epoxy monomers (Epon 862, Epon 828). The slow relaxation behavior is to be expected, considering the matrix viscosity and the Brownian motion of particles at room temperature. Rotational diffusion is hindered by particle-particle interaction and the high viscosity of the epoxy resin formulation.

The magnetic field alignment does not affect the curing chemistry, which agrees with electric field experiments on the same system.

Measurements on the coefficient of thermal expansion (CTE) confirm that morphology control leads to significant differences depending on the alignment of the layered silicates, decreasing CTE the most in the direction of maximum MMT alignment. Understanding the detailed mechanism that leads to a change of the magnetic easy axis within layered silicates opens up opportunities to design novel synthetic layered silicates with unusual magnetic properties.

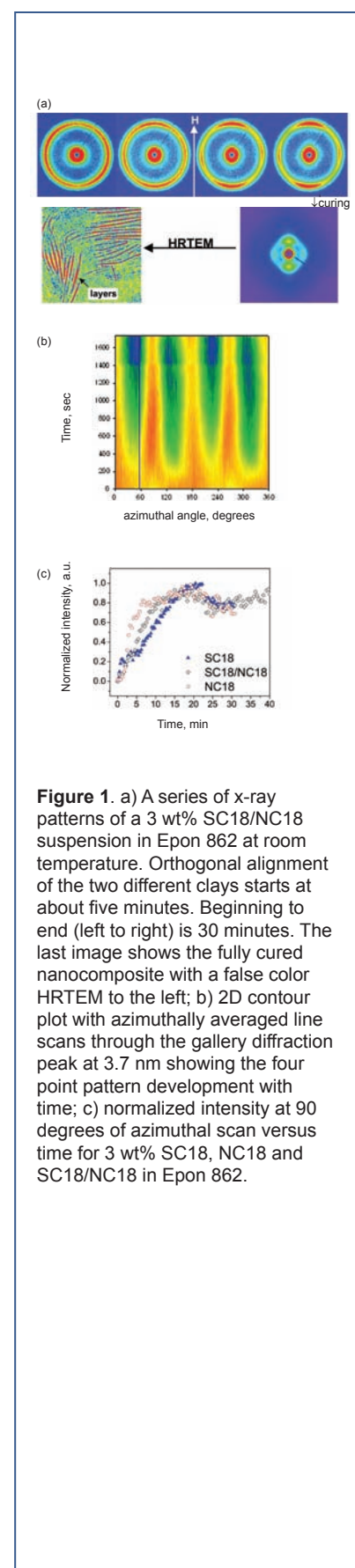


Figure 1. a) A series of x-ray patterns of a 3 wt% SC18/NC18 suspension in Epon 862 at room temperature. Orthogonal alignment of the two different clays starts at about five minutes. Beginning to end (left to right) is 30 minutes. The last image shows the fully cured nanocomposite with a false color HRTEM to the left; b) 2D contour plot with azimuthally averaged line scans through the gallery diffraction peak at 3.7 nm showing the four point pattern development with time; c) normalized intensity at 90 degrees of azimuthal scan versus time for 3 wt% SC18, NC18 and SC18/NC18 in Epon 862.

BEAMLINE U4B**Funding**

Engineering and Physical Sciences Research Council

Publication

L.-A. Míchez, C.H. Marrows, P. Steadman, B.J. Hickey, D.A. Arena, J. Dvorak, H.-L. Zhang, D.G. Bucknall and S. Langridge," *Appl. Phys. Letts.*, **86**, 112502 (2005).

For More Information

C.H. Marrows, School of Physics and Astronomy, E. C. Stoner Laboratory, University of Leeds, United Kingdom

Email: c.h.marrows@leeds.ac.uk

Resonant X-ray Scattering from a Magnetic Multilayer Reflection Grating

L.-A. Míchez¹, C.H. Marrows¹, P. Steadman^{1,2}, B.J. Hickey¹, D.A. Arena³, J. Dvorak⁴, H.-L. Zhang⁵, D.G. Bucknall⁵, and S. Langridge⁶

¹School of Physics and Astronomy, E. C. Stoner Laboratory, University of Leeds, United Kingdom; ²Diamond Light Source, Rutherford Appleton Laboratory, United Kingdom; ³National Synchrotron Light Source, Brookhaven National Laboratory; ⁴Department of Physics, Montana State University; ⁵Department of Materials, University of Oxford, United Kingdom; ⁶ISIS Facility, Rutherford Appleton, United Kingdom

Magnetic multilayers exhibit a very diverse range of fundamental phenomena that underpin much of the data-storage technology we now rely upon, and are of great interest in the emergent technology of spin-electronics. Recently, techniques have allowed the patterning of such systems so that all three spatial dimensions are accessible and controllable at the nanoscale, but it is important to determine how the magnetic microstructure responds to the physical structures imposed upon it. Using soft x-ray magnetic resonant scattering we have studied this behaviour in a system in which the physical structure was deliberately patterned to observe the response of the magnetism to such a perturbation. We found that the magnetisation only tracks the highest Fourier components of the physical structure effectively.

It is well known that the competition between the interaction energies in a ferromagnetic material may lead to the formation of magnetic domains — regions in which there is microscopic ordering of the electron spin to minimise the free energy. If we then impose a physical in-plane pattern on this system, we will have additional competition introduced through the physical shape of the magnetic element. Such a situation has led to the proposal to use patterned arrays to provide ultra-high magnetic storage densities and move beyond the super-paramagnetic limit, in which the magnetic structure becomes thermally unstable ($>100\text{Gb/in}^2$).

To more fully understand this interaction we have prepared antiferromagnetically coupled multilayers of cobalt/ruthenium (Co/Ru) with a nominal structure $[\text{Co}(4\text{nm})/\text{Ru}(3.4\text{nm})]_{x10}$ on top of a polystyrene (PS) line array. The array was produced by micro-contact printing, in which a mold is pressed into the PS at a pressure of 10 kPa to produce a line array with a 400 nm period and a 1:1 mark/space ratio. The advantage of such a technique is that large-area patterning is readily achievable. A scanning electron micrograph of the completed sample is shown in **Figure 1**.

Numerous techniques exist to study the structural morphology of multilayers. However, studying the magnetic structure of the *buried* layers of this patterned Co/Ru multilayer requires a scattering technique such as soft x-ray resonant magnetic scattering (XRMS). By tuning the incident photon energy to the L_{III} absorption edge of the Co (778eV) we can observe both structural morphology and the cross-correlation of the magnetic structure with the physical structure. The diffraction pattern from such a grating structure is shown in **Figure 2a**. In the XRMS measurement we can either change the helicity of the circularly polarized photons or reverse the magnetization of the sample (curves I_+ , I_- in **Figure 2a**). The sum of these two data (**Figure 2b**) is related to the self-correlation of the physical structure whilst the difference is sensitive to the cross-correlation of the physical and magnetic structures. A very sensitive measure is then to plot the asymmetry ratio $(I_+ - I_-)/(I_+ + I_-)$ (**Figure 2c**). Only the first harmonic is present in **Figure 2c**, clearly showing that the magnetic in-plane wave form is significantly different from that of the structural one. The



Chris Marrows

results suggest that the magnetic structure only tracks the gross features of the physical structure, *i.e.* the fundamental period of the physical grating. However, it does not track the finer details that are present in the structural data as higher order harmonics (**Figure 2b**), but are very weak in the asymmetry ratio (**Figure 2c**).

We are complementing these measurements by using polarized neutron scattering, magnetic microscopy, and micromagnetic simulations. This apparent smoothing of the magnetic structure must be accounted for in any patterned recording media based on this type of technology.

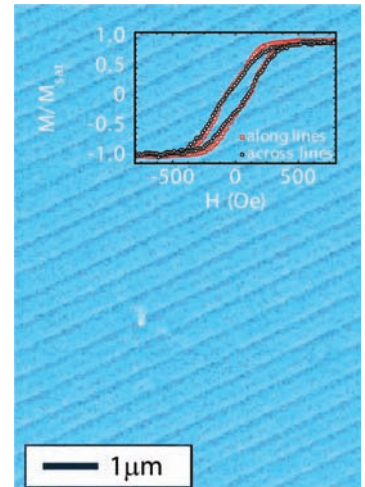


Figure 1. A scanning electron micrograph of the multilayer-coated PS line array. The inset shows the magnetization loop, measured by MOKE, parallel and perpendicular to the line direction. Parallel to the lines is a slightly easier magnetization axis.

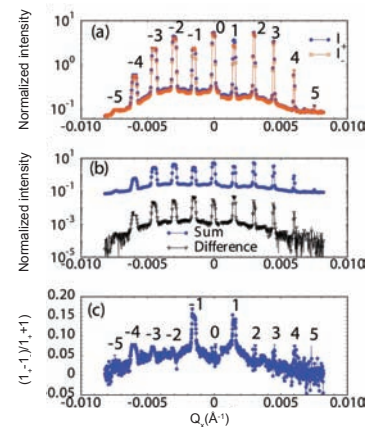


Figure 2. (a) The diffraction pattern from the PS line array. Q_x is the in-plane momentum wave-vector transfer (parallel to the sample surface). The two curves represent the magnetization of the sample. (b) The average and difference of the data presented in panel (a). (c) The asymmetry ratio as defined in the text showing the strong suppression of the higher-order Fourier harmonics.

BEAMLINE X27C

Funding

The National Science Council of Taiwan

Publication

R.-M. Ho, Y.-W. Chiang, C.-C. Lin, and B.-H. Huang, "Crystallization and Melting Behavior of Poly(ϵ -caprolactone) under Physical Confinement," *Macromolecules*, **38**, 4769-4779 (2005).

For More Information

Rong-Ming Ho, Department of Chemical Engineering, National Tsing Hua University, Taiwan

Email: rmho@mx.nthu.edu.tw

Crystallization and Melting Behavior of Poly(ϵ -caprolactone) Under Physical Confinement

R.-M. Ho¹, Y.-W. Chiang¹, C.-C. Lin², and B.-H. Huang²

¹Department of Chemical Engineering, National Tsing Hua University, Taiwan; ²Department of Chemistry, National Chung Hsing University, Taiwan

*We studied the crystallization behavior of poly(ϵ -caprolactone) (PCL) in a physically confined system, the self-assembly of poly(ϵ -caprolactone)/polystyrene-*b*-poly(ethylene-propylene) (PCL/PS-PEP) blends, using simultaneous small-angle x-ray scattering (SAXS) and wide-angle x-ray diffraction (WAXD). The glassy PS-rich phases effectively confined the PCL crystallization due to the localization behavior of PCL. Contrary to a typical microphase-separated morphology of semi-crystalline copolymers (i.e. a chemically confined system), the physically confined system for the crystallization of PCL provides a representative system for understanding crystallization behavior under spatial confinement. With effective confinement, the crystalline chains of PCL appeared in a random orientation at low crystallization temperatures but in a parallel orientation at high crystallization temperatures.*

Crystallization behavior under nanoscale confinement has drawn attention due to the necessity of having a basic understanding of crystallization in order to develop nanotechnology applications. In particular, the crystallization behavior of semi-crystalline block copolymers, in which at least one of the constituted blocks is crystallizable, has been thoroughly studied as illustrated in **Figure 1a** (namely, a chemical confinement). By contrast, the unique morphology with a crystallizable PCL component localized between the lamellar microdomains of PS-PEP gives rise to a specific crystallization environment in which the crystallization is carried out in a nanometer-scale confined environment without the restraint of a chemical connection (**Figure 1b**, a physical confinement). This unique morphology, a crystallizable PCL component localized favorably within PS-rich constituted lamellar in a PS-PEP block copolymer, has been obtained via melt-mixing in a MiniMax mixer. Shear (velocity), vorticity, and velocity gradient directions are labeled *x*, *y*, and *z*, respectively. Two-dimensional SAXS patterns along the *x*, *y*, and *z* directions indicate that microphase-separated microdomains can be oriented after melt-mixing, as illustrated in **Figure 2** for PCL11/PS-PEP blends (the M_w of PCL11 is 11000g/mol). Up to four orders of lamellar scattering peaks ($q/q^* = 1 : 2 : 3 : 4$) can be identified when the incident x-ray beams are along *x* and *y*, as shown in **Figures 2a and 2b**. By contrast, we found no significant scattering peak along the *z* direction in the two-dimensional SAXS pattern (**Figure 2c**). These two-dimensional SAXS results indicate that microphase-separated lamellae of PCL11/PS-PEP are aligned parallel to the *x-y* plane (i.e. the shear plane). Moreover, the oriented microphase-separated lamellar microstructure was preserved after PCL crystallization so that the PCL is completely confined in the PS-PEP lamellar layer.

For PCL crystallization at low crystallization temperatures (for instance, at $T_c = -20^\circ\text{C}$), the two-dimensional WAXD patterns exhibit a typical ring pattern in all directions, suggesting that PCL crystals appear randomly oriented under confinement. However, a specific orientation of the PCL crystals can be identified when the shear-aligned samples are crystallized at high crystallization temperatures (for instance, 40°C). Two-dimensional WAXD patterns along the *x* and *y* directions are practically identical, and exhibit oriented features (**Figures 2d**



Authors (from left) Yeo-Wan Chiang and Rong-Ming Ho

and 2e). Only an isotropic ring pattern along the z direction was observed (Figure 2f). On the basis of the orthorhombic lattice structure of PCL crystals with a unit cell of $a=0.749$ nm, $b=0.498$ nm, $c=1.703$ nm, and $\alpha = \beta = \gamma = 90^\circ$, the corresponding reflections were identified as $\{110\}$ and $\{200\}$. The azimuthal profiles (Figure 3a) were obtained from the two-dimensional WAXD pattern (Figure 2d). The intense $\{110\}$ diffraction peaks are separated into four diffraction arcs and appear at $\Phi=56^\circ$, 124° , 236° , and 304° , and two $\{200\}$ reflections appear at $\Phi=0^\circ$, 180° , respectively. According to the azimuthal results, the diffraction pattern is illustrated in Figure 3b. The fiber-pattern-like diffractions suggest a parallel-type orientation with PCL crystalline chains parallel to the microphase-separated lamellae (i.e. the x and y directions). Figure 3c shows the molecular disposition of crystalline PCL chains, and indicates their parallel orientation at high crystallization temperatures in a physically confined environment. The crystalline orientation is strongly dependent upon the crystallization temperature under physical confinement. As a result, the orientation of the PCL crystalline chain localized between the PS-PEP layers can be thoroughly understood by two-dimensional SAXS and WAXD techniques at a synchrotron light source.

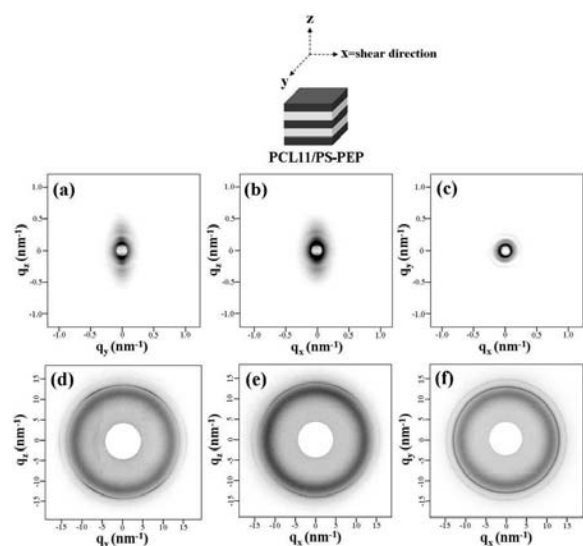


Figure 2. Simultaneous SAXS and WAXD patterns of orientated PCL11/PS-PEP samples isothermally crystallized at 40°C from ordered melt at 100°C . 2D SAXS (top row) and 2D WAXD (bottom row) obtained (a,d) along the x-direction, (b,c) along the y-direction, and (c,f) along the z-direction.

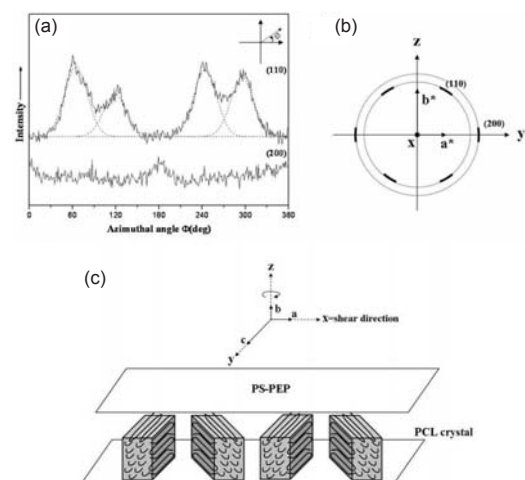


Figure 3. (a) Azimuthal scanning profiles of the $\{110\}$ and $\{200\}$ reflections of the WAXD patterns in Figure 2d for the PCL11/PS-PEP blends isothermally crystallized at 40°C . (b) Schematic diagram of the WAXD pattern with indexed reflections. (c) Schematic diagram of the microstructure of orientated PCL11/PS-PEP samples isothermally crystallized at 40°C from ordered melt at 100°C . The crystallization of PCL is confined between the preformed lamellar PS layers, and the a and c axes of the PCL crystals are preferentially parallel and perpendicular to the axes of the PS lamellar normal, respectively.

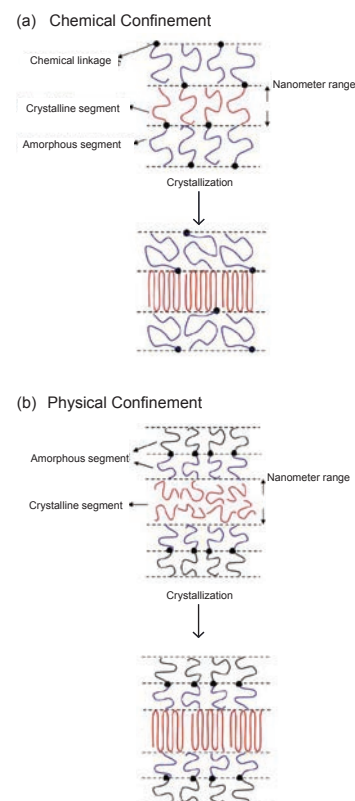


Figure 1. Schematic pictures of (a) chemical confinement and (b) physical confinement.

BEAMLINE X21**Funding**

Marie Curie Program of the European Union

Publication

Taco Nicolai, Fabrice Lafleche, and Alain Gibaud, "Jamming and Crystallization of Polymeric Micelles," *Macromolecules*, **37**, 8066-8071 (2004).

For More Information

Taco Nicolai, Polymères, Colloïdes, Interfaces, UMR CNRS, Université du Maine

Email: Taco.Nicolai@univ-lemans.fr



Authors (from left) Alain Gibaud and Taco Nicolai

Jamming and Crystallization of Polymeric Micelles

T. Nicolai¹, F. Lafleche¹, and A. Gibaud²

¹Polymères, Colloïdes, Interfaces, UMR CNRS, Université du Maine, France; ²Laboratoire de Physique de l'Etat Condensé, UMR CNRS, Université du Maine, France

Polymeric micelles formed by hydrophobically end-capped poly(ethylene oxide) (PEO) copolymers in water show a discontinuous liquid-solid transition, which occurs above a critical concentration that increases with increasing temperature. The solid state contains a body-centered cubic phase in equilibrium with a disordered phase. The fraction of crystalline phase increases with increasing concentration and decreasing temperature. A comparison of the structure and the rheology during cooling shows that the micelles jam before the ordered phase is formed. The discontinuous liquid-solid transition and the distinct bcc phase over a wide range of concentrations are not observed for true star polymers. The difference is perhaps due to the adjustment of the number of arms in the case of close packed polymeric micelles.

Polymeric micelles are formed by the association of block copolymers with a relatively small insoluble block. They show an abrupt transition from a free-flowing liquid to solid-like behaviour above a critical concentration or below a critical temperature. Generally, liquid crystalline order is observed in the solid state. The coincidence between the liquid-solid transition and the appearance of liquid crystalline order has induced some authors to conclude that the solidification is a result of micelle ordering. The objective of our work was to investigate in more detail the correspondence between the liquid-solid transition and the formation of the ordered phase.

We studied poly(ethylene oxide) (PEO) with a molar mass of 4500 g/mol that was end-capped with octadecyl. In water, this polymer forms micelles containing 24 chains. With increasing polymer concentration, the viscosity increases similarly to that observed for equivalent star polymers. However, above a critical concentration that increases with increasing temperature, a discontinuous transition is observed and PEO goes from a viscous liquid to a solid that does not flow when the sample is tilted. The transition, which can also be observed by cooling the sample at a fixed concentration, is fast at temperatures far below the critical value, but can take more than 10 hours just below the critical temperature.

Small-angle x-ray scattering (SAXS) shows narrow Bragg peaks in the solid state, indicating a body-centred cubic phase. However, the amplitude of the peaks is very small when the sample is close to the transition and becomes progressively larger with increasing concentration or decreasing temperature. The underlying amorphous structure can still be clearly distinguished, showing that the solid contains both a crystalline and a disordered phase in equilibrium. The position of the Bragg peaks is independent of the temperature, but shifts to lower scattering wave vectors with increasing concentration. The concentration dependence of the peak position shows that the aggregation number of the micelles in the solid state increases with increasing concentration.

Figure 1 shows, for the same concentration (300 g/L), a comparison of the variation of the shear modulus and the structure factor during a cooling ramp. It is clear that the liquid-solid transition occurs at a higher temperature than the formation of the bcc phase, even though the cooling rate was much faster

for the shear measurement. This implies that the crystalline phase is formed only after the micelles have jammed and, thus, that the formation of the ordered structure is not the origin of the liquid-solid transition.

Polymeric micelles resemble multi-arm star polymers and their behavior is similar at low-volume fractions. The viscosity of true star polymer solutions increases steeply above the overlap concentration, but the increase is continuous. In addition, liquid crystalline order is rarely, and only with difficulty, observed for concentrated star polymers. The essential difference between star polymers and polymeric micelles is that in the latter case the number of arms is variable, which gives the system an extra degree of freedom to minimize the free energy. This is probably the origin of the observed differences.

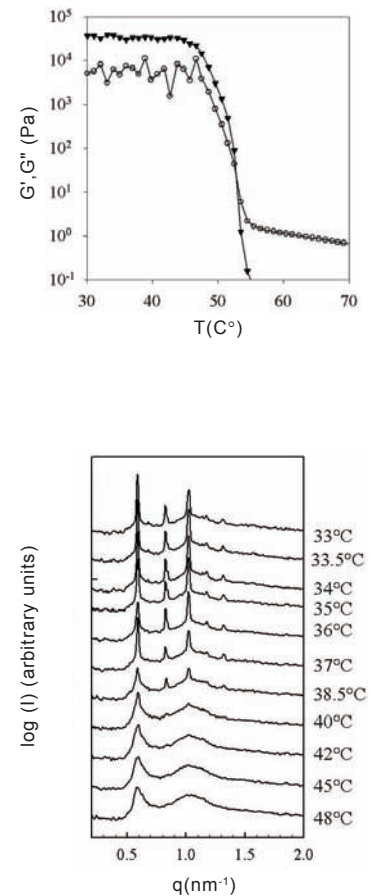


Figure 1. Comparison of the evolution of the shear moduli (top) and the SAXS spectra (bottom) during cooling for suspensions of polymeric micelles at 300g/L. The cooling rate for the rheology experiment was faster (5 degrees/min) than for the SAXS experiment (less than 1 degree/min).

BEAMLINE X3A2**Funding**

Eastman Chemical Company

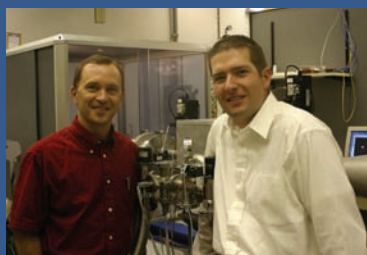
Publication

G.C. Gemeinhardt and R.B. Moore, "Characterization of Ionomer Compatibilized Blend Morphology Using Synchrotron Small Angle X-ray Scattering," *Macromolecules*, **38**, 2813-2819 (2005).

For More Information

Robert B. Moore, Department of Polymer Science, The University of Southern Mississippi

Email: rbmoore@usm.edu



Authors (from left) Robert Moore and Greg Gemeinhardt

Characterization of Ionomer Compatibilized Blend Morphology Using Synchrotron Small-Angle X-ray Scattering

G.C. Gemeinhardt and R.B. Moore

Department of Polymer Science, The University of Southern Mississippi

Synchrotron small-angle x-ray scattering (SAXS) was used to characterize the morphology of a non-crystalline polyester/polyamide blend. The blend's components were made compatible via the addition of a sulfonated, polyester copolymer (that is also an ionomer). We used a two-component correlation function to provide detailed information on the size and structure of the phase-separated domains. With increasing ionic functionality, achieved by varying either the ion content or the ionomer loading, the sizes of the dispersed domains in the blends decreased. In addition, SAXS analysis of the 50/50 blend series indicated that the ionic incorporation led to a shift in the morphology to a more elongated, co-continuous structure.

While small-angle laser light scattering (SALS) has often been used to investigate the micro-scale phase separation of polymer blends, small-angle neutron scattering (SANS) and small-angle x-ray scattering (SAXS) are particularly useful in the study of these complex heterogeneous systems due to their ability to probe much smaller size scales. Although SANS has been used to probe information such as the radius of gyration, correlation lengths, and Flory-Huggins interaction parameters of blend components, recent reports have outlined the advantages of using synchrotron SAXS to measure these important blend parameters. The advantages of using SAXS over SANS include: the elimination of isotopic labeling, the high intensity/resolution that allows for fast data collection, and the ability to dynamically examine the phase-separation process in real time.

In the area of blend compatibilization, research efforts using SAXS have been primarily limited to studying the effect of block copolymers on blend morphology and interfacial properties. Here, we describe our efforts to apply synchrotron SAXS to an amorphous polyester (PETG)/polyamide (T40) blend system. This system is compatibilized through the incorporation of an ionomer (known as SPETG) that bears charged groups capable of forming strong, specific intermolecular interactions with the uncharged, polar blend components. In these blends, the specific interactions (**Figure 1**) act at the interface to lower the interfacial tension and thereby lower the domain size of the dispersed phase.

With SAXS, we investigated the morphological features of the blends using the Debye-Bueche scattering theory, employing a two-parameter correlation function. The resulting scattering curves of the binary blends are shown in **Figure 2**. The solid lines represent the nonlinear regression fits (using the inset equation) to the scattering data and show the excellent agreement between the theoretical and experimental curves. As shown in the inset graph, the two-parameter correlation function divides the scattering into contributions from short-range (a_1) and long-range (a_2) fluctuations present in the system. The relative contribution of each is described by the fractional contribution term, f .

In comparison to the blend with pure PETG, the scattering curves for the

SPETG/T40 samples show a prominent increase in intensity at small values of q . This scattering behavior indicates a decrease in the dimensions of the dispersed phase with the incorporation of functional groups capable of forming intermolecular interactions. From the fits for the SPETG/T40 blend series, the short-range correlation length decreases by 17.6% with increasing ion content, which indicates that the size of the minor phase domain becomes smaller with increasing ion content. In contrast, the long-range correlation length remains relatively constant, while the interfacial surface area of the minor phase (calculated from the volume fractions and values of a_1) increases dramatically with increasing ion content. These trends suggest that the minor phase adopts a more elongated structure and indicate the onset of dual-phase continuity with increasing ion content. A SAXS analysis of the ternary blends containing less than 10% ionomer indicates that these blends behave like the binary blends with varying ion content, as both methods of blending vary only the concentration of ionic functional groups in the blend.

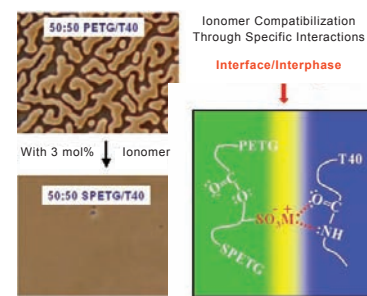


Figure 1. Role of the ionomer (SPETG) in the compatibilization of 50/50 blends of polyamide (T40) and polyester (PETG) binary system. Optical micrographs (left) show that the ionomer yields a profound decrease in dispersed phase size (i.e., below the resolution limit of visible light microscopy/scattering methods).

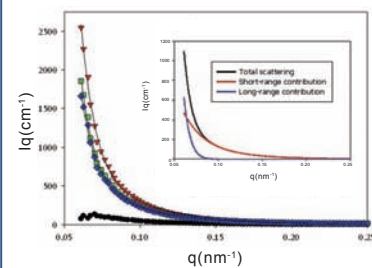


Figure 2. SAXS profiles for the 50/50 polyamide/polyester binary blends: T40/PETG (●), T40/1.9SPETG (▼), T40/3.0SPETG (■) and T40/5.5SPETG (◆). Lines represent the fits to the data from the nonlinear regression analysis using the inset equation. The inset graph shows the relative contribution of the short-range and long-range correlation terms in the nonlinear regression analysis of the measured intensity profiles.

BEAMLINE U7A

Funding

National Science Foundation, Office of Naval Research

Publication

L. Andruzzi, A. Hexemer, X. Li, C. Ober, E. Kramer, G. Galli, E. Chiellini, and D. Fischer, "Control of Surface Properties Using Fluorinated Polymer Brushes Produced by Surface-Initiated Controlled Radical Polymerization," *Langmuir*, **20**, 10498-10506 (2004).

For More Information

Christopher Ober, Francis Norwood Bard Professor of Materials Engineering, Cornell University

Email: cober@ccmr.cornell.edu



Authors (from left) Alex Hexemer and Daniel Fischer

Control of Surface Properties Using Fluorinated Polymer Brushes Produced by Surface-Initiated Controlled Radical Polymerization

L. Andruzzi¹, A. Hexemer², X. Li¹, C.K. Ober¹, E.J. Kramer², G. Galli³, E. Chiellini³, and D. Fischer⁴

¹Cornell University; ²University of California; ³Università di Pisa; ⁴National Institute of Standards and Technology

Fluorinated polymers possess the important technological property of having very low surface energy. One familiar fluoropolymer is Teflon. When a surface prepared using a polymer that contains a fluorinated component is thermally annealed above its glass transition temperature, the low-energy fluorinated component will migrate to the air-coating interface. We are interested in fluorinated block copolymers for the creation of environmentally friendly, fouling-resistant coatings for marine applications. Anyone who owns a boat will know that it can quickly foul, that is, its hull can become coated with a biofilm created by marine flora and fauna. Fluoropolymers may permit the easy removal of foulants without the need for the toxic materials presently used in marine coatings. In a prime candidate for such a coating, surface segregation of a fluorinated block in a block copolymer can be effectively studied by near-edge x-ray absorption fine structure (NEXAFS) and detected by the presence of a sharp peak at 292.0 eV due to the $C\ 1s \rightarrow \sigma_{C-F}^$ transition in the spectrum of Auger electron yield versus energy of the incident x-ray photon. In collaboration with researchers from the National Institute of Standards and Technology (NIST), NEXAFS studies are proving vital in understanding the surface properties of fluoropolymers.*

Grafting a fluoropolymer to a surface seems like an ideal way to coat a substrate with a low-energy polymer. When a block copolymer containing a polystyrene block and a fluorinated block has the free end of the polystyrene block tethered to a substrate, and is then annealed under vacuum, there are surprising results. The mobility of the fluorinated block is so restricted due to chemical bonding with the surface that the air-polymer interface is populated with the higher surface-energy polystyrene block. These were some of the important findings in the paper by Andruzzi et al. [L. Andruzzi, A. Hexemer, X. Li, C. K. Ober, E. J. Kramer, G. Galli, E. Chiellini, D. A. Fisher, *Langmuir*, **20**, 10498-10506 (2004)]. Andruzzi and coworkers prepared fluorinated block copolymer brushes using surface-initiated controlled free radical polymerization. The polymerization reactions were set into motion by initiator molecules covalently bound to a silicon substrate. The thicknesses of the brushes were found to be greater than the radius of gyration of the block copolymer molecules. This indicated that the tethered polymer chains were densely packed on the surface and were in a stretched configuration. The dense packing was also evident when a surface with a tethered polystyrene block and a free fluorinated block had a NEXAFS spectrum almost identical to a fluorinated homopolymer surface. In other words, the polystyrene block in this case was hidden below at least the top 3 nm of the surface, the depth probed by NEXAFS. This was also confirmed by x-ray photoelectron spectroscopy measurements.

The fluorinated block copolymers we studied are unique because of their liquid crystalline properties. The fluoroalkyl side-chains of the block copolymer formed a liquid crystalline phase at the surface, with the $-(CF_2)-$ helices oriented at an angle to the surface. This orientation was quantified from the observed variation in the intensities of the peak at 292.0 eV with the angle of

incidence of the x-ray beam on the surface. We found that a longer fluorinated block resulted in a higher-order parameter of the $-(CF_2)-$ helix. The well-packed fluorinated brushes showed a remarkable stability against reconstruction of the non-polar surface when immersed in a polar environment such as water. There was only a small decrease in the water contact angle when the surfaces were immersed in water for a week.

We propose that, in addition to their fouling-resistant properties, surfaces bearing tethered fluorinated polymer brushes could be used to fabricate analytical devices for microbiology studies, and to create devices for the separation or microfiltration of proteins.

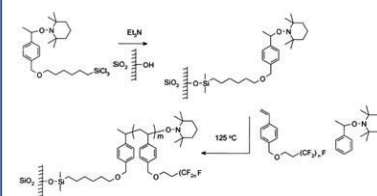


Figure 1. Synthesis of surface-grown fluorinated block copolymer brushes.

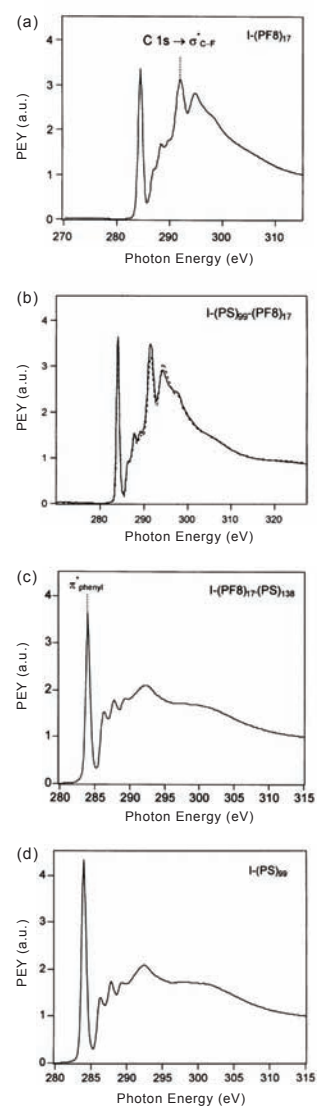
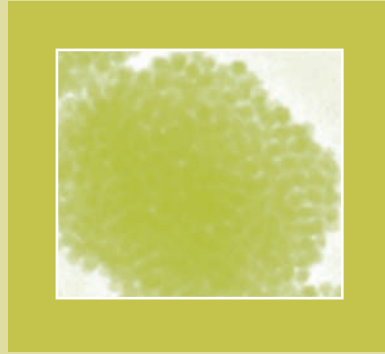


Figure 2. Carbon K-edge NEXAFS spectra of (a) fluorinated brush, (b) block copolymer brush with polystyrene block tethered to surface, (c) block copolymer brush with fluorinated block tethered to surface, and (d) polystyrene brush.



Year in Review

Short Course Participants Learn the Value of Synchrotron Light for Powder Diffraction

January 25-27, 2005

Fifteen participants recently attended the High Resolution Powder Diffraction Data Collection and Analysis Short Course, which was held at the NSLS from January 25-27, 2005. The 3-day course consisted of lectures, guest talks, hands-on data collection, and data analysis, and was co-organized by Peter Stephens (Stony Brook), Christie Nelson (NSLS), and Chi-Chang Kao (NSLS), with administrative support provided by Corinne Messana (NSLS).



Participants of the 2005 High Resolution Powder Diffraction Data Collection and Analysis Short Course

The 15 participants included graduate students, post-docs, and scientists from national labs and universities. While most of the students were familiar with lab-based powder diffraction techniques, very few had synchrotron experience. The participants were all quite eager to learn about the impact that synchrotron-based powder diffraction could have on their own research.

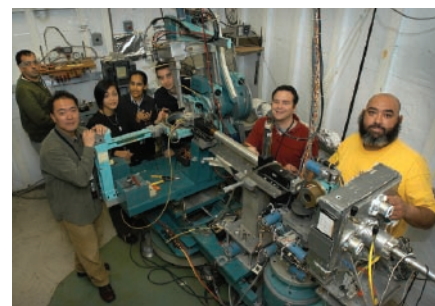
The lectures were presented by Peter Stephens, Pat Woodward (Ohio State), and John Parise (Stony Brook), and covered the basic physics of powder diffraction, experimental aspects of data collection, Rietveld refinement, and indexing. In addition, specialized talks on cutting edge research on high-pressure, high-temperature, and time-resolved powder diffraction were given by guest speakers Yongjae Lee (BNL-CMP), Cam Hubbard (ORNL), and Jonathon Hanson (BNL-Chemistry), respectively.

The hands-on data collection component of the course was carried out on NSLS beamlines X3B1, X7A, and X14A, with beamline instructors Peter Stephens, Yongjae Lee, and Ji-anming Bai (ORNL), respectively. The participants first learned about beamline operation and sample preparation,



Data collection at beamline X3B1

and then collected data from a corundum standard. Next, the participants collected high-resolution data from samples of interest in their own research projects.



Setting up at beamline X7A

In addition to the lectures and data collection, the participants also spent time learning about data analysis techniques. "Homework" assignments included refining the corundum standard data as well as additional data sets, and then students tackled the data obtained from their own samples. The participants were greatly aided in the completion of these tasks by their three lecturers.

At the end of the intensive three-day course, the participants left with a foundation of knowledge about applying high-resolution powder diffraction to their own research projects. Many expressed interest in becoming NSLS general users, and we look forward to seeing them back here soon.

The organizers would like to thank the lecturers, guest speakers, beamline instructors, Elaine Dimasi (NSLS), Jae-Hyuk Her (Stony Brook), Corinne Messana, and the NSLS User Administration Office and safety staff for all of their help in making the short course such a success.

— Christie Nelson

NSLS Engineer John Skaritka Wins BNL's Engineering Award

January 26, 2005

At the BNL Employee Recognition Award Ceremony held on January 26, 2005, NSLS engineer, John Skaritka was presented with a 2005 Engineering Award by BNL's Deputy Director for Operations, Michael Bebon. The award, consisting of a plaque and \$5,000, was also presented to BNL employees Ove Dyling, Joseph Harder, and Alan Raphael.



John Skaritka

The award recognizes distinguished contributions to BNL's engineering and computing objectives over one or more years. Contributions may be in any engineering or computing discipline. Nominees are evaluated on the exceptional nature and level of difficulty of the contributions as well as their benefit to the Lab.

John Skaritka was cited for a body of work that contains semi-

nal as well as sustained contributions. His many achievements speak collectively to outstanding breadth, creativity, drive, and dedication in support of BNL missions.

Skaritka was the sole mechanical engineer for BNL's Accelerator Test Facility (ATF) for many years, making key contributions to the design of elements of the accelerator and experiments that were essential to the success of those projects. He contributed to the design of ATF Gun III and Gun IV, regarded now as standard in the world and running at many other facilities.

He was also the mechanical engineer in charge of coordinating all mechanical design, fabrication, and installation activities at the Source Development Laboratory, resulting in a state-of-the-art facility that produced both a self-amplified spontaneous emission free electron laser and a high gain harmonic generation free electron laser.

Skaritka is also known for his considerable talent in supporting the NSLS User Science programs, recently, for example, in the construction of a unique instrument pivotal in research on three-dimensional strain mapping to study crack propagation and fatigue failure in alloys.

— Liz Seubert

Unique Global Light Source Website Launched

February 17, 2005

On February 17, 2005, the international light source community launched the first website dedicated to providing the media, general public, and scientific community with the latest news and information on the world's accelerator-driven light sources (synchrotrons and free-electron lasers) and the science they produce.



The web site — www.lightsources.org — was developed and is jointly maintained by the Light Source Communicators Group, whose members represent the world's light source facilities in

Europe, North America and Asia. Funding for the project is provided by science funding agencies of many nations.

Accelerator-driven light sources can be large, roughly circular machines or linear machines (usually about the size of a football field to much larger) that accelerate electrons to almost the speed of light. They act like gigantic microscopes that generate intense beams of brilliant light to view the microstructure of materials.

Light sources around the world are advancing research and development in fields as diverse as medicine, drug design,

environmental science, agriculture, minerals explorations, advanced materials, forensics, engineering, and materials fabrication.

Visit www.lightsources.org for the latest news releases on cutting-edge areas of advanced light source applications for science and technology from facilities around the world.

Anyone can subscribe free of charge to "News Flash," which will email subscribers when news releases and other light source information are posted to the website. Also available on the website are an image bank of light source-related photos and graphics, clippings of news stories, links to light source facility websites, and relevant articles and presentations.

Educators will find links to websites relating to light sources and the science conducted at these facilities. Researchers can find specific information regarding each light source facility, including job opportunities and events related to science outreach activities.

Sponsors of this collaborative project include:

- Advanced Light Source (ALS)
- Advanced Photon Source (APS)
- Canadian Light Source (CLS)
- ELETTRA (Sincrotrone Trieste)
- European Synchrotron Radiation Facility (ESRF)
- Hamburger Synchrotronstrahlungs Labor (HASYLAB)
- National Synchrotron Radiation Research Center (NSRRC)
- National Synchrotron Light Source (NSLS)
- Photon Factory (KEK Laboratory)
- Pohang Light Source (PLS)
- Stanford Synchrotron Radiation Laboratory (SSRL)
- SPring-8
- Synchrotron Radiation Center (SRC)
- Synchrotron Ultraviolet Radiation Facility (SURF III)
- Swiss Light Source (SLS)
- The Free-Electron Laser at the Thomas Jefferson National Accelerator Facility (JLab)

X6A Workbench Provides Hands-On Training in Synchrotron Crystallography

March 1-4, 2005

Beamline X6A, the National Institute of General Medical Sciences facility at the National Synchrotron Light Source, offers comprehensive hands-on training in synchrotron data collection and analysis for biophysicists, biochemists, and molecular biologists.



X6A Workbench: Advanced Structural Biology Tools workshop participants

The first “The X6A Workbench: Advanced Structural Biology Tools” workshop took place this year from March 1-4. Participants practiced cryogenic protection of their samples and learned how to load sample cassettes for the X6A automounter. The program followed with hands-on crystallography data collection and analysis. Molecular replacement and multiwavelength anomalous diffraction

(MAD) software suites were discussed. Participants screened their own samples and applied the new data-analysis concepts introduced during the workshop.

The X6A workbench is regularly offered throughout the year. The other three workshops were held on April 26-29, July 12-15, and October 25-28. For more details and registration information, go to: <http://protein.nsls.bnl.gov/news/workbench.php>.

— Vivian Stojanoff

BNLers Help Promote Community Interest in Science

March 4, 2005

Two BNL “Peters” — Peter Wanderer of the Superconducting Magnet Division and Peter Takacs of the Instrumentation Division — are not only passionate about doing their own science



Three BNLers who volunteer time with the Long Island Sciencenter are (from left) Peter Takacs, Marty Woodle, and Peter Wanderer, who are examining model bridges used for demonstration during a recent bridge-building program at the Sciencenter. The bridges are loaned by BNL’s Office of Educational Programs (OEP), examples of previous years’ bridges made for BNL’s annual high-school model bridge-building contest. Woodle, a founder technical advisor in the organization of the contest, helped OEP in this past year’s event that was held on March 12.

but also about spreading the fascination of science to others in the community. That’s how they came to join a group of people who formed a board and set up the Long Island Sciencenter, a new science museum in Riverhead.

“It’s been a busy time,” says Wanderer. “We are still working on the museum and getting more exhibits.” Through the BNL Science Museum, some key current exhibits have been lent to the Sciencenter by the Lab, for example, the Videosphere.

“The BNL Science Museum staff and directors, first Janet Tempel, then Dolores O’Connor, and now, Gail Donoghue, have been very helpful,” Wanderer says.

Another BNLer, retiree Marty Woodle, now a National Synchrotron Light Source Department guest scientist, is a keen Sciencenter supporter. Woodle most recently volunteered his help with a bridge-building program held in late February.

“This March, the Sciencenter is presenting an adult lecture series open to the public, with three interesting talks,” says Takacs. “I believe people at BNL would enjoy them.”

Three LI Sciencenter Lectures, March 4, 11, and 18 were:

- March 4: “Wine: Science or Magic,” Louisa Thomas Hargrave, founder of the first winery on Long Island.

- March 11: “The History and Destiny of Fisheries near Long Island and in the World,” Carl Safina, President, Blue Ocean Institute, Cold Spring Harbor.

- March 18: “The Adventure of Wildlife Photography,” George Loweth, professional photographer.

— Liz Seubert

Scientists Create, Study Methane Hydrates in “Ocean Floor” Lab

Data may help develop strategies for mining natural gas locked up in seafloor sediments

March 13, 2005

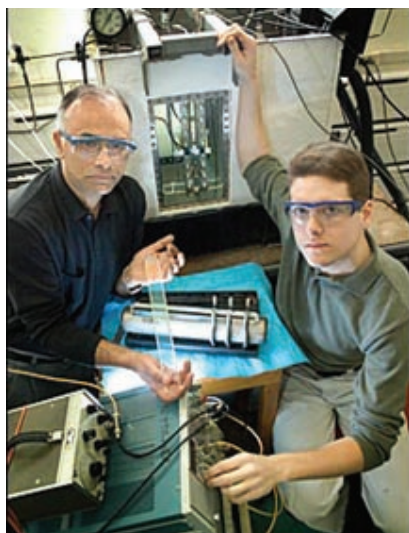
Scientists at BNL have recreated the high-pressure, low-temperature conditions of the seafloor in a tabletop apparatus for the study of methane-hydrates, an abundant but currently out-of-reach source of natural gas trapped within sediments below the ocean floor. Michael Eaton, a Stony Brook University graduate student working for Brookhaven chemist Devinder Mahajan, presented a talk outlining the use of the apparatus for the creation and study of methane hydrates during a special two-day symposium co-organized by Mahajan at the 229th National Meeting of the American Chemical Society in San Diego, California. The talk took place on Sunday, March 13, at 3:05 p.m. in room Madeleine C-D of the Hyatt Regency.

“The amount of natural gas that is tied up in methane hydrates beneath the seafloor and in permafrost on Earth is several orders of magnitude higher than all other known conventional

sources of natural gas — enough to meet our energy needs for several decades,” Mahajan says. But extracting this resource poses several challenges.

For one thing, methane hydrates — which are ice-like cages made of water molecules surrounding individual methane molecules — are only stable at the very low temperatures and high pressures present at the ocean floor. “If you try to bring it up, these things fizzle and decompose, releasing the trapped methane,” Mahajan says.

So a multi-agency team led by the Department of Energy — as part of its mission to secure America’s future energy needs — is trying to learn about the conditions necessary for keeping hydrates locked up so they can be extracted safely and tapped for fuel.



Devinder Mahajan (left) and Michael Eaton

Mahajan’s group has built a vessel that mimics the seafloor temperature and pressure conditions, where they can study the kinetics of methane hydrate formation and decomposition. Unlike other high-pressure research vessels, the Brookhaven apparatus allows scientists to interchange vessels of different volumes, study even fine sediments, and visualize and record the entire hydrate-forming event

through a 12-inch window along the vessel. In addition, mass-balance instrumentation allows the Brookhaven group to collect reproducible data in the bench-top unit. Even better, Mahajan says, they can study the kinetics in actual samples of sediment that once contained hydrates — as close to the natural conditions as you can get in a lab.

“You fill the vessel with water and sediment, put in methane gas, and cool it down under high pressure. After a few hours, the hydrates form. You can actually see it. They look like ice, but they are not. They are stable at 4 degrees Celsius,” he explains.

One further advantage of doing this work at Brookhaven Lab is that the scientists can use the NSLS — a source of intense x-rays, ultraviolet, and infrared light — to measure physical characteristics of the sediments under study. Using x-ray computed microtomography, the scientists gain information about the porosity and other physical characteristics that may affect the availability of nucleation sites where hydrates can form.

Such data about hydrate formation in natural host sediment samples are scarce. By studying different samples and learn-

ing what combinations of pressure and temperature keep the methane locked up, the scientists hope to identify ways to compensate for the changes the hydrates experience as they are brought to the ocean’s surface so they can be extracted with a minimum loss. The comparisons of different sediment samples might also help pinpoint the most abundant sources of locked-up methane.

“It may be at least a decade before we can even think about mining these deposits, but answering these fundamental questions is certainly the place to start,” says Mahajan, who holds a joint appointment as a Stony Brook University professor. “This is a very important issue tied to our future national energy security.”

This research was initially funded by Brookhaven’s Laboratory Directed Research and Development program and is now funded by the Department of Energy’s Office of Fossil Energy. The symposium on Gas Hydrates and Clathrates was co-sponsored by the Petroleum and Fuel Divisions of the American Chemical Society.

— Karen McNulty Walsh

Ceria Nanoparticle Experiments at NSLS Promise Cleaner Fuel Future

March 15, 2005

Experiments on ceria (cerium oxide) nanoparticles carried out at BNL may lead to catalytic converters that are better at cleaning up auto exhaust, and/or to more-efficient ways of generating hydrogen — a promising zero-emission fuel for the future. Jose Rodriguez of the Chemistry Department presented results from two studies exploring the composition, structure, and reactivity of these versatile nanoparticles during the 229th National Meeting of the American Chemical Society on March 15 in San Diego, California. This research was funded by the Office of Basic Energy Sciences within DOE’s Office of Science.

After using a novel technique to synthesize the ceria nanoparticles, Rodriguez and coworkers Xianqin Wang and Jonathan Hanson, also both of Chemistry, used beams of x-rays at the NSLS to study how their composition, structure, and reactivity changed in response to doping with zirconium in one case, and impregnation with gold in another.

“In a catalytic converter, ceria acts as a buffer, absorbing or releasing oxygen depending on the conditions of the engine to maintain the catalyst in its optimum operating condition for converting harmful emissions such as carbon monoxide and nitrogen oxide to carbon dioxide and nitrogen gas,” Rodriguez said. Others have found that adding zirconium improves ceria’s ability to store and release oxygen.

The studies at the NSLS explain why zirconium changes



Jonathan Hanson

the ceria's structure to increase the number of oxygen "vacancies" — or places for oxygen uptake and release.

Furthermore, Rodriguez said, "The ceria nanoparticles we studied have much better performance, higher chemical reactivity, than the bulk form of ceria currently used in catalytic converters."

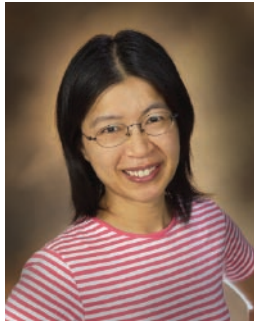
Thus, this research holds promise for more efficient catalytic converters — and cleaner air.

In the second study, Wang, Hanson, and Rodriguez deposited gold on the surface of ceria nanoparticles and used x-rays at the NSLS to determine the catalyst's "active phase" — the conformation responsible for the catalytic activity — in the conversion of water and carbon monoxide to hydrogen gas and carbon dioxide.

This "water-gas shift" reaction is important for generating hydrogen, which can be used for chemical transformations and as a fuel in a hydrogen-based economy. Hydrogen is one of the leading energy sources being investigated by scientists sponsored by DOE as part of its mission to ensure the nation's future energy needs.

"In both cases, we are learning about the fundamental conditions necessary for optimal operation of the catalysts," Rodriguez said. "This kind of knowledge eventually will lead to a rational design of even more effective catalysts."

— Karen McNulty Walsh



Xianqin Wang



Jose Rodriguez



Tom Seda

supplies the initial high energy electrons for the NSLS.

While Seda has not yet worked on plumbing on the job, he has constructed and programmed a single-chip programmable logic device (PLD) to handle the timing that controls the Linac's electron gun. The PLD replaces three logic chassis that control the release of electrons from the electron gun, the origin of electron bunches for x-rays, infrared light and ultraviolet light for experiments at the NSLS.

Seda is now a senior technical specialist assigned to the Operations Group at the NSLS and his primary task is to work on a new design for the extraction magnets of the NSLS Booster Ring. The current magnets — which kick electron bunches at an energy of 800 MeV into the NSLS storage rings, where the energy is ramped up to 2.8 billion eV — are encased in a vacuum chamber.

"The problem with the current design is the short power pulse has to be fed through long conductors to get into the vacuum-encased pulse magnet, known as a kicker. That's not an efficient way to bump the beam," Seda said. "I'm going to try to redesign the system with the pulse magnet outside the vacuum chamber. That would make storing the beam much less troublesome."

The kicker magnets date back to 1983, when the Booster was built, and they are constructed with the standard ferrites that were available at the time. Seda is now investigating newer ferrites for these magnets — specific ferrite alloys currently manufactured for the next generation high-energy accelerators. "We may be able to reconfigure our current bunch patterns with the faster kicker magnets," he said.

"I'm researching the current papers on kicker designs as well as speaking with the scientist and design engineers at other national laboratories," said Seda. "They have been very helpful in identifying vendors who may have the materials and manufacturing skills needed for the new design."

In the past, Seda had constructed and tested a new modulator for the Deep Ultraviolet Free Electron Laser energy upgrade, and he worked on two klystron units in the accelerator Test Facility, which supply RF power to a linear accelerator for advanced laser experiments. Among his suggestions was to replace the PCB-contaminated oil in the klystrons with biodegradable oil.

What Do You Do At Work?

Tom Seda: Bringing Bright Ideas to the Light Source

March 18, 2005

This story was the first in a series entitled "What Do You Do at Work?" featuring BNL employees and their jobs at the Lab.

When I first came to BNL in 1992, I was told that I'd be working on everything from plumbing to programming," said Tom Seda, then a principal technician for the Power Systems Group at NSLS, specializing in the Linac, the linear accelerator that

Seda also helped to test the Marx generator section of the Sandia Pulser Terra Watt Laser, which BNL tested for DOE's Sandia National Laboratory. For his exceptional job performance on this project coupled with helping recover the NSLS after only one week of downtime due to an equipment fire, he is a two-time winner of the BNL Spotlight Award.

"Working as a technician at the NSLS brings opportunities to be involved in all aspects of electronics, with the added benefit of being involved in interesting and ever-changing projects," Seda commented. "I love working firsthand with these amazing machines along with dedicated, talented employees who often go beyond what is expected of them on the job."

Born in the Philippines, Seda, who is of Puerto Rican and Filipino descent, immigrated to the Bronx, NY, with his family when he was an infant. The first in his family to earn a college degree, he received a B.S. in electronic engineering technology from the DeVry Institute of Technology, Chicago, Illinois, in 1988. He then worked as a technician at Magneto of Holtsville, NY, where his responsibilities included designing custom military-grade transformers and inductors, before he joined BNL in February, 1992.

Seda is married to Anna Seda, an administrative assistant in the Energy Sciences & Technology Department. The couple has an 8-year-old son and a 2-year-old daughter. Tom Seda is the president of the BERA Camping Club, and both Anna and Tom Seda are participants in the BERA kickboxing class offered on site. In addition, he and his wife enjoy traveling abroad and going on cruises.

— Diane Greenberg

Brookhaven Town Honors Two BNL Scientists

March 22, 2005

Two BNL scientists — Rita Goldstein and Lisa Miller — were among 11 women honored for their accomplishments at the Brookhaven Town-sponsored Women's Recognition Night at Brookhaven Town Hall on March 22. Goldstein and Miller were recognized for their contributions to science in the Town ceremony, which celebrates National Women's History Month.

Lisa Miller, a biophysicist at the NSLS, uses infrared light and x-rays at the NSLS to study the chemical composition of bone tissue in diseases such as osteoarthritis and osteoporosis. She also investigates protein-folding diseases, such as Alzheimer's disease and scrapie, the sheep form of mad cow disease, in which specific proteins in the brain fold into incorrect shapes and cause damage to brain cells.

Miller also plays an important role in science education and the public understanding of science. She often mentors students from high school to the postgraduate level. In addition, Miller

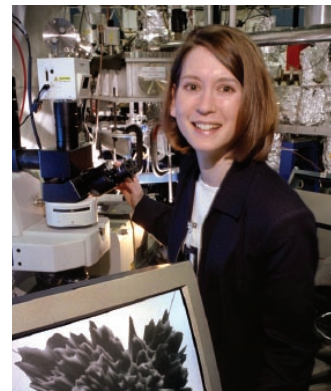
is responsible for outreach activities on behalf of the NSLS, including publications, the website and tours. For example, she organizes an annual open house at the NSLS for BNL's Summer Sundays, when the Lab's facilities are open to the public.

"I am very pleased to receive this honor from Brookhaven Town," Miller said. "I'm glad that my research is recognized, and I am happy that many of the students I've mentored have chosen to pursue scientific careers."

Miller earned a B.S. in chemistry from John Carroll University in 1989, an M.S. in chemistry from Georgetown University in 1992, and a Ph.D. in biophysics from the Albert Einstein College of Medicine in 1995. After serving as a postdoctoral fellow at Lawrence Berkeley National Laboratory and BNL, she joined BNL in 1999 as an assistant biophysicist, and she was promoted to biophysicist in 2003. Since 2002, she also has been an adjunct assistant professor in Stony Brook University's Department of Biomedical Engineering.

This year, Miller was invited to serve on the scientific advisory committee of the Canadian Light Source, a role served only by world-class scientists. For her work with students, Miller received DOE's Outstanding Mentor Award in 2002.

— Diane Greenberg



Lisa Miller

EnviroSuite: Environmental Science at the NSLS

March 30, 2005

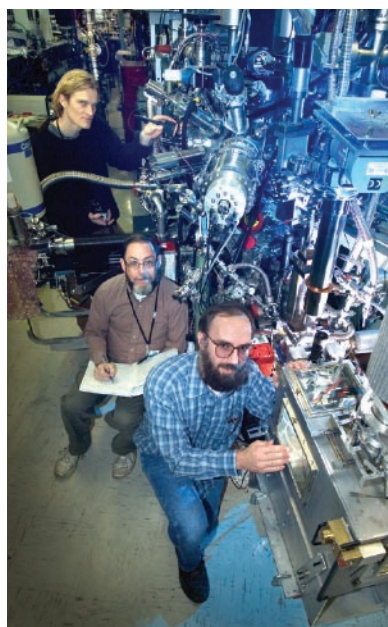
Created in response to rapidly growing interest in environmental synchrotron science, the EnviroSuite Strategic Initiative is designed to support and develop a suite of state-of-the-art resources at the NSLS for molecular environmental science research. Its mission is to optimize and expand synchrotron-based techniques for exploring environmental questions, to establish substantial involvement in several beamlines to bring a multifaceted approach to complex environmental processes, and to introduce new users to these capabilities at the NSLS. EnviroSuite now provides a unified voice for the diverse community of environmental science users.

EnviroSuite is coordinated by the Environmental Research and Technology Division of BNL's Environmental Sciences Department, and is funded by the DOE Office of Biological & Environmental Research, Environmental Remediation Sciences Division (BER:ERSD). Similar programs have been initiated

at all four DOE synchrotron facilities. Its BNL core consists of a number of environmental scientists, who work closely with the NSLS and with CEMS, the NSF/DOE-funded Center for Environmental Molecular Science based at Stony Brook (www.cems.stonybrook.edu).

EnviroSuite is taking an active role in both PRT and NSLS facility beamlines, in order to direct the course of beamline development and harness the resources to conduct leading research. As a result, both capital funding and scientific staff have been brought to the NSLS. Some of these are described in more detail below. In addition, a key goal of the EnviroSuite program is to establish the framework for multi-beamline studies, such as combining bulk EXAFS with microspectroscopy and imaging of elemental and species distributions.

NSLS facility beamline X27A, a new hard X-ray microprobe beamline, was highlighted in the December 2004 NSLS Newsletter. It has a $5 \times 15 \mu\text{m}$ spot size at 3.5 - 32 keV, a 13-element solid state detector, and control software modeled after the beamline X26A system. EnviroSuite collaborated with the NSLS, X26A, and CEMS for the design and commissioning of X27A, and provided the detector. This beamline will greatly increase available microbeam resources at the NSLS. Environmental applications include X-ray fluorescence microanalysis of trace elements, mapping of their distribution, and microspectroscopy.



Environmental scientists (from left) Jeff Fitts (EnviroSuite Coordinator), Mark Fuhrmann (X11 Spokesperson), and Paul Northrup (X15B Spokesperson) at the X15B end station.

Beamline X11 is one of the most scientifically productive and historically important beamlines at the NSLS, being used primarily for bulk EXAFS experiments. It has an unfocused beam ($0.5 \times 10 \text{ mm}$), and operates in the energy range from 4.5 - 35 keV. It is versatile, and can accommodate a variety of sample types as well as in-situ studies. EnviroSuite is adding a new 13-element Ge detector to X11A, to enhance its capabilities for low-concentration and otherwise challenging environmental samples. Detector capability at X11B will also be upgraded.

Beamline X15B is designed for low- to medium-energy bulk and surface XAS (optimized for 1.7 - 5 keV). It has a 1 mm focused spot size, and can address samples in ultra-high vacuum or air/He atmosphere. Current research includes phosphorus, sulfur,

and silicon K-edge, cadmium L-edge, and uranium and lead M-edge spectroscopy.

Beamline X1A is a soft X-ray beamline used for scanning transmission x-ray spectromicroscopy. Its primary emphasis is on organic materials at the carbon and oxygen absorption edges. With a resolution of $\sim 30 \text{ nm}$, X1A is well-suited for imaging molecular chemical features on a sub-cellular scale, such as for research exploring mechanisms of biotransformation of radioactive and toxic species. Recent upgrades include a BER: ERSD-funded laser interferometer.

EnviroSuite provides guidance for new and experienced general users with environmental science research at these and other beamlines. BNL Environmental Science Department resources include laboratory facilities for handling radioactive and hazardous materials and wastes, and for sample preparation. Experimental protocols are being developed to facilitate safe handling and analysis of samples containing radionuclides. For further information, see the EnviroSuite web page (www.bnl.gov/envirosuite) or contact Jeff Fitts (fitts@bnl.gov).

— Paul Northrup

Crystallographers Bloom at RapiData 2005

April 5-11, 2005

Once again in the spring, nearly 50 budding crystallographers from around the world gathered at Brookhaven National Laboratory for RapiData 2005, a week-long course designed to introduce students to the best people, newest equipment, and latest techniques in the field of macromolecular x-ray crystallography.

The course is offered annually by Brookhaven's Biology and NSLS departments, and is always a successful event for participants and instructors alike. In 2005, it ran from April 5 to 11.

The course began with two days of lectures and tutorials taught by scientists from Brookhaven, industry, academia, and other national labs. Then, the instructors and other participants guided the students through a marathon, 60-hour data-collection session on eight NSLS beamlines. Half of the 48 students came with their own specimens to analyze, while the other half learned as observers. Six students left with solved structures that may be publishable in scientific journals.

The course was organized primarily by Bob Sweet and Denise Robertson of Biology. However, they emphasize that its success absolutely depended on enthusiastic help from most of the 24 members of the PXRR (the Biology and NSLS Macromolecular Crystallography Research Resource), NSLS staff members, and several outside teachers.

The majority of the funding for the course comes from the National Institutes of Health's National Center for Research Resources and the Office of Biological & Environmental



Participants in the RapiData 2005 Macromolecular Crystallography course

Research within the U.S. Department of Energy's Office of Science. Additional support is provided by the NSLS and several equipment vendors and drug companies. For more information, go to: www.px.nsls.bnl.gov/RapiData2005/

— Laura Mgrdichian

CFN Site Dedication Draws Special Guests to the NSLS

April 15, 2005

Several distinguished guests visited the NSLS on April 15 as part of activities for the Center for Functional Nanomaterials (CFN) site dedication ceremony. The guests included Congressman David Hobson, Chairman of the Energy and Water Development Appropriations Subcommittee in the House of Representatives; Congressman Tim Bishop; DOE Office of Science Director Raymond Orbach; and Patricia Dehmer, Associate Director of the Office of Basic Energy Sciences within the Office of Science.

After a welcome by NSLS Chairman Steve Dierker, the group gathered in front of the lobby viewing window, which gives an impressive view of the VUV experimental floor. Dierker then gave an overview of the NSLS and its research. He also discussed the bright, new light source proposed at Brookhaven Lab, NSLS-II, and how the new synchrotron would act as a sister facility to the CFN, complementing and enhancing the nanoscience research to be done there.

On this key theme, Hobson mentioned the cutting-edge, third-generation synchrotrons that exist or are under construction in several other countries. "Nanoscience is a whole new era," he said, that requires advanced machinery. In response, Dierker discussed how NSLS-II would take the U.S. to the forefront of synchrotron science and nanoscience. For example, NSLS-II would use CFN instrumentation to focus its beams down to

very small sizes, enabling studies of nanowires, which are the basis for a new class of electronic circuits.

"NSLS x-rays can't get down to the nanoscale," said Dierker. "We need a powerful new photon microscope, a new technology for a whole new industry."

He continued, "It is the remarkable behavior of materials at the nanoscale that is thought to hold the key to the future of United States energy problems. NSLS-II will give us the tools we need to regain world leadership in this area."

Later, at the site dedication ceremony, the CFN site sign was unveiled by several of the invited dignitaries and BNL leaders. A crowd of BNL employees came out to participate in the event and, after a welcome by Lab Director Praveen Chaudhari, heard remarks by Hobson, Bishop, and Orbach.

In his talk, Orbach touched on NSLS-II and its planned relationship to the CFN. "Think of the two as a team," he said. "Without both, we will be robbed of opportunities that they uniquely can bring. NSLS-II will give us a leg up on every other laboratory in the world."

He also had an important message: "We need to convey to the public what science can and will do, to convey to everyone the nature of scientific enterprise and scientific discovery," he said. "What we're doing here today is conveying that message in a whole new era of opportunity. No one knows the dimensions of discoveries that are present."

"Research into nanomaterials is one of the most exciting things since the microchip," said Hobson. "Right here at Brookhaven, you're getting to be in the middle of that."

Hobson also praised BNL for its status as a basic-energy research lab, stressing that basic research is an essential, but waning, component of U.S. science. "The [DOE] labs are the last areas of basic research in our country," he said. "You should all be very proud of what you're doing."



From left, NSLS Chairman Steve Dierker, Congressman Tim Bishop, Congressman David Hobson, DOE Office of Science Director Raymond Orbach, and BNL Director Praveen Chaudhari.

Bishop was equally supportive. “We have on this site some of the world’s best minds. The CFN will bring more of the best minds here, and Long Island will benefit from that.”

Among other distinguished guests invited to the Lab were Dennis Kovar, Associate Director for Nuclear Physics, who is also DOE landlord of the BNL site; Michael Holland, Manager of DOE’s Brookhaven Site Office; Vice Admiral Dennis McGinn, who is Vice President for Strategic Planning for Battelle; and Robert McGrath, SBU Provost and Executive Vice President for Academic Affairs, who also serves as SBU Vice President for Brookhaven Affairs.

Earlier in the day, the special guests also toured BNL’s Relativistic Heavy Ion Collider and the Positron Emission Tomography facility to learn about the research performed at each. The keynote speaker at the luncheon preceding the event was Shirley Strum Kenny, Stony Brook University (SBU) President and also Vice President of Brookhaven Science Associates, an institution formed of SBU and Battelle, which manages BNL for DOE.

— Laura Mgrdichian

Strain-Mapping Workshop Marked by Enthusiasm and Idea-Sharing

April 18-19, 2005

Useful, lively discussions characterized the recent workshop on Strain Mapping in Engineering Materials with High-Energy Synchrotron X-Rays, held at the NSLS from April 18-19. The workshop brought together researchers in the field of strain mapping to discuss their work and talk about how to advance NSLS strain-mapping capabilities. Some of the talks are summarized below.

Asuri Vasudevan, from the U.S. Navy’s Office of Naval Research, discussed how he works to extend and predict the life of aircraft and helicopters by studying “residual stresses” — the stresses within a material left over after a single or repeated use, which are caused by temperature or the material’s chemical environment. Residual stresses can cause cracks on surfaces that may be stable or unstable. Vasudevan is interested in studying these cracks, but said that the tools available to him limit the size of the crack he can study as well as the sample’s thickness and particular composition.

Mel Roquemore and Ruth Sikorski from the Air Force Research Laboratory addressed the potential applications of strain mapping to evaluate jet engine components. Their aims include using the determined stresses that occur within the engine components to predict and model how complicated engine systems will respond to duty-cycle loading. This information will help them determine how to increase the life of engine components.

Another key speaker was Roger Klaffky, who runs the X-Ray

and Neutron Scattering Facilities program within the U.S. Department of Energy’s Office of Science. He spoke about the DOE’s mission to advance nanoscience research for energy needs, and the advantages of x-ray diffraction in this respect. He also gave examples of current stress/strain research now being done at DOE national labs, such as studying why fractures occur over time in stents and how that process may be stunted.

Additionally, an overview of the NSLS beamlines and user community was presented by NSLS scientist Chi-Chang Kao. He laid out the NSLS three-to-five year plan, which aims to continue the growth of life and geo/environmental science user groups, and attempt to reverse the decline in materials and chemical science users. Other initiatives are to advance the biomedical imaging program here and develop a new nanoscience user base. But in the area of strain mapping using high-



Participants in the Strain-Mapping workshop

energy x-rays, Kao said the NSLS needs to win funding for a new end station dedicated solely to that field.

The scheduled discussion period at the end of the workshop, and the several smaller discussions in between, produced many ideas and ways to bolster the strain-mapping program at the NSLS. The participants compiled a “wishlist” of capabilities they would like to see at X17B1, which is where strain-mapping research is now performed, and described current limitations to their research. For example, they discussed how to decrease the time it takes to make a strain map, which is one limitation that may now prevent industrial users from coming to the NSLS.

The group also talked about potential future beamline X17A, which could free up X17B1 to become a strain-mapping-only beamline. Currently, high-energy x-ray scattering and medical researchers share the limited beamtime at X17B1 with scientists in the strain-mapping program.

— Laura Mgrdichian

Four BNLers Win Environmental Stewardship Awards

April 22, 2005

At the annual Earth Day Awards Ceremony held on April 22 by George Goode, Manager of the Environmental and Waste Management Division, Goode and Peter Bond, Interim Deputy Director for Science & Technology, presented four BNL employees with Environmental Stewardship Awards for demonstrating an outstanding effort in pollution prevention, waste minimization, or conservation. The four were: Mary Ann Corwin, National Synchrotron Light Source Department (NSLS); Michael Kindya, Plant Engineering Division (PE); Michael Paquette, PE; and Joel Scott, Collider-Accelerator Department (C-AD).



George Goode (left) and Peter Bond (right) present the awards to (from left) Joel Scott, Mary Ann Corwin, Michael Paquette, and Michael Kindya.

Mary Anne Corwin, who heads the User Administration Office at the National Synchrotron Light Source (NSLS), was awarded for leading the effort to create a virtually “paperless office.” By using the Lab’s web-based Guest Information System and the NSLS Proposal, Access, Safety and Scheduling (PASS) System, considerable resources were saved by reducing the use of paper copies, improving records retention methods, and recovering office space.

— Liz Seubert

NSLS Daughters and Sons are Forensic Scientists for a Day

April 28, 2005

On April 28, approximately 30 daughters and sons of NSLS staff and scientists questioned suspects, analyzed crime-scene evidence, and caught a thief — all in one morning. The activities were part of the national Take our Daughters and Sons to Work Day. This year at the NSLS, the day had a theme: forensic science.

First, the children gathered in the NSLS seminar room to hear a brief safety talk by Nick Gmur, and then learned about

light in its different forms from NSLS scientist Lisa Miller, in her talk, “What Kind of Light?” The kids guessed which type of light is used in many common objects, such as remote controls and microwave ovens.



NSLS scientist Randy Smith demonstrates the process of “blood”-typing.

After the talk, the main event began. Lisa introduced the crime — The Case of the Missing iPod — and then presented the “evidence” that had been found at the scene: a white powdery substance, a black powdery substance, a strand of hair, and a piece of notebook paper. In a nearby trash basket, there was also a soda can with a drop of “blood” on it.

The “victim,” NSLS student researcher Meghan Ruppel, then told her story. She said she was studying for a test in the library, got up to talk to some friends, and returned to find her iPod missing. Her story revealed several possible suspects: Adele Wang, Meghan’s friend; Michael Appel, the library’s custodian; Laura Mrdichian, the librarian; and Steve Giordano, a library patron. The suspects filed in, told their own stories of what happened, and were questioned by several of the children.

After seeing the evidence, hearing the victim’s and suspects’ stories, and interrogating everyone involved, the daughters and sons split into groups to analyze the evidence. They tested the “blood” on the soda can to determine the blood type, and dusted the can and the victim’s notebook paper for fingerprints. They compared their results with the suspects’ blood types and fingerprints.

Next, the children went down to the NSLS experimental floor. There, NSLS scientists Tony Lanzirotti and Bill Rao helped them analyze hair samples from the suspects using x-rays,



Participants in the NSLS Sons and Daughters Day

which measure the levels of various trace elements (such as zinc, copper, or calcium) that are present in the hair. The analysis yielded a unique “signature” for each sample, which was compared to the signature of the strand of hair found at the crime scene. The group also analyzed the powders found at the crime scene with a synchrotron infrared microscope. They determined that the white powder was powdered sugar and the black powder was ground coffee.

With all the evidence properly analyzed, the daughters and sons returned to the seminar room, knowing who had taken the iPod.

And who was the culprit? Laura the librarian! She took the iPod “because iPods are not allowed in the library.” In her introductory story, she only revealed that she made coffee and ate a powdered doughnut that morning. Caught, however, she further explained that she noticed a soda can on Meghan’s desk and, because food and drinks are not allowed in the library, went over to throw it away.



NSLS scientist Lisa Miller uses a synchrotron infrared microscope to identify the unknown white and black powders.

She cut her finger on the top, leaving a blood drop. Then she noticed the iPod, another forbidden item. She took it, but left behind coffee and sugar powders, a strand of hair, and many fingerprints. The NSLS daughters and sons successfully analyzed these clues to catch the true “thief.”

— Laura Mgrdichian

Women in Science Career Day at BNL

May 9, 2005

Ten female students from the Henry Viscardi School, an Albertson, Long Island-based school for children with physical disabilities and health impairments, learned about scientific careers first-hand from female researchers at BNL. The career day was coordinated by Brookhaven Women in Science and funded by Brookhaven Science Associates. During the day, Jeanne Petschauer (standing, left) from the Community Relations Office gave an overview of BNL’s breadth of scientific interests, and Lisa Miller (right) of the NSLS discussed her path to becoming a chemist and her research on such diseases as osteoarthritis, osteoporosis, and Alzheimer’s disease. Linda Bowerman of the Atmospheric Sciences Division explained some of BNL’s environmental research, and physicist Angelika

Drees described her work with other scientists to discover more about the earliest moments of the universe now being studied at the Relativistic Heavy Ion Collider. Among the students present were (front, from left) Adeline Joshua and Stephanie Avramenko.



— Diane Greenberg

BNL Workshop on Intense Coherent THz Pulses

May 10, 2005

The first workshop on intense coherent THz pulses at Brookhaven National Laboratory (BNL) was held during the spring of 2005. Participants included scientists from regional universities and institutions as well as members of the BNL scientific community.

The workshop focused on the science enabled by linac sources of intense coherent terahertz (THz) radiation. The NSLS Source Development Lab (SDL) linac is one such source, producing 100-microjoule, single-cycle coherent pulses with spectral content reaching to a few THz. The full-day workshop began with a presentation by Xijie Wang (NSLS) that described how the SDL linac produces ultra-short, high-charge electron bunches that generate coherent THz pulses or deep ultraviolet free-electron laser light. Larry Carr (NSLS) followed with a description of the SDL’s THz pulses, including measurements of the pulse energy, spectral content, and electro-optic detection instrumentation. He emphasized applications where the



Participants in the Intense Coherent THz Pulses workshop

THz pulses serve as an excitation source rather than simply a probe of a material's response. Tony Heinz (Columbia University) gave an overview of THz methods, current scientific efforts, and the frontiers opened by a source of high intensity THz pulses. Ivan Bozovic (BNL Materials Science) described ultrafast THz studies of correlated electron systems and complex oxides — material systems of great interest at Brookhaven. Toni Taylor (Los Alamos National Laboratory) presented other THz studies of complex materials in a seminar the following day. The National Institute of Standards and Technology (NIST) uses THz methods to study complex biomolecules. Ted Heilweil (NIST) discussed that activity as well as applications of THz in homeland security and imaging. It has been noted that the magnetic field portion of a THz wave could be sufficient to change the magnetization state of some magnetic alloys, a topic Dario Arena (NSLS) summarized in his talk. The connection between THz and magnetization dynamics was also described in Toni Taylor's presentation.

Attendees were given a tour of the SDL facility and the location for future THz studies. This was followed by a discussion session that helped to define experimental directions and provide recommendations on the facility and instrumentation requirements.

For more details, see <http://www.nsls.bnl.gov/newsroom/events/workshops/THz/>. This workshop was sponsored by the NSLS.

— Larry Carr

A Passion for Synchrotron Science and its Future: News from the 2005 NSLS Annual Users' Meeting

May 23-25, 2005

The speakers at the main session of the 2005 National Synchrotron Light Source (NSLS) Annual Users' Meeting, held on Tuesday, May 24, at Brookhaven National Laboratory (BNL), spoke on many different topics. But they all conveyed fierce enthusiasm for the science performed at the NSLS and expressed hope that its proposed successor, the world-leading NSLS-II, would become a reality.

NSLS Users' Executive Committee Vice-Chair Peter Stephens welcomed the audience to the main meeting, setting a positive and enthusiastic tone for the day's events. He then opened the stage to BNL Director Praveen Chaudhari.

Chaudhari commended many attendees for their work to advance NSLS-II. "You've helped tell us what is needed in this new light source, including the workshop last fall that defined NSLS-II," he said. "The struggle to get NSLS-II is just beginning — we need to design it and then get funding. But once the machine is built, you'll have the best machine in the world, and we need your help to make that happen."



Pat Dehmer (third from right), head of the Office of Basic Energy Sciences within the Department of Energy's Office of Science, was a special guest at the 2005 NSLS Annual Users' Meeting. She stands with (from left) NSLS Associate Chair for User Science Chi-Chang Kao, incoming Users' Executive Committee (UEC) Chair Peter Stephens, NSLS Chairman and Associate Lab Director for Light Sources Steve Dierker, BNL Director Praveen Chaudhari, and outgoing UEC Chair Larry Shapiro.

Chaudhari then introduced Patricia Dehmer, head of the Office of Basic Energy Sciences within the U.S. Department of Energy's Office of Science, who plays an important role in efforts to move NSLS-II forward. Dehmer elaborated further on the status of the proposed new facility and made several key points, many concerning the tough budget years ahead.

The Office of Science, she said, led by Raymond Orbach, has set a philosophy in place for fiscal year 2006: making the U.S. the leader in every major field of research, regardless of the declining budgets to come. "These are very scary times, and being bold and aggressive is probably the only way to face this," she said.

However, her talk was full of encouraging messages. NSLS-II, she said, falls into one of the "mission challenges" of the Office of Basic Energy Sciences — that is, enabling the construction of major scientific facilities.

"NSLS-II will undoubtedly be the world's finest synchrotron; it will be a stunning facility," she said. Soon, she added, she and Orbach will present the Laboratory's NSLS-II proposal to Deputy Secretary of Energy Clay Sell for his approval.

She spoke emphatically to NSLS-II supporters. "I think we have a very high probability for success with NSLS-II. But we need your help, too. You have to understand the realities of the budget and be sophisticated when you talk to folks in Washington. You can't rely on Congress to launch something like NSLS-II — you have to talk to the administration."

In her closing remarks, Dehmer left off on a very positive note. "This laboratory has a wonderful history of constructing and operating major user facilities," she said. "The run of the NSLS has been nothing short of remarkable, and NSLS-II will take that tradition and move it into the future." She also praised

NSLS Chairman Steve Dierker. “Steve has been a superb leader for NSLS-II, and there’s no way we could have made our case to Ray Orbach without him. NSLS-II has moved up in the DOE 20-year plan largely because of Steve’s efforts.”

Dierker, who spoke next, showed the audience that the NSLS continues to thrive, even as third-generation synchrotrons draw more and more users. “We’ve held our own and then some,” he said. “The number of users served by the NSLS has been stable at about 2,300 per year.”

He described the NSLS as “very cost effective, highly productive, and highly reliable.” Since 2001, the facility has met many key goals, such as maintaining and strengthening its user program, expanding its user base, and developing a compelling proposal for NSLS-II.

In addition, there has been a “dramatic” evolution of NSLS beamlines, including better support to several beamlines to make them more useful and modern, and many major beamline upgrades.

Looking into the future, Dierker said he looks forward to continuing user input on NSLS-II. “The community has responded very enthusiastically and vigorously,” he said. “I think we have put forward a compelling design that is critically needed in order to probe materials at high-energy resolution, and at spatial resolutions on the order of one nanometer, which would be unprecedented.”

“There is a host of important and exciting scientific opportunities that will be enabled by NSLS-II,” he concluded. “This is something the U.S. absolutely needs to regain leadership in synchrotron radiation science.”

Next, in the first scientific talk of the day, Henk Schenk of the University of Amsterdam discussed “The Structure of Cocoa Butter and the Quality of Chocolate.” In this interesting presentation, Schenk described his group’s work using x-ray diffraction to study the structure of cocoa butter. Cocoa butter is an essential component of chocolate that determines the



The 2005 NSLS Annual Users' Meeting Planning Committee: (from left) Mary Anne Corwin, Liz Flynn, Melissa Abramowitz, Ron Pindak, Lisa Miller, Dan Fischer, Gretchen Cisco, and Peter Stephens.



Speakers at the main meeting included (from left) Bob Casey (BNL-NSLS), John Rehr (University of Washington), Benjamin Chu (Stony Brook University), and Henk Schenk (University of Amsterdam).

chocolate’s characteristic properties, such as its sheen and meltability. By studying the various phases of cocoa butter via melting-cooling processes, he and his group patented a method to produce chocolate that stays fresh longer than other chocolates, and even devised a chocolate-making machine.

Schenk was followed by a talk on safety delivered by Peter Stephens and Bob Casey, the NSLS Associate Chair for Environment, Safety, Health, and Quality. In a back-and-forth style, Casey and Stephens discussed safety from the point of view of NSLS users and administration, particularly in the wake of the electrical incident last year at the Stanford Linear Accelerator (SLAC). The issues raised during their talk were presented in further detail, and subject to more extensive discussion, at a special “Electrical Safety in the Research Community” workshop the following day.

The workshop covered several topics. NSLS Safety Officer Andrew Ackerman discussed National Fire Protection Association electrical standards implemented at the NSLS. He also elaborated on a new NSLS rule that all electrical devices in the NSLS be certified by a nationally recognized testing laboratory within five years, including equipment brought in by users. He showed several photos of unsafe and/or “homemade” electrical equipment and configurations found on the NSLS floor, which illustrated the need for such rules.

Bob Chmiel, the NSLS Environmental, Safety, and Health engineer, expanded on this. He displayed actual examples of unsafe electrical configurations found during routine NSLS inspections, and encouraged users to routinely check their equipment. Finally, Casey gave a more detailed account of the SLAC incident, the many violations of procedure and practice that led to it, and lessons learned. He also went over some recent NSLS electrical incidents, and the lessons learned from them.

The second scientific talk at the main meeting was delivered by John Rehr of the University of Washington. Rehr spoke



This year's poster session winners were (from left) Tejas Telivala (Stony Brook University), Ashtosh Ganjoo (Lehigh University), Angelo Dragone (BNL-Instrumentation Division), Holger Fleckenstein (SBU), Meghan Ruppel (SBU), and Brandon Chapman (BNL-NSLS).

about the theory involved in interpreting x-ray data obtained from many synchrotron analysis techniques, such as extended x-ray absorption fine structure (EXAFS) and nuclear resonant inelastic x-ray scattering.

In the afternoon, Benjamin Chu from Stony Brook University talked about the polymer experiments he performs with his group at beamline X27C, using wide-angle x-ray diffraction (WAXD) and small-angle x-ray scattering (SAXS). Their end station contains several specialized instruments, such as spinning, stretching, and high-pressure devices, which allow them to investigate various properties of the polymers.



Steve Almo

Next, Steve Almo from the Albert Einstein College of Medicine discussed "Structural Genomics in the 3rd Millenium." Almo said that scientists are solving protein structures at amazing rates, but that the future

of structural biology is determining the structures of protein complexes — many proteins interacting at once. He described a new technique to study proteins, called synchrotron x-ray footprinting, which may help structural biologists look beneath cell membranes to study many cell components at once.



Peter Abbamonte

Finally, NSLS scientist Peter Abbamonte presented his work on antiferromagnetism, a state of magnetism in certain materials in which ions orient themselves into regions of opposite alignment, called "stripes." Antiferromagnetic materials can become superconductors, and Abbamonte and his group are trying to determine if stripes play a role

— do they assist or compete with superconductivity?

At the end of Tuesday's main meeting, the outgoing NSLS Users' Executive Committee Chair, Larry Shapiro, announced the three newest members of the UEC: Chris Jacobsen of Stony Brook University (SBU), Steve Almo, and Chris Cahill of George Washington University. NSLS scientist Lisa Miller, the poster session organizer, announced the poster sessions winners: Brandon Chapman (BNL-NSLS), Angelo Dragone (BNL-Instrumentation), Holger Fleckenstein (SBU), Ashtosh Ganjoo (Lehigh University), Meghan Ruppel (SBU), and Tejas Telivala (SBU).

Later that day, meeting participants attended the evening banquet in Berkner Hall for good food, drinks, and conversation. During dinner, photos of the NSLS and NSLS staff cycled on a large screen at the front of the room, sparking conversations. Stephens also presented the UEC Community Service Award to Tony Lenhard.

After dinner, NSLS historian Robert Crease treated everyone to a bit of history during a special presentation. In a narrative accompanied by old photos, he recounted the days before the NSLS was built, the roadblocks encountered before and during its construction, and the ultimate success of the facility.



NSLS historian Bob Crease took the banquet attendees back in time during his presentation on the history of the NSLS.

During the two days surrounding the main meeting, Monday the 23rd and Wednesday the 25th, several additional workshops were held at locations across the Laboratory. They were "Nanomagnetism: Materials and Probes," "Imaging Nanoscale Structure in Biominerals: New Results and Challenges," "The Impact of Cryogenic Specimen Automounters on the Future of Macromolecular Crystallography," "Spectroscopic Studies of Nanoscaled Systems," "Application of Small-Angle X-Ray Scattering to Biological Structures," and "In-situ Analyses in Environmental and Chemical Systems."

— Laura Mgrdichian

Nanomagnetism: Materials and Probes Workshop

May 23, 2005

The connection between magnetism and nanoscience is clear: The nanometer is the natural length scale of magnetism, as it characterizes the domain wall. Unanticipated phenomena occur when the materials' structural scale coincides with the magnetic length scale. To support research into nanomagnetism, recent advances in materials synthesis and nanofabrication technology have made it possible to create a wide range of nanomagnetic systems with unprecedented precision. These novel magnetic systems are used as model systems for testing longstanding theories in magnetism, as well as for exploring new device concepts and applications. In parallel, synchrotron radiation, with its unique polarization properties, tunability, and time structure, has become an indispensable tool for the study of magnetism and magnetic materials.

The 2005 NSLS Users' Meeting Workshop "Nanomagnetism: Materials and Probes" provided an overview of the latest synchrotron characterization techniques as well as introduced new materials concepts for magnetic materials. The workshop was



Nanomagnetism: Materials and Probes workshop attendees

jointly sponsored by the Brookhaven National Laboratory Center for Functional Nanomaterials, a new U.S. Department of Energy nanoscience user facility. Presentations were delivered by seven experts in the application of synchrotron radiation to magnetic materials, and in the synthesis and application of magnetic nanomaterials, with the goal of presenting an up-to-date snapshot of the forefront issues in nanomagnetism.

Daniel Haskel of the Advanced Photon Source at Argonne National Laboratory inaugurated the workshop with a presentation on recent synchrotron characterization advances that elucidate the role surfaces and interfaces at play in the overall magnetic response, especially in thin-film layered systems.

Professor J.M.D. Coey of Trinity College in Dublin, Ireland, followed with surprising but well-documented results that systems with nominally no d-electrons, such as HfO_2 and RhO_2 , exhibit ferromagnetism under certain conditions. The results are currently attributed to the defect state of the material.

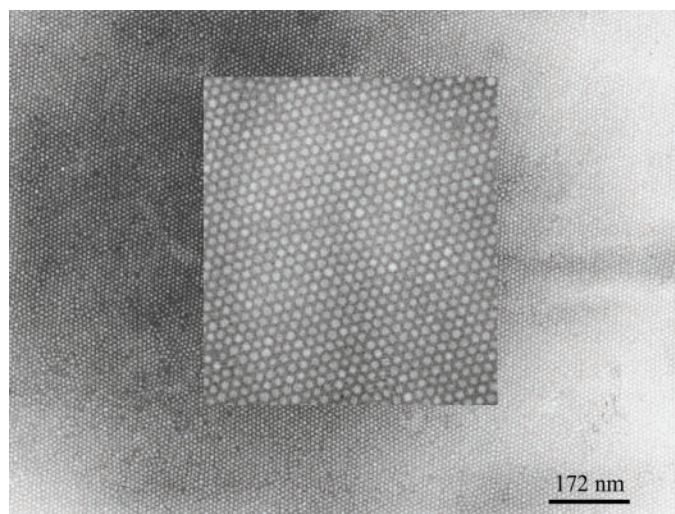


Figure 1. Large view (1.5 mm x 1.5 mm) of uniform ϵ -Co ferromagnetic nanoparticles with a high degree of order induced by lateral compression to form a compressed Langmuir film. The inset shows the presence of dislocations but no grain boundaries in the film. (D. Farrell, Y. Cheng, R.W. McCallum, M. Sachan, and S.A. Majetich, *J. Phys. Chem. B*, **109**(28), 13409-13419 (2005).

Continuing the focus on novel magnetic materials, Distinguished Professor Myriam P. Sarachik of City College-CUNY presented new results on molecular magnets or single-molecule magnets. These systems, which bridge the classical and the quantum worlds, hold potential as quantum computation materials (qubits) and exhibit clear quantum-mechanical tunneling signals under the influence of magnetic fields.

Professor Sara A. Majetich of Carnegie Mellon University discussed recent results obtained from highly uniform monodisperse arrays of ferromagnetic Fe, Co, and FePt nanoparticles (**Figure 1**). The competition between dipolar and anisotropy energies in these systems creates spin-glass-like mictomagnetic behavior, as revealed by small-angle x-ray scattering and small-angle neutron scattering.

Glenn A. Held of the IBM T. J. Watson Research Center in Yorktown Heights, New York, presented an overview of magnetic ferrite nanoparticles encapsulated by biologically active molecules to create bio-functionalized entities for monitoring and influencing cellular processes.

The workshop concluded with two presentations on advanced synchrotron techniques for magnetism characterization. Dario Arena of the NSLS discussed new techniques that probe the dynamics of magnetization precession in the time domain, with element specificity. In this work, time-resolved magnetic circular dichroism in a pump-probe architecture was employed to examine the moment response in permalloy-based systems. Andreas Scholl of Lawrence Berkeley National Laboratory described the application of ultrafast x-ray pulses (picosecond to femtosecond) to image magnetic dynamics with high spatial resolution. As an example of the technique, real-time movies with associated analyses of the precessional dynamics of magnetic vortices were presented.

— Laura H. Lewis and Chi-Chang Kao

Synchrotron Imaging of Biominerals Workshop

May 23, 2005

Biominerals, the mineralized tissues of animals, plants, and microorganisms, have inspired humanity since prehistory. Bones and shells have been used for tools, currency, symbolic objects, and art in every culture. Both the fascination and the importance that biominerals present for science are made clear in Darwin's 19th century writings, and in D'Arcy Wentworth Thompson's 1917 *On Growth and Form*, with its memorable cover illustration of the multi-chambered calcium carbonate nautilus shell.

Now, biomineralization is a field of study in its own right. Biologists, paleontologists, materials chemists, physicists, engineers, and medical professionals all contribute to our understanding of how biominerals grow; how they achieve their submicron hierarchical architectures and their precise control over crystal orientation and habit; how they are able to stabi-



Synchrotron Imaging of Biominerals workshop attendees

lize non-thermodynamically-favored mineral polytypes; and most importantly, how the biomineralization process might be harnessed or mimicked to produce new nanostructured, multi-component materials for medicine and technology.

Recent advances in synchrotron science, as applied to these materials, have uncovered a wealth of new information in the past ten years. Synchrotrons now enable diffraction-enhanced imaging, x-ray microbeam analysis, computed tomography, and phase radiography to probe the microstructures of biominerals. Chemical information is obtained from soft x-ray photoemission and infrared spectromicroscopy techniques, with submicron spatial resolution. High-resolution diffraction, small-angle scattering, and x-ray absorption methods all contribute to the picture of the crystalline and amorphous phases formed. Finally, many of these experiments are sensitive to crucial organic components: the matrix of proteins and polysaccharides that help give biominerals their special properties.

Such new results and challenges were highlighted in a workshop, "Synchrotron Imaging of Biominerals," at the 2005

Annual NSLS Users' Meeting. Our six invited speakers were followed by four short talks from BNL and Stony Brook University scientists, including student presentations. This workshop was also videotaped and is posted on the web at <http://www.solids.bnl.gov/~dimasi/nsls05ws2/>.

Matthias Epple of University Duisburg-Essen, Germany, emphasized the importance of studying well-characterized biological samples in collaboration with biologists, who can help interpret the information. Epple then went on to show how high-resolution powder diffraction, EXAFS, and tomography were used in tandem to obtain structural information from a variety of small animal shells and structural organs. High-resolution measurements are necessary to distinguish between calcite, magnesian calcite, and small amounts of metastable polytypes only observable with synchrotron radiation. In more unusual animals, extremely unlikely minerals, such as calcium sulfate hemihydrate statoliths in deep-sea medusae, were discovered. Finally, selected amorphous calcite carbonate mineral formers were surveyed. Effective measurement of the metastable amorphous biominerals is particularly valuable since biomineralization is thought to often proceed by means of amorphous precursors.



Matthias Epple

Emil Zolotoyabko, from the Technion-Israel Institute of Technology, focused on his newly developed technique for depth-resolved measurements using energy-variable x-ray diffraction. The motivation is that biominerals have complex, multilayered structures. While many synchrotrons have developed micron beam spots to resolve diffraction patterns laterally (across the sample surface), it is necessary to match this spatial resolution in the third direction for a complete picture. Zolotoyabko's technique is based on theoretical analysis of the shapes of diffraction profiles taken under slight misalignment of the diffraction instrument. The interplay between the probability of the x-ray registration in the detecting system and the depth-dependent attenuation of the primary x-ray beam defines at each energy a specific depth from which the maximum diffraction signal is collected. By measuring diffraction profiles at different energies, the depth-dependent effects in the preferred orientation, grain size, microstrain fluctuations, and residual strains could be observed. Zolotoyabko highlighted information obtained from mollusk shells in which microstructural parameters in the successive layers of a material can tell the story of a biomineral growth.



Emil Zolotoyabko

Stuart R. Stock of Northwestern University presented the history and latest advances in x-ray absorption computed microtomography and phase radiography. These non-invasive three-

dimensional imaging techniques can be applied to both medical and materials studies. Stock first gave a detailed discussion of the technique's mathematical basis and practical limitations. He next described how spatial and temporal variations in microstructure could be observed for mouse skull tissue response



Stuart R. Stock

to bone resorption-inducing agents, for the mineralized collagen of regenerated newt limbs, and to study a rabbit model for vascular mineralization, probing treatments to ameliorate the effects of cholesterol. Finally, interesting questions about some similar proteins implicated in skeletal evolution were brought up, contrasting the calcium carbonate skeletons of echinoderms with the calcium phosphate bones of vertebrates: How does the spatial distribution of protein relate

to the microarchitecture and mineral density? Sea-urchin teeth exhibit a remarkable array of materials engineering "tricks" in the design of their composite microstructures, as a *functional* analysis of the images demonstrates.

Gelsomina "pupa" De Stasio, University of Wisconsin - Madison, and Synchrotron Radiation Center. A lively talk from De Stasio showcased SPHINX, an x-ray PEEM spectromicroscope. With monochromatic soft x-rays incident onto the sample surface, photoelectron emission imaging with a



Gelsomina "pupa" De Stasio

field of view of 2 to 200 microns can be accomplished. By scanning the energy, XANES or EXAFS spectra are obtained, with sensitivity to all elements present in biological and mineral systems. This makes chemical and spectroscopic information available with 10 nm spatial resolution. De Stasio discussed wide-ranging examples of biomineralization not previously covered, including the formation of bacterial biofilms and the "reverse-biomineralization" activity of

antifreeze proteins — emphasizing, in all cases, the organic-inorganic interface. She also presented another mystery in mollusk nacre: a polarization dependence, suggesting that the carbonate groups in aragonite do not align along the tablet axis as is currently thought.



Helga Lichtenegger

Helga Lichtenegger, from the Vienna University of Technology, presented research on another unusual family of biominerals: marine worms whose mandibles are reinforced with the copper-based mineral atacamite. Lichtenegger has explored the distribution of copper, zinc and iron in *Glycera* and *Nereis* worm jaws, and the experimental achievement is an elegant combination of microbeam x-ray absorption spectroscopy, diffraction, and small-angle scattering. Each of these

techniques had a necessary role in determining which metals form crystals within the jaws, and which instead are present in trace quantities and may play some role in the tissue other than structural support; and in the case of SAXS, what morphology the mineralized parts exhibit and how that relates to the structure of the whole jaw.

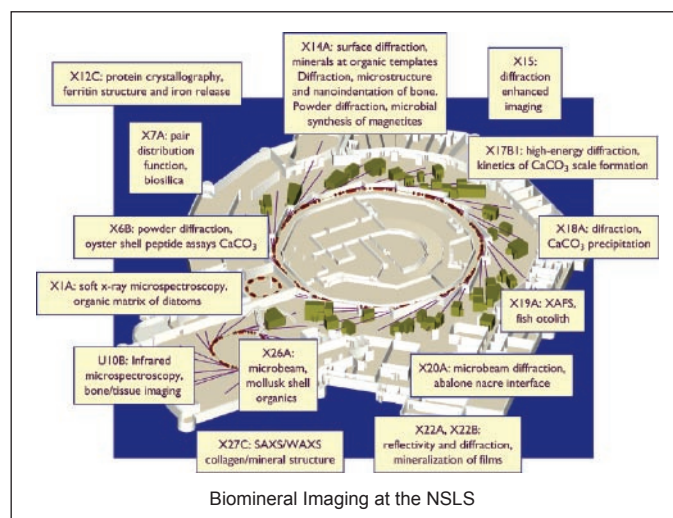
Teresa Nicolson joined us from the Oregon Hearing Research Center and Vollum Institute, Oregon Health and Science University. Nicolson studies the molecular basis of mechanotransduction in sensory hair cells. This research uncovered a puzzle in biomineralization when genes required for hearing and balance in zebrafish were explored. Nicolson demonstrated that a previously unknown gene, *starmaker*, was required for the proper development of the calcium carbonate otoliths or stone-like particles, which serve as balance sensing organs in the ear. The *starmaker* activity was experimentally disrupted in zebrafish embryos. With mild disruption the aragonite mineral otoliths were changed from round to chunky morphologies, and in more excessive cases another calcium carbonate mineral, calcite, was formed. Synchrotron microbeam diffraction was necessary to detect these changes.



Teresa Nicolson

Selected local efforts were showcased in short talks following the invited program. Zhong Zhong (NSLS) presented the superior contrast achieved from Diffraction Enhanced Imaging using x-rays. Meghan Ruppel (NSLS) used infrared spectromicroscopy to compare the chemical makeup of microdamaged versus undamaged bone. Karthikeyan Subburaman (Stony Brook University) described the biomimetic mineralization of synthetic protein films, and Seo-Young Kwak (NSLS) measured the orientation and Mg-incorporation of calcite grown on functionalized self-assembled monolayers.

Interdisciplinary symposia can be a challenge as well as a pleasure for the participants. Aside from the compliments, other



comments (that the organizer, perhaps, was not intended to hear) included: “That was way too technical for me”; “The biology was over my head”; and “Definitely not the way I’m used to thinking about problems.” It’s our hope that such symposia can continue to increase awareness of the problems and methods encountered in a research area like biomineralization, which presents so many faces. For this reason, we are especially appreciative of the support and participation that this workshop received. We would like to thank the NSLS, the NSLS Users’ Executive Committee, the Center for Functional Nanomaterials, and BNL videographer Alex Reben.

— Elaine DiMasi

The Impact of Cryogenic Specimen Automounters on the Future of Macromolecular Crystallography Workshop

May 23, 2005

Cryogenic “automounters” are becoming common at synchrotron x-ray sources and in a few commercial laboratories, employed especially in macromolecular crystallography (PX). There are several commercially available models, and several home-built ones, used in a range of synchrotron radiation sources around the world. This workshop gave the PX community an opportunity to hear the major builders of these instruments describe important features of the operation of their instruments, and the ways the scientific community is using them.

Thomas Earnest’s group at Lawrence Berkeley National Laboratory’s Advanced Light Source (LBL-ALS) designed one of the most imitated automounter systems, based on pneumatic actuators. He summarized their experience at the ALS with the design, now exported to several locations (the NSLS, the Advanced Photon Source (APS), and the Macromolecular Diffraction Facility at the Cornell High-Energy Synchrotron Source (CHESS)). He emphasizes an “open source” view of the design to encourage information sharing and described many small improvements since the original design. They’re working on a Cartesian robot to replace the current system, which would not require the crystal-supply dewar to move, and would have a larger capacity. Dieter Schneider, BNL Biology Department, described his group’s refinement of the LBL-ALS system. They devised a three-jaw gripper that is being adopted at several places, developed innovations that minimize frosting of the lid, and are beginning to develop EPICS-based control. Gerd Rosenbaum, of the Southeast Regional Collaborative Access Team at the APS, described his group’s adaptation of this design. This instrument is just now coming into operation. Quan Hao, CHESS, gave the same sort of report, one innovation being a miniature liquid nitrogen pump for filling the sample dewar, and described his use of a Java-based camera system for sample viewing.

Aina Cohen represented the Stanford Synchrotron Radiation Laboratory (SSRL) robot effort, one of the earliest in the PX community, whose device depends on an industrial robot for flexibility. They have very much experience and have made many refinements to the original system to provide reliability. The SSRL group has developed a web site for sharing ideas about automounters: <http://smb.slac.stanford.edu/robosync/>.

Franck Felisaz, of the Joint Structural Biology Group at the European Synchrotron Radiation Facility’s (ESRF) European Molecular Biology Laboratory (EMBL), Medical Research Council Grenoble, described a robot named SC3 that was developed at the EMBL. Eight of these have been built for ESRF, commercialized through Maatel and marketed through Accel. An especially attractive feature is the software, which can be used with a pocket PC to read bar code labels on crystal-growth trays in order to transfer that information to the data-collection software. Bernard Lavault, also from EMBL, described image-recognition software (“C3D”) for locating and centering crystals on the goniometer. It has an impressive record of finding the real crystal in globs of vitrified liquid. He emphasized the importance of lighting and the ability to vary lighting direction and in-



The Impact of Cryogenic Specimen Automounters on the Future of Macromolecular Crystallography Workshop attendees

tensity. Deming Shu, a member of the instrument-development group at the APS, described their design of a custom robotic system based on a commercial six-axis robot. There are many refinements, in particular a force-sensing gripper.

Several commercially available robotic systems were described as well. Ross Doyle of Mar USA described the MAR Cryogenic Sample Changer, which can be provided as part of MAR dtb (desk-top beamline). This system is used at several places in Europe and at the Structural GenomiX beam line at the APS. Anne Mulichak, a member of the Industrial Macromolecular Crystallography Association Collaborative Access Team (IMCA-CAT) at the APS, described their experience using ACTOR, the six-axis robot produced by Molecular Structure Corporation of The Woodlands, Texas. This instrument is an engineered adaptation of the first such robot ever produced (by Abbott Pharmaceuticals for their internal use). After a few years’ experience at IMCA-CAT the machine is in fairly routine use now. Ehmke Pohl of the Swiss Light Source reported that they purchased one two-Dewar ACTOR system. They put special effort into accurately intersecting the x-ray beam with the crystal, employing x-ray beam position monitors to provide

feedback for 10-micrometer positional stability. They're looking into using ultraviolet sensing together with visible light to locate the sample. Finally, Bob He, from the Bruker-Nonius company of Madison, Wisconsin, described yet another quite successful commercial robot based on a six-axis system. This system has found acceptance in the home-lab small-molecule community, and it works just fine in PX.

An hour and a half were reserved at the end of the workshop for open discussion. Both builders and users seriously discussed the standardization of the fixtures the experimenters use to handle their specimens: crystal "caps" and pins, and the cassettes used to carry the caps to the automount robot. The discussion yielded important, detailed ideas that have been passed on to the American Crystallographic Association Data, Standards, and Computing Committee.

— Robert Sweet

Spectroscopic Studies of Nanoscaled Systems Workshop

May 25, 2005

A workshop titled "Spectroscopic Studies of Nanoscaled Systems" was held on May 25, 2005, as part of the National Synchrotron Light Source 2005 Annual Users' Meeting. This workshop was intended to be a forum on the connection between nanoscience and the physics of interacting electron systems, particularly the occurrence of electronic ordering at the nanoscale in oxides, both in extended crystals and in artificial heterostructures. Our hope was that this session might feed the discussion concerning the correlated electron thrust area at Brookhaven Lab's planned Center for Functional Nanomaterials.

The day opened with a presentation on quantum confinement effects in thin films by Tai Chiang from the University of Illinois. Chiang's group carried out angle-resolved photoemission measurements on thin films of lead and determined a direct correlation between the thermal stability of layers of different thickness and the binding energy of the highest occupied orbital. This stability arises from the confinement of the electron in the direction perpendicular to the film and turns out to be periodic in the layer thickness. This periodicity can be thought of as a one-dimensional analogue of the periodic table.

The next speaker was Seamus Davis from Cornell University, who presented scanning tunneling spectroscopy (STS) measurements of the copper-oxide superconductor $\text{Ca}_{2-x}\text{Na}_x\text{CuO}_2\text{Cl}_2$. In an earlier study this material was reputed to contain an electronic (i.e. Wigner) crystal, and the current presentation contained additional measurements showing spectral weight modulations at a large binding energy (~ 200 meV). These measurements spurred a continuation of the debate over the definition of the term "Wigner crystal" and what

aspect of STS measurements may be thought of as charge order.

After Davis, Ali Yazdani from Princeton University presented similar measurements on underdoped $\text{Bi}_2\text{Sr}_2\text{CaCu}_2\text{O}_{8+\delta}$ with trace quantities of zinc. These STS measurements were carried out in the pseudogap state, i.e. $T_c < T < T^*$. Yazdani observed a "checkerboard" pattern that appears to be electronic in origin, disappears when the sample is cooled into the superconducting state, and was speculated to arise from some competing order responsible for the pseudogap. What relation these measurements have to Davis' Wigner crystal, or to the stripe phases seen with neutron scattering, is still a mystery.

After a lunch break, Girsh Blumberg of Bell Laboratories presented Raman measurements of very lightly doped $\text{La}_2\text{CuO}_{4+y}$ (LCO), as well as the spin ladder material $\text{Sr}_{14}\text{Cu}_{24}\text{O}_{41}$, to characterize the nature of the inhomogeneity in these systems. From his measurements he concludes that the inhomogeneity in LCO is actually two dimensional ("giraffe disorder"), rather than one-dimensional ("zebra disorder").

The discussion turned from intrinsic-occurring order to artificial



Spectroscopic Studies of Nanoscaled Systems Workshop attendees

order with a presentation on quantum wires of underdoped $\text{YBa}_2\text{Cu}_3\text{O}_{6+y}$ by Dale Van Harlingen of the University of Illinois. The Van Harlingen group carried out four-probe transport measurements on such wires and observed quasi-random "telegraph" noise in the IV characteristics. This noise was seen only at temperatures around the pseudogap temperature T^* , and was speculated to arise from stripe domains that exist above T_c and thermally switch at random times. Such switching is not seen in optimally doped wires.

A major topic of discussion at the workshop was whether the physics of oxides differs substantially if patterned into nanostructures. Insight into this subject was provided by Antonio Castro-Neto of Boston University, who gave a theoretical perspective on the edge states that might arise at the surface of a (1,0,0) terminated doped Mott insulator. In a study based on density matrix renormalization group techniques, carried out in collaboration with Stephen White of the University of California at Irvine, Castro-Neto concluded that static stripes form near a terminated surface and, with increasing U , spread out from the bulk and move to the surface. These effects may be important for the properties of transition metal oxide devices.

The session closed with a presentation by Satoshi Okamoto of Columbia University on the subject of electronic reconstruction in oxides with reduced dimensions, such as at surfaces and interfaces in artificial structures. Okamoto carried out a computational study of the interface between LaTiO_3 (a Mott insulator) and SrTiO_3 (a band insulator), and found that the interface between the two is, in fact, highly metallic and exhibits orbital ordering. The precise form of the orbital ordering depends on the thickness of the interface and the geometry of the structure. Such effects may have already been seen by groups at Bell Labs and in Korea.

— Peter Abbamonte and Peter Johnson

Application of SAXS to Biological Structures Workshop

May 25, 2005

The development new synchrotron sources has enabled challenging small-angle x-ray scattering (SAXS) experiments that require extremely small, yet intense x-ray beams. An example is time-resolved scattering from proteins undergoing folding at millisecond or better time resolution. However, the emergence of these new sources does not make SAXS instruments that are based on older second-generation sources, such as the NSLS, obsolete. Instead, these instruments continue to contribute to biology and biomaterials research. This workshop was intended to show the user community how SAXS can be used to facilitate structural studies of biological systems with examples of studies achievable at second-generation synchrotron sources.

The morning session of this workshop focused on solution scattering from proteins and protein complexes. Dmitri Svergun (European Molecular Biology Laboratory) described applications of the low-resolution structural modeling programs developed in his group. These data analysis methods are based on static measurements that do not require very high source brightness. He gave examples for a broad range of sizes, from individual macromolecules to multi-domain proteins and large macromolecular assemblies. Structural modelling of molecular complexes is particularly effective when combined with high-resolution structures of the constituting subunits.

The scattering at higher angles corresponds to structures at smaller length scales. Lee Makowski (Argonne National Laboratory) showed that scattering within this region contains information on the secondary structures and folding motif of the protein. Wide-angle x-ray scattering (WAXS) data can therefore be utilized to quantify the structural difference between protein structures as a distance in the WAXS space. Proteins known to have similar structural motifs have the shortest distances. This method, therefore, may be a sensitive, global method for detecting structural changes in proteins, narrowly categorizing proteins based on their scattering homology to known folds

and elucidating the differences between crystal structures and aqueous conformations.

Scattering from protein solutions is not only capable of charactering the structure of proteins, but also the interaction potential between them. This capability is employed by Annette Tardieu (Centre Nationale de la Recherche Scientifique) to study the conditions that are optimal to obtain protein crystals. The major result from her research is that attraction between protein molecules may be tuned with salt and/or with PEG. The optimal condition depends upon the macromolecular size: With small compact proteins the Hofmeister effect may be sufficient to induce an attractive regime and crystallization, whereas the presence of PEG is required with higher molecular weight complexes.

The last speaker of the morning session was Jack Johnson (The Scripps Research Institute), who studied the maturation of HK97 bacteriophage capsid. This dynamical process proceeds at a moderate speed (on the order of seconds) and was monitored with time-resolved SAXS. This study is a great example of how protein crystallography, electron microscopy, small-



Application of SAXS to Biological Structures Workshop attendees

angle scattering, and fluorescence complement each other to provide a more complete picture of the biological process that may not be elucidated by any of these techniques alone.

The afternoon session moved on to the application of SAXS to more complex structures in biological tissues. Due to the presence of various periodic structures, scattering data from tissues often contain diffraction peaks and there is no uniform method of analyzing the data. Ben Hsiao (Stony Brook University) modeled the shape and position of small-angle diffraction peaks from fish bones. His data analysis quantified the diameter of collagen fibrils, the orientation distribution of fibrils, the coherence length, as well as the mineral (calcium phosphate) dimensions and orientation in the bones. Myosins and actin fibers in muscle also produce diffraction peaks. Leepo Yu (National Institutes of Health) studied the structural change in muscles as the chemical-to-mechanical energy conversion that drives muscle movement takes place. In search for materials for replacing defective heart valves, Jun Liao (University of Pittsburgh) studied candidate tissues under biaxial stretch either with constant force or constant displacement. The response of the tissue gives a good indication of its mechanical integrity.

The workshop also included a brief tour of SAXS beamlines X27C and the newly renovated wiggler-based X21 beamline, and ended with a discussion session during which a number of NSLS SAXS users presented their results.

— Lin Yang

In-Situ Kinetic Analyses in Environmental and Chemical Systems Workshop

May 25, 2005

Natural environmental systems, such as soils, sediments, and subsurface aquifers, are always in a state of disequilibrium. Changes in porewater chemistry, biological activity, and chemical properties, such as particle-water interfacial composition, redox potential, and pH, occur over time scales ranging from microseconds to years. Research on the kinetics of chemical and physical processes at different time scales is essential for understanding the fate and transport of environmental contaminants. A workshop organized by Dean Hesterberg and Jeff Fitts for the NSLS Annual Users' Meeting on May 25, 2005, brought together a multidisciplinary group of scientists who discussed *in-situ* approaches for studying time-dependent chemical processes.

The workshop was dedicated to the memory of the late Dale E. Sayers. Ed Stern (University of Washington) provided a historical perspective on Sayers, discussing how, as a Ph.D. student in 1971, Sayers pioneered (along with Stern and Farrell Lytle) the first correct physical model explaining the extended x-ray absorption fine structure (EXAFS). This breakthrough led to development of XAFS spectroscopy as an analytical tool for determining the local molecular structure of condensed phases. Stern discussed the unique advantages of XAFS spectroscopy in determining short-range structure, valence, local symmetry, and angular deviation of atoms from collinearity. He also described nanosecond-scale time-dependent studies involving laser excitations of atoms in tandem with photon pulses inherent in synchrotron radiation.

Donald L. Sparks (University of Delaware) gave an overview of the importance of understanding the kinetics of reactions and processes in soils and sediments. Given the extreme complexity of such matrices, it is challenging to measure chemical kinetics separate from diffusion. Soil chemical reactions involving inorganic and organic contaminants often show an initially rapid rate followed by a slow approach to steady state, with hysteresis upon reversal. Very short, real-time, molecular-scale analyses are needed to determine chemical kinetics in isolation from transport, and elucidate reaction mechanisms that determine the fate of environmental contaminants.

One promising method for measuring short-term kinetics is Quick-EXAFS. Wolfgang Caliebe (NSLS) compared various Quick-EXAFS systems and showed Quick-EXAFS spectra collected at the NSLS on time scales of seconds. The rate-

limiting component for Quick-EXAFS is typically the detector. The application of time-resolved *in-situ* EXAFS analysis was illustrated for battery materials by Mali Balasubramanian (Advanced Photon Source). These examples showed how quasi-equilibrium states of chemical reactions could be probed on times scales of three to 30 minutes. For example, XAFS spectra revealed how chromium ions migrate between octahedral and tetrahedral positions in Mn-oxide systems.

The precipitation, growth, and crystallization of naturally occurring iron oxides under various redox and pH conditions regulate the mobility of chemicals in the environment by, for example, adsorption and encapsulation. Sam Shaw (Oxford University) described *in-situ*, synchrotron-based time-resolved small-angle x-ray scattering (SAXS) and time-resolved x-ray diffraction (TRXRD) studies that followed the growth of poorly ordered iron oxyhydroxide (ferrihydrite) and its transformation into goethite and hematite, which are more stable crystalline endproducts. Rapid (seconds to minutes) precipitation and crystal growth of ferrihydrite was followed with SAXS using a stopped-flow reaction cell. Adsorption of chemical species such



In-Situ Kinetic Analyses in Environmental and Chemical Systems Workshop attendees

as phosphate on freshly precipitated mineral phases slows the overall crystal growth and retards growth on specific crystal faces. Based on activation energies calculated from TRXRD, ferrihydrite apparently transforms to goethite by dissolution and precipitation and to hematite by solid-state transformations.

John Parise (Stony Brook University) and James D. Martin (North Carolina State University) gave additional examples of using TRXRD to follow chemical kinetics. Parise showed how this technique could be used to optimize the synthesis of a titanium silicate material to maximize its selectivity for cesium, an important radioactive contaminant in nuclear waste. Highly selective binding of this element by ion exchange was attributed to structural distortions in the material. By following total scattering from nanocrystalline materials over time, evolution of the pair-distribution functions for FeS minerals were also determined. Martin used TRXRD coupled with differential scanning calorimetry to study the nucleation and growth of $ZnCl_2$ from melts. The rate of crystal growth was inversely related to the initial temperature of the melt. For sodalite, templating was

found to be critical to crystal growth, with isothermal crystallization only occurring if the melt reached a critical temperature below the melting temperature, which allowed proper ordering of the templating cations.

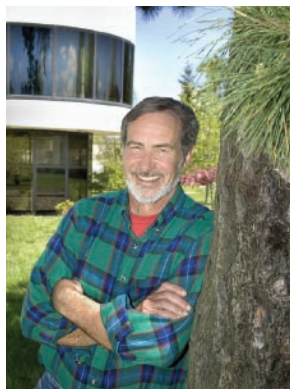
In summary, in-situ synchrotron-based x-ray absorption, scattering, and diffraction are successfully used to follow the kinetics and mechanisms of chemical processes in a variety of systems. Further developments and applications of these methods to probe reactions at increasingly shorter time scales in highly heterogeneous natural systems will advance our understanding of the short- and long-term fate of chemical contaminants in the environment.

— Dean Hesterberg and Jeff Fitts

Tony Lenhard Receives the 2005 UEC Community Service Award

May 24, 2005

This year, the NSLS Users' Executive Committee (UEC) presented the UEC Community Service Award to Tony Lenhard, Senior Technical Supervisor, NSLS User Science Division. The award is given for service, innovation, and dedication to NSLS users, and Tony is well deserving of that honor.



Tony Lenhard

As a tribute to nearly 25 years of dedicated support for NSLS experimenters and beamlines, members of the NSLS user community nominated Tony Lenhard for this year's award. Tony has demonstrated an uncommon dedication to improving the experimental setups at the NSLS. Here are quotes and paraphrased comments from some of the users who nominated Tony:

- Tony has supervised the Beamline Development and Support group that has been central to the construction, upgrade, and maintenance of all of the User Science Division beamlines: x-ray, ultraviolet, and infrared, including the insertion devices.
- As supervisor of that group, his superior traits have set the standard and inspired all of the NSLS User Science Division technical staff to excellence.
- "Tony is always ready to advise on the mechanical design of users' experimental apparatus, even under acute time pressure."
- "Tony is a treasure house of technical knowledge and skill in setting up beamlines and experiments. He has had a huge impact on the user community, based on his supervision of the technical work on every one of the NSLS-operated beamlines. Since many of the PRT beamlines look to the NSLS-construct-



NSLS UEC Vice Chair Peter Stephens presents the 2005 UEC Community Service Award to Tony Lenhard at the Users' Meeting banquet.

ed beamlines for technical guidance, Tony's mark is probably on every single beamline at the NSLS."

- Many of the people who wrote in support of his nomination made particular mention of his special talent for coming up with a simple solution to a mechanical problem, often quite different from what the experimenter initially visualized.
- "I don't believe the community properly appreciates his contributions to the many experiments that otherwise would have been delayed."
- Tony is patient and unflappable to a remarkable degree, especially considering the excited state that experimenters are often in when facing technical difficulties at the start of an experiment.
- "Tony may be one of the most underappreciated treasures in the NSLS. He is often on the spot when users arrive and he has to make some quick modifications to equipment to allow them to complete an experiment."
- "Tony plays a crucial role in assisting NSLS users while they are performing experiments. Every user facility needs a person like Tony: someone who knows how to build or modify any mechanical part in a short amount of time, and someone who is kind enough to help guide experimenters in the right direction."
- Tony has served the NSLS User Community in the ways described above for essentially the entire life of the NSLS. Ironically, many of the users whose experiments run well have never even met him. It is time for him to be recognized for this service via this Community Service Award.

Peter Stephens vice chair of the UEC, presented the award to Tony at the NSLS Users' Meeting banquet on the evening of Tuesday, May 24th. Tony received a \$250 gift certificate and his name was engraved on the plaque on display in the NSLS lobby. Congratulations Tony, and thanks for a job well done!

— Peter Stephens

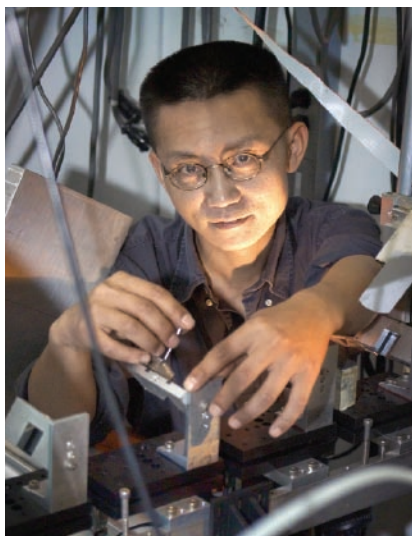
NLSL Physicist, Zhong Zhong, Awarded Tenure

June 1, 2005

BSA granted tenure on June 1 to five Brookhaven scientists. They were: Ivan Bozovic, Materials Science Department; Sergei Lymar, Chemistry Department; James Misewich, Materials Science; Werner Vogelsang, Physics Department; and Zhong Zhong, National Synchrotron Light Source Department.

Tenure appointments are granted by action of the BSA Board after a rigorous selection procedure overseen by the BSA Science & Technology Steering Committee.

In making tenure decisions, the BSA Board is advised by members of the Brookhaven Council, an elected body that



Zhong Zhong

advises the Director on matters affecting the scientific staff.

At the NLSL, physicist Zhong Zhong received tenure for his contributions to instrumentation, leadership, and for his innovative and creative original research. “Zhong is widely recognized for his major and creative contributions to the design and implementation of novel x-ray optics and as the co-inventor of a new medical imaging

technique that has great potential as a powerful and unique diagnostic tool,” said Steven Dierker, Brookhaven’s Associate Laboratory Director for Light Sources.

Conducting theoretical and experimental studies, Zhong devised a novel method for focusing high-energy x-rays and also a powerful new tool for fluorescence detection — offering scientists new ways to study previously inaccessible materials. Zhong is also coinventor of diffraction-enhanced imaging, or DEI, a technique that makes use of variations in how tissues refract and/or scatter x-rays, rather than absorption, which can be used to visualize soft tissues as well as bone at considerably lower x-ray doses than traditional radiography. DEI shows promise in diagnosing breast cancer and other soft-tissue diseases. In addition, Zhong serves as spokesperson for two NLSL beam lines, and is expected to help establish a Biomedical Imaging Research Resource at the facility.

According to Dierker, “Zhong’s talent and expertise in finding creative solutions to the most challenging optics and instrumentation problems will be especially crucial at NLSL-II, which will present new and difficult instrumentation challenges to take

advantage of its world-leading brightness.”

Zhong received a B.S. in physics from Beijing University in 1990, an M.S. in applied physics from Michigan Technological University in 1992, and a Ph.D. in physics from Stony Brook University in 1996. He joined the NLSL as a postdoctoral research associate in 1997, and has since been promoted to assistant scientist (1998), x-ray ring manager (1999), associate physicist (2000), and physicist (2002). He has also been an adjunct assistant professor in Biomedical Engineering at Stony Brook University since 2001.

— Karen McNulty Walsh

Crystallization Workshop Gets Top Marks From Participants

June 6-8, 2005

The “Crystallization: Focus on Optimization Techniques, Soluble and Membrane Proteins” course organized by Naomi Chayen (Imperial College of London) and Vivian Stojanoff (NLSL) took place at the NLSL from June 6 through June 8. During those three days, 55 researchers from the U.S. and abroad discussed and experienced hands-on the complexity of the protein-crystal growth process.

Several lectures to introduce the subject and eight parallel practical sessions were held by experts in the field during three days. Neer Asherie (Yeshiva University) discussed “Understanding of the Protein Phase Behavior,” Pat Loll (Drexel University) discussed the “Effects of Detergents,” Marie Claude Marchand (Nextal) discussed the “Vapor Diffusion Method and



Crystallization Workshop attendees

Optimization Techniques,” Gwen Nneji (Imperial College of London) discussed “Non-standard Crystallization Techniques,” Petra Fromme (Arizona State University) discussed “Phase Diagrams: A Way for the Rational Design of Membrane Protein Crystallization,” and Peter Nollert (deCODE Genetics) discussed “Micro Crystallization Using the Lipidic Cubic Phase Methodology.”

The practical sessions also included talks on “Purification Tech-

niques" by Janmeet Anand and Debbie Cohen (GE Healthcare), "The Light Scattering as a Diagnosis of Protein Purity" by Trevor Harvard (Precision Detectors), and "High-Throughput Screening of Crystallization Conditions" by Chris Gawronski (Fluidigm).

The 40 participants were divided into eight groups and rotated through the two-hour practical sessions. The course was designed to allow participants to experience different crystallization techniques and discuss the available optimization tools. The importance of protein purity and knowledge of phase diagrams were stressed in several lectures and practical sessions. Participants had the opportunity to try the different methods on standard or known proteins, such as lysozyme, thaumatin proteinase K, photosystem I, and bacteriorhodopsin.

Several participants brought their own proteins and tried the different methods and screening techniques to screen or optimize crystallization conditions. They used plates from Nextal, Hampton Research, Douglas Instruments, Molecular Dimensions, and Jena Biosciences. Several participants characterized their proteins by light scattering using the system provided by Precision Detectors, first finding possible improvements in the crystallization conditions they were using.

Overall, all the participants recommended organizing similar workshops in the future, as this is the only course in the U.S. that offers real experience in protein crystallization.

— Laura Mgrdichian

BioCD-2005

June 20-24, 2005

An intensive weeklong course on circular dichroism (CD) was presented at the NSLS at Brookhaven National Laboratory, from June 20-24.

CD is the difference in absorption of left and right circularly polarized light. It is observed in the spectral regions of absorption of molecules that are chiral, i.e. lacking a center of symmetry. While most CD spectra are small — only a tiny fraction of the total absorption — biopolymers with helical structures, such as proteins, DNA, RNA and polysaccharides, exhibit informative CD spectra.

The objective of BioCD-2005 was to acquaint the participants with the theory of ultraviolet CD spectroscopy, techniques, and instrumentation for acquiring CD data with laboratory and synchrotron-source instruments, as well as computational tools for analysing CD spectra, with special emphasis on determinations of the net secondary structure of proteins.

The motivation for a new course on CD spectroscopy is due, in part, to recent advances in CD spectrometers and accessory equipment, plus the development of new software for data analysis. The initial synchrotron beamlines for CD spectroscopy

were built at Tantalus and SURF II, moving to Aladdin and the NSLS, respectively, when these facilities opened. Within recent years, there has been a significant increase in interest in synchrotron radiation CD (SRCD). NSLS beamline U11 is being commissioned as a dedicated facility for UV CD spectroscopy and the Synchrotron Radiation Source at Daresbury (United Kingdom) recently brought beamline 12.1 online in the same role. SRCD instruments are also operating at the Institute for Storage Ring Facilities in at the University of Århus in Denmark, BESSY II in Berlin, HiSOR in Hiroshima, and the Beijing Synchrotron Radiation Facility. Additionally, there are plans for new CD beamlines at the Diamond Light Source in the UK and at SOLEIL in France.

Students attending BioCD-2005 were from the United States, the UK, Sweden, Ireland, Portugal, and Mexico, and included graduate students, postdoctoral researchers, and established investigators from industrial and governmental laboratories. Lectures were presented by Bonnie Wallace and Lee Whitmore (Birkbeck College, University of London), Robert Janes (Queen Mary College, University of London), John Sutherland and Lisa Miller (BNL), and Eugene Stevens (State University of New York at Binghamton). Sutherland, Wallace, Janes, and Miller organized the course. John Trunk, Denise Monteleone, and Michael Appel provided technical support. The hands-on laboratories included data collection on beamlines U9B and U11



BioCD-2005 participants

plus a conventional (lab-based, commercial) CD spectrometer. On-line data analysis of protein structures used the DichroWeb web site, based at Birkbeck College in London.

Topics covered by the workshop included: "Principles of CD Spectroscopy," "CD of Proteins, Analyses of Protein Secondary Structures and Practical Considerations in Measurements of CD Spectra," "Instrumentation for CD and SRCD," "CD Bioinformatics," "Demonstrations of Software for CD Spectroscopy," "Time Resolved Spectroscopy," "CD of Membrane Proteins," "Data Bases for Analysis of CD Spectra," "CD of Nucleic Acids and Polysaccharides (ES)," "Vibrational Spectroscopy," and "Linear Dichroism and Applications of SRCD to Structural and Functional Genomics". The workshop ended with an open dis-

cussion on the future of CD and SRCD in structural molecular biology.

BioCD-2005 was supported by the Office of Biological and Environmental Research within the U.S. Department of Energy's Office of Science, and BNL's Biology and NSLS departments.

— John Sutherland

Changes to NSLS User Access Policy

June 30, 2005

Important changes to operations at the NSLS were incorporated into the NSLS User Access Policy. This policy will support the NSLS in its mission to perform outstanding science in a safe and environmentally friendly manner. The document outlines the general policies for user access to the NSLS and is designed to ensure open and fair access to the NSLS by the scientific community at large, to sustain the highest standards of scientific and technical excellence, and to be responsive and adaptable to varying user needs and funding realities. The policy changes were made after consulting with the NSLS User Executive Committee and were approved by the NSLS Science Advisory Committee.

Facility Beamlines

One major change in the new policy is the creation of "facility" beamlines, which are controlled and managed by the NSLS. At least 75% of the available beam time on each facility beamline will be allocated to general users and one or more contributing users, with at least 50% of the available beam time going to general users.

Contributing Users

Another major change is the establishment of a new mode of user access, known as contributing users (CUs). CUs are individuals or groups who carry out research at facility beamlines as well as enhance the capabilities of those beamlines or contribute to their operation. CUs typically develop instrumentation in some manner, bringing external financial and/or intellectual capital into the development of the beamlines or making an external contribution to the operation of the beamlines. To encourage involvement, and in exchange for supporting the general user program, CUs may be recognized for their investments by receiving a specified percentage of beam time on one or more beamlines for a period of up to three years, with the possibility of renewal. The first group of CUs will be selected on September 1, 2005.

The new NSLS User Access Policy can be found at:
<http://www.nsls.bnl.gov/newsroom/publications/manuals/ppm/>.

— Chi-Chang Kao

NSLS Scientists Recognized by the American Physical Society

June 30, 2005

Three NSLS user researchers —Jan Genzer, Thomas Russell, and Gabriel Aeppli — were honored with prestigious American Physical Society (APS) awards. Additionally, two other NSLS scientists — user Robert Bartynski and the NSLS' own Li-Hua Yu — were elected as fellows of the APS.

"For his highly creative manipulation of surface properties via monolayer and macromolecular films," Genzer, a materials scientist at North Carolina State University, was awarded the Dillon Medal.

The Polymer Physics Prize went to Russell, a polymer scientist with the University of Massachusetts. He was cited "for his pioneering research and fundamental elucidation of the surface and interfacial behavior of polymers."

Aeppli, a condensed matter physicist with University College London, received the Oliver Buckley Prize "for fundamental contributions to experimental studies of quantum spin dynamics and spin coherence in condensed matter systems."

Bartynski, a condensed matter physicist at Rutgers University, was elected "for pioneering experiments to determine the electronic properties of surfaces, especially for leadership in developing Auger Photoelectron Coincidence Spectroscopy (APECS) with synchrotron radiation as a tool for local electronic structure."

Yu, a beam physicist at the Deep Ultraviolet Free-Electron Laser at the NSLS, was elected "for creative contributions to the theory of self-amplified spontaneous emissions and high-gain harmonic-generation, and the experimental demonstration of the high-gain harmonic-generation free-electron laser."

More information on the awards is available at

<http://www.aps.org/praw/05winners.cfm>.

— Laura Mgrdichian



Jan Genzer



Thomas Russell



Gabriel Aeppli



Robert Bartynski



Li-Hua Yu

Protein Rush at the NSLS

July 1, 2005

In the spring of 2005, the Protein Structure Initiative (PSI) launched the second phase of its national effort to find the three-dimensional shapes of a wide range of proteins. This is good news for the NSLS, since many of those structures will be determined here. But more importantly, the structural information will help reveal the roles that proteins play in health and disease and will help point the way to designing new medicines.

The highlight of the PSI second phase was the announcement of 10 new research centers, which marks the second half of the decade-long initiative. The centers are slated to receive about \$300 million in grants over the next five years.

When the PSI established its pilot centers in 2000, its goal was twofold: to develop innovative approaches and tools, such as robotic instruments, that streamline and speed many steps of generating protein structures, and to incorporate those new methods into pipelines that turn DNA sequence information into protein structures.



Now, the focus shifts to production. The new centers will use methods developed during the pilot period to rapidly determine thousands of protein structures found in organisms ranging from bacteria to humans. These efforts will facilitate structure determination on a much larger number of proteins through computer modeling.



The PSI production phase includes two types of centers. Four large-scale centers, established during the pilot phase, hope to generate between 3,000 and 4,000 structures. Six smaller, specialized centers will develop novel methods for quickly determining the structures of proteins that traditionally have been difficult to study. These include small protein complexes, proteins that attach to a cell's outer "skin," or membrane, and many proteins from higher organisms, including humans.

As before, the PSI centers will submit their structures



Three protein structures determined at the NSLS as part of the Protein Structure Initiative (Images courtesy www.nysgrc.org.)

and related findings to the Protein Data Bank, an NSF- and NIH-supported public repository of three-dimensional biological structure data.

The Protein Structure Initiative is funded largely by the National Institute of General Medical Sciences (NIGMS) and also receives funding from the National Center for Research Resources. Both centers are part of the National Institutes of Health.

More on how BNL and NSLS are involved

In 2000, an organization called the New York Structural GenomiX Research Consortium was formed as part of the PSI pilot program. During the pilot period, members of this consortium developed many innovative methods and determined approximately 200 new protein structures. The majority of these structures were deciphered at the NSLS, with about 50 of them being determined by Brookhaven scientists. In fact, two of the consortium's principal investigators are Brookhaven Lab biologists Subramanyam Swaminathan and William Studier.

In the second PSI phase, the Brookhaven group will continue to solve structures at the NSLS and work to improve their methods. Over the five years, the consortium will receive approximately \$48 million, with about \$9.5 million of that supporting research at Brookhaven Lab.

The consortium's other member institutions are Albert Einstein College of Medicine, Mount Sinai School of Medicine, The Rockefeller University, and Weill Medical College of Cornell University.

— Laura Mgrdichian

Highlights from the 2005 NSLS Summer Sunday

August 7, 2005

An enthusiastic crowd of 700-plus visitors came to the National Synchrotron Light Source on August 7 as part of Brookhaven Lab's Summer Sundays program, crowding the lobby, seminar room, and front patio to see what the NSLS had in store for them. The program welcomes the public to the Lab on several consecutive Sundays in the summer, highlighting a different facility each week.

Guests arrived at Berkner Hall, where an NSLS scientist first gave a brief NSLS overview talk and discussed how



Out on the patio there were several fun, interesting exhibits



Summer Sunday volunteers help young guests build "crystals" out of toothpicks and gumdrops

and patio to show visitors how the NSLS works and teach them about the science performed there. For example, the new "Electron Catapult" display showed visitors how different amounts of energy are required to propel an electron from an atom's "ground state" level to higher levels. This concept is key to many NSLS experiments.



"MC" Gerry Van Derlaske with a happy raffle winner

off, to shrivel down to a smaller size than when the experiment began. Guests learned that the shrunken candies were still edible (perhaps even tastier that way).

And at "See the Light," visitors could see actual synchrotron light, guided to the lobby from the experimental floor by a fiber-optic cable.

Upon entering the building, each guest received a quiz with several questions that could be answered by visiting each display. Every finished quiz was handed in and redeemed for an NSLS keychain flashlight and, every half-hour, one quiz was selected raffle-style to receive another prize



Volunteer Ted Feldman shows visitors how the "Electron Catapult" display works

they use the NSLS to perform their own research. From there, visitors boarded a bus to the NSLS.

There were many things to do and see at the facility. Fifteen hands-on displays were set up in the lobby, seminar room,



A steady stream of visitors filled the NSLS lobby

— an NSLS baseball cap or BNL polo shirt.

Always a powerful sight for guests are the lobby and second-floor viewing windows that look down over the NSLS experimental floor. Looking down across the expanse of hardware, aluminum foil, and wiring is always fascinating for first-time visitors. At both windows, NSLS scientists were available to answer questions. Large neon numbers placed on the floor clearly labeled various components.

Outside the building, on the patio, NSLS scientists demonstrated how solar cars and water rockets worked, among other fun and interesting toys.

The day's success was made possible by many volunteers: Marc Allaire, Michael Appel, Steve Bennett, Mike Buckley, Wolfgang Caliebe, Shailendra Chouhan, John Dabrowski, Elaine Di Masi, Matt Engel, Larry Fareria, Ted Feldman, Ed Haas, Sarah Heins, Steve Hulbert, Anubav Jain, Ariane Kretlow, Kathryn Krycka, Tony Kuczewski, Tony Lanzirotti, Alan Levine, Andreana Leskovjan, William Little, Ebrahim Mahajna, Corinne Messana, Laura Mgrdichian, Laura Miller, Lisa Miller, Eileen Morello, Wendy Morrin, Susila Ramamoorthy, Perumal Ramasamy, Lydia Rogers, Ray Raynis, Meghan Ruppel, Sami Khouri Salameh, Sharadha Sambasivan, Cecilia Sanchez-Hanke, Anne Schirmer, Randy Smith, Peter Stephens, Raji Sundaramoorthy, Tejas Telivala, Heather Turbush, Gerry Van Derlaske, Adele Wang, Gary Weiner, Marty Woodle, Nancye Wright, Lin Yang, and Zhong Zhong.



Three successful crystal-builders

— Laura Mgrdichian

Meet the NSLS Summer Students of 2005

August 31, 2005

Each summer, a number of high school and college students perform research projects at the NSLS. Most of the students work at the NSLS as part of Laboratory-sponsored research internship programs.

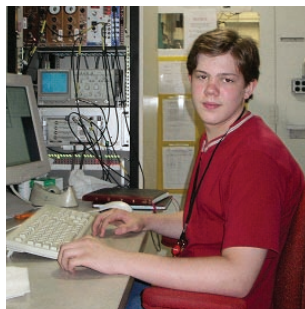
The students work with scientists and engineers from the department in a wide range of research fields: medical sciences, geology and environmental sciences, chemistry, materials science, physics, and electrical and mechanical engineering. The students also attend scientific lectures, tour BNL research facilities, and participate in numerous social activities.



Jeff Borack

Interested students apply to these programs in the spring and the programs range from six to 10 weeks long. More information and application procedures can be found on the BNL Science Education website at <http://www.bnl.gov/scied/>.

Jeff Borack, now a senior at SUNY Binghamton, spent his summer trying to determine how to differentiate between two forms of chronic lymphocytic leukemia (CLL). In his project, developed by Dr. Nick Chiorazzi from the North Shore Long Island Jewish Hospital and NSLS scientist Lisa Miller, he analyzed B-cells (a type of white blood cell) using an infrared microscope. This research may lead to the development of a new diagnostic tool capable of helping doctors and patients determine which treatment options are best for CLL.

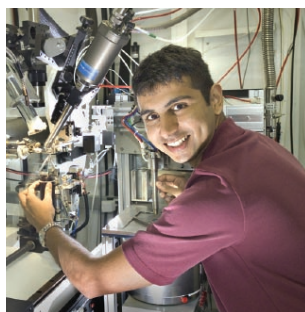


Michael DiBiccari

For the past two summers, **Michael DiBiccari**, a senior at Hauppauge High School, has

worked with Elaine DiMasi, studying the growth process of biological minerals. They examined the diffraction patterns of x-rays that reflected off the mineral crystals, which helped them understand how the crystals formed. This research will be helpful in understanding the process of biomineralization.

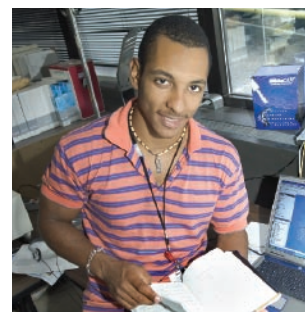
Anubhav Jain is now a senior at Cornell University. Both this summer and last, he worked with NSLS scientist Vivian Stojanoff, developing software to help automate the process of determining the molecular struc-



Anubhav Jain

ture of proteins. This research will help structural biologists get three-dimensional structures of proteins more quickly, allowing scientists to develop treatments

Jean Christian Brutus is a sophomore at Stony Brook University. This summer, he worked with engineer John Skaritka in the NSLS design room. His project involved designing a superconducting undulator (a device used in synchrotron rings), manufacturing it, and finding a way to wind and cool down the system. This undulator will be used as an insertion device for the electron accelerator in NSLS-II, the planned NSLS successor.



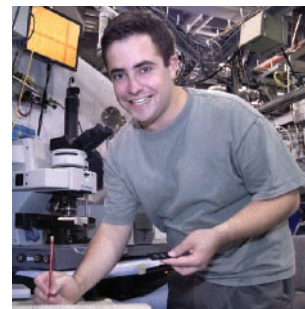
Jean Christian Brutus

Gabriel Sanchez, a senior at Stony Brook University, worked with mentor Cheo Teng, the NSLS systems administrator. His project involved systems/network administration. The NSLS uses Hewlett-Packard UniX machines to monitor the daily operations and data collection of the particle accelerators. These machines are configured on a network; Sanchez' objective was to successfully add another machine to this existing network. This involved the setup of a Network Information Service, the Domain Name System, and a Network File System.



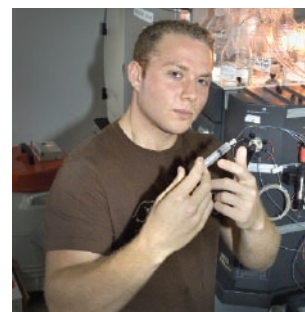
Gabriel Sanchez

Theodore Feldman, now a junior at Stony Brook University, worked with Lisa Miller studying compositional changes in developing mouse bone. They used infrared microspectroscopy to study changes in the chemical makeup of bone as it mineralizes by analyzing the infrared spectrum of bone's organic and inorganic components. This work may help elucidate the role chemistry plays in determining bone strength and quality, which may be used to better treat and diagnose osteoporosis and similar bone diseases.



Theodore Feldman

Matthew Engel worked with NSLS scientist Marc Allaire on a protein crystallography project. The particular protein he isolated and worked with is from



Matthew Engel



Ebrahim Mahajna, Mahmoud Simri, and Sami Khouri Salameh

the capsid (protein coating) of a human virus that surrounds its DNA and controls its infectivity. Solving the protein's structure will allow researchers to engineer capsids with less ability to produce an immune-system response or even target specific membrane receptors.

Ebrahim Mahajna, Mahmoud Simri, and Sami Khouri Salameh are seniors at Ben Gurion University in Israel. They performed research at the NSLS as part of a U.S. Department of Energy Cooperative Research Program. Simri, working with Vivian Stojanoff, crystallized a protein and determined its structure using x-ray crystallography. Salameh, with Lisa Miller, studied a potential therapy for skin melanoma by imaging skin cancer cells using infrared light. Mahajna worked with Zhong Zhong and Avraham Dilmanian, studying whether diffraction-enhanced imaging could detect early stages of Alzheimer's disease.

— Laura Mgrdichian

NSLS-II Gets CD-0!

September 9, 2005

The Laboratory received fantastic news in September 2005: The Department of Energy granted "Critical Decision Zero" (CD-0) status to National Synchrotron Light Source-II, the planned world-leading NSLS successor. This is the key first step in the long process to make NSLS-II a reality at Brookhaven.



ALD for Light Sources Steve Dierker

Accompanied by Lab Director Praveen Chaudhari and Steve Dierker, Associate Laboratory Director for Light Sources, DOE Brookhaven Site Office Manager Michael Holland announced the news at an NSLS All-Hands meeting on Friday, September 9.

"This is a tremendous step forward for science," said Holland. "The effort that went into this by Steve

Dierker and others on the project was tremendous. I thank everyone for their hard work and accomplishments."

Holland noted that as part of the process that leads to CD-1, the next critical decision for the project, the physical site for

the facility will be chosen, determining whether NSLS-II will be located at BNL. "There will certainly be a strong case made for NSLS-II at Brookhaven. There is an awful lot of work ahead of us in the next eight to 12 months," he said.

In his comments, Chaudhari congratulated the NSLS staff and many others for their efforts in maintaining the NSLS while working to make the case for NSLS-II. "You ought to take a moment and clap for yourself," he said. "It's been difficult to keep the NSLS running and design a new machine. You are going to have to continue to work very hard, but I expect that you can do it."

Dierker called the announcement a "wonderful occasion." He then presented an overview of the history of the NSLS-II project, from the initial idea to the proposal to the major reviews by DOE, as well as the large and successful NSLS-II workshop in March 2004 — all the results of hard, hard work and cooperation. He thanked everyone for helping to achieve this critical milestone and emphasized the continuing teamwork necessary to continue the process and secure the site.

"There is a strong research community in the Northeast and a tremendous density of academic and research institutions," he said. "Moreover, U.S. synchrotrons are far oversubscribed. We need NSLS-II more than ever, or the science and benefits from that science will move overseas."

— Laura Mgrdichian



DOE Brookhaven Site Office Manager Michael Holland



Lab Director Praveen Chaudhari

Synchrotron Environmental Science III (SES) Meeting

September 19-21, 2005

On September 19-21, the Synchrotron Environmental Sciences III (SES III) conference was held at Brookhaven National Laboratory (BNL). Continuing the tradition established by previous SES conferences held at Argonne National Lab, SES-III brought together the diverse community of scientists who apply

synchrotron-based radiation techniques to study the biological and geochemical aspects of both local and global environmental issues. The conference included two days of topical sessions that addressed the application of innovative synchrotron methods in environmental science along with applications in bioavailability and remediation science. The third day included a workshop on microbeam methods. Attendees reported on environmental science activities conducted at synchrotron facilities worldwide.

The SES meetings are an outgrowth of EnviroSync, a grass roots organization with almost 400 members established in early 1998 to represent the growing multidisciplinary community of synchrotron radiation users who focus on molecular environmental science problems (<http://www.cems.stonybrook.edu/envirosync/history.html>). Stephen Sutton (GSECARS, University of Chicago) has been Chair of EnviroSync since 2002. An EnviroSync open meeting was also held as part of the SES-III conference, during which Richard Reeder (Stony Brook University) was elected as the new EnviroSync Chair and John Bargar (Stanford Synchrotron Radiation Lab) its Secretary for 2005-2007.



Synchrotron Environmental Science III (SES-III) Meeting attendees

BNL Director Praveen Chaudhari opened the SES-III conference with very supportive comments emphasizing the increasingly important role environmental science research plays at BNL and how well suited light sources are to answer the questions asked by environmental scientists. There were also welcoming remarks from Martin Schoonen, Stony Brook University's Associate Vice President for Research, and Creighton Wirick, Chair of BNL's Environmental Sciences Department. Steve Dierker, BNL's Associate Lab Director for Light Sources, then gave an update on the National Synchrotron Light Source (NSLS) and in particular the progress that the NSLS has made in bringing additional beamlines into operation that support environmental science users. He emphasized that this is need driven by the rapidly increasing number of environmental science users at the NSLS and the over-subscription of beamlines that cater to the community. Steve also updated the attendees on the status of NSLS-II, which was recently granted "Critical Decision Zero" (CD-0) status by the Department of

Energy (DOE). NSLS-II is a proposed new state-of-the-art medium energy storage ring designed to deliver world leading brightness and flux with top-off operation for constant output. DOE program managers Nicolas Woodward (Basic Energy Sciences – Geosciences Research Program) and Roland Hirsch (Biological & Environmental Research – Environmental Remediation Sciences Division) also gave updates on DOE support for environmental research and how these programs have stressed availability of synchrotrons to earth and environmental scientists. Todd Anderson from the Office of Biological & Environmental Research was also in attendance.

Gordon Brown (Stanford University) opened the scientific presentations of the first day with an overview of recent environmental science activities that have been made possible by using synchrotron-based approaches, as well as future possibilities. The first day's sessions also included talks by Ken Kemner (Argonne National Lab), Neil Sturchio (Univ. Illinois), Sanjit Kumar Ghose (GSECARS, Univ. Chicago), David Shuh (Lawrence Berkeley Lab), and Lynda Soderholm (Argonne National Lab). Talks on the first day focused on the use of innovative synchrotron based techniques in biogeosciences and how studies of mineral surfaces can employ x-ray standing wave imaging, resonant anomalous x-ray reflectivity, and crystal truncation rod scattering. There were also discussions about the application of soft x-ray emission spectroscopy, resonant inelastic x-ray scattering, and extended x-ray absorption fine structure investigations in the study of actinides. The first day concluded with a poster session.

Sessions on the second day included a number of talks on the application of synchrotron techniques to biological-environmental systems. Topics included metal ions in living systems, the structural chemistry of bacteriogenic manganese oxides, the reduction of U(VI) by Fe(II) at cell surfaces, and the application of synchrotron infrared microspectroscopy to environmental studies. There were also discussions of the use of multiple synchrotron x-ray techniques in the study of plant-metal-soil interactions, the effect of microbial siderophores on Pb speciation and adsorption, and the application of synchrotron micro-diffraction in prediction of environmental risks associated with arsenic-bearing mine wastes. Attendees also heard about the benefits of combining x-ray and neutron scattering techniques for obtaining fundamental information about processes of importance to environmental sciences. Speakers included Graham George (Univ. of Saskatchewan), John Bargar (Stanford Synchrotron Radiation Lab), Maxim Boyanov (Argonne National Lab), Stefan Vogt (Argonne National Lab), Lisa Miller (Brookhaven National Lab), Ryan Tapperro (Univ. of Delaware), Bhoopesh Mishra (Univ. of Notre Dame), John Parise (Stony Brook Univ.), Heather Jamieson (Queen's Univ., Canada), and Matthew Ginder-Vogel (Stanford Univ.). The day's sessions concluded with a classic Long Island clambake, where attendees gorged themselves on fresh lobsters, clams, and mussels well into the evening.

The meeting concluded with a workshop on the application

of microbeam methods to environmental sciences. Workshop speakers included Steve Sutton, Daniel Grolimund (Swiss Light Source), Matthew Marcus (Lawrence Berkeley Lab), Mary Gilles (Lawrence Berkeley Lab), and Chris Jacobsen (Stony Brook Univ.). The speakers described beamlines at the Advanced Photon Source, Advanced Light Source, National Synchrotron Light Source, and the Swiss Light Source and applications of hard x-ray microbeam fluorescence, absorption, diffraction, and tomography techniques and soft x-ray spectro-microscopy techniques for characterization of environmental materials.

Overall, the meeting proved to be a rousing success, and everyone looks forward to SES-IV in the near future. This workshop was co-sponsored by EnviroSync, the National Synchrotron Light Source, the Center for Environmental Molecular Science (Stony Brook Univ.), Brookhaven National Laboratory, Stony Brook University, the National Science Foundation, and the Department of Energy.

— Antonio Lanzarotti

The 2005 NSLS Barbeque Wraps Up the Year

September 23, 2005

The unusually warm, sunny weather of September 23 did not hint at the cool autumn days to come, but did make for an enjoyable 2005 NSLS Barbeque. However, it was the NSLS staff members in attendance, particularly the service and spotlight-award winners, that made the event memorable.



NSLS Chairman Steve Dierker

Service Awards

Nick Gmur and Dennis Carlson were honored for 30 years of service at Brookhaven Lab, and 25-year awards went to Shu Cheung, John Klug, Gloria Ramirez, and Peter Zuhoski.

In the 20-year category were Erik Johnson, Eileen Morello, Mihai (Mike) Radulescu, Lydia Rogers, David (Peter) Siddons, and Yong-Nian Tang. Mary Anne Corwin and Zhijian Yin celebrated 10 years.

Not available to receive their awards at the barbeque were Wayne Rasmussen, for a very impressive 40-year award; John Bohenek for 25 years of service; Sorin Pop, Leonard Pharr, and Madeline Hughes for 20 years; and Syed Khalid and Elio Vescovo for 10 years.

Spotlight Awards

The Spotlight awards are tributes to NSLS staff members who



Steve Dierker presents a 30-year service award to Nick Gmur

have shown exceptional dedication to their jobs during the year. This year, the winners were: John Aloï, nominated by Bob Casey; Angela Bowden, nominated by Laura Miller; Michael Caruso, nominated by Gary Nintzel; Bob Kiss, nominated by Gerry Van Derlaske; Patrick Moylan, nominated by Ed Haas; Dennis Poshka, nominated by Anthony Kuczewski; John Vaughn, nominated by Gloria Ramirez; and Zhijian Yin, nominated by Peter Siddons.

John Aloï: John installed and commissioned a complex request-tracking system for the User Science Division that keeps a more accurate record of requests. The system, a significant programming effort one would expect to take several months, took John just a month and a half. This effort involved many late hours, during which John experimented with and tested the system. Now, jobs are easier to monitor and requests are handled much more efficiently.

Angela Bowden: For five weeks in April and into May, Angela worked under the pressure of a tight deadline to bring the NSLS into compliance with a Department of Energy "Corrective Action" item. She volunteered to learn two new computer programs, and then used them to create more than 3,000 safety warning labels for hazardous equipment on the NSLS experimental floor. All the labels were accurate and completed before the deadline.

Michael Caruso: Caruso is recognized for providing invaluable assistance to the NSLS Vacuum Group over the past several years. Notably, he helped develop a coating process that greatly reduces the time necessary to coat a ceramic chamber, and then used the method to titanium-coat three ceramic chambers. He demonstrated excellent knowledge and skills in vacuum processes, and all three chamber coatings proved to have excellent mechanical and electrical properties.

Bob Kiss: In response to a Brookhaven Lab directive, Bob crafted and implemented new and improved procedures for the NSLS Hoisting and Lifting program. He created new check-out sheets tailored for equipment at each beamline, came up with an NSLS-specific rigging-training program, took control of 49 NSLS overhead cranes by preventing unauthorized people



A group of NSLS staff members watch the awards ceremony

from operating them, and assigned to each beamline a person responsible for hoisting and lifting activities at that beamline. These actions helped make the NSLS experimental floor a safer place.

Patrick Moylan: Pat demonstrated exceptional initiative and written skills by putting together Worker Qualification and Training forms for the Mechanical Tech Group, which falls outside of his own training and work area. On top of that, he put together a training program designed to enhance on-the-job safety in the x-ray ring tunnel for workers who need unescorted access to the tunnel. He then presented that training to all NSLS staff, to inform them of potential hazards in the tunnel.

Dennis Poshka: By starting up a verification and maintenance routine for the facility beamline user interlock systems, a project he undertook on his own accord, Dennis uncovered many beamlines in which legacy interlocks were disconnected or inadequately instrumented. Identifying these interlocks prevented a potentially huge loss of equipment and greatly added to the measure of safety at the NSLS.

John Vaughn: After a period of repeated beam dumps on the x-ray ring in 2004, caused by random trips of a faulty power supply, John assisted in several studies to trace the origin of the trips in the power supply. When nothing surfaced, he set up diagnostics, and logged and charted events to establish a correlation between the trip frequency and the x-ray ring maintenance periods. These efforts led him to a solution after months of efforts by other staff members did not.

Zhijian Yin: Zhijian installed and commissioned a complex request-tracking system for the User Science Division over a very short time period. He discovered an open-source software package that fit the needs of the division and successfully incorporated it into the existing email, web, and database servers. This complex task involved many extended hours of experimenting and testing to make sure the software worked properly. Since then, more than 100 requests have been tracked without problems and the system has proved to be easy to use and efficient.

— Laura Mgrdichian

SBU Student Wins First Dr. Mow Shiah Lin Scholarship

September 27, 2005

Yuanzhi Tang, a graduate student in the Department of Geosciences at Stony Brook University (SBU), won the first annual Dr. Mow Shiah Lin Scholarship. The Asian Pacific American Association (APAA) at the Lab initiated the scholarship, which consists of \$1,000 and a plaque, to honor the late distinguished Brookhaven Lab scientist for which it is named.

Mow Shiah Lin began his career at BNL in 1975 as a postdoctoral fellow and advanced to co-lead a research team working with an environmental remediation company to use selected bacteria to convert toxic oil wastes, such as used motor oils, into useful products. In 2001, Lin shared the R&D 100 Award, given by R&D Magazine to the top 100 technological achievements of the year, for a technology to recover silica from geothermal brine. Lin died suddenly due to a brain aneurysm at the height of his career in 2003, and his fellow employees, friends, and family contributed funds to establish the scholarship.



With Mow Lin Scholarship winner Yuznhi Tang (fifth from left) in the photo are: (from left) Susan Eng Wong, co-coordinator, APAA; Thomas Butcher, BNL scientist and head of the scholarship selection committee; Satoshi Ozaki, BNL scientist/administrator and APAA advisor; Beth Y. Lin, APAA co-coordinator and widow of Mow Shiah Lin; Lucinda Lin, daughter of Beth and Mow Shiah Lin; Richard J. Reeder, Director, SBU Center for Environmental Molecular Sciences and thesis advisor for Tang; Samantha Lin Alvarado, daughter of Beth and Mow Shiah Lin; Marie Van Buren, member of the APAA scholarship committee, and (front, center) Josephine Alvarado, granddaughter of Beth and Mow Shiah Lin.

In honor of Lin's research, achievements, and inventions, the scholarship will be granted annually to an Asian immigrant with a student visa who is matriculating toward a graduate degree at an accredited institution of higher education in environmental science, biology, or chemistry, in remembrance of the manner in which Lin began his career.

Tang's research at SBU involves the use of various analytic techniques — including x-ray imaging at the NSLS — to study the mechanisms of the reaction of contaminants in natural environments, especially reactions at the interfaces of minerals and water.

— Diane Greenberg

New Grant for Catalysis Research at the NSLS

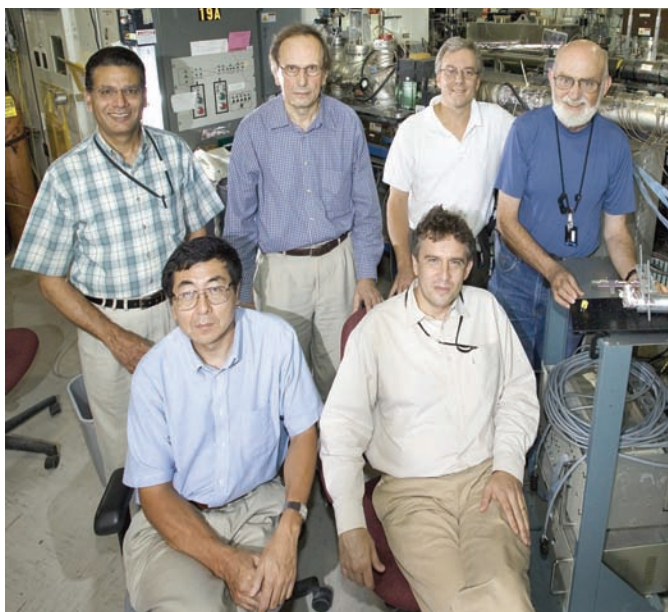
September 28, 2005

A group of scientists was awarded a \$900,000 grant by the Department of Energy to create dedicated facilities for catalysis research at NSLS beamlines X18B and X19A. The two facilities will be operated by the Synchrotron Catalysis Consortium, charged with improving and expanding catalysis research by taking advantage of the unique investigation tools available at the NSLS.

Catalysis is a major area of research in the United States because it is very important to U.S. industry, particularly the chemical and petroleum industries. It is estimated to be involved in 90% of all chemical processes and the creation of 60% of the chemical products available on the market. In addition, catalysis is becoming more important to several other fields, including environmental protection, pharmaceuticals and bioengineering, and the development of fuel cells.

The consortium's main investigation tool will be x-ray absorption fine-structure (XAFS) spectroscopy, which measures how a material absorbs x-rays to learn about its molecular structure and electronic behavior.

"XAFS is well suited to studying catalysis, and can often yield more in-depth information on a material's structural, electronic, and catalytic properties than more widely used techniques," said Anatoly Frenkel of Yeshiva University, one of the consortium's principal investigators. "We hope to help make more scientists aware of the advantages of using synchrotron radiation in general, and XAFS in particular, and provide support for



Some of the key members of the Synchrotron Catalysis Consortium. In the front row, from left, are principal investigators Jingguang Chen and Anatoly Frenkel. In the back, from left, is NSLS scientist Syed Khalid, who runs beamline X18B, and co-principal investigators Radoslav Adzic, Steve Hulbert, and Jonathan Hanson.

scientists who wish to start catalysis experiments at the NSLS."

The two other principal investigators are Jingguang Chen of the University of Delaware and Radoslav Adzic of Brookhaven's Chemistry Department. Chen said, "Synchrotron techniques are currently underutilized or unexplored by the catalysis community due to various perceived and real barriers. The primary purpose of the consortium is to promote the utilization of synchrotron techniques to perform cutting-edge catalytic research under *in-situ* conditions."

Said Adzic, "This consortium is expected to have a particularly strong impact on the research and development of fuel cell electrocatalysts. Capabilities for *in situ* characterization of electrocatalysts in fuel cell environment under various conditions will be provided by adequate cell designs."

The consortium's co-principal investigators are Chi-Chang Kao and Steve Hulbert (NSLS), Jan Hrbek, Jose Rodriguez and Jonathan Hanson (BNL-Chemistry), David Mullins and Steve Overbury (Oak Ridge National Laboratory), and Simon Bare (UOP, LLC).

The grant will fund new hardware additions and changes at X18B and X19A, allowing scientists to study chemical transformations in catalytic materials over a wide range of energies in real time and at realistic operation conditions. Examples of new devices that will benefit the catalysis-research community are state-of-the-art reactor cells, gas-handling equipment, and detectors. The upgrades will also include the latest advances in beamline instrumentation. All these changes will provide new experimental opportunities for scientists interested in catalysis.

In addition, the grant includes funds to hire a beamline staff to run the new facility and provide support for visiting research groups. The budget also includes funds for travel, which will help new user scientists start synchrotron research programs as well as attend catalysis workshops and training courses.

Most components at X18B and X19A will be in place by April 2006. Catalysis users are now being contacted with invitations to start their research program at the NSLS, and the first users will start experiments in February 2006. The grant covers a time span of three years.

— Laura Mgrdichian

EXAFS Course: Theory, Experiment, and Advanced Applications

September 28-30, 2005

X-ray absorption fine structure (XAFS) data collection and analysis courses have been held at the NSLS annually since 2001. While previous courses were aimed at beginners and thus broad in scope, this three-day (September 28-30) course was devoted to one technique: extended XAFS (EXAFS).



Participants in the EXAFS course

Participants in this course (32 scientists from U.S. and Canada, representing universities, national laboratories, and industrial companies) had prior familiarity with the basics of the technique and were interested in learning how to correctly design, perform, and analyze EXAFS experiments in application to their research. The course was self-contained, starting with the fundamentals and proceeding to the more advanced topics, including recent theoretical developments, data analysis techniques, and specific applications of EXAFS.

The course consisted of three lecture sessions in the mornings, two hands-on experimental sessions in the afternoons, and one data analysis session during the last day of the course. The organizers identified four areas of interest: nanocatalysis, environmental/bio/geo chemistry, disordered alloys/thin films, and transition metal oxides, and designed several research experiments in each of these areas. Experiments were conducted at eight beamlines.

Lectures were taught by invited speakers: Edward Stern and Josh Kas (University of Washington), Grant Bunker (Illinois Institute of Technology), Anatoly Frenkel (Yeshiva University), Trevor Tyson (New Jersey Institute of Technology), Joseph Woicik (National Institute of Standards and Technology), Douglas Hunter (Savannah River National Laboratory), Scott Calvin (Sarah Lawrence College), and Douglas Pease (University of Connecticut). Among the highlights of the course were two talks, "History of EXAFS" and the "Pitfalls of the Experiment and Data Analysis," which was taught by Edward Stern, one of the founders of the technique.

Beamline instructors were F. Alamgir (City University of New York), T. Tyson, A. Frenkel, J. Woicik, A. Ignatov (Case Western Reserve University), K. Pandya (Brookhaven National Laboratory), P. Northrup (Brookhaven National Laboratory), W. Caliebe (Brookhaven National Laboratory), S. Khalid (Brookhaven National Laboratory). Data analysis sessions were led by S. Calvin, A. Frenkel, F. Alamgir, T. Tyson, J. Woicik, S. Khalid and P. Northrup.

The course administrator was Corinne Messana (BNL). The course was possible due to generous sponsorship by the National Synchrotron Light Source, Yeshiva University, and the DOE Synchrotron Catalysis Consortium.

— Anatoly Frenkel

Brookhaven Lab Breaks Ground for New Nanocenter

October 3, 2005

The U.S. Department of Energy's (DOE) Brookhaven National Laboratory held a groundbreaking ceremony on October 3 for the Center for Functional Nanomaterials (CFN). The CFN will provide researchers with advanced probes and the ability to use new fabrication techniques to study materials at nanoscale dimensions — typically, billionths of a meter, or 1,000 times smaller than a human hair. These materials have different chemical and physical properties than bulk materials and could form the basis of new technologies.

The CFN — one of five Nanoscale Science Research Centers to be built at DOE national laboratories — was designed by HDR Architecture, Inc., of Alexandria, Virginia, and is being constructed by E. W. Howell Co., Inc., of Woodbury, New York. The 94,500-square-foot state-of-the-art laboratory/office facility is expected to attract an estimated 300 researchers from the Northeast annually.



(L to R) Laboratory Director Praveen Chaudhari, DOE Brookhaven Site Office Manager Michael Holland, Battelle Memorial Institute Senior Vice President and Chief Operating Officer Donald McConnell, Associate Director for the DOE Office of Basic Energy Sciences Patricia Dehmer, Congressman Timothy Bishop, CFN Director Robert Hwang, and Associate Lab Director for Basic Energy Sciences Doon Gibbs.

Brookhaven employees and distinguished guests, including local Congressman Tim Bishop and Dr. Patricia Dehmer, Associate Director for the U.S. Department of Energy's Office of Basic Energy Sciences, attended the ceremony against a backdrop of heavy equipment at the CFN location in the center of Brookhaven's 5,300-acre site.

"The Center for Functional Nanomaterials will be at the forefront of research that is expected to lead to new technologies, such as faster computers, new communications devices, improved solar energy and new energy alternatives," Congressman Bishop said. "Long Island is fortunate to have this center here. Everyone reaps benefits when the best minds and the best technology merge to explore the frontiers of science."

DOE's Office of Basic Energy Sciences is funding the \$81-

million CFN project. The contemporary building, which has a metal and glass exterior, will cost \$38 million to build, while specialized equipment, such as electron microscopy facilities and lithography-based fabrication facilities, and engineering and project management will account for the balance of the budget. The facility, which will occupy nine square acres and will accommodate 150 people, will be considered “green,” or energy efficient and environmentally friendly, based on the U.S. Green Building Council’s rating system. Construction is expected to be completed by March 2007, and experiments are due to begin shortly after that date.

The overarching research goal of the CFN is to help solve energy problems in the U.S. by exploring materials that use energy more efficiently and by researching practical alternatives to fossil fuels, such as hydrogen-based energy sources and improved, economical solar energy systems.

Under the energy banner, CFN studies will focus on three key areas: nanocatalysis, the acceleration of chemical reactions using nanostructures; biological and soft nanomaterials, such as polymers and liquid crystals, in which specialized design is expected to lead to new functions; and electronic nanomaterials that exhibit unprecedented control of electrons, which are expected to lead to new communication and energy-control devices.

— Diane Greenberg

NSLS Users Recognized

October 21, 2005

Each year, a number of NSLS users win prestigious awards in their field of scientific research. The following represent a collection of some of the awards from 2005.

Russell Hemley and David Mao Win the Balzan Prize



Russell Hemley

This year, the International Balzan Foundation Prize for Mineral Physics was awarded to Russell Hemley and Ho-Kwang (David) Mao, both scientists with the Geophysical Laboratory at the Carnegie Institute of Washington.

Hemley and Mao received the award “for the impressive impact of their joint work leading to fundamental breakthroughs, theoretical and experimental, in the field of minerals submitted to extreme physical conditions.” Much of their work — particularly their early, pioneering studies — has been, and is currently, performed at the NSLS.

They began working at the NSLS in 1986, using beamline

X13A (later renamed X7A) to perform x-ray diffraction studies of materials subjected to extremely high pressures. Later, they helped build X17C — the world’s first dedicated high-pressure beamline — and also conducted high-pressure infrared spectroscopy studies at U4IR, U2B, and U2A (the world’s only dedicated beamline for that type of research).



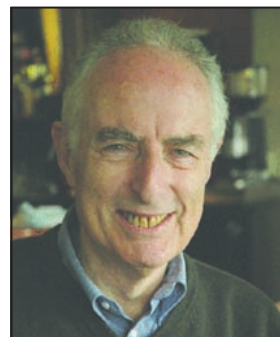
David Mao

“They have operated as a highly effective team,” remarked the award committee, “characterized by twenty years of research contributions at the highest level. They have developed techniques which allow them to study the behavior of a wide range of minerals, such as hydrogen, the most abundant ‘mineral’ in the universe. Their results have deep implications for our understanding of nature.”

The prize will be given out on November 11 in Berne, Switzerland at the Swiss Federal Parliament Buildings. Each prize consists of one million Swiss francs (about \$773,000), half of which must be used to fund research projects by students and young scientists at the winners’ home institution.

Philip Coppens Receives the Ewald Prize

Longtime NSLS user scientist Philip Coppens, a Distinguished Professor and Henry M. Woodburn Chair of Chemistry at the State University of New York at Buffalo, was awarded the prestigious Ewald Prize by the International Union of Crystallography (IUCr).



Philip Coppens

The prize honors Coppens’ contributions to developing the fields of electron density determination and the crystallography of molecular excited states. He was also recognized for his commitment to the education of future crystallographers through many courses and workshops.

A significant part of the work for which he received the award is the result of studies at former NSLS beamline X3, which was operated by a collaboration of several SUNY campuses and for which Coppens was principal investigator for many years.

At X3, Coppens developed many of the methods he now uses in his research. Early on, he and his group performed several studies to determine the charge densities in various materials using x-ray diffraction. These experiments provided valuable insight into the properties of crystalline materials and the nature of chemical bonds within molecules and interactions between molecules. In later research, the group performed their first time-resolved studies at X3, using x-rays to determine the nature of molecular excited states that exist for very short

periods but are highly reactive. The first results of this research were published in 2002.

Coppens formally received the Prize during the IUCr's Florence Congress Opening Ceremony on August 23. The Prize, presented just once every three years at the triennial International Congresses of Crystallography, consists of a medal, certificate, and \$30,000.

2005 Chief's Honor Award for Distinguished Science Goes to Barbara Illman



Barbara Illman

Research plant pathologist and NSLS user Barbara L. Illman, who is Director of the Institute for Microbial and Biochemical Technology at the Forest Products Lab in Madison, Wisconsin, received the USDA Forest Service's 2005 Chief's Honor Award for Distinguished Science for her studies in four major areas of research.

The award recognizes Illman for her efforts in "applying solid-state

physics techniques to forestry problems, invasive species mitigation research, bioremediation research, and contributions to long-term ecological research programs."

At the NSLS, Illman developed techniques for using x-rays to study wood decay, recycling of wood biomass material, and bioremediation of toxic chemicals in the environment. This work led to discoveries about the biochemical mechanisms of brown-rot fungi, the most destructive wood-decay organisms. Nearly 10 percent of the 300 million tons of trees harvested annually in the United States are used to replace wood products damaged by the decay fungi. The discoveries could lead to improved methods for protecting wood from fungi.

Illman's many other achievements include measures to control the spread of highly destructive non-native insects, especially in shipping materials. Roughly half of all international trade goods move in wood crates or on wood pallets or spools, or involve other wood material, creating a major pathway for the spread of invasive insects.

The award was presented to Illman in a Washington, D.C. ceremony by Dale Bosworth, chief of the Forest Service.

Noel Clark: Co-Winner of the APS Oliver E. Buckley Prize

The 2006 American Physical Society Oliver E. Buckley Prize, recognizing "outstanding theoretical or experimental contributions to condensed matter physics," was awarded to Noel Clark, physicist at the University of Colorado and a user at beamline X10. He shares the prize with Robert Meyer of Brandeis University.

The two scientists received the award "for groundbreaking experimental and theoretical contributions to the fundamental science and applications of liquid crystals, particularly their fer-

roelectric and chiral properties."

Clark and Meyer have made very significant contributions to developing the concepts that underlie the fields of liquid-crystal science and technology. Beyond that, they have designed novel, highly creative experiments that verify these concepts. Their efforts also extend to studies of other complex fluid systems, such as liquid-crystal polymers, colloids, and protein solutions.

Individually, Clark has performed a great deal of significant research. One example is his groundbreaking studies of ferroelectric liquid-crystal display cells that made it possible for display-cell manufacturers to use them in commercial devices. And recently, using freeze-fracture electron microscopy and x-ray diffraction, he studied the liquid crystal phases exhibited by banana-shaped molecules and determined their complex structure, which had perplexed the liquid-crystal research community.



Noel Clark

The Buckley prize was formally awarded to Clark and Meyer on March 16 during the March 2006 APS meeting in Baltimore, Maryland. It consists of \$10,000 and a certificate.

— Laura Mgrdichian

Highlights from the COMPRES Sponsored Workshop on Synchrotron Infrared Spectroscopy for High Pressure Geoscience and Planetary Science

November 3-5, 2005

In recent years, infrared (IR) microscopy and spectroscopy have greatly benefited from new synchrotron techniques. New infrared synchrotron radiation sources provide a tremendous improvement in flux on a sample, with well-collimated beams from far- to near-IR that give high spatial resolution with unmatched signal-to-noise. This has opened up new scientific directions in a range of fields, including physics, biology, chemistry, materials science, high-technology, and forensics. One of the most exciting areas, however, is high-pressure geoscience and planetary science. High-pressure synchrotron IR spectroscopy is an ideal coupling of the diamond anvil cell device and synchrotron IR radiation. In addition, the technique serves as a useful, if not unique, tool to study minerals quenched from high pressures and temperatures, and natural samples (including natural high-pressure assemblages) at ambient conditions.

Sponsored by COMPRES (the Consortium for Materials Properties Research in Earth Sciences) and the NSLS, the work-



Synchrotron Infrared Spectroscopy for High Pressure Geoscience and Planetary Science workshop participants

shop on Synchrotron Infrared Spectroscopy for High Pressure Geoscience and Planetary Science was held at the NSLS in November. The conveners were Zhenxian Liu and Russell J. Hemley (Geophysical Laboratory, Carnegie Institution of Washington). Thanks to the members of the COMPRES Executive Committee and the NSLS staff for suggesting, promoting, and supporting this IR workshop. It was a great success in terms of the excellence of the lectures, its broad attendance that included many new potential users and student participation, its extensive program, and plenty of hands-on experience for new users. More than 50 attendees took part (this was the maximum allowed by the budget and the size of the lecture room).

The workshop consisted of five sessions designed to accommodate the broad spectrum of attendees, ranging from experts to new users. The Friday morning session was directed toward attendees who were new to the modern IR spectroscopy techniques used in this field, but, for experienced users, it was also a very useful review of the fundamentals and new developments. Q. Williams (University of California at Santa Cruz) gave a thorough overview on IR spectroscopy (and FT techniques in general) and its applications in the Earth sciences. G. Rossman (California Institute of Technology) gave a talk on hydrous components in nominally anhydrous minerals, which was crucially important for users who are interested in the calibration of the water content in minerals. A. Hofmeister (Washington University in St. Louis) discussed the high-pressure far-IR spectroscopy of mantle candidate minerals that are worth pursuing with the synchrotron technique. Finally, J. Tse (University of Saskatchewan, Canada) described theoretical methods for vibrational spectroscopy and many other applications.

The Friday afternoon session was started by L. Carr (NSLS). He gave a very comprehensive talk on Fourier transform spectroscopy techniques using the synchrotron infrared source as well as an overview of the IR programs at the NSLS. There were seven additional speakers (A. Goncharov, V. Struzhkin, and S. Jacobsen, Geophysical Laboratory; D. Klug, Canadian Research Council; H. Scott, Indiana University at South Bend; G. Lager, University of Louisville; and Y. Lee, Brookhaven National Laboratory) who discussed different topics related to the work they have done at NSLS beamline U2A. These talks

not only addressed a broad range of problems in the Earth and planetary sciences but also reflected new techniques developed at U2A in past years.

The third session, held Saturday morning, focused on imaging techniques combined with synchrotron sources. L. Miller (NSLS) gave an extensive overview of chemical imaging at high spatial resolution using a synchrotron infrared microscope. Other speakers (L. Wang, Stony Brook University; L. Dobrzhi-netskaya, University of California at Riverside; M. Koch-Müller, GeoForschungsZentrum Potsdam, Germany; and S. Clark, Advanced Light Source) gave talks featuring the applications of imaging techniques as well as high-pressure IR studies at other synchrotron sources. The facility tour and hands-on session on Saturday afternoon attracted more than 30 people. At the IR beamline, new users received detailed information on the beamline facility and its capabilities, as well as first-hand experience on how to perform high-pressure IR experiments from beginning to end.

The last session, for student/post-doc experiments at U2A, started right after the workshop. Two students and one post-doc submitted their research proposals and one day of beam-time was allocated per proposal. This new session offered not only a great opportunity to learn how to use the synchrotron IR facility but also a chance to collect valuable data for their research projects. The experiments went very well and the IR data they obtained were very interesting and publishable in scientific journals.

— Zhenxian Liu

The NSLS Remembers Bill Oosterhuis

November 16, 2005

Bill Oosterhuis, Team Leader for Condensed Matter Physics and Materials Chemistry in the U.S. Department of Energy's Office of Basic Energy Sciences, passed away on November 16.

Bill was a true friend of synchrotron radiation science. While at DOE, a position he had held since 1991, he made significant contributions to the field, spearheading several major changes to the Condensed Matter Physics and Materials Chemistry team.

These include the creation of the X-ray and Neutron Scattering program, the Theoretical and Computational Materials Physics program, and the Experimental Program to Stimulate Competitive Research.

Before joining the DOE, Oosterhuis he worked for 17 years at the National Science Foundation, where he was a section head for its



Bill Oosterhuis

Division of Materials Research. During this time, he became a driving force for progress during the U.S. transition from first-generation to second-generation synchrotrons.

Similarly, while at DOE, he provided support and guidance as third-generation synchrotrons were developed. As a result of his presence during these years, he is widely credited for playing a major role in the growth of synchrotron radiation research. Upon his death, he leaves behind this important legacy.

Bill is remembered for his overall passion for science, and materials research in particular, his finely honed sense of progress and forward-thinking, and, more personally, his pervasive optimism and ability to earn the trust of others. He will be missed by many.

— Laura Mgrdichian

BNL Establishes NSLS-II Project In Light Sources Directorate

December 9, 2005



Steve Dierker

In the fall of 2005, Laboratory Director Praveen Chaudhari named Steve Dierker, Associate Laboratory Director (ALD) for Light Sources, as Project Director of the newly established National Synchrotron Light Source II (NSLS-II) Project. The move was triggered by the Lab's recent success in getting DOE approval for "Critical Decision Zero" (CD-0, Approval of Mission Need) for NSLS-II, the planned world-leading successor to BNL's NSLS. NSLS-II will meet

critical scientific challenges of the future, provide state-of-the-art technology for research — complementing BNL's Center for Functional Nanomaterials — and play a pivotal role in fostering economic growth in the northeastern United States.

CD-0 is the first of five Critical Decisions that the project will need to achieve in order to progress through the successively more detailed stages of conceptual design, preliminary design, and final design, followed by construction, and then operations. While the site for NSLS-II is not formally selected until the next Critical Decision (CD-1, Approved Alternative Selection and Cost Range), BNL believes that there are strong reasons for citing NSLS-II at BNL.

"At Brookhaven, we have long experience and deep technical knowledge in the synchrotron light source field, along with an

excellent infrastructure, demonstrated support from potential facility users of national and international standing, and an extraordinarily skilled and experienced workforce," states Dierker. "For these and other reasons, we believe NSLS-II should be located here at BNL."

NSLS-II will be a major project, with an estimated cost of \$800M, and will employ up to 200 people during the peak of construction. The NSLS-II Project organization is being created in the Light Sources Directorate to put in place the management systems and infrastructure required to execute this complex undertaking. Building upon the groundwork laid by NSLS staff, the first task of the new organization will be to develop the documents required for CD-1, including a Conceptual Design Report and more refined cost and schedule estimates.

As NSLS-II Project Director, Dierker will retain his position as ALD for Light Sources and step down as Chair of the NSLS Department. Chi-Chang Kao, the current NSLS Department Deputy Chair, was named Interim NSLS Chair and assumed his new responsibilities in mid-January, 2006.

The NSLS-II Project Office is housed in Building 817. The organization plan is well under way, and includes an Administration & Finance Office, headed by an Associate Director for Administration & Finance; and three technical Divisions — Accelerator Systems, Experimental Facilities, and Conventional Facilities — each headed by a Division Director. Several advisory committees are being formed to provide broad perspective and expert advice, including an NSLS-II Advisory Board and advisory committees for each of the three Divisions.

Each Division will be responsible for design and construction activities within its specialty area, and will be staffed with a range of specialty groups. Many of these positions are expected to be filled by existing Lab personnel. With an estimated annual operating cost of \$90M, the staff required to operate NSLS-II will be about twice as large as that required to operate the present NSLS, adding about 200 new positions to the Laboratory.

— Liz Seubert

2005 NSLS Tours

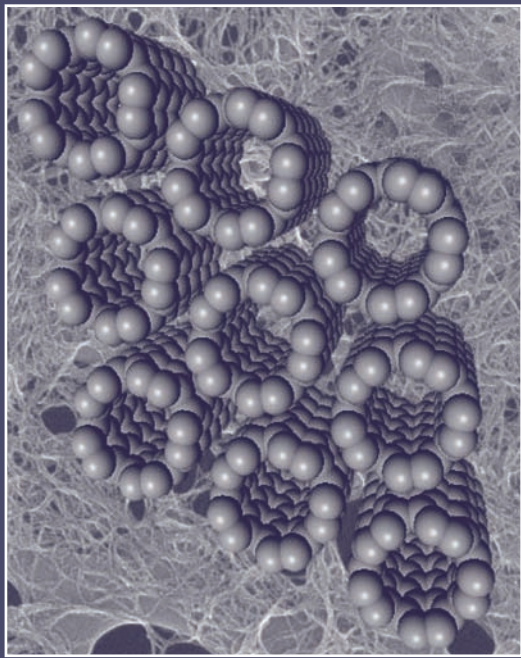
1/11/2005	Infotonics Technology Center and Javelin Assoc., Rochester Federal Subcontracting Initiative
1/24/2005	City College of New York
1/28/2005	Islip School District Science Faculty
2/17/2005	Rochester Institute of Technology
2/24/2005	United States Department of the Navy
2/25/2005	Hofstra University, Society of Physics Students
3/18/2005	BNL Employee Tour
3/28/2005	City College of New York
4/4/2005	Stony Brook University Undergraduates
4/6/2005	League of Women Voters - Suffolk County Brookhaven Chapter
4/7/2005	University of Connecticut
4/14/2005	Charterhouse School
4/15/2005	Congressman David Hobson
4/21/2005	Queens College
4/28/2005	DOE Facility Managers Conference
4/29/2005	Suffolk Community College
4/29/2005	Nassau Community College - Physics & Engineering
5/5/2005	The Roundtable at Stony Brook University
5/6/2005	City College of New York - IEEE Chapter
5/10/2005	Suffolk Community College
5/10/2005	Suffolk County Commissioner of Public Health Services
5/12/2005	Senator Schumer's Staff
5/12/2005	Invision
5/13/2005	Literacy Volunteers of America
5/17/2005	NASA Users' Workshop
5/26/2005	SUNY at Farmingdale - Institute of Retirement and Learning
6/6/2005	Stony Brook University Research Experience for Undergraduate (REU) Students
6/7/2005	OEP Summer Program Students
6/20/2005	DOE - Materials Science Review for BES
6/20/2005	Nuclear Chemistry Summer Students
6/24/2005	DOE Contractor Attorneys Conference
6/28/2005	Stony Brook University - BioPrep Program
7/6/2005	Columbia University REU Students
7/11/2005	Stony Brook University - Garcia Center for Material Science
7/12/2005	SUNY - REU Physics & Chemistry Program

2005 NSLS Tours

7/13/2005	Korean Ministry of Government Legislation (MOLEG)
7/14/2005	Stony Brook University - Masters in Business Administration
7/21/2005	New York State Community College Summer Program
7/21/2005	Columbia University (Summer Chemistry Program)
7/27/2005	BNL QUARK.NET Summer Program
8/8/2005	Mt. Sinai Rotary Club
8/9/2005	Dr. Rohatgi - DOE Review
8/9/2005	Senior Advisor for Science and Engineering Workforce, NSF
8/12/2005	U.S. Army Recruits
8/15/2005	Senator Clinton's Washington Staffers
8/16/2005	Industrial Center Workshop
8/23/2005	Richard Gelfond
8/25/2005	IBM Group
9/14/2005	New York State Assemblyman Philip Ramos
9/16/2005	DOE - Materials Science Review for BES
9/28/2005	Merchant Marine Academy - Nuclear Engineering and Physics
9/28/2005	SUNY at Stony Brook - Biomedical Engineering Program
9/30/2005	Atomic Energy Regulatory Board
10/7/2005	Small Business Administration
10/19/2005	Green Mens Club
10/25/2005	SUNY at Stony Brook - Cytotechnology Group
11/4/2005	Suffolk Community College
11/7/2005	Green Mens Club
11/9/2005	United Federation of Teachers (retired)
11/10/2005	U.S. States Department Tour - Kazakhstan Visitors
11/14/2005	Chinese Academy of Sciences, Shanghai Institute of Applied Physics
11/15/2005	Dr. Alan Friedman, Director & CEO, New York Hall of Science
11/16/2005	Quark.Net Physics Teachers
11/22/2005	SUNY at Stony Brook - Physics Department
12/2/2005	Green Mens Club
12/6/2005	Columbia University
12/12/2005	Southern Methodist University
12/12/2005	Office of Science and Technology Policy (OSTP)
12/15/2005	Rensselaer Polytechnic Institute

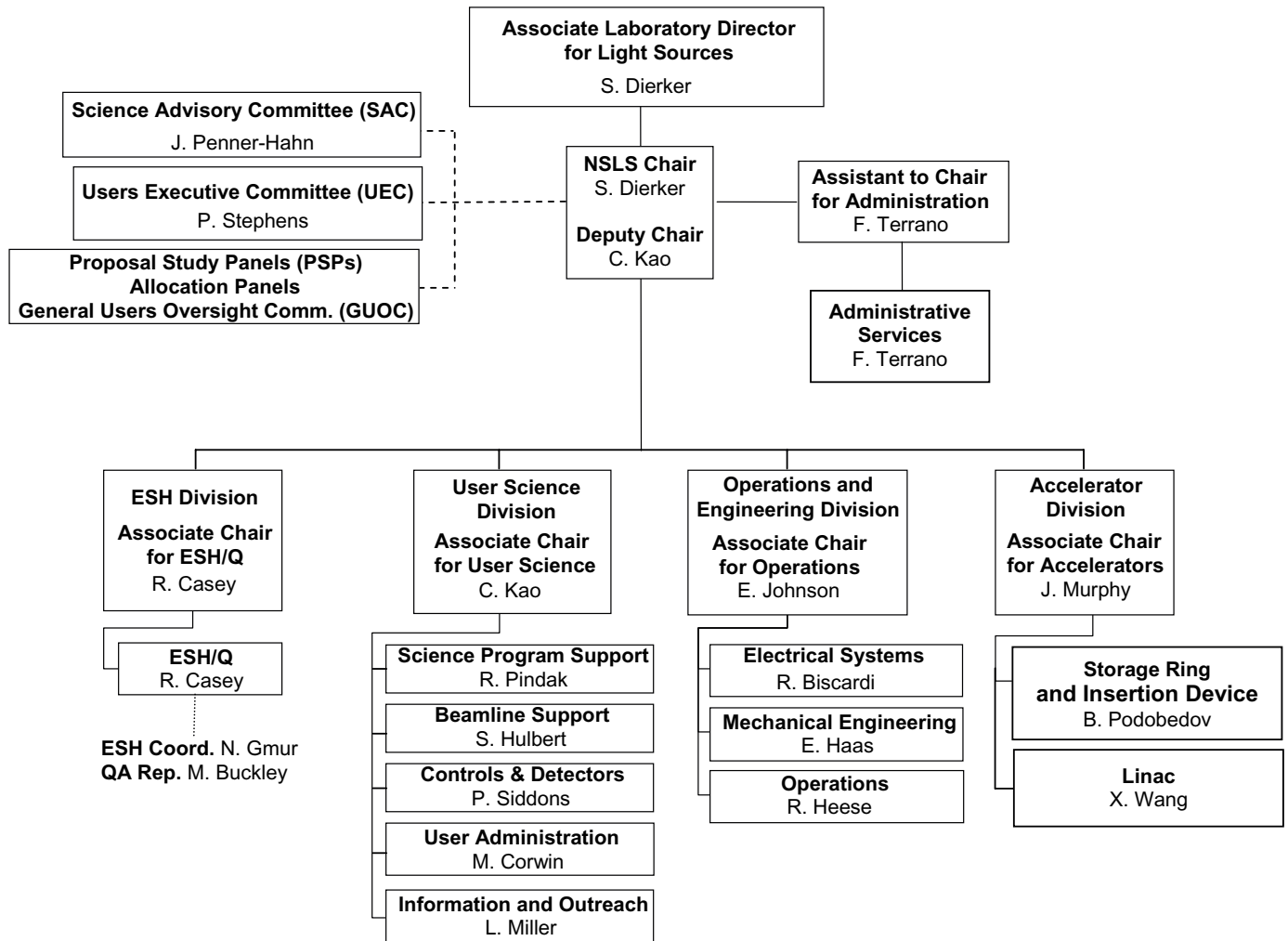
2005 NSLS Workshops

1/25/2005	Synchrotron Light for Powder Diffraction
3/1/2005	X6A Workbench: Hands-On Training in Synchrotron Crystallography
4/5/2005	RapiData 2005
4/18/2005	Strain-Mapping Workshop
4/26/2005	X6A Workbench: Hands-On Training in Synchrotron Crystallography
5/10/2005	Workshop on Intense Coherent THz Pulses
5/23/2005	Nanomagnetism: Materials and Probes
5/23/2005	Synchrotron Imaging of Biominerals
5/23/2005	The Impact of Cryogenic Specimen Automounters on the Future of Macromolecular Crystallography
5/25/2005	Spectroscopic Studies of Nanoscaled Systems
5/25/2005	Application of SAXS to Biological Structures
5/25/2005	<i>In-Situ</i> Kinetic Analyses in Environmental and Chemical Systems
6/6/2005	Crystallization Workshop
6/20/2005	BioCD-2005
7/12/2005	X6A Workbench: Hands-On Training in Synchrotron Crystallography
9/19/2005	Synchrotron Environmental Science III (SES) Meeting
9/28/2005	EXAFS Course: Theory, Experiment, and Advanced Applications
10/25/2005	X6A Workbench: Hands-On Training in Synchrotron Crystallography
11/3/2005	COMPRES Sponsored Workshop on Synchrotron Infrared Spectroscopy for High Pressure Geoscience and Planetary Science



Organization

National Synchrotron Light Source Organization



NSLS Advisory Committees

USERS' EXECUTIVE COMMITTEE

The Users Executive Committee (UEC) provides for organized discussions among the user community, NSLS administration, and laboratory directorate. It aims to communicate current and future needs, concerns, and trends within the user community to NSLS staff and management, and to disseminate to the users information about the NSLS and BNL plans.

CHAIR

Peter Stephens, Stony Brook Univ.

VICE CHAIR

Chris Jacobsen, Stony Brook Univ.

PAST CHAIR

Larry Shapiro, Columbia Univ.

SECRETARY/SPIG REP

Jeff Keister, SFA, Inc.

MEMBER

Steve Almo, AECOM

MEMBER

Chris Cahill, George Washington Univ.

MEMBER

Trevor Tyson, NJIT

MEMBER

Hao Wu, Cornell Univ.

EX-OFFICIO

Chi-Chang Kao, NSLS User Science Division

EX-OFFICIO

Mary Anne Corwin, User Administration Office

EX-OFFICIO

Lisa Miller, NSLS Information and Outreach Office

SPECIAL INTEREST GROUP REPRESENTATIVES

Special Interest Groups in areas of common concern communicate with NSLS management through the UEC.

BIO. SCATTERING AND DIFFRACTION

Ann Stock, Univ. of Medicine and Dentistry of NJ

INDUSTRIAL USERS

Paul Stevens, Exxon Mobil Research & Engineering Company

IMAGING

Sue Wirick, Stony Brook Univ.

INFRARED USERS

Randy Smith, BNL-NSLS

NUCLEAR PHYSICS

Mahbub Khandaker, TJNL

STUDENTS AND POST DOCS

Meghan Ruppel, Stony Brook Univ.

XAFS

Paul Northrup, BNL-Environ. Sci.

X-RAY SCATTERING AND CRYSTALLOGRAPHY

Ben Ocko, BNL-Physics

TIME RESOLVED SPECTROSCOPY

John Sutherland, BNL-Biology

TOPOGRAPHY

Michael Dudley, Stony Brook Univ.

UV PHOTOEMISSION AND SURFACE SCIENCE

Jeff Keister, SFA, Inc.

SCIENCE ADVISORY COMMITTEE

The Science Advisory committee (SAC) evaluates science programs at the NSLS and makes recommendations to the Chairman.

Mario Amzel, Johns Hopkins School

Joel Brock, Cornell Univ.

Thomas Ellenberger, Harvard School

Eric D. Isaacs, ANL

Edward Kramer, Univ. of California

Simon Mochrie, Yale Univ.

James Penner-Hahn, Univ. of Michigan

Peter Stephens, Stony Brook Univ.,
Ex-Officio, UEC Chair

William Thomlinson, CLS



UEC and SPiG Members (standing, from left): Chi-Chang Kao, Gretchen Cisco, Larry Shapiro, Steve Almo, Trevor Tyson, Sue Wirick, Paul Stevens, Hao Wu, Jeff Keister, Meghan Ruppel, John Sutherland, Mary Anne Corwin, Chris Cahill, Paul Northrup, and Ben Ocko. (Sitting, from left) Peter Stephens and Chris Jacobsen.

NLSL Advisory Committees

GENERAL USER PROPOSAL REVIEW PANEL

The Proposal Review Panel (PRP) reviews and rates General User Proposals. Members are drawn from the scientific community and generally serve a two-year term.

IMAGING AND MICROPROBES: BIOLOGICAL AND MEDICAL

Leroy Chapman, Univ. of Sask.
Max Diem, City Univ. of New York
Paul Dumas, Soleil
Kathleen Gough, Univ. of Manitoba
Lindsay Keller, NASA
Barry Lai, ANL
Irit Sagi, Weizmann Institute of Sci.

IMAGING AND MICROPROBES: CHEMICAL AND MATERIALS SCIENCES

Harald Ade, N.C. State Univ.
David Black, NIST
Gene Ice, ORNL
Nobumichi Tamara, LBNL

IMAGING AND MICROPROBES: ENVIRONMENTAL AND GEOSCIENCES

Don Baker, McGill Univ.
David Black, NIST
Jeffrey Fitts, BNL-Environ. Sci.
George Flynn, SUNY @ Plattsburgh
Lindsay Keller, NASA
Kenneth Kemner, ANL
David Wetzel, Kansas State Univ.

IR/UV/SOFT X-RAY SPECTROSCOPY: CHEMICAL SCIENCES/SOFT MATTER/ BIOPHYSICS

Jingguang Chen, Univ. of Delaware
Daniel Fischer, NIST
Jan Genzer, N.C. State Univ.
David Mullins, ORNL
Michael White, BNL-Chemistry

IR/UV/SOFT X-RAY SPECTROSCOPY: MAGNETISM/STRONGLY CORRELATED ELECTRONS/SURFACES

Robert Bartynski, Rutgers Univ.
Di-Jing Huang, SRRG
Hong Ding, Boston College
Boris Sinkovic, Univ. of Connecticut
Jiufeng Tu, CUNY
Tonica Valla, BNL-Physics
Barrett Wells, Univ. of Connecticut

METHODS AND INSTRUMENTATION

Leroy Chapman, Univ. of Sask.
Kenneth Finkelstein, Cornell Univ.
Albert Macrander, ANL
Ralf-Hendrik Menk, Sincrotrone Trieste
Peter Takacs, BNL-Instrumentation

MACROMOLECULAR CRYSTALLOGRAPHY

Alex Bohm, Tufts Univ.
Daniel Leahy, Johns Hopkins Univ.
Brenda Schulman, St. Jude Hospital
Da Neng Wang, New York Univ.
Joshua Warren, Duke Univ.

POWDER/SINGLE CRYSTAL CRYSTAL- LOGRAPHY

Simon Billinge, Michigan State Univ.
Thomas Duffy, Princeton Univ.

Stefan Kycia, Univ. of Guelph
Peter Lee, ANL
Peter Stephens, Stony Brook Univ.

X-RAY SCATTERING: MAGNETISM/ STRONGLY CORRELATED ELECTRONS/ SURFACE

Sean Brennan, Stanford Univ.
Kenneth Finkelstein, Cornell Univ.
Valery Kiryukhin, Rutgers Univ.
Karl Ludwig, Boston Univ.
George Srajer, ANL
Trevor Tyson, NJIT

X-RAY SCATTERING: SOFT MATTER AND BIOPHYSICS

Paul Heiney, Univ. of Pennsylvania
Ben Hsiao, Stony Brook Univ.
Huey Huang, Rice Univ.
Robert Leheny, Johns Hopkins Univ.
H. Miriam Rafailovich, Stony Brook U.
Detlef Smilgies, Cornell Univ.
Helmut Strey, Stony Brook Univ.

X-RAY SPECTROSCOPY: BIOLOGICAL, ENVIRONMENTAL, AND GEOSCIENCES

Martine Duff, Westinghouse Savannah
Dean Hesterberg, N.C. State Univ.



SAC Committee members (from left): Eric Isaacs, Peter Stephens, Joel Brock, Tom Ellenberger, Bill Thomlinson, Jim Penner-Hahn, and Simon Mochrie. (Missing from photo): Ed Kramer and Mario Amzel.

NSLS Advisory Committees

GENERAL USER PROPOSAL REVIEW PANEL (CONT.)

X-RAY SPECTROSCOPY: BIOLOGICAL, ENVIRONMENTAL, AND GEOSCIENCES

Douglas Hunter, Univ. of Georgia
Kenneth Kemner, ANL
Satish Myneni, Princeton Univ.

X-RAY SPECTROSCOPY: CHEMICAL AND MATERIAL SCIENCES

Uwe Bergmann, SLAC
Simon Bare, UOP
Anatoly Frenkel, Yeshiva Univ.
Steven Heald, ANL
Jean-Pascal Rueff, Jussieu
Tsun Sham, Univ. of Western Ontario
Trevor Tyson, NJIT

ALLOCATION PANEL

The Allocation Panel allocates general user beam time to both new proposals and beam time requests based on ratings provided by the Proposal Study Panels. Members are drawn from the scientific community and generally serve a two-year term.

BIOLOGY-PX

Marc Allaire, BNL-NSLS
Annie Heroux, BNL-Biology

EXAFS

Jeffrey Fitts, BNL-Environ. Sci.
Syed Khalid, BNL-NSLS

IMAGING AND MICROPROBES

James Ablett, BNL-NSLS
Kenneth Evans-Lutterodt, BNL-NSLS
Antonio Lanzirotti, Univ. of Chicago
Lisa Miller, BNL-NSLS

IR/UV/SOFT X-RAY

Larry Carr, BNL-NSLS

VUV ALLOCATIONS

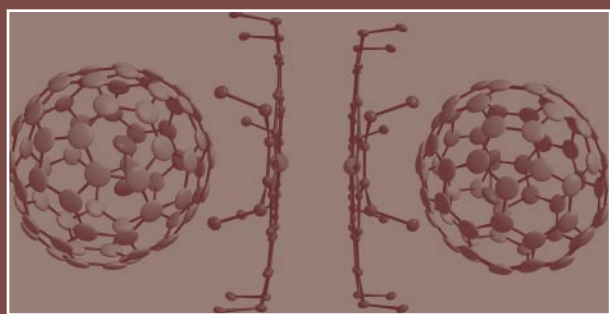
Elio Vescovo, BNL-NSLS

POWDER/SINGLE CRYSTAL/HIPRESS/ OPTICS

Zhong Zhong, BNL-NSLS

SCATTERING

Elaine DiMasi, BNL-NSLS
Cecilia Sanchez-Hanke, BNL-NSLS
Jean Jordan-Sweet, IBM
Christie Nelson, BNL-NSLS
Lin Yang, BNL-NSLS



Facility Report

Accelerator Division Report

James B. Murphy

Associate Chair for Accelerators

Organization and Mission

The NSLS Accelerator Division (AD), headed by James B. Murphy, is organized into two sections: the Linear Accelerator (Linac) section, headed by Xijie Wang, and the Storage Ring & Insertion Device section (SR & ID), headed by Boris Podobedov. The AD staff consists of ten accelerator physicists, two engineers, three technicians, and four postdocs.

The NSLS Accelerator Division has a four-part mission:

- To ensure the quality of the electron beam in the existing NSLS booster and linear accelerator, and the x-ray & vacuum ultraviolet (VUV) storage rings
- To participate in the NSLS-II project, in particular the design of the storage ring and injection system
- To operate the Magnet Measurement Lab (MML) and the Source Development Laboratory
- To perform fundamental research and development in accelerator and free-electron laser physics

2005 Activities

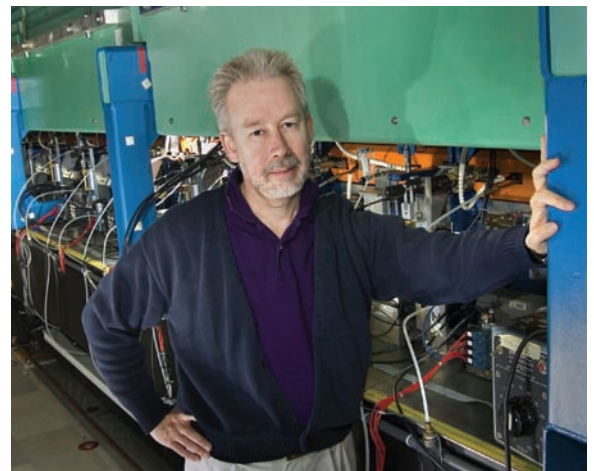
Storage Ring & Injection System Improvements

Both storage rings have seen a steady rate of improvements in 2005. Several new or upgraded diagnostics, including electron beam profile imaging hardware and a turn-by-turn beam position monitor for injection studies, have been made operational in the x-ray ring. Machine studies took place to better understand and improve the injection process into the rings. Additional work has been done to better calibrate the x-ring lattice model, specifically to improve the control of the horizontal-vertical coupling and vertical dispersion. Machine studies were also performed to prepare for the installation of the new X25 undulator in January 2006.

One activity that brought an immediate improvement to the VUV ring users was the fine-tuning of the lattice, which resulted in a beam lifetime increase. Using the “Middle Layer” software tools incorporated into the NSLS control system last year, the VUV ring symmetry was restored by correcting the quadrupole settings and adjusting the revolution frequency. With the restored periodicity, the lattice has a 15-20% higher lifetime, depending on the ring current.

A task force on “Storage Ring Closed Orbit Measurement, Reproducibility, Stability & Feedback” was formed to develop a plan to provide improvements on orbit stability. The task force drew upon the experimental and theoretical expertise of the Accelerator, Operations & Engineering and User Science divisions. Its objective was to determine the factors that influence beam stability and reproducibility in the x-ray and VUV storage rings, determine the present performance of related systems, and make recommendations for improvements to these systems, up to the state-of-the-art. In the course of their work, the task force systematically examined the requirements of the users, the status of key subsystems, such as beam position monitors, orbit feedbacks, orbit correction algorithms, and the noise sources that degrade beam stability. A report of the task force’s findings and recommendations is being prepared and those recommendations will be followed up on in the coming year.

Tremendous progress was made in FY05 to improve the NSLS injection system. Working in collaboration with the Operation & Engineering Division (OED), the beam profile monitors, wall current monitors, and synchrotron light monitor for the NSLS linac and booster were successfully upgraded. Those newly upgraded diagnostic tools are now being used to improve the injection efficiency and reduce beam loss. An RF klystron was successfully re-built by Communications Power Industries (CPI) to ensure that the NSLS linac has sufficient spare klystrons for future operations.



Magnet Measurement Laboratory

During the December 2005 shutdown, the existing 15-year-old X25 hybrid wiggler was replaced by a new, state-of-the-art, cryo-ready, in-vacuum “mini-gap undulator” (MGU), optimized for a dedicated macromolecular crystallography program. The X25 MGU is expected to provide X25 with between 2 and 30 times brighter x-ray beams over its entire tuning range, compared with the old X25 wiggler. It will also be substantially brighter, with better spectral coverage than the previous MGUs at X13 and X29. The mechanical and vacuum system was designed and fabricated by Advanced Design Consultants, Inc. of Lansing, NY; the magnet arrays were assembled at NSLS. The new MGU’s one-meter-long hybrid permanent magnet structure has a period of 18 mm, a minimum operating gap of 5.6 mm, and a peak on-axis design field of 0.91 T. The device will provide continuously tunable spectral coverage from 1.9 to 20 keV, using the fundamental, 2nd, 3rd, 5th, and 7th harmonics. We used a new high-remnance, high-temperature grade of NdFeB developed for hybrid car motors (NEOMAX 42AH) with $B_r = 1.3\text{T}$ and $H_{c_j} = 24\text{ kOe}$ at room temperature. The high intrinsic coercivity (H_{c_j}) allows the undulator to be baked to 100 °C without a loss of magnetization for ultra-high vacuum (UHV) compatibility. Baking under vacuum in the lab for half a day at 90 °C showed only a 0.4% decrease in the peak field, and an additional five-day 85 °C bake showed negligible additional demagnetization. The final pressure after cool-down was less than 5×10^{-10} torr, well within x-ray ring requirements.

The new MGU design incorporates several novel features, the most important being a provision for cryo-cooling the magnet arrays to 150 K. This will increase the remanence (B_r) of the NdFeB magnets to about 1.45 T and raise the peak field to 1.0 T, thereby increasing the tuning range of all harmonics by 11%, as well as increasing the source brightness at some key photon energies.



Proud X25 team surrounding the new mini gap X25 undulator

To minimize stress and deformation of the magnet support beams during welding of the cooling channels, a low-temperature “friction stir welding” technique was used for the first time in a UHV device. The cooling channels proved to be vacuum-tight under repeated cryogenic cycling and baking. A provision for stress-free thermal expansion and contraction of the magnet support structure was also demonstrated during the thermal cycling.

A novel gap-measurement system using a commercial, high-precision, LED-based optical micrometer was incorporated to back up the linear encoders and to correct for gap changes due to differential contraction during cryogenic operation. The system optically monitors the magnet gap through viewports at either end of the MGU, ensuring a gap accuracy of ± 2 micrometers.

Magnetic measurements were performed using both pulsed wire and Hall probe mapping. A pair of full-length, rectangular Helmholtz coils was added to the exterior of the vacuum chamber to compensate for Earth’s field and to cancel a small systematic dipole error in the magnet array. These coils will be powered by one of the existing end-pole supplies from the old X25 wiggler. Despite very little time for trajectory, multipole, and phase error shimming, we achieved an RMS phase error of 2.5 degrees (sufficiently low to assure good spectral quality up to the 7th harmonic) and met the x-ray ring’s multipole tolerances.

The new X25 MGU was completed, tested, measured, and shimmed on schedule, thanks to the outstanding efforts of NSLS staff members from all divisions, who worked many nights and weekends to make it happen. Most of them can be seen in the photo above.

NSLS-II Machine Design

The NSLS-II storage ring is the future of the NSLS, and it will provide unprecedented high-brightness photons to the user community. The AD staff worked in collaboration with the OED staff to produce the pre-conceptual machine design, which served as the technical basis for achieving “Critical Decision Zero” status for the NSLS-II project in August 2005.

Source Development Laboratory (SDL)

The Source Development Laboratory is a platform for the development and applications of new radiation sources, such as free electron lasers and coherent terahertz (THz) radiation. Funding was obtained from the Office of Navy Research to pursue the development of laser-seeded free electron amplifiers in the 0.8 - 1.0 micron range. The SDL has also measured a record 100 microjoules per pulse of THz radiation, which will be used for materials science applications by BNL and external users.

Operations and Engineering Division

Erik D. Johnson

Associate Chair for Operations and Engineering

Organization and Mission

The Operations and Engineering Division (OED) has three sections: Operations, which is led by Richard Heese; Electrical Systems, led by Richard Biscardi; and Mechanical Engineering, led by Ed Haas. To serve the NSLS user community, our mission falls into three main areas:

- Operating on of the NSLS 24 hours a day, seven days a week, an average of 44 weeks a year
- Designing, fabricating, and maintaining of the NSLS accelerators, infrastructure, and instruments, including upgrades, modifications, and proposal development
- Providing engineering and technical support for other NSLS divisions and the NSLS user community

The OED staff includes one scientist, 19 engineers, and 55 technicians, making it the largest of the NSLS divisions. In addition to its own staff, the division coordinates the activities of five full-time skilled tradesmen from the laboratory, as well as shops and trades assigned for specific jobs. The breadth of our mission is such that we need to draw on the capabilities of the other NSLS divisions for support, and in turn provide specialized support for their activities.

2005 Activities

Thankfully, this year was not punctuated by some of the major equipment failures that we have experienced in recent years. An overview of machine performance summarized for calendar year 2005 is provided in Section 6, "Facility Facts and Figures." For Fiscal Year 2005, which is the DOE reporting period, overall reliability was 96% for the x-ray ring and 99% for the VUV ring. For a facility now into its third decade of operations, high reliability depends critically on an aggressive maintenance program as well as the skill of the staff operating the machine. Faults and operations disruptions are carefully monitored to extract trends and help us focus our efforts on the most fragile systems. A comparatively small number of disruptions over four hours in duration accounts for much of the down time. For FY 2005, roughly one-third of the downtime came from only six events on the x-ray ring and three on the VUV ring. This distribution is an indication of a mature operation with an effective preventive maintenance program.

Along with our maintenance program, a number of initiatives were undertaken this year aimed at improving the safety, performance, and reliability of the facility. After an extensive evaluation of hazards at the NSLS, our staff members located, identified, and labeled potential sources of stored energy that could cause injury to staff or visitors. Placing informational signs sounds like a mundane activity, but it was actually an important milestone in our program to enhance worker safety around the facility. During the spring shutdown, in addition to our equipment upgrade and preventative maintenance activities, NSLS staff members placed more than two thousand warning signs on equipment around the facility, much of it in use since the start of NSLS operations. This activity required a bottom-up assessment of the stewardship and hazards for all of the NSLS equipment, capturing the information in a systematic manner and providing suitable warning signs with information pointing to the correct procedures for servicing the equipment. This monumental investment of effort is worthwhile, since we anticipate continuing use and development of the facility for some years ahead.



Significant effort was also directed toward becoming compliant with various code requirements. Major investments were made to facilitate compliance with the National Fire Protection Association code on electrical safety (NFPA 70E) in a way that minimizes impact on operations. This included providing specialized personnel protective equipment (PPE) required by the code, providing training on its use, and, where possible, installing systems to verify that equipment that does not require the use of PPE is de-energized.

An Electrical Equipment Inspection (EEI) program has also been developed to assure that electrical equipment is free from reasonably foreseeable risk due to electrical hazards. This goal can be met when equipment is certified by a

Nationally Recognized Testing Laboratory (NRTL) or through further inspection through the EEI program. In either case, the equipment must be inspected and inventoried. Equipment that does not carry NRTL certification will be subject to further examination to ensure that it will be safe for its intended use. This work will be performed by a cadre of inspectors comprised of longtime members of the NSLS community with extensive experience as electrical technicians or engineers. This effort will be an ongoing program, and full inspection of all equipment is expected by DOE by 2009.

The spring shutdown also saw a complete rebuild and upgrade of the UV RF1 temperature control system, substantially improving its thermal response. This is important because the old system could not adjust quickly enough to keep up with the change in load from injection at maximum rate, and hence extended the minimum fill time for the VUV ring. After the shutdown, with the new system in place, one fill was completed from 0 to 1000 mA in less than two minutes. Of course, this also depended on the ability of the injector to rapidly supply charge to the machine.

Working with the Accelerator Division staff, this year the injection system was fitted with enhanced diagnostics to allow tracking of its performance. Wall current monitors were installed on existing ceramic breaks to follow current loss from the linac through the transport lines. Improved flags installed in key areas provide better imaging of the electron beam to help with machine tune-up. These upgrades are part of an ongoing effort to reduce lost charge and the radiation it produces around the facility. They also have the benefit of providing more user beam through reduced injection times.

Several other major activities underway in 2005, aimed at improving the capabilities of the facility, achieved significant milestones during the winter 2005 shutdown. The new undulator constructed for X25 was installed, providing a much brighter source for the X25 program. The construction, measurement, and testing of this novel device was a monumental and sustained undertaking for the whole department. The X25 mini-gap undulator (MGU) is described in detail by the Accelerator Division on page 5-4. This is only fitting, since their Magnetic Measurement Lab became a center of activity as the device came together for final assembly and testing starting in October.

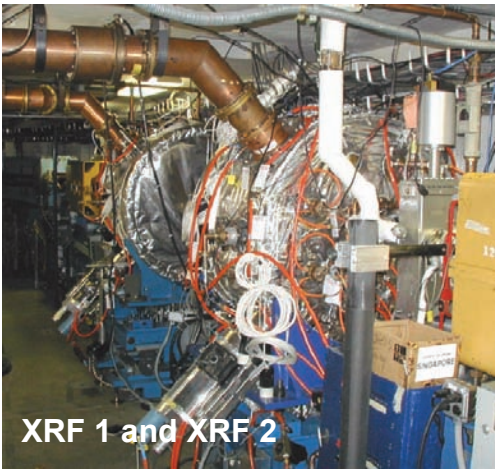
Another major program effort revolves around the creation of an insertion device based on a small angle x-ray scattering (SAXS) beamline to support research for the Center for Functional Nanomaterials. As it happens, the only available insertion device location in the x-ray ring is the RF straight, which feeds the X9 beamline, a slot already occupied by two very active beamlines that need to be relocated to make way for the new program. A suitable new home for the current Case Western X9 beamlines is the space at X3, although it was occupied by the Stony Brook University powder diffraction program. This program was relocated to X16C, which was refurbished for powder diffraction work. This cascade of moves is well underway, with the User Science Division coordinating and supporting the relocation of SBU program to X16C and dismantling the old beamline at X3 during 2005. This seemingly Byzantine series of moves was planned after careful consideration of many alternative sequences that would address the need to make a significant program change in a facility that is fully built out. Of the options considered it was easily the most cost effective way to free the space at X9 with minimal

FY05 Summary Fault Analysis

Group Area/System	Number of Faults			Downtime [hr]	
	Total	X- DT	U- DT	X-ray	UV
Total Charges to Down Time					
Controls and Diagnostics	121	37	11	29.8	8.4
Power Systems	195	41	45	60.7	57.3
Utilities	95	47	26	54.3	10.7
Miscellaneous	136	86	8	36.1	1.6
	547	211	90	180.9	77.9
Significant Disruptions					
Ground Faults on XQB				22.5	
VUV RF System Intermittant Short					20.3
X-ray Sextupole overheating (XSD1)				13.1	
Trim system failures				8.1	
LIPA Switchover Power Dip				4.1	
VUV RF 100 W amplifier failure					4.3
XRF2 Contactor Replacement				3.6	
VUV Dipole PS Water Leak					3.7
				51.4	28.3
Balance to 'Routine' Faults					
				129.5	49.7



The X25 MGU in the tunnel (not surrounded by the legion who built it; see Accelerator Division article for more information).



disruption for most of the user community.

To provide sufficient space within the x-ray ring for the insertion device that is to be located in the RF straight, the last of the new RF cavities was installed during the winter shutdown. Beyond making space for a new insertion device, as was done in the X29 RF straight, this last new cavity for the x-ray ring completes a long upgrade campaign. The new cavity design has improved thermal performance and eliminates weld joints that separated vacuum from water.

Further work is planned for the winter 2006 shutdown to install an insertion-device-capable exit chamber on the ring and to complete preparations of the RF straight such that it can receive an insertion device. The critical front-end components for the current X9 beamline will be relocated during the May 2006 shutdown, with relocation of the beamline to occur during the summer of 2006.

With the award of CD0 for NSLS-II in 2005, the whole NSLS community looks forward to bringing the exciting capabilities the proposal envisions into reality. In the meantime, the OED will continue to work with the other NSLS divisions to keep our user community on the existing facility — one of the most productive synchrotrons in the world.

User Science Division Report

Chi-Chang Kao

Associate Chair for User Science

Organization and Mission

The User Science Division coordinates major facility activities related to users so that we can be more effective in communicating with the user community, strengthening existing scientific programs, fostering the growth of new scientific programs, and raising the visibility of the exciting science produced by our users both inside and outside the scientific community. The division consists of five sections: User Administration (Mary Anne Corwin), Information and Outreach (Lisa Miller), Beamline Development and Support (Steve Hulbert), Scientific Program Support (Ron Pindak), and Detectors and Controls (Peter Siddons). The major initiatives and accomplishments of the User Science Division and the NSLS user community for 2005 are summarized below.

2005 Activities

Beamline Reviews

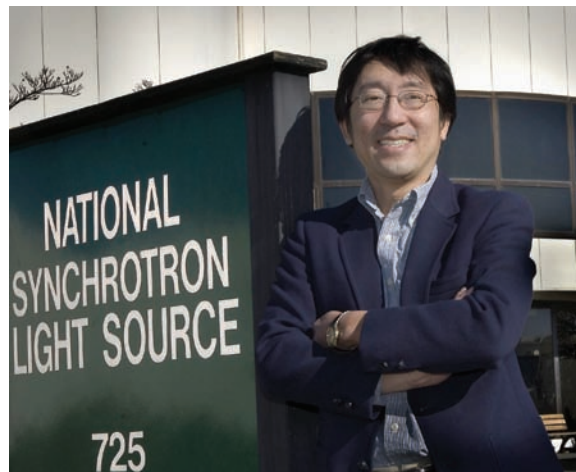
With the cooperation of participating research teams (PRTs) and assistance from a large number of NSLS staff, all operational beamlines at the NSLS were reviewed in January-February 2005 by the NSLS Scientific Advisory Committee (SAC). In this round of review, beamlines were divided into seven groups: macromolecular crystallography, x-ray scattering/soft condensed matter, x-ray scattering/hard condensed matter, powder/single crystal diffraction and high pressure, imaging and microprobe, x-ray spectroscopy, and IR/UV/soft x-ray spectroscopy. Each group was reviewed by an ad hoc beamline review committee led by one or two members of the SAC. The goal of the review was to ensure the highest scientific productivity and safe operation of these beamlines. Specifically, the following areas were evaluated by the review committee for each beamline: (1) importance of the scientific program; (2) quality and quantity of scientific productivity; (3) quality of beamline instrumentation, including beamline optics/controls, endstations, detectors, and software; (4) funding for the beamline operation and beamline/endstation upgrades; (5) effectiveness in beamline usage; (6) level of beamline staffing; and (7) safety-related issues, including beamline operation procedures and user training. The evaluation and recommendations from the beamline review were accepted by NSLS management and communicated to the PRTs soon after the review. Most of the PRTs have been renewed for another three years. We are working closely with the remaining PRTs to resolve the issues raised by the review.

User Access Policy

Another major undertaking in 2005 was the establishment of facility beamlines (FBs) under the new NSLS User Access Policy. A set of approximately 15 beamlines were selected as FBs in the first phase, based on coverage of the primary research directions of the user community, available resources, and considerations of complementary capabilities provided by the PRTs. The goal of these beamlines is to allow general users to have access to all wavelengths and major synchrotron techniques. In addition, general users will also have better coordinated support from the facility's scientific and technical staff. Users will also benefit from enhanced instrumentation at these beamlines as a result of the beamline/endstation upgrade projects carried out over the last few years. These FBs were put into operation starting from the fall cycle of 2005. We are looking forward to working with and receiving feedback from users at these beamlines. Finally, we initiated a contributing user (CU) program on the FBs, with the first CU proposals submitted in September 2005. The CUs enhance the endstation capabilities on the FBs. In some cases, this enhancement involves specialized instrumentation to meet the needs of specific research communities, such as catalysis or environmental sciences. In other cases, the enhancement involves the implementation of a specific x-ray technique, such as x-ray standing wave or strain-mapping. The CUs also provide supplemental user support to strengthen the scientific impact of the FBs.

Education and Outreach

We continue to take steps to enhance user education, training, and outreach at the NSLS. In the area of user training, we organized a "High Resolution Powder Diffraction Data Collection and Analysis"



short course, with the help of Peter Stephens (Stony Brook University) and Christie Nelson (NSLS). It was an intensive three-day course that included lectures on the basic physics of powder diffraction, indexing, and Rietveld refinement, as well as cutting-edge research using powder diffraction. The course also involved hands-on data collection carried out on NSLS beamlines X3B1, X7A, and X14A. Feedback on the short course was very positive, and we are considering running it annually. We also continued our annual EXAFS short course in 2005, which was entitled "EXAFS Course: Theory, Experiment, and Advanced Applications." We worked closely with users to organize additional focused scientific workshops, including "RapidData 2005," a workshop on "Strain Mapping in Engineering Materials with High-Energy Synchrotron X-Rays," a "BNL Workshop on Intense Coherent THz Pulses," a "Crystallization Workshop," "Bio-CD 2005," the "Synchrotron Environmental Sciences III (SES-III)" conference, a workshop on "Synchrotron Infrared Spectroscopy for High-Pressure Geoscience and Planetary Science," and three tutorials entitled the "X6A Workbench: Hands-On Training in Synchrotron Crystallography." These workshops were very effective in introducing the use of synchrotron techniques to a particular area of science to non-synchrotron users. Many new research opportunities and fruitful collaborations have resulted from them. Finally, a concerted effort has been made this year to coordinate closely with the Center for Functional Nanomaterials, in order to reach out to nanoscience researchers through joint seminars, workshops, and visits to interested universities and institutions.

Beamline Upgrades

There were a number of significant beamline upgrade projects completed this year by the NSLS and PRTs, including an upgrade of the X18B monochromator, the construction of a micro-beam diffraction endstation at X13B, an upgrade of the U13 photoemission spectrometer, the design and testing of Quick-EXAFS, the development of a double-focusing high-energy monochromator for X17, and the implementation of high field magnets at several beamlines around the ring. These highlights are described in detail below.

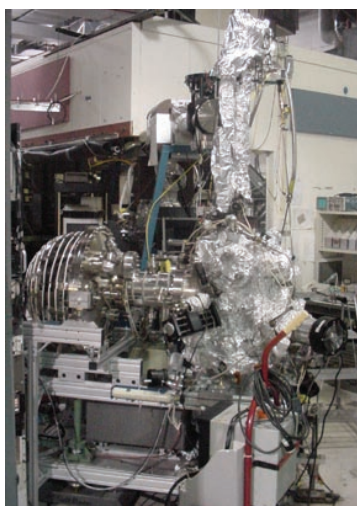


Figure 1. Photograph of the U13UB experimental endstation, the heart of which is a very high resolution Scienta SES200 photoelectron spectrometer.

New High-Resolution Electron-Energy Analyzer Installed on Beamline U13UB

The 1990s renaissance in the field of angle-resolved photoemission spectroscopy (ARPES) resulted from the combination of new parallel-detection (in energy and angle) photoelectron spectrometers with high-brightness VUV synchrotron beamlines. At the NSLS, such a beamline/endstation combination was constructed and commissioned at beamline U13UB in the late 1990s.

In 2004, the original Scienta photoelectron spectrometer that had been used since 1998 was replaced by a higher-resolution instrument from the same company. Shown in **Figure 1**, the new instrument has a measured energy resolution of 0.7 meV, which is a significant improvement over the ~ 5 meV resolution of the previous model. A photoelectron spectrum recorded at low temperature from an evaporated gold film in the vicinity of the Fermi edge is shown in **Figure 2**. The energy width of the Fermi edge in this spectrum is limited by the temperature of the sample.

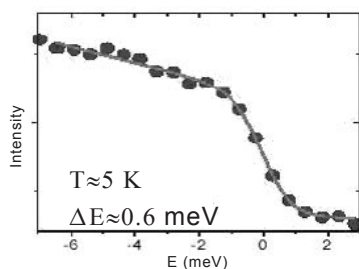


Figure 2. A photoelectron spectrum recorded at low temperature (~ 5 K) from an evaporated gold film in the vicinity of the Fermi edge, demonstrating the superior (sub meV) electron energy resolution of the new Scienta photoelectron spectrometer at beamline U13UB.

This new instrument has been used by U13UB PRT members and general users since late 2004. The U13UB PRT members (Brookhaven Lab's Physics Department, Boston University, Boston College, and Columbia University) are using the enhanced energy resolution of this new instrument to study detailed information on the electronic structure and dynamics of complex electronic systems. In particular, a recent study of the quasiparticle scattering rates around the Fermi surface of Sr_2RuO_4 was reported in Physical Review Letters by the Brookhaven group (PRL 94, 107003 (2005)). This study provided a microscopic picture of the origin of the crossover from non-Fermi liquid to Fermi liquid behavior observed in macroscopic transport measurements.

An X-ray Micro-Diffraction Instrument for Materials Research

A new x-ray micro-diffraction instrument was developed at X13B to take advantage of the small source size of the in-vacuum mini-gap undulator in the X13 straight section of the NSLS x-ray ring. This instrument combines sub-micron spatial resolution, exceptional reciprocal space access, a choice of focusing optics, and a modular design to accommodate different experimental needs.

A New High-Energy X-ray Side Station for High-Pressure Research

A new side-diffracting double-focusing high-energy x-ray monochromator was developed to provide 30-100 keV monochromatic x-rays to a new endstation in beamline X17B2, which includes a new high-pressure press and a MAR345 image-plate detector. It will enable high-resolution angle-resolved diffraction and pair-distribution function measurements to allow structure refinement for materials under high pressure.

A Fast Scanning Monochromator for X-ray Absorption Spectroscopy

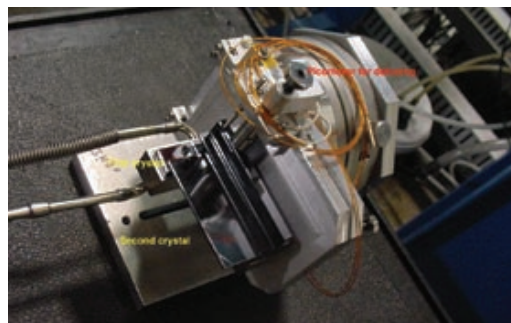
A new monochromator drive and data-collection scheme has been developed to allow fast measurement of x-ray absorption spectra. This new method reduces the collection time of a typical extended x-ray absorption fine structure (EXAFS) spectrum to less than one second. It will be particularly important for the study of kinetics in catalytic reactions.

X18B: A New Monochromator for X-Ray Absorption Spectroscopy Between 4.9 and 40keV

A new monochromator has been installed at beamline X18B to lower its lower energy limit from 5.6 keV down to 4.9 keV. This change might sound small, but it opens significant opportunities for research — especially in solid-state physics, materials science, and catalysis research — since the K-edges of two important 3d-transition metals, titanium and vanadium, have their energies at 4.966 and 5.465 keV, respectively.

Beamline X18B is optimized for hard x-ray absorption spectroscopy. The original monochromator covered an energy range between 5.7 and 40 keV (Cr – Ce K-edges, Ce – U L-edges). An overlapping lower energy range (2-7 keV) is covered by beamline X19A, which is optimized for x-ray absorption spectroscopy below 4 keV. However, several research groups, especially in the field of catalysis research, do experiments at the K-edges of several 3d-transition metals. The typical duration for one of their experiments is two to three days, including a few hours of research at photon energies below 5.7 keV (i.e. the V and Ti K-edges).

Rather than attempt to schedule and setup experiments at both X18B and X19A, we decided to extend the lower energy range of X18B down to 4.9 keV via a simple modification of its monochromator. The monochromator at X18B is a standard channel-cut monochromator with a 3mm gap between the two crystals. The original length of the first crystal was 34 mm, which limited the maximum usable angle of operation of the monochromator, and in turn limited the low end of the photon energy range to 5.7 keV. The 34 mm length of the first crystal was chosen in order to intercept the entire beam vertically at higher energies, where the Bragg angle, and thus the vertical acceptance of the crystal, is smaller.



New X18B monochromator with smaller first crystal.

However, as it turns out, the vertical opening angle worsens the energy resolution at higher energies, so it is better to limit the vertical beam size at high energies, thereby shortening the required length of the first crystal and increasing the usable angular and photon energy ranges of the monochromator. By optimizing both the energy resolution and intensity, the footprint of the white beam on the monochromator remains almost constant over the energy range of this monochromator. This allowed us to shrink the length of the first crystal to 16 mm, which is still enough to prevent heat-load problems like the thermal bump.

The monochromator was first mounted in the beamline in the end of April, and tested and commissioned in April and May.

Beam Stability Tests at X18B

One important parameter in the success of experiments at the NSLS is the stability of the x-ray beam on the sample. Properties such as intensity, beam position, energy stability, and in a few cases degree of polarization play crucial roles in this success, and some can be neglected based on the experiment. Ideally, these properties, when normalized by their dependence on ring current, do not change over the course of an experiment. Change from the ideal performance can be caused by motions of the electron beam in the storage ring or by motions of the beamline optics. The latter are often thermally driven, their effect is not proportional to beam current, and they can cause any combination of beam position changes, intensity changes, or energy changes. Ideally, these motions are eliminated by stable supports (beamlines and storage ring), feedback systems (electron beam and, in some cases, beamline optics), and efficient cooling schemes. In practice, however, both the electron beam and the beamline optics move slightly over time, requiring regular realignment.

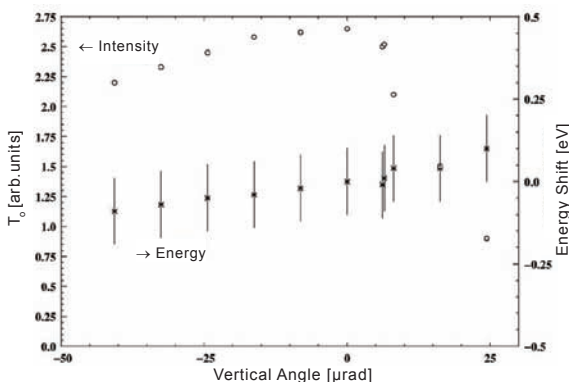


Figure 1. Intensity and energy shift for changes of the vertical angle. The stability of the beam is better than 5 μrad .

During a beam studies period, we measured the effect of beam motion on the intensity and energy of beamline X18B, which is equipped with a channel-cut Si(111) monochromator located at a distance of 18 meters from the source. X18B accepts a vertical (horizontal) divergence of 50 μrad (0.5-1 mrad). Since X18B is optimized for x-ray absorption spectroscopy, we do not care too much about position stability. In contrast, we care a lot about source angular stability, since this directly affects the photon energy selected by our monochromator.

Based on the geometry of the X18B beamline (slit sizes and positions), we calculate that vertical offsets of the source (electron beam) by 60 μm or angular changes by 5 μrad cannot be observed in a typical experiment. In order to test these calculations, we aligned the beamline slits such that the beamline becomes sensitive to beam motions in one direction (angle or position), but not the other. We then moved the beam (angle and position) around the nominal values and measured the intensity and energy stability. We did not study the effects of orbit motion (position or angle) in the horizontal plane, since X18B is not sensitive to motion in this plane.

The results of the orbit studies described above on the intensity and energy of beamline X18B are shown in **Figures 1** and **2**. It is apparent that vertical angular changes have only a small effect on the energy calibration, independent of the slit position, but have a relatively large effect on intensity. Theoretically, the energy should remain constant as a function of vertical source angle, which demonstrates that the X18B

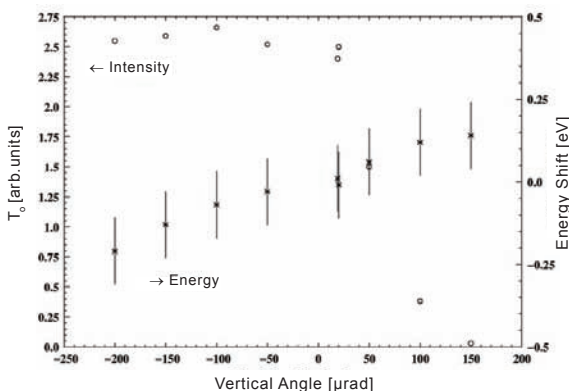


Figure 2. Intensity and energy shift for changes of the vertical position. The stability of the beam is better than 50 μm .

beamline saw a positional shift in addition to an angular change during these studies. The photon energy shifts significantly more for changes in the vertical source position, about 0.1 eV for 100 μm , as expected. The intensity profile in **Figure 2** is an asymmetric function of vertical source position relative to the standard orbit value. The reason for this is that we aligned our three beamline slits/apertures (5 mm vertical Be-window, 1mm vertical white beam slit, 0.5 mm vertical hutch slit) such that the lower edges of their upper jaws were aligned, as viewed from the source point. In this situation, if the electron beam moves up, one of the slits intercepts the beam and the intensity is reduced immediately. Beam motions in the other direction, however, move the beam more towards the center of the three slits, so the intensity is much less strongly reduced, as can be observed in the data.

In summary, we confirmed our calculations for the sensitivity of the X18B beamline to electron beam motions and demonstrated that the intensity can vary significantly if the beamline is not aligned appropriately. For normal operations, we align the slits symmetrically about the nominal beam axis in order to maximize intensity and to maximize the intensity stability. During normal operations, the intensity varies less than 0.4%, and the energy is stable within 0.05 eV.

High Resolution Terahertz Spectroscopy in Magnetic Field

Over the past few years a new magneto-optical facility has been developed at the U12IR beamline at the NSLS. The main components are an Oxford Instrument superconducting magnet, and a Bruker IFS 125HR high-resolution spectrometer. -The principal reason for using the synchrotron source in far-IR spectroscopy is the brightness advantage over a conventional light source -- depending on the frequency range and on the sample geometry, the synchrotron results in a factor of 50 - 200 gain in the intensity, making a vast array of new measurements possible.

The Bruker spectrometer is essentially an interferometer where spectral resolution is proportional to the available path difference (between the two interferometer "arms"). This particular spectrometer has an extremely long path difference, yielding a 0.001 cm^{-1} ($0.125 \text{ } \mu\text{eV}$) resolution. The available spectral range is from 5 cm^{-1} (0.63 meV) to over 7000 cm^{-1} . The magnet can produce fields up to 16 Tesla and its 20 liter He reservoir has a hold time of nearly 1 week. A set of three wedged single crystal quartz windows at the bottom provide optical access to the sample from below, along the vertical axis of the magnet (see figure). The sample temperature can be varied between 1.8 K and room temperature.



The Oxford Instruments magnet, installed next to the Bruker IFS 125HR spectrometer. The stainless steel tubes contain the optical coupling to the VUV-IR ring and between the spectrometer and the magnet.

The facility was tested extensively and the first results have been published on LaMnO_3 , a well-known antiferromagnet and the parent compound of the so-called colossal magnetoresistance materials. Other projects currently in progress include: the study of the single molecular magnet Mn_{12} -acetate (in collaboration with Myriam Sarachik, City College of New York), spin resonance on NaNiO_2 (with Sophie De Brion, Grenoble HMFL), the investigation of correlated magnetic systems, including LiCu_2O_2 and others (with Laszlo Forro, EPFL, Lausanne), and magneto-optical studies on superconductors, including carbon-doped MgB_2 .

A 10T Superconducting Magnet for Magneto-Structural and Magneto-Electronic Research and Education

A horizontal-field, split-coil superconducting magnet has become available for magneto-structural and magneto-electronic research at the NSLS. The magnet can operate over the temperature range from 1.6 to 300 K and over the field range 0 to 10 T. The horizontal field enables x-ray absorption measurements with linearly polarized x-rays with the electric field of the beam parallel to or normal to the magnetic field. Care was taken in the design to ensure that the samples can be measured in transmission mode for energies down to 5 keV (and in small steel hutches).

In general, this magnet is being used to study the lattice-spin coupling in complex materials. It was designed to be used on beamlines X11A, X19A, X21A and X23B for structural measurements (XAFS and powder XRD) in magnetic fields. With the use of a quarter wave plate, hard x-ray circular dichroism measurements on these beamlines will be feasible. With a differential pumping configuration, a future upgrade will make possible x-ray magnetic circular dichroism (XMCD) measurements on beamlines X13A and U4B. This will enable the study of magnetism in hard magnets as well as the induced moments on oxygen sites in metal oxide systems. Optical access is possible by replacing the kapton windows with quartz windows and/or replacing the variable temperature insert windows and external windows with all-quartz windows. The magnet was funded by a NSF IMR Grant and is now operational.



The magnet set up at X19A. It is mounted on a xyz table, which can be motor-controlled for ease of alignment. Samples are loaded from the top on a vertical rod into the samples space and are cooled by helium vapor or liquid from the magnet reservoir.

User Administration Report

Mary Anne Corwin
User Administrator

User Statistics

In FY05, there were 2,256 users from academia, government, industry, and other institutions (see Figure) who performed experiments at the NSLS.

Consistent with past years, more than a third were first-time users. The majority of our users come from the materials and life sciences arenas. Slight increases were noticed in medical applications and in the biological and life sciences. The numbers of users in the fields of chemistry and engineering decreased slightly. Other areas remained fairly stable.

PASS System

Proposal Allocation Safety Scheduling

Education and employment levels vary. Scientists, faculty members, or other professionals make up the largest user population at 43%. Graduate students account for 39% and post-docs make up 14%. Users that are between 30 and 39 years of age and are male are the most numerous. In FY05, 410 unique academic, government, non-government laboratory, and industrial institutions sent users to the NSLS. Nearly 260 were academic institutions.

Contributing Users

A new mode of access to beam time became available in FY05. Proposals by contributing users (CUs), who are individuals or groups who carry out research at facility beamlines and also contribute to their operation, were approved.

PASS System

The NSLS Proposal Allocation Safety and Scheduling (PASS) System, a web-based resource for proposal submissions, feasibility and peer review, allocation and scheduling of beam time, safety review, and maintenance of beam-line information received several enhancements in FY05. Managers of crystallography data were provided with automated feeds to manage information more efficiently. Proprietary proposals and an automated billing system for proprietary charges were incorporated. User interface changes were made to provide more information to PASS users and to simplify the tasks of copying existing proposal and safety approval forms. The development of a component for requesting rapid access to beam time has been started. Plans for FY06 include completing of rapid access proposals, including contributing user access, and expanding the beam time scheduling component.



The User Administration Group (top, from left) Mary Anne Corwin and Gretchen Cisco, (bottom, from left) Liz Flynn and Mercy Baez.

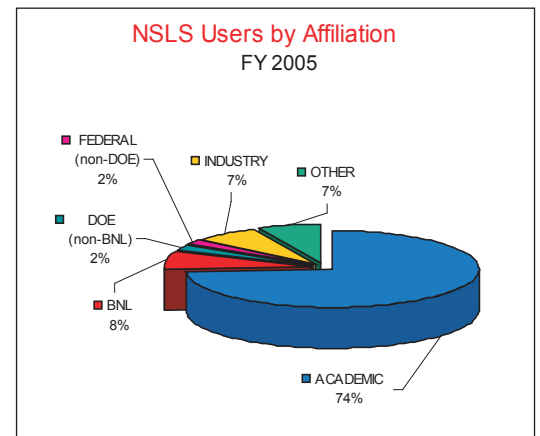
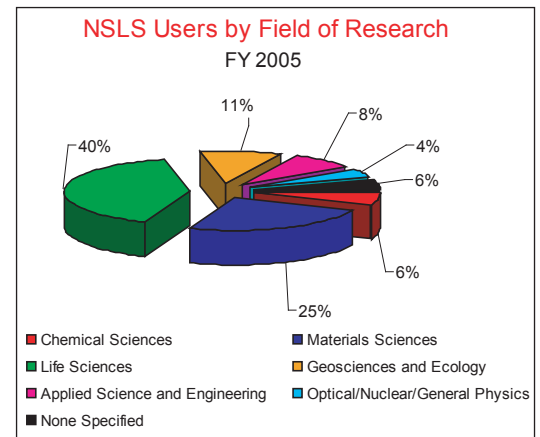
Safety Compliance

Due to two measures implemented in the prior fiscal year, non-compliances related to safety and security by users accessing the experimental floor were nearly eliminated in FY05. The measures involved encoding badges for timed access and the inclusion of various user expiration dates (e.g., training, badge, etc.) on the safety approval form.

Final Comments

As many of you know, I recently accepted the position of NSLS Training Coordinator in the ESH&Q Division, following Eva Rothman's footsteps again! So, this will be my last report. I've learned so much through all the interactions that become part of the regular routine of a user administrator. The roles are complex, and often challenging

and demanding. I'm grateful for having had the opportunity to work in all these areas. My experience will have many benefits in carrying out my new responsibilities and has provided me with a strong foundation for my new position. As I leave this position, one thing is evident: NSLS User Administration staff have always been very productive, handling hefty workloads and challenges in a prompt, expert, and courteous manner. Please welcome our new User Administrator, Kathleen Nasta (formerly the BNL Science Museum Program Coordinator), as your liaison between the NSLS and the user community. Your support will promote a smooth transition for the NSLS and our users.



Safety Report

Bob Casey

Associate Chair For ESH

Organization and Mission

The NSLS Environment, Safety, Health and Quality Division, headed by Bob Casey, consists of seven professionals servicing ESH, Training, and Quality Assurance, and one administrative assistant.

ESH performance within the NSLS and at Brookhaven National Laboratory in general remains an important issue for NSLS staff, PRT members, and users. There is great emphasis at BNL on reducing the frequency of injuries and incidents, and this emphasis produces heightened visibility for all matters relating to safety. The NSLS Activity Report provides an excellent opportunity to comment on ESH performance at the NSLS and to discuss issues that will be of importance in the year ahead.

2005 Activities

Safety performance was high in 2005 in all areas.

1. We had no injuries that met recording criteria or resulted in lost or restricted time during 2005. In fact, at the time of this writing, we have worked more than 1.5 million person hours without a lost-time injury at the NSLS. This parameter is given a major weighting by BNL and Department of Energy management in judging safety performance. In the figure, on the next page, the significant reduction in DART rate since FY 1997 is clear. We can all take pride in that accomplishment.
2. We had no reportable occurrences related to ESH issues in 2005.
3. Radiation exposure remains very low — the total recorded dose to NSLS staff and users for 2005 was less than 50 mRem.
4. There were no spills or releases of hazardous materials to the environment.
5. The generation of hazardous and industrial waste continues near all-time lows. Inspections of work sites indicate a high degree of compliance with hazardous waste and environmental requirements.
6. Our responsiveness to inspection and audit findings and training requirements was prompt and complete in general.
7. Our compliance with safety requirements, as indicated through numerous audits, is viewed as high.

These performance measures are a good indicator that NSLS staff and users are seriously addressing safety. Because of the effort of many people, the NSLS is a safe place to work. More than 1,200 experiments were conducted safely and approximately 2,300 users conducted research in our facility without significant incident or injury. I want to acknowledge the ongoing commitment and dedication of the NSLS management and staff, and that of our user community. A pat on the back is due to everyone involved.



ESH Initiatives of Importance in 2006

Two issues of importance to the user community will receive particular emphasis during 2006.

Electrical Safety

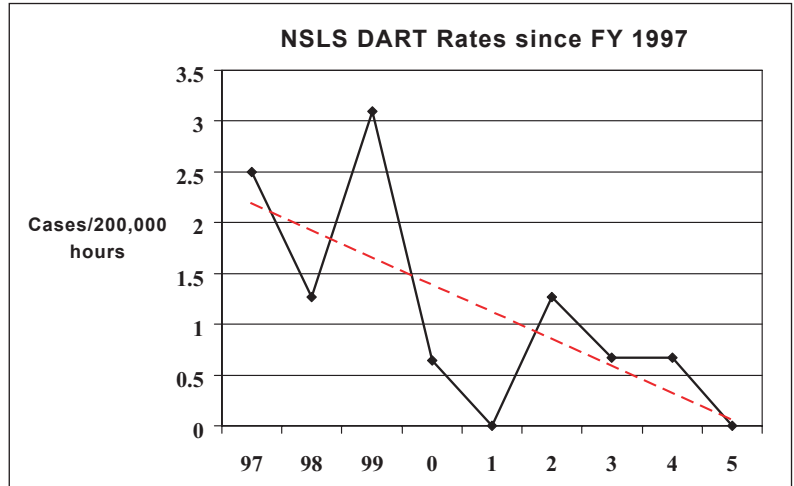
Much has been done in the past year to identify equipment that has the potential to create electrical shock hazards if improperly handled. Labeling, increased training, and inspections have been a major commitment. A similar emphasis will continue this year to re-enforce the previous efforts. Inspections will begin on beamline equipment that does not have a label or sticker from a nationally recognized test laboratory (e.g. U.L). In addition, all equipment brought in by visiting users must be labeled or inspected by designated staff before it can be used on the experimental floor.

Integrated Safety Management

The NSLS Safety Program is based on the principles described by the Department of Energy as Integrated Safety Management (ISM). It is the intent of the ISM program to ensure that all work is effectively performed by trained and qualified personnel and that hazards associated with the work have been fully identified and properly controlled. These concepts are embodied in the safety program requirements established for all users and staff. We will seek to ensure a good understanding and implementation of these practices and requirements throughout this year.

Conclusion

We must maintain a sharp focus on working safely, and we must continue efforts to ensure that our research programs capture the requirements of the NSLS Safety Program and the essence of ISM. World-class research and a rigorous safety program are compatible. Most importantly, a successful safety program is built on an ongoing awareness, involvement, and commitment from everyone. We all know that one problem can quickly override and out-shine many successes. Whether you are at your home institution or at the NSLS, keep an eye on the workplace. Make sure that all requirements are respected and that work is conducted safely. We all have a stake in safety performance.



Building Administration Report

Gerry Van Derlaske
NSLS Building Manager

Nearly 25 years since first commissioning the VUV ring, the NSLS remains one of the most widely visited research facilities in the DOE complex. Previous large-scale construction projects have been replaced with building upgrades, which have been taking place during monthly maintenance sessions and scheduled shutdown periods. As always, the experimental halls remain a hotbed of activity, as many trades groups, technicians, scientists, staff members, and visitors work side by side conducting cutting-edge research in a safe and efficient manner. Staff and users are asked to report concerns that may arise regarding safety or security issues to any NSLS staff member. We do appreciate having others act as our eyes and ears. Contacts may be reached via phone, e-mail, or in person. Our aim is to provide a safe and secure environment for carrying out quality scientific research programs.

Work Planning and Controls for Maintenance and Operations

Overseeing the work-planning and work-permit process for safety and controls for a majority of the work being accomplished within the facility now resides with Al Boerner, Operations Division, who assumed the position of NSLS work control manager in January 2005. In keeping with the effort to have all work planned and properly reviewed prior to the commencement of tasks, several programs and training modules have been implemented to assure a safe and consistent application of the work-planning process. The work control manager, assisted by many work control coordinators, ensures that proper work planning policy is followed by both in-house staff and NSLS users.

Material Handling and Overhead Hoists

Due to serious events across the DOE sites, material handling devices, overhead cranes, and below the hook lifting devices were given a high priority for assessment regarding compliance, inventory tracking, and inspections. At the NSLS, the point of contact for all material handling/ hoisting and lifting devices is Robert Kiss. During this assessment period, new training requirements were developed, responsible individuals were named for each of the overhead cranes, and administrative locks were placed on overhead cranes to prevent use by unauthorized individuals. These programs were established to create a safe and consistent policy for our staff and users of material-handling and lifting devices. All below-the-hook devices, such as slings, shackles, and lifting fixtures, are required to be inspected on an annual basis and inventoried into our database, along with being assigned to a responsible individual. This program also applies to the purchase of any lifting device for use at BNL. Prior to submitting an order to purchase any lifting device, the device should be reviewed by BNL Quality Assurance to check its compliance with the applicable American National Standards Institute (ANSI) requirements.

Changes in the Experimental Halls

The changing landscape of the x-ray experimental hall is most dramatically noticed as one proceeds past the control room towards the LEGS facility. Over the course of the year, various groups have worked together to "green field" the X3 beamline area, preparing for relocation of the PRT from the Case Center for Synchrotron Biosciences from beamline X9.



During 2005, Stony Brook University beamline components and staff were moved from the existing X3 beamline to new quarters at X16. Green fielding of the X3 area began after X16 was commissioned and user operations were initiated. Major reconstruction of the X3 area will take place in 2006, in preparation for the Case PRTs' move.

Fall Arrest Protection Equipment

NSLS compliance with OSHA regulations prompted various groups to assess their needs and enhance worker safety when performing tasks at elevated heights. In an effort to mitigate falls from heights, the NSLS safety group, coupled with the NSLS assigned carpenter, installed various fall-protection devices throughout the facility. Areas such as the roofs of experimental end station enclosures (EESes), the exterior build-

ing AC cooling towers, and x-ray saw tooth areas above grade level were the areas of focused attention. Additional areas of concern will be evaluated as they are reviewed during the work-planning sessions, or during Tier 1 inspections.

New AEDs Installed

Two additional automated external defibrillators (AEDs) have been installed in building 725. Along with the existing AEDs in the main lobby and in the control room area of building 729 (the DUV-FEL facility), there is an AED in the RF power supply area in the center of the x-ray ring, along with the AED adjacent to the north elevator on the second floor. Familiarity with these units and their exact locations could save a co-worker's life. The life saved could be yours!

HSSD System Installed to Protect the Power Supply Area Electrical Components

Due to funding secured via requests submitted to the general laboratory upgrade process, during the winter 2006 shutdown highly sensitive smoke detectors (HSSDs) were installed in the NSLS power supply area, near the center roll-up doors. These detectors perform numerous air samplings over a short time interval, and can detect very minute signs of possible electrical fires, thereby giving operations coordinators a chance to investigate and shut down equipment prior to an event that would trigger less sensitive smoke-detection equipment. Testing of the system, in order to fine-tune the lowest possible thresholds prior to tripping the sensors that signal the control room, will be conducted as the winter shutdown ends, thereby establishing a real-time, true-test scenario.



Work Control Coordinators (standing from left, back row) Gary Nintzel, Ron Beauman, Mike Buckley, Steve Kramer, Wayne Rambo, Bob Kiss, Nick Gmur, Frank Zafonte, Emil Zitvogel, and Bob Chimel. (Standing from left, middle row) Bob Scheuerer, Payman Mortazavi, Toshiya Tanabe, John Gallagher, John Aloj, Dave Harder, Walter DeBoer, and Tony Kuczewski. (Sitting from left, front row) Randy Church, Al Boerner (Work Control Manager), and Andrew Ackerman (Experiment Review Coordinator). (Missing from photo) Gerry Van Derlaske (Work Control Manager), Mike Schwarz, Mike Fulkerson, Pete Zuhoski, Scott Buda, Gloria Ramirez, Wayne Rasmussen, Conrad Foerster, Anthony Lenhard, Jim Rose, and Peter Siddons.

ADA Compliant Doors Installed at Facility Entrances

Again, through funding supplied by General Plant Projects, Americans with Disabilities Act (ADA) compliant doors were installed at the main entrances to building 725. The ground-level south and north lobby entrance doors have remote operational "push buttons" identified with the familiar international wheelchair symbol, allowing hands-free passage through the vestibule area. The push-button door switches are keyed into the NSLS card-swipe system for access during evening, holiday, and weekend periods. An additional plus is the ability to have the doors remotely open when one's hands are full.

NSLS Trailer Park Closes

Without much ado, the fabled NSLS trailer park, located east of Railroad Avenue on the north side of Brookhaven Avenue, is now a memory. Once host to many of the original NSLS user groups who utilized these trailers as both office and technical shop space, the trailers' useful lifetimes have come to an end. Many of the original groups still conducting research at the NSLS have since moved to more pleasant accommodations in building 535. The trailers have been severed from BNL utilities and are no longer considered as space occupied or serviced by the NSLS.

RF Penthouse Repairs and Upgraded AC Installed

Once again, with the assistance of Plant Engineering Building & Maintenance trades, a major restoration project was accomplished transparently to most NSLS staff and the user community. During several Tier 1 inspections, and from information passed along to the building management team by RF supervisors and technical staff, deficiencies with the structural integrity of the RF penthouse were noted and corrected. During the summer months, when weather permitted, the exterior siding and the sub-flooring of the RF penthouse was replaced without interrupting services to the research program. Original windows were saved for reinstallation, and the sub-floor replaced where water had seeped behind the exterior walls and allowed dry rot to occur. Plant Engineering carpenters worked under tarps to keep the

interior temperatures of the penthouse at a level appropriate to keep the power supplies fully functional. Once the sub-floors were replaced, wet insulation in the walls was replaced and new T-111 exterior siding installed over the failing Dri-vet exterior walls. Painting of the siding to match the remaining Dri-vet siding is planned during the spring of 2006.

NSLS utilities and operations support group staff, in conjunction with varied Plant Engineering groups, continue the process of installing additional cooling capacity within the RF penthouse. This additional supply of cooled, conditioned air will allow a level of redundancy that did not previously exist, which is necessary to prevent "fault conditions," such as those that occur in times of heavy heat loading during peak summer months and during interruptions in service of the chilled-water supply. In the spring of 2006, final connections of the ductwork will take place and the additional cooling is expected to be fully operational.

Conclusion

As in past years, we encourage the NSLS staff and user community to keep the building management team abreast of any concerns with the physical plant utilities, the condition of the facilities, and daily quality-of-life issues. We will work to correct these issues as quickly as possible.



Facts and Figures

Facility Facts & Figures

The National Synchrotron Light Source (NSLS) is a national user research facility funded by the U.S. Department of Energy's Office of Basic Energy Science. The NSLS operates two electron storage rings: an x-ray ring (2.8 GeV, 280 mA) and a vacuum ultraviolet (VUV) ring (800 meV, 1.0 A), which provide intense light spanning the electromagnetic spectrum from the infrared through x-rays. The properties of this light, and the specially designed experimental stations, called beamlines, allow scientists in many fields of research to perform experiments not otherwise possible at their own laboratories.

Over 2,200 scientists representing more than 400 institutions, more than 60 of them corporations, come to Brookhaven National Laboratory annually to conduct research at the NSLS. The facility operates seven days a week, 24 hours a day throughout the year, except during periods of maintenance and studies.

As a national user facility, the NSLS does not charge for its beamtime, providing that the research results are published in the open literature. Proprietary research is conducted on a full cost recovery basis. The primary way to obtain beamtime at the NSLS is through the General User program. General Users are independent investigators interested in using the NSLS for their research. Access is gained through a peer-reviewed proposal system.

The NSLS currently has 53 x-ray and 13 VUV-IR operational beamlines available to users for performing a wide range of experiments. There are two types of beamlines at the NSLS: Facility Beamlines (FBs) and Participating Research Team (PRT) beamlines. In 2005, the NSLS had 19 FBs and 47 PRT beamlines. FBs are operated by the NSLS and reserve at least 50% of their beamtime for General Users. Some FBs host contributing users (CUs), who enhance the endstation capabilities and provide specialized user support on FBs. PRT beamlines are operated by user groups with related interests from one or more institutions. PRT beamlines reserve 25% of their beamtime for General Users. Membership in a PRT or CU program is open to all members of the scientific community who can contribute significantly to the program of the beamline, (i.e., funding, contribution of equipment, scientific program, design and engineering, operations manpower, etc).

The following pages list the operational beamlines at the NSLS and their unique characteristics.

Beamline Guide Abbreviations

TECHNIQUE	DESCRIPTION	TECHNIQUE	DESCRIPTION	TECHNIQUE	DESCRIPTION
ARPES	UV PHOTOELECTRON SPECTROSCOPY, ANGLE-RESOLVED	MCD	MAGNETIC CIRCULAR DICHROISM	WAXD	WIDE-ANGLE X-RAY DIFFRACTION
DAFS	X-RAY DIFFRACTION ANOMALOUS FINE STRUCTURE	NEXAFS	NEAR EDGE X-RAY ABSORPTION SPECTROSCOPY	WAXS	WIDE-ANGLE X-RAY SCATTERING
DEI	DIFFRACTION-ENHANCED IMAGING	PEEM	PHOTO EMISSION ELECTRON MICROSCOPY	XAFS	X-RAY ABSORPTION SPECTROSCOPY, FINE STRUCTURE
EXAFS	X-RAY ABSORPTION SPECTROSCOPY, EXTENDED FINE STRUCTURE	SAXS	SMALL ANGLE X-RAY SCATTERING	XANES	X-RAY ABSORPTION SPECTROSCOPY, NEAR EDGE STRUCTURE
GISAXS	GRAZING INCIDENCE SMALL ANGLE X-RAY SCATTERING	SPARPES	UV PHOTOELECTRON SPECTROSCOPY, SPIN- AND ANGLE-RESOLVED	XAS	X-RAY ABSORPTION SPECTROSCOPY
IRMS	INFRARED MICROSPECTROSCOPY	STXM	SCANNING TRANSMISSION X-RAY MICROSCOPY	XPS	X-RAY PHOTOELECTRON SPECTROSCOPY
MAD	MULTI-WAVELENGTH ANOMALOUS DISPERSION	UPS	UV PHOTOELECTRON SPECTROSCOPY	XRD	X-RAY DIFFRACTION
		UV-CD	ULTRAVIOLET CIRCULAR DICHROISM	XSW	X-RAY STANDING WAVES

VUV-IR Beamlines

Beamline	Source	Technique	Energy Range	Type	Organization
U1A	Bend	XAS XAFS NEXAFS XANES	270-900 eV	PRT	ExxonMobil Research and Engineering Co.
U2A	Bend	IRMS High pressure research IR spectroscopy	30-8000 cm ⁻¹	FB	BNL-NSLS Carnegie Institution of Washington COMPRES
U2B	Bend	IRMS IR spectroscopy	50-4000 cm ⁻¹	PRT	Case Western Reserve University
U3C	Bend	Metrology	50-1000 eV	PRT	Bechtel Nevada Lawrence Livermore National Laboratory Los Alamos National Laboratory Sandia National Laboratory
U4A	Bend	UPS	10-250 eV	PRT	Army Research Laboratory North Carolina State University Rutgers University University of North Carolina
U4B	Bend	X-ray scattering, resonant MCD UPS X-ray fluorescence spectroscopy XPS	20-1200 eV	PRT	Montana State University Northeastern University
U5UA	Insertion Device	ARPES UPS, spin-resolved PEEM	15-150 eV	FB	BNL-NSLS BNL-CFN
U7A	Bend	NEXAFS XANES XPS	180-1200 eV	PRT	BNL-Chemistry Dow Chemical Company NIST University of Michigan
U9B	Bend	UV-CD UV florescence spectroscopy	0.8 - 8.0 eV	PRT	BNL-Biology
U10A	Bend	IRMS	100-4000 cm ⁻¹	FB	BNL-NSLS

Beamline	Source	Technique	Energy Range	Type	Organization
U10B	Bend	IRMS	500-4000 cm ⁻¹	FB	BNL-NSLS
U11	Bend	UV-CD	3-10 eV	PRT	BNL-Biology
U12A	Bend	XAS XPS	100-800 eV	PRT	Oak Ridge National Laboratory
U12IR	Bend	IR spectroscopy THz / mm wave spectroscopy Time-resolved spectroscopy	6-600 cm ⁻¹	FB	BNL-NSLS
U13UB	Insertion Device	UPS ARPES	3-30 eV	PRT	Boston College Boston University BNL-Physics Columbia University

X-ray Beamlines

X1A1	Insertion Device	STXM	0.25-0.50 keV	PRT	BNL-Environmental Science ExxonMobil Research and Engineering Co. SUNY @ Plattsburgh Stony Brook University University of Texas @ Houston
X1A2	Insertion Device	STXM	0.25-1 keV	PRT	Stony Brook University
X1B	Insertion Device	X-ray scattering, coherent XAS X-ray fluorescence spectroscopy XPS	0.2-1.6 keV	PRT	Boston University TJNL University of Illinois
X2B	Bend	X-ray microtomography	8-35 keV	PRT	ExxonMobil Research and Engineering Co.
X4A	Bend	MAD Macromolecular crystallography	3.5-20 keV	PRT	Albert Einstein College of Medicine City University of New York (CUNY) Columbia University Cornell University Mount Sinai School of Medicine New York Structural Biology Center New York University SUNY @ Buffalo Sloan-Kettering Institute Wadsworth Center

Beamline	Source	Technique	Energy Range	Type	Organization
X4C	Bend	MAD Macromolecular crystallography	7-20 keV	PRT	Albert Einstein College of Medicine City University of New York (CUNY) Columbia University Cornell University Mount Sinai School of Medicine New York Structural Biology Center New York University Rockefeller University SUNY @ Buffalo Sloan-Kettering Institute Wadsworth Center
X5A	Bend	Laser backscattering	150-420 MeV	PRT	BNL-Physics Forschungszentrum Juelich (KFA) James Madison University Norfolk State University Ohio University University of Rome II University of South Carolina University of Virginia Virginia Polytechnic Institute
X6A	Bend	MAD Macromolecular crystallography	6.0-23 keV	FB	BNL-NSLS National Institutes of Health
X6B	Bend	XRD, surface WAXD X-ray reflectivity SAXS GISAXS	7-19 keV	FB	BNL-NSLS
X7B	Bend	XRD, single crystal XRD, time resolved WAXD WAXS	5-21 keV	PRT	BNL-Chemistry General Electric
X8A	Bend	Metrology	1.0-5.9 keV	PRT	Bechtel Nevada Lawrence Livermore National Laboratory Los Alamos National Laboratory Sandia National Laboratory
X8C	Bend	MAD Macromolecular crystallography	5-19 keV	PRT	Biogen Incorporated BNL-Biology Hoffmann-La Roche National Research Council of Canada
X9A	Bend	MAD Macromolecular crystallography	5-15 keV	PRT	Albert Einstein College of Medicine Case Western Reserve University Rockefeller University Sloan-Kettering Institute

Beamline	Source	Technique	Energy Range	Type	Organization
X9B	Bend	XAS EXAFS XAFS NEXAFS XANES	5-15 keV	PRT	Case Western Reserve University
X10A	Bend	XRD, powder XRD, time resolved WAXD X-ray reflectivity SAXS WAXS	6-15.2 keV	PRT	ExxonMobil Research and Engineering Co.
X10B	Bend	XRD, powder XRD, surface WAXD X-ray reflectivity X-ray scattering, surface WAXS	14 keV	PRT	ExxonMobil Research and Engineering Co.
X10C	Bend	XAS EXAFS XAFS NEXAFS XANES	4-24 keV	PRT	ExxonMobil Research and Engineering Co.
X11A	Bend	DAFS XAS EXAFS XAFS NEXAFS XANES	4.5-35 keV	PRT	BNL-Environmental Science BNL-Material Sciences Canadian Light Source ETH Labs - Zuerich Naval Research Laboratory (NRL) Naval Surface Warfare Center New Jersey Institute of Technology Sarah Lawrence College Stony Brook University
X11B	Bend	DAFS XAS EXAFS XAFS NEXAFS XANES	5.0-23 keV	PRT	BNL-Environmental Science BNL-Material Sciences Canadian Light Source ETH Labs - Zuerich Naval Research Laboratory (NRL) Naval Surface Warfare Center New Jersey Institute of Technology Sarah Lawrence College Stony Brook University
X12B	Bend	MAD Macromolecular crystallography	5-20 keV	PRT	BNL-Biology

Beamline	Source	Technique	Energy Range	Type	Organization
X12C	Bend	MAD Macromolecular crystallography	5.5-20.0 keV	PRT	BNL-Biology
X13A	Insertion Device	X-ray scattering, resonant MCD	0.2-1.6 keV	FB	BNL-NSLS
X13B	Insertion Device	Microdiffraction Imaging	4-16 KeV	FB	BNL-NSLS
X14A	Bend	MAD XRD, powder XRD, single crystal XRD, time resolved WAXD X-ray reflectivity	5-26 keV	PRT	Oak Ridge National Laboratory Tennessee Technological University University of Tennessee
X15A	Bend	XSW DEI	3-25 keV XSW 10-60 keV DEI	FB	BNL-NSLS Northwestern University
X15B	Bend	XAS EXAFS XAFS NEXAFS XANES	0.8-15 keV	PRT	BNL-Environmental Sciences Lucent Technologies, Inc. Stony Brook University Temple University University of Texas @ Austin
X16C	Bend	XRD, powder	6-30 keV	PRT	Stony Brook University
X17B1	Insertion Device	XRD, powder	55-80 keV mono 20-150 keV white	FB	BNL-NSLS Rutgers University
X17B2	Insertion Device	XRD, powder XRD, time resolved High pressure research	20-130 keV	FB	BNL-NSLS COMPRES Stony Brook University
X17B3	Insertion Device	XRD, powder XRD, single crystal High pressure research	5-80 keV	FB	BNL-NSLS COMPRES University of Chicago
X17C	Insertion Device	XRD, powder XRD, single crystal High pressure research	5-80 keV	FB	BNL-NSLS University of Chicago

Beamline	Source	Technique	Energy Range	Type	Organization
X18A	Bend	XRD, powder XRD, single crystal XRD, surface WAXD X-ray reflectivity X-ray scattering, surface WAXS	4-19 keV	PRT	BNL-Chemistry Indiana University @ Indianapolis Pennsylvania State University Purdue University Stony Brook University University of Missouri @ Columbia
X18B	Bend	XAS EXAFS XAFS NEXAFS XANES	4.8-40 keV	FB	BNL-NSLS BNL-Chemistry BNL-Electrochemistry ORNL UOP LLC University of Delaware Yeshiva University
X19A	Bend	X-ray scattering, resonant XAS EXAFS XAFS NEXAFS XANES	2.1-17 keV	FB	BNL-NSLS University of Delaware Yeshiva University
X19C	Bend	XRD, surface X-ray topography X-ray reflectivity X-ray scattering, liquid X-ray scattering, surface	6-17 keV	PRT	Arizona State University Fairfield Crystal Technology, LLC Kansas State University Kyushu University SUNY @ Albany Stony Brook University University of Illinois @ Chicago
X20A	Bend	XRD, single crystal Microdiffraction Imaging X-ray reflectivity X-ray scattering, surface	4.5-13 keV	PRT	IBM Research Division
X20C	Bend	XRD, single crystal XRD, surface XRD, time resolved X-ray reflectivity X-ray scattering, surface	4-11 keV	PRT	IBM Research Division
X21	Insertion Device	XRD, single crystal X-ray scattering, magnetic X-ray scattering, resonant SAXS	5-20 keV	FB	BNL-NSLS Boston University University of Vermont

Beamline	Source	Technique	Energy Range	Type	Organization
X22A	Bend	XRD, single crystal XRD, surface WAXD X-ray reflectivity X-ray scattering, surface WAXS	10.7 keV 32keV	PRT	BNL-X-Ray Scattering Group BNL-Chemistry
X22B	Bend	X-ray scattering, liquid X-ray scattering, surface	6.5-10 keV	PRT	Bar-Ilan University BNL-X-Ray Scattering Group BNL-CFN Harvard University
X22C	Bend	XRD, single crystal XRD, surface X-ray reflectivity X-ray scattering, magnetic X-ray scattering, surface	3-12 keV	PRT	BNL-X-Ray Scattering Group Massachusetts Institute of Technology Rutgers University
X23A2	Bend	XRD, powder DAFS XAS EXAFS XAFS NEXAFS XANES	4.7-30 keV	PRT	NIST
X23B	Bend	XRD, powder XAS EXAFS XAFS NEXAFS XANES	4-10.5 keV	PRT	Hunter College Montana State University Naval Research Laboratory (NRL) New Jersey Institute of Technology Sarah Lawrence College
X24A	Bend	XSW Auger spectroscopy EXAFS X-ray fluorescence spectroscopy XPS	1.8-5 keV	PRT	NIST
X24C	Bend	X-ray reflectivity UV photoabsorption spectroscopy UPS XAS	0.006-1.8 keV	PRT	Naval Research Laboratory (NRL)
X25	Insertion Device	MAD Macromolecular crystallography	3-28 keV	FB	BNL-NSLS BNL-Biology

Beamline	Source	Technique	Energy Range	Type	Organization
X26A	Bend	Microdiffraction Imaging X-ray microprobe	3-30 keV	PRT	BNL-Environmental Science University of Chicago University of Georgia
X26C	Bend	MAD Macromolecular crystallography	5-20 keV	PRT	BNL-Biology Cold Spring Harbor Laboratory Stony Brook University
X27A	Bend	X-ray microprobe	4.5-20 keV	FB	BNL-NSLS BNL-Environmental Science Stony Brook University
X27C	Bend	XRD, time resolved WAXD SAXS WAXS	9 keV	PRT	Air Force Research Laboratory National Institutes of Health Naval Surface Warfare Center Stony Brook University
X28C	Bend	X-ray footprinting	White Beam	PRT	Case Western Reserve University
X29A	Insertion Device	MAD Macromolecular crystallography	6-15keV	PRT	Case Western Reserve University BNL-Biology

NSLS Linac Parameters as of December 2005

Electron Gun Injection Energy	100 keV
Linac Final Energy	120 MeV
Number of Accelerating Sections	3
Number of Klystrons	3
Linac Frequency	2856 MHz
Horizontal Emittance into Booster (ϵ_x)	7.6×10^{-1} m-rad

NSLS BOOSTER PARAMETERS

Booster Injection Energy	120 MeV
Booster Extraction Energy	750 MeV
Circumference	28.35 m
Number of Superperiods (N_s)	4
Dipole Bend Radius (ρ)	1.91 m
Nominal Tunes (ν_x, ν_y)	2.42, 1.37
Betatron Function (β_x, β_y)	8.63 to 1.01, 5.26 to 1.73 m
Dispersion Function (η_x, η'_x)	1.21 to 0.41 m
Momentum Compaction (α)	0.106
RF Frequency (f_{rf})	52.88 MHz
RF Peak Voltage (V_{rf})	25 keV
Horizontal Acceptance	1.66×10^{-4} m-rad
Vertical Acceptance	6.11×10^{-5} m-rad
Momentum Acceptance	± 0.0025
Horizontal Emittance at Extraction (ϵ_x)	7.6×10^{-7} to 1.0×10^{-7} m-rad
Energy Spread at Extraction ($\sigma E/E$)	1.4×10^{-4}
Bunch Length at Extraction	110 mm

BOOSTER MAGNETIC ELEMENTS (FIELDS AT 750 MeV)

Name	Type	Quantity	B (kG)	B' (kG/m)	B'' (kG/m)	Effective Length (m)
BB	Dipole	8	13.099	-7.97	-125	1.5
Q1	Quadrupole	4		68.82		0.3
Q2	Quadrupole	4		93.60		0.3
SF	Sextupole	4			1223.7	0.2

VUV Storage Ring Parameters as of December 2005

Stored Electron Beam Energy	0.808 GeV
Injected Current	1.0 amp
Lifetime @ 200 mA unstretched (stretched)	~6 (9.8) hr
Circumference	51.0 meters

PHOTON CRITICAL WAVELENGTH (ENERGY)

Dipole Source 1.41 T $\lambda_c(E_c)$	19.9 Å (622 eV)
---------------------------------------	-----------------

LATTICE STRUCTURE (CHASMAN-GREEN) SEPARATED FUNCTION, QUAD DOUBLETS

Number of Superperiods (N_s)	4			
Magnet Complement	<table> <tr> <td>8 Bending Magnets (1.5 meters long each)</td> </tr> <tr> <td>24 Quadrupole (0.3 meters long each)</td> </tr> <tr> <td>12 Sextupole in two families (0.20 meters long each)</td> </tr> </table>	8 Bending Magnets (1.5 meters long each)	24 Quadrupole (0.3 meters long each)	12 Sextupole in two families (0.20 meters long each)
8 Bending Magnets (1.5 meters long each)				
24 Quadrupole (0.3 meters long each)				
12 Sextupole in two families (0.20 meters long each)				

STORAGE RING CHARACTERISTICS

Number of Dipole Ports	18
Number of Insertion Device Straight Sections	2
Maximum Length of Insertion Devices	2.25 meters
Dipole Bend Radius	1.91 meters
Radiated Bending Magnet Power (I= 1A)	20.4 kW
Power per Horizontal Milliradian (I= 1A)	3.2 W
RF Frequency (f_{rf})	52.887 MHz
Electron Orbital Period	170.2 nanoseconds
Number of RF Buckets	9
Typical Bunch Mode (filled buckets)	7
Damping Times	$\tau_x = \tau_y = 13$ msec; $\tau_z = 7$ msec
Nominal Tunes (ν_x, ν_y)	3.14, 1.26
Momentum Compaction	0.0235
RF Peak Voltage with 52 MHz (with 211 MHz) (V_{rf})	80 keV (20 keV)
Design RF Power with 52 MHz (with 211 MHz)	50 kW (6 KW)
Synchrotron Tune (ν_s)	0.0018
Natural Energy Spread [$I_b < 20$ mA] ($\sigma E/E$)	5.0×10^{-4}
Natural Bunch Length [$I_b < 20$ mA] 52 MHZ (211 MHZ) (2σ)	9.7 mm (360 mm)
Horizontal Damped Emittance (ϵ_x)	1.6×10^{-7} m-rad
Vertical Damped Emittance (ϵ_y)	3.5×10^{-10} m-rad (4×10^{-9} in normal ops.)*

ARC SOURCE PARAMETERS

Betatron Function (β_x, β_y)	1.18 to 2.25 m, 10.26 to 14.21 m
Dispersion Function (η_x, η'_x)	0.500 to 0.062 m, 0.743 to 0.093 m
$\alpha_{x,y} = -\beta'_{x,y}/2$	-0.046 to 1.087, 3.18 to -0.96
$\gamma_{x,y} = (1 + \alpha_{x,y}^2)/\beta_{x,y}$	0.738 to 0.970 m ⁻¹ , 1.083 to 0.135 m ⁻¹
Source Size (σ_x, σ_y)	536 to 568 μ m, >60 to >70 μ m (170-200 μ m in normal ops.)*
Source Divergence (σ'_x, σ'_y)	686 to 373 μ rad, 19.5 to 6.9 μ rad (55-20 μ rad in normal ops.)*

INSERTION DEVICE PARAMETERS

Betatron Function (β_x, β_y)	11.1 m, 5.84 m
Source Size (σ_x, σ_y)	1240 μ m, >45 μ m (220 μ m in normal ops.)*
Source Divergence (σ'_x, σ'_y)	112 μ rad, >7.7 μ rad (22 μ rad in normal ops.)*

X-Ray Storage Ring Parameters as of December 2005

Stored Electron Beam Energy	2.800 GeV
Injected Current	0.3 A
Lifetime	~20 hours
Circumference	170.1 meters

PHOTON CRITICAL WAVELENGTH (ENERGY)

Dipole Source $1.36 T \lambda_c(E_c)$	1.75 Å (7.1 keV)
Wiggler Source $5.0 T \lambda_c(E_c)$	0.48 Å (26.1 keV)

LATTICE STRUCTURE (CHASMAN-GREEN SEPARATED FUNCTION, QUAD DOUBLETS)

Number of Superperiods (N_s)	8
Magnet Complement	16 Bending (2.7 meters long each) 40 Quadrupole A,C and D type (0.45 meters each) 16 Quadrupole B type (0.8 meters long each) 32 Sextupole in two families (0.20 meters long each)

STORAGE RING CHARACTERISTICS

Number of Dipole Ports	30
Number of Insertion Device Straight Sections	6
Maximum Length of Insertion Devices	4.50 meters
Dipole Bend Radius	6.875 meters
Radiated Bending Magnet Power (1=0.25A)	198 kW
Power per Horizontal Milliradian (1=0.25A)	32 W
RF Frequency (f_{rf})	52.88 MHz
Electron Orbital Period	567.2 nanoseconds
Number of RF Buckets	30
Typical Bunch Mode (filled buckets)	25
Damping Times	$\tau_x = \tau_y = 4$ msec; $\tau_z = 2$ msec
Nominal Tunes (ν_x, ν_y)	9.8, 5.7
Momentum Compaction	4.1×10^{-3}
RF Peak Voltage (V_{rf})	1120 keV
Design RF Power	450 kW
Synchrotron Tune (ν_s)	0.0023
Natural Energy Spread ($\sigma E/E$)	9.2×10^{-4}
Natural Bunch Length (2σ)	87 mm
Horizontal Damped Emittance (ϵ_x)	7.5×10^{-8} m-rad
Vertical Damped Emittance (ϵ_y)	1.5×10^{-10} m-rad

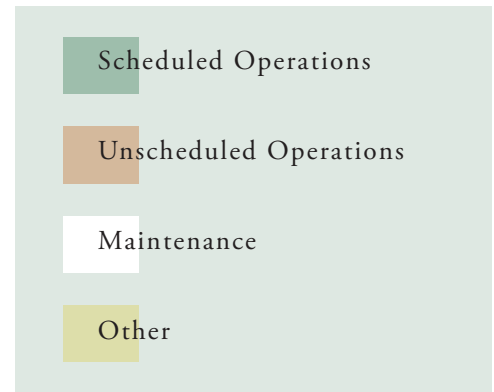
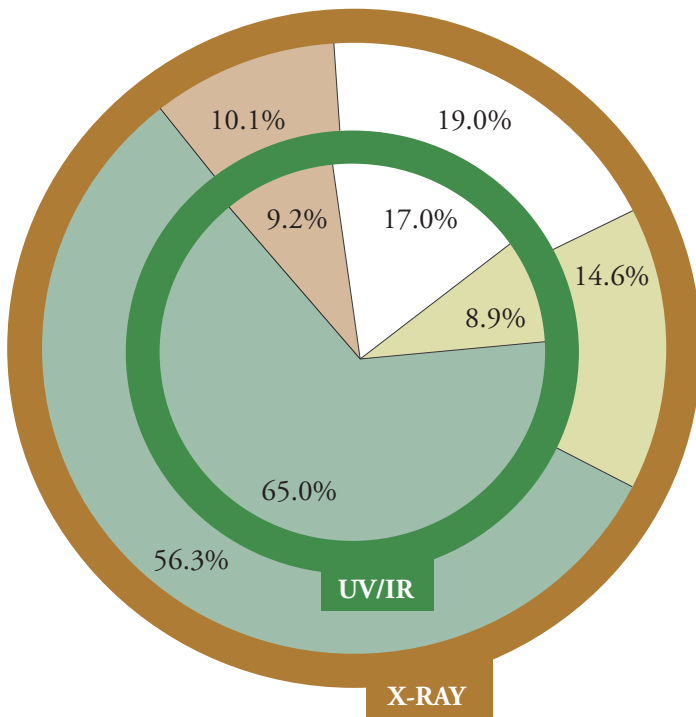
ARC SOURCE PARAMETERS

Betatron Function (β_x, β_y)	1.0 to 3.8 m, 7.9 to 26.5 m
Dispersion Function (η_x, η'_x)	0.47 to -0.11, -0.39 to 0.22
$\alpha_{x,y} = -\beta'_{x,y}/2$	-0.49 to 1.62, -3.4 to 4.5
$\gamma_{x,y} = (1 + \alpha_{x,y}^2)/\beta_{x,y}$	0.952 to 0.962 m ⁻¹ , 0.81 to 0.52 m ⁻¹
Source Size (σ_x, σ_y)	371 to 612 μm, 27 to 53 μm
Source Divergence (σ'_x, σ'_y)	476 to 324 μrad, 9 to 7 μrad

INSERTION DEVICE PARAMETERS

Betatron Function (β_x, β_y)	1.60 m, 0.35 m
Source Size (σ_x, σ_y)	300 μm, 6 μm
Source Divergence (σ'_x, σ'_y)	260 μrad, 35 μrad

Calendar Year 2005 NSLS Machine Activities



Other Activities	UV/IR	X-ray
Studies	2.3%	4.2%
Comm/Cond.	2.8%	4.1%
Holiday	1.9%	1.9%
Injection	0.9%	1.7%
Unscheduled Downtime	1.0%	2.0%
Interlock	0.0%	0.7%

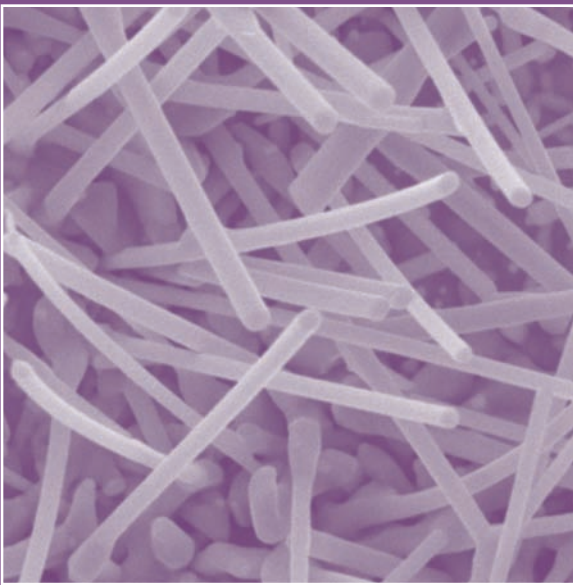
CALENDAR YEAR 2005

MONTH	VUV ACTUAL CY 05			X-RAY ACTUAL CY 05		
	PLANNED HOURS	RELIABILITY ¹	AVAILABILITY ²	PLANNED HOURS	RELIABILITY ¹	AVAILABILITY ²
January	468	98.3%	125.2%	334	93.7%	126.1%
February	551	98.4%	117.4%	557	98.8%	104.7%
March	623	99.9%	108.6%	516	91.7%	111.4%
April	592	99.0%	111.6%	534	95.7%	112.2%
May	216	99.7%	144.6%	175	96.8%	110.1%
June	623	99.6%	110.1%	578	95.3%	107.5%
July	463	98.2%	108.5%	429	96.8%	109.5%
August	571	94.6%	103.0%	521	98.7%	128.4%
September	591	99.5%	109.2%	545	98.8%	119.2%
October	591	97.2%	108.7%	552	96.8%	114.3%
November	488	99.6%	111.5%	365	98.5%	110.8%
December	0	-	-	0	-	-
	5777			5106		
Calendar 2005						
Delivered	5690	98.5%	112.4%	4929	96.5%	113.9%

Note: Delivered hours are only those accumulated during scheduled operations. Unscheduled operations do not contribute to this total.

¹ Operations during scheduled time

² Operations compared to total scheduled time



Publications

The following pages list all papers published in the 2005 calendar year as reported to the NSLS by February 28, 2006. Citations are listed in order of beamline number and then alphabetically by the last name of the first author. This list contains reported citations for journal articles, published conference proceedings, books, chapters in books, formal reports, informal reports, technical reports, theses, dissertations, and patents. For citation submissions where research was performed on more than one beamline, the citation is listed under each beamline. However, each citation was only counted once.

The first column in the table (right) lists the number of publications reported to the NSLS during the 2005 fiscal year (Oct. 1, 2004 – Sept. 30, 2005) and published between 2002 and 2005. Although some of these publications were published earlier than FY 2005, they were not reported to the NSLS until this fiscal year. Thus, they have not been counted in prior years' activity reports.

The second column in the table lists the number of publications published in the 2005 calendar year and reported to the NSLS as of Feb. 28, 2006. These numbers are slightly lower than the fiscal year values because they contain only publications from 2005 and it often takes many months or years to account for user and staff publications.

Several types of journal articles are reported in this list, including premier journals, peer-reviewed journals, and a few that are not peer-reviewed. A publication is considered premier if the journal has an impact factor of 6 or greater (from Journal Citation Report 2003, Thomson Institute for Scientific Information). These journals represent approximately the top 3% of all journals.

For calendar years 2002-2005, the NSLS users and staff published in 40 premier journals. These premier journals are: Accounts of Chemical Research, Advanced Materials, Angewandte Chemie, Annual Review of Biophysics and Biomolecular Structure, Annual Review of Genomics and Human Genetics, Applied Physics Letters, Cancer Cell, Cell, Chemical Reviews, Chemistry and Biology, Current Biology, Current Opinion in Chemical Biology, Current Opinion in Structural Biology, EMBO Journal, Faseb Journal, Genes and Development, Genome Research, Human Molecular Genetics, Immunity, Journal of Biological Chemistry, Journal of Experimental Medicine, Journal of Immunology, Journal of Neuroscience, Journal of the American Chemical Society, Molecular and Cellular Biology, Molecular and Cellular Proteomics, Molecular Cell, Nano Letters, Nature, Nature Immunology, Nature Materials, Nature Structural & Molecular Biology, Neuron, Nucleic Acids Research, Physical Review Letters, PNAS, Reports on Progress in Physics, Science, Structure, Trends in Biochemical Sciences, and Trends in Neurosciences. Two additional journals are included in the premier list, Applied Physics Letters (impact factor 4.0) and Environmental Sciences and Technology (impact factor 3.6), because these journals represent the "best in class" for the NSLS industrial and environmental science users, even though their impact factors are less than 6.

In FY 2005, NSLS users and staff had 849 publications – a record for high for the facility. Moreover, 239 papers were published in premier journals, representing 28% of the total publications from the facility, and demonstrating the high impact of NSLS science.

	Reported in Fiscal Year 2005*	Published in Calendar Year 2005**
Journals, peer-reviewed, premier	239	189
Journals, other peer-reviewed	503	438
Journals, non peer-reviewed	23	23
Total Journals and Magazines	765	650
Books/Chapters in Books	7	5
Published Conference Proceedings	49	43
Reports: Technical, Formal, Informal	3	3
Theses/Dissertations	24	17
Patents	1	4
Total Misc. Publications	84	72
Total Publications	849	722
NSLS VUV User Publications	68	77
NSLS X-Ray User Publications	718	586
NSLS Staff Publications	63	59
	849	722

* Publications reported to the NSLS from Oct 1, 2004 – Sept. 30, 2005 and published between 2002 – 2005.
** Publications published in 2005 as reported to the NSLS by Feb. 28, 2006.

NSLS Users

Beamline U1A

- S Bocharov, Z Zhang, T Beebe, Jr., A Teplyakov. Structure of a Thin Barrier Film Deposited from Tetrakis-(dimethylamino)-Titanium onto a Si(100)-2x1 Substrate. *Thin Solid Films*. **471** (1-2), 159-165 (2005).
- G Hahner, M Zwahlen, W Caseri. Solvent Dependence of the Molecular Order in Ion-Exchanged Self-Assembled dialkylammonium Monolayers on Mica Studied with Soft X-ray Absorption. *J. Colloid Interface Sci.* **291** (1), 45-52 (2005).
- G Hahner, M Zwahlen, W Caseri. Chain-Length Dependence of the Conformational Order in Self-Assembled Dialkylammonium Monolayers on Mica Studied with Soft X-ray Absorption. *Langmuir*. **21**, 1424-1427 (2005).
- J Horn, Z Song, D Potapenko, J Hrbek, M White. Characterization of Molybdenum Carbide Nanoparticles Formed on Au(111) Using Reactive-Layer Assisted Deposition. *J. Phys. Chem. B*. **109**, 44-47 (2005).
- H Hwu, M Zellner, J Chen. The Chemical and Electronic Properties of Oxygen-Modified C/Mo(110): A Model System for Molybdenum Oxycarbides. *J. Catal.* **229**, 30-44 (2005).
- G Liu, S Natarajan, S Kim. Photochemical Production of Oligothiophene and Polythiophene Micropatterns from 2,5-diiodothiophene on Au in UHV. *Surf. Sci.* **592** (1-3), L305-L309 (2005).
- K Rao, D Kumaran, T Binz, S Swaminathan. Structural Analysis of the Catalytic Domain of Tetanus Neurotoxin. *Toxicon*. **45** (7), 929-939 (2005).
- M Sahiner, D Downey, S Novak, J Woicik, D Arena. The Local Structural Characterization of the Inactive Clusters in B, Bf2 and B23 Implanted Si Wafers using X-ray Techniques. *Microelectr. J.* **36**, 522-526 (2005).

Beamline U2A

- R Hemley, H Mao, V Struzhkin. Synchrotron Radiation and High Pressure: New Light on Materials Under Extreme Conditions. *J. Synch. Rad.* **12**, 135-154 (2005).
- M Koch-Müller, P Dera, Y Fei, H Hellwig, Z Liu, J Van Orman, R Wirth. Polymorphic Phase Transition in Superhydrophobic Phase B. *Phys. Chem. Miner.* **32** (5-6), 349-361 (2005).
- G Lager, W Marshall, Z Liu, R Downs. Re-Examination of the Hydrogarnet Structure at High Pressure using Neutron Powder Diffraction and Infrared Spectroscopy. *Am. Mineral.* **90**, 639 (2005).
- H Liu, J Tse, J Hu, Z Liu, L Wang, J Chen, D Weidner, Y Meng, D Hausermann, H Mao. Structural Refinement of the High-Pressure Phase of Aluminum Trihydroxide: In-Situ High-Pressure Angle Dispersive Synchrotron X-ray Diffraction and Theoretical Studies. *J. Phys. Chem. B*. **109**, 8857 (2005).
- J Lu, G Rozgonyi, A Schonecker, A Gutjahr, Z Liu. Impact of Oxygen on Carbon Precipitation in Polycrystalline Ribbon Silicon. *J. Appl. Phys.* **97**, 033509 (2005).
- Y Song, Z Liu, R Hemley, H Mao, D Herschbach. High-Pressure Vibrational Spectroscopy of Sulfur Dioxide. *J. Chem. Phys.* **122**, 174511 (2005).
- Y Song, R Hemley, H Mao, D Herschbach. Nitrogen-Containing Molecular Systems at High Pressures and Temperatures. *Chemistry under Extreme Conditions*, p. 189-222, Elsevier Science, St. Louis. (2005).

Beamline U2B

- K Dokken, L Davis, N Marinkovic. Synchrotron Radiation Fourier Infrared Microspectroscopy (SR-IMS) as a Tool to study the Fate and Transport of Organic contaminants in Plants. *Spectroscopy*. **20** (9), 14-20 (2005).
- K Dokken, L Davis, N Marinkovic. Use of Fourier Transform Infrared Microspectroscopy in Plant Growth and Development. *Appl. Spectrosc. Rev.* **40**, 1-26 (2005).
- K Dokken, L Davis, L Erickson, S Castro-Diaz, N Marinkovic. Synchrotron Fourier Transform Infrared Microspectroscopy: A New Tool to Monitor the Fate of Organic Contaminants in Plants. *Microchem. J.* **81** (1), 86-91 (2005).
- V Joshi, D Ramamurthy, R Powell, F Furuya, J Hainfeld. High Z Metal Carbonyls for Imaging and Microspectroscopy. *Microsc. Microanal.* **11** (S2), 974 (2005).
- J Joshi, D Ramamurthy, R Powell, F Furuya, J Hainfeld. High Z Metal Carbonyls for Imaging and Microscopy. *Microsc. Microanal.* **10**, 912 (2005).
- N Marinkovic, M Chance, K Dokken, L Davis, D Linkous, J Flinn. Synchrotron Infrared Spectroscopy at NSLS Beamline U2B. *Am. Biotechnol. Lab.* **23**, 12 (2005).
- N Marinkovic, S Gupta, C Zhan, M Chance. Synchrotron Radiation in Biosciences. *Nucl. Instrum. Meth. B*. **241** (1-4), 242-246 (2005).
- L Pietrzak, S Miller. Microchemical Structure of Soybean Seeds Revealed in Situ by Ultraspatially Resolved Synchrotron Fourier Transformed Infrared Microspectroscopy. *J. Agr. Food Chem.* **53** (24), 9304-9311 (2005).
- M Shao, J Warren, N Marinkovic, P Faguy, R Adzic. In-Situ ATR-SEIRAS Study of Electrooxidation of Dimethyl Ether on a Pt Electrode in Acid Solutions. *Electrochem. Commun.* **7**, 459 (2005).
- D Wetzel, G Post, R Lodder. Synchrotron Infrared Microspectroscopic Analysis of Collagens I, III, and Elastin on the Shoulders of Human Thin-Cap Fibroatheromas. *Vib. Spectrosc.* **38** (1-2), 53-59 (2005).
- P Yu. Molecular Chemistry Imaging to Reveal Structural Features of Various Plant Feed Tissues. *J. Struct. Biol.* **150** (1), 81-89 (2005).
- P Yu. Application of Cluster Analysis (CLA) in Feed Chemical Imaging to Accurately Reveal Structural-Chemical Features of Feeds within Cellular Dimension. *J. Agr. Food Chem.* **53** (8), 2872-2880 (2005).
- P Yu. Applications of Cluster Analysis (CLA) and Principal Component Analysis (PCA) in Feed Structure and Feed Molecular Chemistry Research, Using Synchrotron-Based FTIR Microspectroscopy. *J. Agr. Food Chem.* **53**, 7115-7127 (2005).
- P Yu, C Christensen, J McKinnon, D Christensen. Ultrastructural-Chemical Makeup of Yellow- (Brassica Rapa) and Brown-Seeded (Brassica Napus) Canola within Cellular Dimensions, Explored with Synchrotron Reflection FTIR Microspectroscopy. *Can. J. Plant. Sci.* **85**, 533-541 (2005).

Beamline U4A

- A Chan, G Wertheim, H Wang, M Ulrich, J Rowe, T Madey. Surface Atom Core-Level Shifts of Clean and Oxygen-Covered Re(1231). *Phys. Rev. B*. **72**, 035442 (2005).
- L Webb, E Nemanick, J Biteen, D Knapp, D Michalak, M Traub, A Chan, B Brunschwig, N Lewis. High-Resolution X-ray Photoelectron Spectroscopic Studies of Alkylated Silicon(111) Surfaces. *J. Phys. Chem. B*. **109**, 3930-3937 (2005).
- A Yang, Z Chen, X Zuo, D Arena, J Kirkland, C Vittoria, V Harris.

Cation-Disorder-Enhanced Magnetization in Pulsed-Laser-Deposited CuFe₂O₄ Films. *Appl. Phys. Lett.* **86**, 252510 (2005).

Beamline U4B

- J Dvorak, Y Idzerda, D Arena, Y Zhao, S Ogale, T Wu, T Venkatesan, R Godfrey, R Ramesh. Are Strain-Induced Effects Truly Strain Induced? A Comprehensive Study of Strained LCMO Thin Films. *J. Appl. Phys.* **97**, 10C102 (2005).
- T Funk, A Deb, S George, H Wang, S Cramer. X-ray Magnetic Circular Dichroism-A High Energy Probe of Magnetic Properties. *Coordin. Chem. Rev.* **249**, 3-30 (2005).
- Y Guan, Z Dios, D Arena, L Cheng, W Bailey. Transmission-Mode X-ray Magnetic Circular Dichroism Characterization of Moment Alignment in Tb-Doped Ni₈₁Fe₁₉. *J. Appl. Phys.* **97**, 10A719 (2005).
- A Lussier, J Dvorak, Y Idzerda, S Shinde, S Ogale, T Venkatesan. XAS Characterization of Growth Parameter Effects for Pulsed Laser Deposited Co₂Ti_{1-x}O₂? Films. *Phys. Scr.* **T115**, 623-625 (2005).
- C Marrows, P Steadman, A Hampson, L Michez, B Hickey, N Telling, D Arena, J Dvorak, S Langridge. Probing Magnetic Ordering in Multilayers using Soft X-ray Resonant Magnetic Scattering. *Phys. Rev. B: Condens. Matter.* **72**, 024421 (2005).
- L Michez, C Marrows, P Steadman, B Hickey, D Arena, J Dvorak, H Zhang, D Bucknall, S Langridge. Resonant X-ray Scattering from a Magnetic Multilayer Reflection Grating. *Appl. Phys. Lett.* **86**, 112502 (2005).
- E Negusse, Y Idzerda. Extraction of Roughness Parameters from Specular X-ray Resonant Scattering. *J. Appl. Phys.* **97**, 10C901 (2005).
- S Stadler, D Minott, D Harley, J Craig, M Khan, I Dubenko, N Ali, K Story, J Dvorak, et al.. Element-Specific Magnetic Properties of Co₂MnSi Thin Films. *J. Appl. Phys.* **97**, 10C302 (2005).

Beamline U4IR

- X Hu, C Hirschmugl. Long-Range Metal-Mediated Interactions Between S and CO on Cu(100). *Phys. Rev. B.* **72**, 205439 (2005).
- O Mercier, R Buckley, H Trodahl, C Bernhard, G Balakrishnan. Low-Energy Excitations in La_{1.2}Sr_{1.8}Mn₂O₇ Investigated by Ellipsometry. *Phys. Rev. B.* **72**, 214437 (2005).

Beamline U5UA

- E Vescovo, H Kim, J Ablett, S Chambers. Spin-polarized Conduction in Localized Ferromagnetic Materials: The Case of Fe₃O₄ on MgO(100). *J. Appl. Phys.* **98**, 084507 (2005).

Beamline U7A

- L Andruzzi, W Senaratne, A Hexemer, E Sheets, B Ilic, E Kramer, B Baird, C Ober. Oligo(ethylene glycol) Containing Polymer Brushes as Bioselective Surfaces. *Langmuir.* **21**, 2495-2504 (2005).
- S Banerjee, T Hemraj-Benny, S Sambasivan, D Fischer, J Misewich, S Wong. Near-Edge X-ray Absorption Fine Structure Investigations of Order in Carbon Nanotube-Based Systems. *J. Phys. Chem. B.* **109** (17), 8489-8495 (2005).
- R Bhat, J Genzer. Using Spectroscopic Ellipsometry for Quick Prediction of Number Density of Nanoparticles Bound to Non-transparent Solid Surfaces. *Surf. Sci.* **596**, 187 (2005).
- R Bubeck, L Thomas, S Rendon, W Burghardt, A Hexemer, D

Fischer. Characterization of the Skin Orientation of Thermotropic Liquid-Crystalline Copolyester Moldings with Near-Edge X-ray Absorption Fine Structure. *J. Appl. Polym. Sci.* **98**, 2473-2480 (2005).

- R Bubeck, P Dvornic, J Hu, A Hexemer, X Li, S Keinath, D Fischer. Near Edge X-ray Absorption Fine Structure (NEXAFS) Studies of Copper Ion-Containing PAMAMOS Dendrimer Networks. *Macromol. Chem. Physic.* **206**, 1146 - 1153 (2005).
- D Burnett, A Gabelnick, D Fischer, A Marsh, J Gland. Mechanism of Acetylene Oxidation on the Pt(111) Surface using in situ Fluorescence Yield Near-Edge Spectroscopy. *J. Catal.* **230**, 282-290 (2005).
- D Burnett, A Gabelnick, D Fischer, A Marsh, J Gland. In Situ Soft X-ray Studies of Ethylene Oxidation Mechanisms and Intermediates on the Pt(111) Surface. *J. Phys. Chem. B.* **109**, 5659-5666 (2005).
- C Cox, D Fischer, W Schwartz, Y Song. Improvements in the Low Energy Collection Efficiency of Si(Li) X-ray Detectors. *Nucl. Instrum. Meth. B.* **241** (1-4), 436-440 (2005).
- D DeLongchamp, S Sambasivan, D Fischer, E Lin, P Chang, A Murphy, J Frechet, V Subramanian. Direct Correlation of Organic Semiconductor Film Structure to Field-Effect Mobility. *Advanced Materials.* **17**, 2334-2338 (2005).
- D DeLongchamp, E Lin, D Fischer. Organic Semiconductor Structure and Chemistry from Near-Edge X-ray Absorption Fine Structure (NEXAFS) Spectroscopy. *SPIE Organic Thin Film Transistors IV*, Vol 5940, p. 54-64, sponsored by SPIE - The International Society for Optical Engineering. (2005).
- D DeLongchamp, B Vogel, Y Jung, M Gurau, C Richter, O Kirillov, J Obrzut, D Fischer, S Sambasivan, et al.. Variations in Semiconducting Polymer Microstructure and Hole Mobility with Spin-Coating Speed. *Chem. Mater.* **17** (23), 5610-5612 (2005).
- K Efimenko, J Crowe, E Manias, D Schwark, D Fischer, J Genzer. Rapid Formation of Soft Hydrophilic Silicone Elastomer Surfaces. *Polymer.* **46**, 9329-9341 (2005).
- L Gamble, C Lee, G Harbers, P Gong, D Grainger, D Castner. Characterization of Surface order and Structure of Thiolated Single Stranded and Hybridized DNA. *Society for Biomaterials 30th Annual Meeting*, Vol , p. 121, sponsored by Society for Biomaterials. (2005).
- J Genzer. Templating Surfaces with Gradient Assemblies. *J. Adhes. Sci. Technol.* **81**, 417 (2005).
- T Hemraj-Benny, S Banerjee, S Sambasivan, D Fischer, W Han, J Misewich, S Wong. Investigating the Structure of Boron Nitride Nanotubes by Near-edge X-ray Absorption Fine Structure (NEXAFS) Spectroscopy. *Phys. Chem. Chem. Phys.* **6**, 1103-1106 (2005).
- D Krapchetov, H Ma, A Jen, D Fischer, Y Loo. Solvent-Dependent Assembly of Terphenyl- and Quaterphenyldithiol on Gold and Gallium Arsenide. *Langmuir.* **21**, 5887-5893 (2005).
- J Lenhart, D Fischer, S Sambasivan, E Lin, R Jones, C Soles, W Wu, D Goldfarb, M Angelopoulos. X-ray Absorption Spectroscopy to Probe Surface Composition and Surface Deprotection in Photoresist Films. *Langmuir.* **21**, 4007-4015 (2005).
- H Lewis, D Burnett, A Gabelnick, D Fischer, J Gland. Enhanced Low-Temperature CO Oxidation on a Stepped Platinum Surface for Oxygen Pressures Above 10⁻⁵ Torr. *J. Phys. Chem. B.* **109**, 21847-21857 (2005).
- A Murphy, P Chang, P VanDyke, J Liu, J Frechet, V Subramanian, D DeLongchamp, S Sambasivan, D Fischer, E Lin. Self-Assembly, Molecular Ordering, and Charge Mobility in Solution-Processed Ultrathin Oligothiophene Films. *Chem. Mater.* **17**, 6033-6041 (2005).
- L Pattison, A Hexemer, E Kramer, P Petroff, D Fischer. Temperature Dependence of the Ordering of Semiconducting Fluorene-Thiophene Copolymers on Rubbed Polyimide Alignment Layers.

- Proc. SPIE Int. Soc. Opt. Eng.*, Vol , p. 5398, sponsored by Soc. Opt. Eng.. (2005).
- N Samuel. Structural Characterization of Adsorbed Helical and Beta-Sheet Peptides. Ph.D. Thesis. University of Washington, Seattle. (2005).
- J Sayan, N Nguyen, J Ehrstein, D Yoder, I Levin, D Fischer, M Paunescu, O Celik, E Garfunkel. Effect of Nitrogen on Band Alignment in HfSiON Gate Dielectrics. *Appl. Phys. Lett.* **87**, 212905-3 (2005).
- W Yoon, M Balasubramanian, K Chung, X Yang, J McBreen, C Grey, D Fischer. Investigation of the Charge Compensation Mechanism on the Electrochemically Li-Ion Deintercalated Li_{1-x}Co_{1/3}Ni_{1/3}Mn_{1/3}O₂ Electrode System by Combination of Soft and Hard X-ray Absorption Spectroscopy. *J. Am. Chem. Soc.* **127** (49), 17479-17487 (2005).
- X Zhao, P Liu, J Hrbek, J Rodriguez, M Perez. The Chemisorption of SO₂ on the Cu/Au (1 1 1) Surface: Interplay Between Ensemble and Electronic Effects. *Surf. Sci.* **592** (1-3), 25-36 (2005).
- X Zhao, J Hrbek, J Rodriguez. The Decomposition and Chemistry of Ru₃(CO)₁₂ on TiO₂(110) Studied with X-ray Photoelectron Spectroscopy and Temperature Programmed Desorption. *Surf. Sci.* **575**, 115-124 (2005).

Beamline U9B

- S Badre, C Goncalves, K Norinaga, G Gustavson, O Mullins. Molecular Size and Weight of Asphaltene and Asphaltene Solubility Fractions from Coals, Crude Oils and Bitumen. *Fuel* **85** (1), 1-11 (2005).
- Y Nie, S Vignes, J Hobbs, G Conn, S Munger. Distinct Contributions of T1R2 and T1R3 Taste Receptor Subunits to the Detection of Sweet Stimuli. *Curr. Biol.* **15** (21), 1948-1952 (2005).
- B Wallace. Shining New Light on Protein Structure and Function thru Synchrotron Radiation Circular Dichroism (SRCD) Spectroscopy. *Aust. Biochem.* **35**, 47-50 (2005).
- F Wien, A Miles, J Lees, S Vronning Hoffmann, B Wallace. VUV Irradiation Effects on Proteins in High-Flux Synchrotron Radiation Circular Dichroism Spectroscopy. *J. Synch. Rad.* **12**, 517-523 (2005).
- F Wien, A Miles, J Lees, A Cuff, R Janes, B Wallace. A New Circular Dichroism Reference Dataset Covering Fold Space. *Biophysical Journal*, Vol 88, p. 554a, (2005).

Beamline U10A

- S Dordevic, C Homes, J Tu, T Valla, M Strongin, P Johnson, G Gu, D Basov. Extracting the Electron-Boson Spectral Function $\alpha^2F(\omega)$ from Infrared and Photoemission Data using Inverse Theory. *Phys. Rev. B: Condens. Matter* **71**, 104529 (2005).
- C Homes. Scaling Laws in High-Temperature Superconductors as Revealed through Infrared Spectroscopy. *Synch. Rad. News* **18** (3), 9-14 (2005).
- I Kezsmarki, G Mihaly, R Gaal, N Barisic, H Berger, L Forro, C Homes, L Mihaly. Pressure-induced Suppression of the Spingapped Insulator Phase in BaVS₃: An Infrared Optical Study. *Phys. Rev. B* **71**, 193103 (2005).
- J Kim, S Oh, Y Lee, E Choi, C Homes, J Rhyee, B Cho. Optical Spectroscopy Study on the electronic Structure of Eu_(1-x)Ca_xB₆. *Phys. Rev. B* **71**, 075105 (2005).
- R Lobo, J LaVigne, D Reitze, D Tanner, Z Barber, E Jacques, P Bosland, M Burns, G Carr. Photoinduced Time-Resolved Electrodynamics of Superconducting Metals and Alloys. *Phys. Rev. B* **72**, 024510 (2005).
- S Miller, L Pietrzak. Preparation of Soybean Seed Samples for FT-

IR Microspectroscopy. *Biotech. Histochem.* **80** (3-4), 117-121 (2005).

- A Zimmers, J Tomczak, R Lobo, N Bontemps, C Hill, M Barr, Y Dagan, R Greene, A Millis, C Homes. Infrared Properties of Electron-Doped Cuprates: Tracking Normal-State Gaps and Quantum Critical Behavior in Pr_(2-x)Ce_xCuO₄. *Europhys. Lett.* **70** (2), 225-231 (2005).

Beamline U10B

- S Chakraborty, B Sahoo, I Teraoka, L Miller, R Gross. Enzyme-Catalyzed Regioselective Modification of Starch Nanoparticles. *Macromolecules* **38** (1), 61-68 (2005).
- V Joshi, D Ramamurty, R Powell, F Furuya, J Hainfeld. High Z Metal Carbonyls for Imaging and Microspectroscopy. *Microsc. Microanal.* **11** (S2), 974 (2005).
- J Lehmann, B Liang, D Solomon, M Lerotic, F Luizao, J Kinyangi, T Schäfer, S Wirick, C Jacobsen. Near-Edge X-ray Absorption Fine Structure (NEXAFS) Spectroscopy for Mapping Nano-Scale Distribution of Organic Carbon Forms in Soil: Application to Black Carbon Particles. *Global Biogeochem. Cy.* **19**, GB1013 (2005).
- L Miller, R Smith. Synchrotrons Versus Globars, Point-Detectors Versus Focal Plane Arrays: Selecting the Best Source and Detector for Specific Infrared Microspectroscopy and Imaging Applications. *Vib. Spectrosc.* **38** (1-2), 237-240 (2005).
- S Miller, L Pietrzak. Preparation of Soybean Seed Samples for FT-IR Microspectroscopy. *Biotech. Histochem.* **80** (3-4), 117-121 (2005).
- M Petra, J Anastassopoulou, T Theologis, T Theophanides. Synchrotron Micro-FT-IR Spectroscopic Evaluation of Normal Paediatric Human Bone. *J. Mol. Struct.* **733**, 101-110 (2005).
- L Pietrzak, S Miller. Microchemical Structure of Soybean Seeds Revealed in Situ by Ultraspatially Resolved Synchrotron Fourier Transformed Infrared Microspectroscopy. *J. Agr. Food Chem.* **53** (24), 9304-9311 (2005).
- D Solomon, J Lehmann, J Kinyangi, B Liang, T Schäfer. Carbon K-Edge NEXAFS and FTIR-ATR Spectroscopic Investigations of Organic Carbon Speciation in Soils. *Soil Sci. Soc. Am. J.* **69**, 107-119 (2005).
- T Telivala, L Miller. Effect of Metal Ions on the Secondary Structure of Amyloid beta (Ab) in Alzheimer's disease. Masters Thesis. SUNY at Stony Brook, Stony Brook. (2005).
- Q Wang, A Kretlow, M Beekes, D Naumann, L Miller. In Situ Characterization of Prion Protein Structure and Metal Accumulation in Scrapie-Infected Cells by Synchrotron Infrared and X-ray Imaging. *Vib. Spectrosc.* **38**, 61-69 (2005).
- Q Wang, W Sanad, L Miller, A Voigt, K Klingel, R Kandolf, K Stangl, G Baumann. Infrared Imaging of Compositional Changes in Inflammatory Cardiomyopathy. *Vib. Spectrosc.* **38**, 217-222 (2005).
- B Wood, K Bamberg, L Miller, M Quinn, L Chiriboga, M Diem, D McNaughton. Infrared Imaging of Normal and Diseased Cervical Tissue Sections. *Biomedical Applications of Micro- and Nanoengineering II*, Vol 5651, p. 78-84, sponsored by SPIE--The International Society for Optical Engineering. (2005).
- P Yu, R Wang, Y Bai. Reveal Protein Molecular Structural-Chemical Differences Between Two Types of Winterfat (Forage) Seeds with Physiological Differences in Low Temperature Tolerance Using Synchrotron-Based Fourier Transform Infrared Microspectroscopy. *J. Agr. Food Chem.* **53**, 9297-9303 (2005).
- P Yu. Application of Cluster Analysis (CLA) in Feed Chemical Imaging to Accurately Reveal Structural-Chemical Features of Feeds within Cellular Dimension. *J. Agr. Food Chem.* **53** (8), 2872-2880 (2005).

- P Yu. Molecular Chemistry Imaging to Reveal Structural Features of Various Plant Feed Tissues. *J. Struct. Biol.* **150** (1), 81-89 (2005).
- P Yu. Applications of Cluster Analysis (CLA) and Principal Component Analysis (PCA) in Feed Structure and Feed Molecular Chemistry Research, Using Synchrotron-Based FTIR Microspectroscopy. *J. Agr. Food Chem.* **53**, 7115-7127 (2005).
- P Yu, C Christensen, J McKinnon, D Christensen. Ultrastructural-Chemical Makeup of Yellow- (Brassica Rapa) and Brown-Seeded (Brassica Napus) Canola within Cellular Dimensions, Explored with Synchrotron Reflection FTIR Microspectroscopy. *Can. J. Plant. Sci.* **85**, 85: 533-541 (2005).

Beamline U11

- A Miles, F Wien, J Lees, B Wallace. Calibration and Standardisation of Synchrotron Radiation and Conventional Circular Dichroism Spectrometers. Part 2: Factors Affecting Magnitude and Wavelength. *Spectroscopy*. **19**, 43-51 (2005).
- Y Nie, S Vignes, J Hobbs, G Conn, S Munger. Distinct Contributions of T1R2 and T1R3 Taste Receptor Subunits to the Detection of Sweet Stimuli. *Curr. Biol.* **15** (21), 1948-1952 (2005).
- B Wallace. Shining New Light on Protein Structure and Function thru Synchrotron Radiation Circular Dichroism (SRCD) Spectroscopy. *Aust. Biochem.* **35**, 47-50 (2005).
- F Wien, A Miles, J Lees, A Cuff, R Janes, B Wallace. A New Circular Dichroism Reference Dataset Covering Fold Space. *Biophysical Journal*, Vol 88, p. 554a, (2005).

Beamline U12A

- S Senanayake, G Waterhouse, H Idriss, T Madey. Coupling of Carbon Monoxide Molecules over Oxygen Defected UO₂ (111) Single Crystal and Thin Film Surfaces. *Langmuir*. **21**, 11141-11145 (2005).

Beamline U12IR

- R Lobo, J LaVeigne, D Reitze, D Tanner, Z Barber, E Jacques, P Bosland, M Burns, G Carr. Photoinduced Time-Resolved Electrodynamics of Superconducting Metals and Alloys. *Phys. Rev. B*. **72**, 024510 (2005).

Beamline U13UB

- S Dordevic, C Homes, J Tu, T Valla, M Strongin, P Johnson, G Gu, D Basov. Extracting the Electron-Boson Spectral Function $\alpha^2F(\omega)$ from Infrared and Photoemission Data using Inverse Theory. *Phys. Rev. B: Condens. Matter*. **71**, 104529 (2005).
- P Glans, T Learmonth, K Smith, T Valla, P Johnson, S Hulbert, W McCarroll, M Greenblatt. Charge-Density-Wave Gap in the Quasi-Two-Dimensional Conductor Na_{0.9}Mo₆O₁₇ Measured by Angle-Resolved Photoemission Spectroscopy. *Phys. Rev. B*. **72**, 035115 (2005).
- T Kidd, T Valla, A Fedorov, P Johnson, R Cava, M Haas. Orbital Dependence of the Fermi Liquid State in Sr₂RuO₄. *Phys. Rev. Lett.* **94**, 107003 (2005).
- M Kralj. Hybridization Schemes for Ag Films on V(1 0 0). *Surf. Sci.* **599** (1-3), 150-159 (2005).
- T Valla. Electronic Interactions in Strongly Correlated Systems: What is the Glue for High Temperature Superconductivity?. *Proceedings of the SPIE, Strongly Correlated Electron Materials: Physics and Nanoengineering*, Vol 5932, p. 5932-03, sponsored by SPIE-The International Society for Optical Engineering. (2005).

Beamline X1A1

- A Bauer, T Rabung, F Claret, T Schäfer, G Buckau, T Fanghänel. Influence of Temperature on Sorption of Europium onto Smectite: The Role of Organic Contaminants. *Appl. Clay Sci.* **30** (1), 1-10 (2005).
- A Braun, N Shah, F Huggins, K Kelly, A Sarofim, C Jacobsen, S Wirick, H Francis, J Havsky, et al.. X-ray Scattering and Spectroscopy Studies on Diesel Soot from Oxygenated Fuel Under Various Engine Load Conditions. *Carbon*. **43** (12), 2588-2599 (2005).
- A Braun, F Huggins, N Shah, Y Chen, S Wirick, S Mun, C Jacobsen, G Huffman. Advantages of soft X-ray Absorption over TEM-EELS for Solid Carbon Studies - a Comparative Study on Diesel Soot with EELS and NEXAFS. *Carbon*. **43**, 117-124 (2005).
- F Claret, T Schäfer, T Rabung, M Wolf, A Bauer, G Buckau. Differences in Properties and Cm(III) Complexation Behavior of Isolated Humic and Fulvic Acid Derived from Opalinus Clay and Callovo-Oxfordian Argillite. *Appl. Geochem.* **20** (6), 1158-1168 (2005).
- M Haming. Spectroscopy on Poly-L-Lysine and Spectromicroscopy Study on Biomineralized Proteins in Jaws of Glycera Dibranchiata. M.A. Thesis. SUNY at StonyBrook, StonyBrook. (2005).
- R Kretzschmar, T Schäfer. Metal Retention and Transport on Colloidal Particles in the Environment. *Elements*. **1** (4), 205-210 (2005).
- J Lehmann, B Liang, D Solomon, M Lerotic, F Luizao, J Kinyangi, T Schäfer, S Wirick, C Jacobsen. Near-Edge X-ray Absorption Fine Structure (NEXAFS) Spectroscopy for Mapping Nano-Scale Distribution of Organic Carbon Forms in Soil: Application to Black Carbon Particles. *Global Biogeochem. Cy.* **19**, GB1013 (2005).
- M Lerotic, C Jacobsen, J Gillow, A Francis, S Wirick, S Vogt, J Maser. Cluster Analysis in Soft X-ray Spectromicroscopy: Finding the Patterns in Complex Specimens. *J. Electron. Spectrosc. Relat. Phenom.* **144-147**, 1137-1143 (2005).
- M Lerotic. Finding Patterns in Complex Specimens by Improving the Acquisition and Analysis of X-ray Spectromicroscopy Data. Ph.D. Thesis. SUNY at StonyBrook, StonyBrook. (2005).
- D Mancosky, L Lucia, H Nanko, S Wirick, A Rudie, R Braun. Novel Visualization Studies of Lignocellulosic Oxidation Chemistry by Application of C-near Edge X-ray Absorption Fine Structure Spectroscopy. *Cellulose*. **12**, 35-41 (2005).
- M Plaschke, J Rothe, M Altmaier, M Denecke, T Fanghaenel. Near Edge X-ray Absorption Fine Structure (NEXAFS) of model compounds for the humic acid / actinide ion interaction. *J. Electron. Spectrosc. Relat. Phenom.* **148**, 151-157 (2005).
- T Schäfer, G Buckau, R Artinger, J Kim, S Geyer, M Wolf, W Bleam, S Wirick, C Jacobsen. Origin and Mobility of Fulvic Acids in the Gorleben Aquifer: Implications from Isotopic Data and Carbon/Sulfur XANES. *Org. Geoch.* **36**, 567-582 (2005).
- T Schäfer, F Claret, M Lerotic, G Buckau, T Rabung, A Bauer, C Jacobsen. Source Identification and Characterization of Humic and Fulvic Acids Isolated from Oxfordian Argillite and Opalinus Clay. *Humic Substances: Molecular Details and Applications in Land and Water Conservation*, p. 43-62, Tayloe and Francis, Inc., New York. (2005).
- M Schumacher. Microheterogeneity of Soil Organic Matter investigated by C-1s NEXAFS Spectroscopy and X-ray Microscopy. Ph.D. Thesis. Swiss Federal Institute of Technology Zurich, Zurich. (2005).
- M Schumacher, I Christl, A Scheinost, C Jacobsen, R Kretzschmar. Chemical Heterogeneity of Organic Soil Colloids Investigated by

- Scanning Transmission X-ray Microscopy and C-1s NEXAFS Microspectroscopy. *Environ. Sci. Tech.* **39** (23), 9094-9100 (2005).
- D Solomon, J Lehmann, J Kinyangi, B Liang, T Schäfer. Carbon K-Edge NEXAFS and FTIR-ATR Spectroscopic Investigations of Organic Carbon Speciation in Soils. *Soil Sci. Soc. Am. J.* **69**, 107-119 (2005).

Beamline X1A2

- M Haming. Spectroscopy on Poly-L-Lysine and Spectromicroscopy Study on Biomineralized Proteins in Jaws of Glycera Dibranchiata. M.A. Thesis. SUNY at StonyBrook, StonyBrook. (2005).
- M Lerotic. Finding Patterns in Complex Specimens by Improving the Acquisition and Analysis of X-ray Spectromicroscopy Data. PH.D. Thesis. SUNY at StonyBrook, StonyBrook. (2005).
- T Schäfer, F Claret, M Lerotic, G Buckau, T Rabung, A Bauer, C Jacobsen. Source Identification and Characterization of Humic and Fulvic Acids Isolated from Oxfordian Argillite and Opalinus Clay. *Humic Substances: Molecular Details and Applications in Land and Water Conservation*, p. 43-62, Tayloe and Francis, Inc., New York. (2005).
- D Shapiro, P Thibault, T Beetz, V Elser, M Howells, C Jacobsen, J Kirz, E Lima, H Miao, et al.. Biological Imaging by Soft X-ray Diffraction Microscopy. *Proc Natl Acad Sci USA*. **102** (43), 15343-15346 (2005).

Beamline X1B

- C McGuinness, J Downes, P Sheridan, P Glans, K Smith, W Si, P Johnson. X-ray Spectroscopic Study of the Electronic Structure of the High-Dielectric-Constant Material CaCu₃Ti₄O₁₂. *Phys. Rev. B* **71**, 195111 (2005).
- A Rüdél, U Hergenhanh, K Maier, E Rennie, O Kugeler, J Vieffhaus, P Lin, R Lucchese, A Bradshaw. Exchange Interaction Effects in NO Core Level Photoionization Cross Sections. *New J. Phys.* **7**, 189 (2005).
- C Schubler-Langeheine, J Schlappa, A Tanaka, Z Hu, C Chang, E Schierle, M Benomar, H Ott, E Weschke, et al.. Spectroscopy of Stripe Order in La_{1.8}Sr_{0.2}NiO₄ Using Resonant Soft X-Ray Diffraction. *Phys. Rev. Lett.* **95**, 156402 (2005).
- Y Zhang, S Wang, T Learmonth, L Plucinski, A Matsuura, S Bernardis, C O'Donnell, J Downes, K Smith. Electronic Excitations in Vanadium Oxide Phthalocyanine Studied via Resonant Soft X-ray Emission and Resonant Inelastic X-ray Scattering. *Chem. Phys. Lett.* **413** (1-3), 95-99 (2005).

Beamline X2B

- J Borah, E Ritman, T Dufresne, S Jorgensen, S Liu, J Sacha, R Phipps, R Turner. The Effect of Risdrionate on Bone Mineralization as Measured by Micro-Computed Tomography with Synchrotron Radiation: Correlation to Histomorphometric Indices of Turnover. *Bone*. **37** (1), 1-9 (2005).

Beamline X3A1

- P Coppens, I Vorontsov, T Graber, M Gembicky, A Kovalevsky. The Structure of Short-Lived Excited States of Molecular Complexes by Time-Resolved X-ray Diffraction. *Acta Cryst. A*. **61**, 162-172 (2005).
- R Poulsen, A Bentien, M Chevalier, B Iverson. Synthesis, Physical Properties, Multitemperature Crystal Structure, and 20 K Synchrotron X-ray Charge Density of a Magnetic Metal Organic

Framework Structure, Mn₃(C₈O₄H₄)₃(C₅H₁₁ON)₂. *J. Am. Chem. Soc.* **127**, 9156-9166 (2005).

Beamline X3A2

- D Dikovsky, G Marom, C Avila-Orta, R Somani, B Hsiao. Shear-Induced Crystallization in Isotactic Polypropylene Containing Ultra-High Molecular Weight Polyethylene Oriented Precursor Domains. *Polymer*. **46** (9), 3096-3104 (2005).
- K Fukukawa, L Zhu, P Gopalan, M Ueda, S Yang. Synthesis and Characterization of Silicon-Containing Block Copolymers from Nitroxide-Mediated Living Free Radical Polymerization. *Macromolecules*. **38**, 263-270 (2005).
- G Gemeinhardt, R Moore. Characterization of Ionomer-Compatibilized Blend Morphology Using Synchrotron Small-Angle X-ray Scattering. *Macromolecules*. **38**, 2813-2819 (2005).
- D Kawakami, B Hsiao, C Burger, S Ran, C Avila-Orta, I Sics, T Kikutani, K Jacob, B Chu. Deformation-Induced Phase Transition and Superstructure Formation in Poly(ethylene terephthalate). *Macromolecules*. **38**, 91-103 (2005).
- J Keum, R Somani, F Zuo, C Burger, I Sics, B Hsiao, H Chen, R Kolb, C Lue. Probing Flow-Induced Precursor Structures in Blown Polyethylene Films by Synchrotron X-rays During Constrained Melting. *Macromolecules*. **38**, 5128-5136 (2005).
- J Miao, G Xu, L Zhu, L Tian, K Uhrich, C Avila-Orta, B Hsiao, M Utz. Chain-folding and Overall Molecular Conformation in a Novel Amphiphilic Starlike Macromolecule. *Macromolecules*. **38**, 7074-7082 (2005).
- S Poompradub, M Tosaka, S Kohjiya, Y Ideda, S Toki, I Sics, B Hsiao. Mechanism of Strain-Induced Crystallization in Filled and Unfilled Natural Rubber Vulcanizates. *J. Appl. Phys.* **97**, 103529 (2005).
- R Somani, L Yang, B Hsiao, T Sun, N Pogodina, A Lustiger. Shear-Induced Molecular Orientation and Crystallization in Isotactic Polypropylene: Effects of the Deformation Rate and Strain. *Macromolecules*. **38**, 1244-1255 (2005).

Beamline X3B1

- C Blome, T Tschentscher, J Davaasambuu, P Durand, S Techert. Femtosecond Time-Resolved Powder Diffraction Experiments using Hard X-ray Free-Electron Lasers. *J. Synch. Rad.* **12**, 812-819 (2005).
- L Chi, I Swainson, L Cranswick, J Her, P Stephens, O Knop. The Ordered Phase of Methylammonium Lead Chloride CH₃ND₃PbCl₃. *J. Solid State Chem.* **178** (5), 1376-1385 (2005).
- O Chmaissem, B Dabrowski, S Kolesnik, J Mais, J Jorgenson, S Short, C Botez, P Stephens. Effects of A-Site Ordering on the Structures and Properties of La_{1-x}BaxMnO₃(x~0.5). *Phys. Rev. B*. **72**, 104426 (2005).
- L Hildebrandt, R Dinnebier, M Jansen. Crystal Structure and Ionic Conductivity of Cesium Trifluoromethyl Sulfonate, CsSO₃CF₃. *Z. Anorg. Allg. Chem.* **631**, 1660-1666 (2005).
- A Huq, P Stephens. Transition Temperatures and Vacancies in Superconducting Rb₃C₆₀. *Phys. Rev. B: Condens. Matter*. **72**, 092511 (2005).
- C Kenney, Y Maham, A Nelson. Characterization of Monofunctional ZrO₂-MnO₃ Catalysts for Methylcyclopentane Conversion. *Thermochem. Acta*. **434** (1-2), 55-61 (2005).
- J Majzlan, C Botez, P Stephens. The Crystal Structure of Synthetic Fe₂(So₄)₃(H₂O)₅ and the type specimen of lausenite. *Am. Mineral.* **90**, 411-416 (2005).
- M Navarro, E Pannunzio-Miner, S Pagola, M Gomex, R Carbonio.

- Structural Refinement of Nd[Fe(CN)₆] 4H₂O and Study of NdFeO₃ Obtained by its Oxidative Thermal Decomposition at Very Low Temperatures. *J. Solid State Chem.* **178** (3), 847-854 (2005).
- I Schottenfeld, A Benesi, P Stephens, G Chen, P Eklund, T Mallouk. Structural Analysis and Characterization of Layer Perovskite Oxynitrides made from Dion-Jacobson oxide precursors. *J. Solid State Chem.* **178**, 2313-2321 (2005).
- A van der Lee, P Richez, C Tapiero. Crystal Structure of Nitarsone Determined from Synchrotron X-ray Powder Diffraction Data. *J. Mol. Struct.* **743**, 223-228 (2005).
- R Von Dreele. Binding of N-acetylglucosamine Oligosaccharides to Hen Egg-White Lysozyme: A Powder Diffraction Study. *Acta Cryst. D* **61**, 22-32 (2005).
- P Whitfield, I Davidson, L Cranswick, I Swainson, P Stephens. Investigation of Possible Superstructure and Cation Disorder in the Lithium Battery Cathode Material Li Mn(1/3)Ni(1/3)Co(1/3)O(2) Using Neutron and Anomalous Dispersion Powder Diffraction. *Solid State Ionics*. **176**, 463-471 (2005).
- ### Beamline X4A
- J Avalos, K Bever, C Wolberger. Mechanism of Sirtuin Inhibition by Nicotinamide: Altering the NAD⁺ Cosubstrate Specificity of a Sir2 Enzyme. *Mol. Cell*. **17** (6), 855-868 (2005).
- P Bachhawat. Regulation In The OmpR/PhoB Family of Response Regulators. PhD Thesis. Graduate School of Biomedical Sciences, University of Medicine and Dentistry, NJ and Rutgers University, NJ, Piscataway. (2005).
- P Bachhawat, G Swapna, G Montelione, A Stock. Mechanism of activation for transcription factor PhoB suggested by different modes of dimerization in the inactive and active states. *Structure*. **13** (9), 1353-1363 (2005).
- A Banerjee, W Yang, M Karplus, G Verdine. Structure of a Repair Enzyme Interrogating Undamaged DNA Elucidates Recognition of Damaged DNA. *Nature*. **434**, 612-618 (2005).
- S Bouyain, P Longo, S Li, K Ferguson, D Leahy. The Extracellular Region of ErbB4 Adopts a Tethered Conformation in the Absence of Ligand. *Proc Natl Acad Sci USA*. **102**, 15024-15029 (2005).
- R Depetris, J Hu, I Gimpelevich, L Holt, R Daly, S Hubbard. Structural Basis for Inhibition of the Insulin Receptor by the Adaptor Protein Grb14. *Mol. Cell*. **20** (2), 325-333 (2005).
- D Eckert, D Chan, V Malashkevich, P Carr, P Kim. Inhibitors of HIV Membrane Fusion. US Patent No. 6,841,657. (2005).
- Q Fan, W Hendrickson. Structure of Human Follicle-Stimulating Hormone in Complex with its Receptor. *Nature*. **433**, 269 (2005).
- F Forouhar, Y Yang, D Kumar, Y Chen, E Fridman, S Park, Y Chiang, T Acton, G Montelione, et al.. Structural and Biochemical Studies Identify Tobacco SABP2 as a Methyl Salicylate Esterase and Implicate it in Plant Innate Immunity. *Proc Natl Acad Sci USA*. **102**, 1773-1778 (2005).
- F Forouhar, I Lee, J Vujcic, S Vujcic, J Shen, S Vorobiev, R Xiao, T Acton, G Montelione, et al.. Structural and Functional Evidence for *Bacillus subtilis* PaiA as a Novel N1-spermidine/spermine acetyltransferase (SSAT). *J. Biol. Chem.* **280**, 40328-40336 (2005).
- H Furukawa, S Singh, R Mancusso, E Gouaux. Subunit Arrangement and Function in NMDA Receptors. *Nature*. **438**, 185-192 (2005).
- B Geisbrecht, B Hamakoa, B Perman, Z Zemla, D Leahy. The Crystal Structure of EAP Domains from *Staphylococcus Aureus* Reveal an Unexpected Hology to Bacterial Superantigens. *J. Biol. Chem.* **280**, 17243 (2005).
- J Gorman, L Shapiro. Crystal Structures of the Tryptophan Repressor binding Protein WrbA and complexes with Flavin Mononucleotide. *Protein Sci.* **14**, 3004-3012 (2005).
- S Hausmann, S Zheng, C Fabrega, S Schneller, C Lima, S Shuman. Encephalitozoon Cuniculi MRNA Cap (Guanine N-7) Methyltransferase: Methyl Acceptor Specificity, Inhibition by S-Adenosylmethionine Analogs, and Structure-Guided Mutational Analysis. *J. Biol. Chem.* **280**, 20404 (2005).
- W Hendrickson, X Jiang, K Langley, R Syed, Y Hsu. Conjugated Ligands for the Stimulation of blood Cell Proliferation by Effecting Dimerization of the Receptor for Stem Cell Factor. US Patent No. 6,904,369. (2005).
- J Hu, S Hubbard. Structural Characterization of a Novel Cbl Phosphotyrosine Recognition Motif in the APS Family of Adapter Proteins. *J. Biol. Chem.* **280** (19), 18943 (2005).
- O Ibrahimi, B Yeh, A Eliseenkova, F Zhang, S Olsen, M Igarashi, S Aaronson, R Linhardt, M Mohammadi. Analysis of Mutations in Fibroblast Growth Factor (FGF) and a Pathogenic Mutation in FGF Receptor (FGFR) Provides Direct Evidence for the Symmetric Two-End Model for FGFR Dimerization. *Mol. Cell. Bio.* **25**, 671-684 (2005).
- A Inanobe, H Furukawa, E Gouaux. Mechanism of Partial Agonist Action at the NR1 Subunit of NMDA Receptors. *Neuron*. **47**, 71-84 (2005).
- R Jin, S Clark, A Weeks, J Dudman, E Gouaux, K Partin. Mechanism of Positive Allosteric Modulators Acting on AMPA Receptors. *J. Neurosci.* **25**, 9027-9036 (2005).
- G Jogl, Y Hsiao, L Tong. Crystal Structure of Mouse Carnitine Octanoyltransferase and Molecular Determinants of Substrate Selectivity. *J. Biol. Chem.* **280**, 738 (2005).
- J Khan, B Dunn, L Tong. Crystal Structure of Human Taspase1, a Crucial Protease Regulating the Function of MLL. *Structure*. **13** (10), 1443-1452 (2005).
- L Lois, C Lima. Structures of the Small Ubiquitin-like Modifier E1 Activating Enzyme Provide Insights into SUMO Activation and the Mechanism for E2 Recruitment to E1. *EMBO J.* **24**, 439-451 (2005).
- A Malay, K Allen, D Tolan. Structure of the Thermolabile Mutant Aldolase B, A149P: Molecular Basis of Hereditary Fructose Intolerance. *J. Mol. Biol.* **347** (1), 135-144 (2005).
- A Marina, C Waldburger, W Hendrickson. Structure of the Entire Cytoplasmic Portion of a Sensor Histidine-kinase Protein. *EMBO J.* **24**, 1-13 (2005).
- E Michelotti, K Moffett, D Nguyen, M Kelly, R Shetty, X Chai, K Northrop, V Nambodiri, B Campbell, M Karpusas. Two Classes of p38 β MAP Kinase Inhibitors Having a Common Diphenylether Core but Exhibiting Divergent Binding Modes. *BioOrg. Med. Chem.* **15** (23), 5274-5279 (2005).
- R Olson, E Gouaux. Crystal Structure of the *Vibrio cholerae* Cytolysin (VCC) Pro-toxin and its Assembly into a Heptameric Transmembrane Pore. *J. Mol. Biol.* **350**, 997-1016 (2005).
- D Reverter, K Wu, T Gan-Erdene, Z Pan, K Wilkinson, C Lima. Structure of the Complex Between the Ulp/Senp Protease Family Member Den1 and Nedd8. *J. Mol. Biol.* **345**, 141-151 (2005).
- S Rubin, A Gall, N Zheng, N Pavletich. Structure of the Rb C-Terminal Domain Bound to E2F1-DP1: A Mechanism for Phosphorylation-Induced E2F Release. *Cell*. **123** (6), 1093-1106 (2005).
- M Rudolph, G Amodeo, Y Bai, L Tong. Crystal Structure of the Protein Kinase Domain of Yeast AMP-Activated Protein Kinase Snf1. *Biochem. Biophys. Res. Commun.* **337**, 1224-1228 (2005).
- A Ruthenburg, D Graybosch, J Huetsch, G Verdine. A Superhelical Spiral in the *Escherichia coli* DNA Gyrase A C-terminal Domain

- Imparts Unidirectional Supercoiling Bias. *J. Biol. Chem.* **280**, 26177-26184 (2005).
- C Steegborn, T Litvin, K Hess, A Capper, R Taussig, J Buck, L Levin, H Wu. A Novel Mechanism for Adenylyl Cyclase Inhibition from the Crystal Structure of its Complex with Catechol Estrogen. *J. Biol. Chem.* **280**, 31754 (2005).
- C Steegborn, T Litvin, L Levin, J Buck, H Wu. Biocarbonate Activation of Adenylyl Cyclase via Promotion of Catalytic Active Site Closure and Metal Recruitment. *Nat. Struct. Mol. Biol.* **12**, 32 (2005).
- X Tao. Structural and Functional Studies on Human DJ-1 (PARK7), a Protein Associated with Early-Onset Parkinson's Disease. PhD Thesis. Columbia University, New York. (2005).
- A Toro-Roman, T Mack, A Stock. Structural Analysis and Solution Studies of the Activated Regulatory Domain of the Response Regulator ArcA: A Symmetric Dimer Mediated by the alpha4-beta5-alpha5 Face. *J. Mol. Biol.* **349** (1), 11-26 (2005).
- A Toro-Roman, T Wu, A Stock. A Common Dimerization Interface in Bacterial Response Regulators KdpE and TorR. *Protein Sci.* **14** (12), 3077-3088 (2005).
- A Toro-Roman. A Model for the Mechanism of Activation of Response Regulators from the OmpR/PhoB Subfamily of Transcription Factors. Ph.D. Thesis. Rutgers, The State University of New Jersey, New Brunswick. (2005).
- L Vedula, M Rynkiewicz, H Pyun, R Coates, D Cane, D Christianson. Molecular Recognition of the Substrate Diphosphate Group Governs Product Diversity in Trichodiene Synthase Mutants. *Biochemistry*. **44**, 6153 (2005).
- J Williams, C Sue, G Banting, H Yang, D Glerum, W Hendrickson, E Schon. Crystal Structure of Human SCO1: Implications for Redox Signaling by a Mitochondrial Cytochrome C Oxidase „Assembly“ Protein. *J. Biol. Chem.* **280**, 15202 (2005).
- J Williams, H Xie, W Hendrickson. Crystal Structure of Dynein Light Chain TCTEX-1. *J. Biol. Chem.* **280**, 21981 (2005).
- P Worley, J Tu, B Xiao, D Leahy, J Beneken, A Lanahan, P Brakeman. Nucleic Acid Molecule Encoding Homer 2a Protein. US Patent No. 6,864,083. (2005).
- Q Xu, R Roberts, H Guo. Two Crystal Forms of the Restriction Enzyme MspI-DNA Complex Show the Same Novel Structure. *Protein Sci.* **14**, 2590-2600 (2005).
- A Yamashita, S Singh, T Kawate, Y Jin, E Gouaux. Crystal Structure of a Bacterial Homologue of Na⁺/Cl⁻-Dependent Neurotransmitter Transporters. *Nature*. **437**, 215 (2005).
- J Yang, L Wang, L Zheng, F Wan, M Ahmed, M Lenardo, H Wu. Crystal Structure of MC159 Reveals Molecular Mechanism of DISC Assembly and FLIP Inhibition. *Mol. Cell*. **20**, 939 (2005).
- M Zweifel, D Leahy, D Barrick. Structure and Notch Receptor Binding of the Tandem WWE Domain of Deltex. *Structure*. **13**, 1599-1611 (2005).
- Beamline X6A**
- M Adams, Z Jia. Structural and Biochemical Evidence for an Enzymatic Quinone Redox Cycle in Escherichia Coli: Identification of a Novel Quinol Monooxygenase. *J. Biol. Chem.* **280**, 8358 (2005).
- R DeSilva, G Kovacicova, W Lin, R Taylor, K Skorupski, F Kull. Crystal Structure of the Virulence Gene Activator Apha from Vibrio Cholerae Reveals it is a Novel Member of the Winged Helix Transcription Factor Superfamily. *J. Biol. Chem.* **280**, 13779 (2005).
- J Helliwell. Protein Crystal Perfection and its Application. *Acta Cryst. D*. **61**, 793-798 (2005).
- T Kajander, A Cortajarena, E Main, S Mochrie, L Regan. A New Folding Paradigm for Repeat Proteins. *J. Am. Chem. Soc.* **127**, 10188-10190 (2005).
- T Kuzuyama, J Noel, S Richard. Structural Basis for the Promiscuous Biosynthetic Prenylation of Aromatic Natural Products. *Nature*. **435** (7044), 983-7 (2005).
- A Mildvan, Z Xia, H Azurmendi, V saraswat, P Legler, M Massiah, S Gabelli, M Bianchet, L Kang, L Amzel. Structures and Mechanisms of Nudix Hydrolases. *Arch. Biochem. Biophys.* **433** (1), 129-43 (2005).
- M Nadella, M Bianchet, S Gabelli, J Barrila, L Amzel. Structure and Activity of the Axon Guidance Protein MICAL. *Proc Natl Acad Sci USA*. **102** (46), 16830-16835 (2005).
- D Nair, R Johnson, L Prakash, S Prakash, A Aggarwal. Rev1 Employs a Novel Mechanism of DNA Synthesis using a Protein Template. *Science*. **309**, 2219 (2005).
- M Nicholson, M Hahn, K Wucherpfennig. Unusual features of Self-Peptide/MHC Binding by Autoimmune T Cell Receptors. *Immunity*. **23** (4), 351-360 (2005).
- K Pant, B Crane. Structure of a Loose Dimer: an Intermediate in Nitric Oxide Synthase Assembly. *J. Mol. Biol.* **352** (4), 932-940 (2005).
- E Pozharski, A Moulin, A Hewagama, A Shanafelt, G Petsko, D Ringe. Diversity of Hapten Recognition: Structural Study of an Anti-Cocaine Antibody M82G2. *J. Mol. Biol.* **349** (3), 570-582 (2005).
- A Vahedi-Faridi, V Stojanoff, J Yeh. The Effects of Flash-Annealing on Glycerol Kinase Crystals. *Acta Cryst. D*. **61** (7), 982-989 (2005).
- Z Xia, H Azurmendi, L lairson, S Withers, S Gabelli, M Bianchet, L Amzel, A Mildvan. Mutational, Structural, and Kinetic Evidence for a Dissociative Mechanism in the GDP-mannose Mannosyl Hydrolase Reaction. *Biochemistry*. **44** (25), 8989-97 (2005).
- Beamline X6B**
- S Kwak, E DiMasi, Y Han, J Aizenberg, I Kuzmenko. Orientation and Mg Incorporation of Calcite Grown on Functionalized Self-Assembled Monolayers: A Synchrotron X-ray Study. *Cryst. Growth Des.* **5** (6), 2139-2145 (2005).
- Beamline X7A**
- D Cox, B Noheda, G Shirane. Low-Temperature Phases in PbZr_{0.52}Ti_{0.48}O₃: A Neutron Powder Diffraction Study. *Phys. Rev. B: Condens. Matter*. **71**, 134110-10 (2005).
- M Crawford, R Harlow, S Ceemyad, V Tissen, J Schilling, E McCarron, S Tozer, D Cox, N Ichikawa, et al.. High-Pressure Study of Structural Phase Transitions and Superconductivity in La_{1.48}Nd_{0.4}Sr_{0.12}CuO₄. *Phys. Rev. B*. **71**, 104513 (2005).
- F Drymiotis, Y Lee, G Lawes, J Lashley, T Kimura, S Shapiro, A Migliori, V Correa, R Fisher. Tunable Thermal Expansion Behavior in the Intermetallic YbGaGe. *Phys. Rev. B*. **71**, 174304 (2005).
- M Gateshki, V Petkov, S Pradhan, T Vogt. Structure of Nanocrystalline MgFe₂O₄ from X-ray Diffraction, Rietveld and Atomic Pair Distribution Function Analysis. *J. Appl. Cryst.* **38**, 772-779 (2005).
- J Graetz, Y Lee, J Reilly, S Park, T Vogt. Structures and Thermodynamics of the Mixed Alkali Alanates. *Phys. Rev. B*. **71**, 184115 (2005).
- J Lai, K Shafi, A Ullman, K Loos, R Popovitz-Biro, Y Lee, T Vogt, C Estournes. One-Step Synthesis of Core(Cr)/Shell(gamma-Fe₂O₃) Nanoparticles. *J. Am. Chem. Soc.* **127**, 5730-5731 (2005).
- Y Lee, J Hriljac, T Vogt. Pressure-Induced Migration of Zeolitic Water in Laumontite. *Phys. Chem. Miner.* **31**, 421-428 (2005).
- Y Lee, J Hriljac, T Vogt. Variable-Temperature Structural Studies of

- Tetranatrolite from Mt. Saint-Hilaire: Synchrotron X-ray Powder Diffraction and Rietveld Analysis. *Am. Mineral.* **90**, 247-251 (2005).
- Y Lee, J Hriljac, J Parise, T Vogt. Pressure-Induced Stabilization of Ordered Paratrolite: A new Insight into the Paratrolite controversy. *Am. Mineral.* **90**, 252-257 (2005).
- R Macquart, S Kim, W Gemmill, J Stalick, Y Lee, T Vogt, H zur Loye. Synthesis, Structure, and Magnetic Properties of Sr₂NiOsO₆ and Ca₂NiOsO₆: Two New Osmium-Containing Double Perovskites. *Inorg. Chem.* **44**, 9676-9683 (2005).
- Y Mudryk, Y Lee, T Vogt, K Gschneidner, Jr., V Pecharsky. Polymorphism of Gd₅Si₂Ge₂: The Equivalence of Temperature, Magnetic Field, and Chemical and Hydrostatic Pressures. *Phys. Rev. B* **71**, 174104 (2005).
- S Park, K Kang, W Si, W Yoon, Y Lee, A Moodenbaugh, L Lewis, T Vogt. Synthesis and Characterization of Na_{0.3}RhO₂·0.6H₂O-A Semiconductor with a Weak Ferromagnetic Component. *Solid State Commun.* **135** (1-2), 51-56 (2005).
- S Park, Y Lee, W Si, T Vogt. Synthesis and Structure of the Monolayer Hydrate K_{0.3}CoO₂·4H₂O. *Solid State Commun.* **134** (9), 607-611 (2005).
- V Petkov, V Parvanov, D Tomalia, D Swanson, D Bergstrom, T Vogt. 3D Structure of Dendritic and Hyper-Branched Macromolecules by X-ray Diffraction. *Solid State Commun.* **134** (10), 671-675 (2005).
- V Petkov, V Parvanov, P Trikalitis, C Malliakas, T Vogt, M Kanatzidis. Three-Dimensional Structure of Nanocomposites from Atomic Pair Distribution Function Analysis: Study of Polyaniline and (Polyaniline)_{0.5}V₂O₅·1.0H₂O. *J. Am. Chem. Soc.* **127**, 8805-8812 (2005).
- C Petrovic, Y Lee, T Vogt, N Lazarov, S Bud'ko, P Canfield. Kondo Insulator Description of Spin State Transition in FeSb₂. *Phys. Rev. B: Condens. Matter* **72**, 045103 (2005).
- K Wallwork, B Kennedy, Q Zhou, Y Lee, T Vogt. Pressure and Temperature-Dependent Structural Studies of Ba₂BiTaO₆. *J. Solid State Chem.* **178** (1), 201-211 (2005).
- X Yang, B Toby, M Cambor, Y Lee, D Olson. Propene Adsorption Sites in Zeolite ITQ-12: a Combined Synchrotron X-ray Neutron Diffraction Study. *J. Phys. Chem. B* **109** (16), 7894-7899 (2005).
- Q Zhou, B Kennedy, K Wallwork, M Elcombe, Y Lee, T Vogt. Temperature and Pressure Dependent Structural Studies of the Ordered Double Perovskites Sr₂TbRu_{1-x}Ir_xO₆. *J. Solid State Chem.* **178** (7), 2282-2291 (2005).
- H zur Loye, M Smith, Y Lee, T Vogt. High-Pressure Investigation of Sr₃PbNiO₆. *J. Alloys Compd.* **390** (1-2), 35-40 (2005).
- Processes. *J. Magn. Magn. Mater.* **295** (2), 145-154 (2005).
- M Helliwell, R Jones, V Kaucic, N Logar. The use of Softer X-rays in the Structure Elucidation of Microporous Materials. *J. Synch. Rad.* **12** (4), 420-430 (2005).
- L Hildebrandt, R Dinnebier, M Jansen. Crystal Structure and Ionic Conductivity of Cesium Trifluoromethyl Sulfonate, CsSO₃CF₃. *Z. Anorg. Allg. Chem.* **631**, 1660-1666 (2005).
- T Jensen, A Christensen, J Hanson. Hydrothermal Transformation of the Calcium Aluminum Oxide Hydrates CaAl₂O₄ · 10H₂O and Ca₂Al₂O₇ · 8H₂O to Ca₃Al₂(OH)₁₂ Investigated by In Situ Synchrotron X-ray Powder Diffraction. *Cem. Concr. Res.* **35**, 2300-2309 (2005).
- H Jeong, Z Lai, M Tsapatsis, J Hanson. Strain of MFI Crystals in Membranes: An in situ Synchrotron X-ray Study. *Microporous Mesoporous Mater.* **84** (1-3), 332-337 (2005).
- Y Meng, G Ceder, C Grey, W Yoon, M Jiang, J Breger, Y Shao-Horn. Cation Ordering in Layered O₃ Li[NiLi_{1/3-2/3}Mn_{2/3-x}]/O₂. *Chem. Mater.* **17**, 2386-2394 (2005).
- J Rodriguez, X Wang, G Liu, J Hanson, J Hrbek, C Peden, A Iglesias-Juez, M Fernandez-Garcia. Physical and Chemical Properties of Ce_{1-x}Zr_xO₂ Nanoparticles and Ce_{1-x}Zr_xO₂(1 1 1) Surfaces: Synchrotron-Based Studies. *J. Mol. Catal. A: Chem.* **228**, 11-19 (2005).
- L Solovyov, O Belousov, R Dinnebier, A Shmakov, S Kirik. X-ray Diffraction Structure Analysis of MCM-48 Mesoporous Silica. *J. Phys. Chem. B* **109**, 3233-3237 (2005).
- J Szanyi, J Kwak, J Hanson, C Wang, T Szailer, C Peden. Changing Morphology of BaO/Al₂O₃ During NO₂ Uptake and Release. *J. Phys. Chem. B* **109**, 7339-7344 (2005).
- S van Smalen, R Dinnebier, J Hanson, J Gollwitzer, F Bullesfeld, A Prokofiev, W Assmus. High-Temperature Behavior of Vanadyl Pyrophosphate (VO)₂P₂O₇. *J. Solid State Chem.* **178** (7), 2225-2230 (2005).
- X Wang, J Rodriguez, J Hanson, D Gamarra, A Martinez-Arias, M Fernandez-Garcia. Unusual Physical and Chemical Properties of Cu in Ce_{1-x}Cu_xO₂ Oxides. *J. Phys. Chem. B* **109**, 19595-19603 (2005).
- X Wang, J Hanson, J Rodriguez, C Bolver, M Fernandez-Garcia. The Structural and Electronic Properties of Nanostructured Ce(1-x-y)Zr(x)Tb(y)O(2) Ternary Oxides: Unusual Concentration of Tb(3+) and Metal-Oxygen-Metal Interactions. *J. Chem. Phys.* **122** (15), 154711 (2005).
- X Wang, J Rodriguez, J Hanson, M Perez, J Evans. In Situ Time-Resolved Characterization of Au-CeO₂ Catalysts During Water Gas Shift Reactions: presence of Au and O Vacancies in the Active Phase. *J. Chem. Phys.* **123**, 221101 (2005).
- W Wen, B Kumarasamy, S Mukerjee, M Auinat, Y Ein-Eli. Origin of 5 V Electrochemical Activity Observed in Non-Redox Reactive Divalent Cation Doped LiM_{0.5-x}Mn_{1.5+x}O₄ (0<X). *Electrochem. Soc.* **152** (9), A1902 (2005).
- W Yoon, M Balasubramanian, X Yang, J McBreen, J Hanson. Time Resolved XRD Study on the Thermal Decomposition of Li_{1-x}Ni_{0.8}Co_{0.15}Al_{0.05}O₂ Cathode Materials for Li-ion Batteries. *Electrochem. Solid-State Lett.* **8**, A83 (2005).
- J Zhang, F Lima, M Shao, K Sasaki, J Wang, J Hanson, R Adzic. Platinum Monolayer on Nonnoble Metal-Nobel Metal Core-Shell Nanoparticle Electrocatalysts for O₂ Reduction. *J. Phys. Chem. B* **109**, 22701-22704 (2005).

Beamline X7B

- A Celestian, D Medvedev, A Tripathi, J Parise, A Clearfield. Optimizing Synthesis of Na₂Ti₂SiO₇ · 2H₂O (Na-CST) and Ion Exchange Pathways for Cs_{0.4}H_{1.6}Ti₂SiO₇ · H₂O (Cs-CST) Determined from in situ Synchrotron X-ray Powder Diffraction. *Nucl. Instrum. Meth. B* **238**, 61-69 (2005).
- R Dinnebier, S Vensky, M Jensen, J Hanson. Crystal Structure and Topological Aspects of the High-Temperature Phases of the Alkali-metal Oxalates M₂C₂O₄ (M= K, Rb, Cs). *Chem. Eur. J.* **11** (4), 1119-1129 (2005).
- M Fernandez-Garcia, X Wang, C Bolver, A Iglesias-Juez, J Hanson, J Rodriguez. Ca Doping of Nanosize Ce-Zr and Ce-Tb Solid Solutions: Structural and Electronic Effects. *Chem. Mater.* **17**, 4181-4193 (2005).
- X Guo, B Ravi, P Devi, J Hanson, J Margolies, R Gambino, J Parise, S Sampath. Synthesis of Yttrium Iron garnet (YIG) by Citrate-Nitrate Gel Combustion and Precursor Plasma Spray

Beamline X8C

- J Adams, G Pal, K Yam, H Spencer, Z Jia, S Smith. Purification and Crystallization of a Trimodular Complex Comprising the Type II Cohesin-Dockerin Interaction from the Cellulosome of *Clostridium thermocellum*. *Acta Cryst. F* **61**, 46-48 (2005).

- A Athanasiadis, D Placido, S Maas, B Brown, II, K Lowenhaupt, A Rich. The Crystal Structure of the ZB Domanin of the RNA-Editing Enzyme ADAR1 Reveals Distinct Conserved Surfaces Among Z-Domains. *J. Mol. Biol.* **351** (33), 496-507 (2005).
- R Crowther, M Georgiadis. The Crystal Structure of 5-Keto-4-Deoxyuronate Isomerase from *Escherichia Coli*. *Proteins: Struct. Func. Genet.* **61**, 680 (2005).
- C Goulding, M Apostol, M Sawaya, M Phillips, A Parseghian, D Eisenberg. Regulation by Oligomerization a Mycobacterial Folate Biosynthetic Enzyme. *J. Mol. Biol.* **349**, 61-72 (2005).
- M Huang, A Mazar, G Parry, A Higazi, A Kuo, D Cines. Crystallization of Soluble Urokinase Receptor (suPAR) in Complex with Urokinase Amino-Terminal Fragment (1-143). *Acta Cryst. D.* **61**, 697-700 (2005).
- J Johnston, V Arcus, E Baker. Structure of Naphthoate Synthase (MenB) From *Mycobacterium Tuberculosis* in Both Native and Product-Bound Forms. *Acta Cryst. D.* **61** (9), 1199-1206 (2005).
- A Kim, T Dobransky, R Rylett, B Shilton. Surface-Entropy Reduction used in the Crystallization of Human Choline Acetyltransferase. *Acta Cryst. D.* **61** (9), 1306-1310 (2005).
- T Kuzuyama, J Noel, S Richard. Structural Basis for the Promiscuous Biosynthetic Prenylation of Aromatic Natural Products. *Nature.* **435** (7044), 983-7 (2005).
- P Lario, R Pfuetzner, E Frey, L Creagh, C Haynes, A Maurelli, N Strynadka. Structure and Biochemical Analysis of a Secretin Pilot Protein. *EMBO J.* **24**, 1111-1121 (2005).
- R Liu, P Loll, R Eckenhoff. Structural Basis for High Affinity Volatile Anesthetic Binding in a Natural 4-helix Bundle Protein. *Faseb J.* **19**, 567-576 (2005).
- J Meng, D Vardar, Y Wang, H Guo, J Head, C McKnight. High-Resolution Crystal Structures of Villin Headpiece nad Mutants with Reduced F-Actin Binding Activity. *Biochemistry.* **44**, 11963-11973 (2005).
- A Mezzetti, J Schrag, C Cheong, R Kazlauskas. Mirror-Image Packing in Enantiomer Discrimination Molecular Basis for the Enantioselectivity of B. Cepaci Lipase Toward 2-Methyl-3-Phenyl-1-Propanol. *Chem. Bio.* **12**, 427 (2005).
- I Mirza, I Nazi, M Korczynska, G Wright, A Berghuis. Crystal Structure of Homoserine Transacetylase from *Haemophilus Influenzae* Reveals a New Family of alpha/beta-Hydrolases. *Biochemistry.* **44**, 15768-15773 (2005).
- J Pedelacq, G Waldo, S Cabantous, E Liong, T Terwilliger. Structural and Functional Features of a nNDP Kinase from the Hyperthermophile Crenarchaeon *Pyrobaculum Aerophilum*. *Protein Sci.* **14**, 2562 (2005).
- E Rangarajan, Y Li, P Iannuzzi, M Cygler, A Matte. Crystal Structure of *Escherichia coli* Crotonobetianyl-CoA: Carnitine CoA-Transferase (CaiB) and Its Complexes with CoA and Carnitiny-CoA. *Biochemistry.* **44**, 5728-5738 (2005).
- S Raymond, A Tocilj, E Ajamian, Y Li, M Hung, A Matte, M Cygler. Crystal Structure of Ureidoglycolate Hydrolase (AIIA) from *Escherichia coli* O157:H7. *Proteins: Struct. Func. Genet.* **61** (2), 454-459 (2005).
- J Schuermann, S Prewitt, C Davies, S Deutscher, J Tanner. Evidence for Structural Plasticity of Heavy Chain Complementarity-determining Region 3 in Antibody-ssDNA Recognition. *J. Mol. Biol.* **347**, 965 - 978 (2005).
- J Sivaraman, R Myers, L Boju, T Sulea, M Cygler, V Davisson, J Schrag. Crystal Structure of *Methanobacterium thermoautotrophicum* Phosphoribosyl-AmP. *Biochemistry.* **44**, 10071-10080 (2005).
- D Snyder, Y Chen, N Denissova, T Acton, J Aramini, M Ciano, R Karlin, J Liu, P Manor, et al.. Comparisons of NMR Spectral Quality and Success in Crystallization Demonstrate that NMR and X-ray Crystallography are Complementary Methods for Small Protein Structure Determination. *J. Am. Chem. Soc.* **127**, 16505-16511 (2005).
- M St-Jean, J Lafrance-Vanasse, B Liotard, J Sygusch. High Resolution Reaction Intermediates of rabbit Muscle Fructose-1,6-bisphosphate Aldolase: Substrate Cleavage and Induced Fit. *J. Biol. Chem.* **280** (29), 27262-70 (2005).
- P Telmer, B Shilton. Structural Studies of an Engineered Zinc Biosensor Reveal an Unanticipated Mode of Zinc Binding. *J. Mol. Biol.* **354** (4), 829-840 (2005).
- A Tocilj, J Schrag, Y Li, B Schneider, L Reitzer, A Matte, M Cygler. Crystal Structure of N-succinylarginine Dihydrolase AstB, Bound to Substrate and Product, an Enzyme from the Arginine Catabolic Pathway of *Escherichia Coli*. *J. Biol. Chem.* **280** (16), 15800-15808 (2005).
- Z Yang, J Horton, R Maunus, G Wilson, R Roberts, X Cheng. Structure of HinP1I Endonuclease Reveals a Striking Similarity to the Monomeric Restriction Enzyme MspI. *Nucleic Acids Res.* **33** (6), 1892-1901 (2005).

Beamline X9A

- T Ball, W Edstrom, L Mauch, J Schmitt, B Leistler, H Fiebig, W Sperr, A Hauswirth, P Valent, et al.. Gain of Structure and IgE Epitopes by Eukaryotic Expression of the Major Timothy Grass Pollen Allergen, Phl p. 1. *FEBS Lett.* **272**, 217 (2005).
- W Barton, D Tzvekova, D Nikolov. Structure of the Angiopoietin-2 Receptor Binding Domain and Identification of Surfaces Involved in Tie2 Recognition. *Structure.* **13** (5), 825-832 (2005).
- I Berke. Nuts and Bolts of the NPC: The Structure of Nup133. Ph.D. Thesis. Rockefeller University, New York. (2005).
- M Chlenov, Y Masuda, K Murakami, V Nikiforov, S Darst, A Mustaev. Structure and Function of Lineage-Specific Sequence Insertions in the Bacterial RNA Polymerase beta' Subunit. *J. Mol. Biol.* **353**, 138-154 (2005).
- B Hao, N Zheng, B Schulman, G Wu, J Miller, M Pagano, N Pavletich. Structural Basis of the Cks1-Dependent Recognition of P27Kip1 by the SCF skp2 Ubiquitin Ligase. *Mol. Cell.* **20** (1), 9-19 (2005).
- S Hegde, M Vetting, S Roderick, L Mitchenall, A Maxell, H Takiff, J Blanchard. A Fluoroquinolone Resistance Protein from *Mycobacterium tuberculosis* That Mimics DNA. *Science.* **308**, 1480 (2005).
- R Janjusevic, R Abramovitch, G Martin, C Stebbins. A Bacterial Inhibitor of Host Programmed Cell Death Defenses is an E3 Ubiquitin Ligase. *Science.* **311**, 222-226 (2005).
- D Jian, y Kim, K Maxwell, S Beasley, R Zhang, g Gussin, A Edwards, S Darst. Crystal Structure of Bacteriophage lamda cII and its DNA Complex. *Mol. Cell.* **19**, 259-269 (2005).
- S Li, K Schmitz, P Jeffrey, J Wiltzius, P Kussie, K Ferguson. Structural Basis for Inhibition of the Epidermal Growth Factor Receptor by Cetuximab. *Cancer Cell.* **7** (4), 301-311 (2005).
- B Manjasetty, F Niesen, C Scheich, Y Roske, F Goetz, J Behlke, V Sievert, U Heinemann, K Buessow. X-ray Structure of Engineered Human Aortic Preferentially Expressed Protein-1 (APEG-1). *BMC Struct. Bio.* **5**, 21 (2005).
- N Marinkovic, S Gupta, C Zhan, M Chance. Synchrotron Radiation in Biosciences. *Nucl. Instrum. Meth. B.* **241** (1-4), 242-246 (2005).
- D Nikolov, C Li, W Barton, J Himanen. Crystal Structure of the Ephrin-B1 Ectodomain: Implications for Receptor Recognition and Signaling. *Biochemistry.* **44**, 10947-10953 (2005).
- L Patskovska, Y Patskovsky, S Almo, R Hirsch. COHbC and COHbS Crystallize in the R2 Quaternary State at Neutral pH in the Presence of PEG 4000. *Acta Cryst. D.* **61**, 566 (2005).

- U Ramagopal, Z Dauter, R Thirumuruhan, E Fedorov, S Almo. Radiation-Induced Site-Specific Damage of Mercury Derivatives: Phasing and Implications. *Acta Cryst. D.* **61** (9), 1289-1298 (2005).
- E Sickmier, D Brekasis, S Paranawithana, J Bonanno, M Paget, S Burley, C Kielkopf. X-ray Structure of a Rex-Family Repressor/NADH Complex Insights into the Mechanism of Redox Sensing. *Structure.* **13**, 43-54 (2005).
- J Sun, W Wang, H Yang, S Liu, F Liang, A Fedorov, S Almo, Z Zhang. Structure and Biochemical Properties of PRL-1, a Phosphatase Implicated in Cell Growth, Differentiation, and Tumor Invasion. *Biochemistry.* **44**, 12009-12021 (2005).
- T Tellinghuisen, J Marcotrigiano, C Rice. Structure of the Zinc-Binding Domain of an Essential Component of the Hepatitis C Virus Replicase. *Nature.* **435**, 374 (2005).
- N Thoma, B Czyzewski, A Alexeev, A Mazin, N Pavletich. Structure of the SW12/SNF2 Chromatin-Remodeling Domain of Eukaryotic Rad54. *Nat. Struct. Mol. Biol.* **12**, 350-356 (2005).
- H Yang, Q Li, J Fan, W Hollomon, N Pavletich. The BRCA2 Homologue Brh2 Nucleates RAD51 Filament Formation at a dsDNA-ssDNA Junction. *Nature.* **433**, 653-657 (2005).
- Beamline X9B**
- R Breece, A Costello, B Bennett, T Sigdel, M Matthews, D Tierney, M Crowder. A Five-Coordinate Metal Center in Co(II)-Substituted VanX. *J. Biol. Chem.* **280**, 11074-11081 (2005).
- M Chlenov, Y Masuda, K Murakami, V Nikiforov, S Darst, A Mustae. Structure and Function of Lineage-Specific Sequence Insertions in the Bacterial RNA Polymerase beta' Subunit. *J. Mol. Biol.* **353**, 138-154 (2005).
- A Fokine, p Leiman, M Shneider, B Ahvazi, K Boeshans, A Steven, L Black, V Mesyanzhinov, M Rossman. Structural and Functional Similarities Between the Capsid Proteins of Bacteriophages T4 and HK97 Point to a Common Ancestry. *Proc Natl Acad Sci USA.* **102**, 7163-7168 (2005).
- A Guarne, T Brendler, Q Zhao, R Ghirlando, S Austin, W Yang. Crystal Structure of a SeqA-N Filament: Implications for DNA Replication and Chromosome Organization. *EMBO J.* **24**, 1502-1511 (2005).
- K Gunter, M Aschner, L Miller, R Eliseev, J Salter, K Anderson, S Hammond, T Gunter. Determining the Oxidation States of Manganese in PC12 and Nerve Growth Factor-Induced PC12 Cells. *N/A.* **39** (2), 164-181 (2005).
- A Gustchina, M Li, S Wunschmann, M Chapman, A Pomes, A Wlodawer. Crystal Structure of Cockroach Allergen Bla g2, an Unusual Zinc Binding Aspartic Protease with a Novel Mode of Self-Inhibition. *J. Mol. Biol.* **348** (2), 433-444 (2005).
- A Hansen, Y Gu, M Li, M Andrykovitch, D Waugh, D Jin, X Ji. Structural Basis for the Function of Stringent Starvation Protein A as a Transcription Factor. *J. Biol. Chem.* **280**, 17380-17391 (2005).
- M Jensen, M Costas, R Ho, J Kaizer, A Payeras, E Umnck, L Que, Jr., J Rohde, A Stubna. High-Valent Nonheme Iron. Two Distinct Iron(IV) Species Derived from a Common Iron(II) Precursor. *J. Am. Chem. Soc.* **127**, 10512-10525 (2005).
- J Kim, S Sitaraman, A Hierro, B Beach, G Odorizzi, J Hurley. Structural Basis For Endosomal Targeting by The Bro1 Domain. *N/A.* **8**, 937-947 (2005).
- D Lansky, B Mandimutsira, B Ramdhanie, M Clausen, J Penner-Hahn, S Zvyagin, J Telser, J Krzystek, R Zhan, Z Ou. Synthesis, Characterization, and Physicochemical Properties of Manganese(III) and Manganese(V)-Oxo Corrolazines. *Inorg. Chem.* **44**, 4485-4498 (2005).
- Y Li, J Blaszczyk, Y Wu, G Shi, X Ji, H Yan. Is the Critical Role of Loop 3 of Escherichia coli 6-Hydroxymethyl-7,8-dihydropterin Pyrophosphokinase in Catalysis Due to Loop-3 Residues Arginine-84 and Tryptophan-89? Site-Directed Muagenesis, Biochemical, and Crystallographic Studies. *Biochemistry.* **44**, 8590-8599 (2005).
- A Longo, C Leonard, G Bassi, D Berndt, J Krahn, T Tanaka Hall, K Weeks. Evolution from DNA to RNA Recognition by the b13 LAGLIDADG Maturase. *Nat. Struct. Mol. Biol.* **12** (9), 779 (2005).
- M Mayer. Crystal Structures of the GluR5 and GluR6 Ligand Binding Cores: Molecular Mechanisms Underlying Kainate Receptor Selectivity. *Neuron.* **45**, 539-552 (2005).
- O Pasternak, J Biesiadka, F Dolot, L Hanschuh, G Bujacz, M Sikorski, M Jaskolski. Structure of a Yellow Lupin Pathogenesis-Related PR-10 Protein Belonging to a Novel Subclass. *Acta Cryst. D.* **61**, 99-107 (2005).
- J Penner-Hahn. Characterization of "Spectroscopically Quiet" Metals in Biology. *Coord. Chem. Rev.* **249**, 161-177 (2005).
- B Ramakrishnan, E Boeggeman, P Qasba. Mutation of Arginine 228 to Lysine Enhances the Glucosyltransferase Activity of Bovine beta-1,4-Galactosyltransferase I. *Biochemistry.* **44**, 3202-3210 (2005).
- K Saikrishnan, G Manjunath, P Singh, J Jeyakanthan, Z Dauter, K Sekar, K Muniyappa, M Vijayan. Structure of Mycobacterium smegmatis Single-Stranded DNA-Binding Protein and a Comparative Study Involving Homologous SSBs: Biological Implications of Structural Plasticity and Variability in Quaternary Association. *Acta Cryst. D.* **61** (8), 1140-1148 (2005).
- F Schubot, S Cherry, B Austin, J Tropea, D Waugh. Crystal Structure of the Protease-Resistant Core Domain of Yersinia Pestis Virulence Factor Yopr. *Protein Sci.* **14**, 1679 (2005).
- K Sekar, V Rajakannan, D Gayathri, D Velmurugan, M Poi, M Dauter, Z Dauter, M Tsai. Atomic Resolution (0.97 Angstrom) Structure of the Triple Mutant (K53,56,121M) of Bovine Pancreatic Phospholipase A2. *Acta Cryst. F.* **61**, 3-7 (2005).
- W Shi, C Zhan, A Lgnatov, B Manjasetty, N Marinkovic, M Sullivan, R Huang, M Chance, H Li, et al.. Metalloproteomics: High-Throughput Structural and Functional Annotation of Proteins in Structural Genomics. *Structure.* **13** (10), 1473-1486 (2005).
- B Strokopytov, A Fedorov, N Mahoney, M Kessels, D Drubin, S Slmo. Phased Translation Function Revisited: Structure Solution of the Cofilin-Homology Domain from Yeast Actin-Binding Protein 1 Using six-Dimensional Searches. *Acta Cryst. D.* **61**, 285-293 (2005).
- P Thomas, E Stone, A Costello, D Tierney, W Fast. The Quorum-Quenching Lactonase from Bacillus thuringiensis is a Metalloprotein. *Biochemistry.* **44**, 7559-7569 (2005).
- W Wen, B Kumarasamy, S Mukerjee, M Auinat, Y Ein-Eli. Origin of 5 V Electrochemical Activity Observed in Non-Redox Reactive Divalent Cation Doped LiM0.5-xMn1.5+xO4 (0<XJ. *Electrochem. Soc.* **152** (9), A1902 (2005).
- Beamline X10A**
- H Cui, V Krikorian, J Thompson, A Nowak, T Deming, D Pochan. Preparation and Characterization of Synthetic Polypeptide Single Crystals with Controlled Thickness. *Macromolecules.* **38**, 7371-7377 (2005).
- S Guthrie, G Mazzanti, S Idziak. X-ray phase Identification of Chocolate is Possible. *Eur. J Lipid Sci. Tech.* **107**, 656-659 (2005).
- M Lamm, K Rajagopal, J Schneider, D Pochan. Laminated Morphology of Nontwisting beta-Sheet Fibrils Constructed via Peptide Self-Assembly. *J. Am. Chem. Soc.* **127**, 16692-16700 (2005).

- M May, I Lim, J Luo, Z Rab, D Rabinovich, T Liu, C Zhong. Mediator-Template Assembly of Nanoparticles. *J. Am. Chem. Soc.* **127**, 1519-1529 (2005).
- G Mazzanti, A Marangoni, S Idziak. Modeling Phase Transitions During the Crystallization of a Multicomponent Fat Under Shear. *Phys. Rev. E*. **71**, 041607 (2005).

Beamline X10B

- S Guthrie, G Mazzanti, S Idziak. X-ray phase Identification of Chocolate is Possible. *Eur. J Lipid Sci. Tech.* **107**, 656-659 (2005).
- S Harton, T Koga, F Stevie, T Araki, H Ade. Investigation of Blend Miscibility of a Ternary PS/PCHMA/PMMA System Using SIMS and Mean-Field Theory. *Macromolecules*. **38**, 10511-10515 (2005).
- S Harton, F Stevie, R Spontak, T Koga, M Rafailovich, J Sokolov, H Ade. Low-Temperature Reactive Coupling at Polymer-Polymer Interfaces Facilitated by Supercritical Carbon Dioxide. *Polymer*. **46**, 10173-10179 (2005).
- T Koga, J Jerome, M Rafailovich, J Sokolov, C Gordon. Metalizable Polymer Thin Films in Supercritical Carbon Dioxide. *J. Adhes.* **81**, 751-764 (2005).
- T Koga, C Li, Y Sun, M Rafailovich, J Sokolov, J Douglas, D Mahajan. Surface Modification of Polymeric Nanocomposite Thin Films using Supercritical Carbon Dioxide. *Top. Catal.* **32**, 257-262 (2005).
- Y Seo, T Koga, J Sokolov, M Rafailovich, M Tolan, S Sinha. Deviations from Liquidlike Behavior in molten Polymer Films at Interfaces. *Phys. Rev. Lett.* **94**, 157802 (2005).

Beamline X10C

- J Calla, R Davis. X-ray Absorption Spectroscopy and CO Oxidation Activity of Au/Alumina Treated with NaCN. *Catal. Lett.* **99** (1-2), 21-26 (2005).
- J Calla, R Davis. Investigation of Alumina-Supported Au Catalyst for CO Oxidation by Isotopic Transient Analysis and X-ray Absorption Spectroscopy. *J. Phys. Chem. B*. **109** (6), 2307-2314 (2005).
- J Calla, R Davis. Influence of Dihydrogen and Water Vapor on the Kinetics of CO Oxidation over Au/Alumina. *Ind. Eng. Chem. Res.* **44**, 5403 (2005).
- P Haider, Y Chen, S Lim, G Haller, L Pfefferle, D Ciuparu. Application of the Generalized 2D Correlation Analysis to Dynamic Near-Edge X-ray Absorption Spectroscopy Data. *J. Am. Chem. Soc.* **127**, 1906-1912 (2005).
- H Isaacs, K Sasaki, C Jeffcoate, V Laget, R Buchheit. Formation of Chromate Conversion Coatings on Aluminum and Its Alloys. *J. Electrochem. Soc.* **152**, B460 (2005).
- V Murthi. Electrochemistry at Interfaces with Low Water Content: Applications to Proton Exchange Membrane Fuel Cells and Growth of Anodic Oxide Films. Ph.D Thesis. Northeastern University, Boston. (2005).
- Y Yang, S Lim, G Du, Y Chen, D Ciuparu, G Haller. Synthesis and Characterization of Highly Ordered Ni-MCM-41 Mesoporous Molecular Sieves. *J. Phys. Chem. B*. **109**, 13237-13246 (2005).

Beamline X11A

- O Alexeev, F Li, M Amiridis, B Gates. Effects of Adsorbates on Supported Platinum and Iridium Clusters: Characterization in Reactive Atmospheres and During Alkene Hydrogenation Catalysis by X-ray Absorption Spectroscopy. *J. Phys. Chem. B*. **109** (6), 2338-2349 (2005).

- Y Arai, D Sparks, J Davis. Arsenate Adsorption Mechanisms at the Allophane-Water Interface. *Environ. Sci. Tech.* **39**, 2537-2544 (2005).
- T Boonfueng, L Axe, Y Xu. Properties and Structure of Manganese Oxide-Coated Clay. *J. Colloid Interface Sci.* **281** (1-2), 80-92 (2005).
- S Calvin, S Luo, C Caragianis-Broadbridge, J McGuinness, E Anderson, A Lehman, K Wee, S Morrison, L Kurihara. Comparison of Extended X-ray Absorption Fine Structure and Scherrer Analysis of X-ray Diffraction as Methods for Determining Mean Sizes of Polydisperse Nanoparticles. *Appl. Phys. Lett.* **87** (23), 233102 (2005).
- S Calvin, C Riedel, E Carpenter, S Morrison, R Stroud, V Harris. Estimating Crystallite Size in Polydispersed Samples using EXAFS. *Phys. Scr.* **T115**, 744-748 (2005).
- I Drake, K Furdala, A Bell, T Tilley. Dimethyl Carbonate Production Via the Oxidative Carbonylation of Methanol Over Cu/SiO₂ Catalysts Prepared Via Molecular Precursor Grafting and Chemical Vapor Deposition Approaches. *J. Catal.* **230** (1), 14-27 (2005).
- M Grafe, D Sparks. Kinetics of Zinc and Arsenate Co-sorption at the Goethite-water Interface. *Geochim. Cosmochim. Acta*. **69** (19), 4573-4595 (2005).
- A Holland, G Li, A Shahin, G Long, A Bell, T Tilley. New Fe/SiO₂ Materials Prepared using Diiron Molecular Precursors: Synthesis, Characterization and Catalysis. *J. Catal.* **235** (1), 150-163 (2005).
- A Keimowitz, Y Zheng, S Chillrud, B Mailloux, H Bok Jung, M Stute, H Simpson. Arsenic Redistribution Between Sediments and Water Near a Highly Contaminated Source. *Environ. Sci. Tech.* **39**, 8606-8613 (2005).
- Y Lee, E Elzinga, R Reeder. Cu(II) Adsorption at the Calcite-Water Interface in the Presence of Natural Organic Matter: Kinetic Studies and Molecular-Scale Characterization. *Geochim. Cosmochim. Acta*. **69**, 49-61 (2005).
- Y Lee, E Elzinga, R Reeder. Sorption Mechanisms of Zinc on Hydroxyapatite: Systematic Uptake Studies and EXAFS Spectroscopy Analysis. *Environ. Sci. Tech.* **39**, 4042-4048 (2005).
- S Maeng, L Axe, T Tyson, A Jiang. An Investigation on Structure of Thermal and Anodic Tantalum Oxide Films. *J. Electrochem. Soc.* **152** (2), B60-B64 (2005).
- A Mansour, L Croguennec, C Delmas. A Unique Structure of Ni(III) in LiNi_{0.30}Co_{0.30}O₂ Without Jahn-Teller Distortion. *Electrochem. Solid-State Lett.* **8** (10), A544-A548 (2005).
- A Mansour, P Smith, M Balasubramanian, J McBreen. In Situ X-Ray Absorption Study of Cycled Ambigel V₂₀/5.nH₂O (n ~ 0.5) Composite Cathodes. *N/A*. **152** (7), A1312-A1319 (2005).
- S Morrison, C Cahill, E Carpenter, S Calvin, V Harris. Atomic Engineering of Mixed Ferrite and Core-Shell Nanoparticles. *J. Nanosci. Nanotechnol.* **5** (9), 1323-1344 (2005).
- V Murthi. Electrochemistry at Interfaces with Low Water Content: Applications to Proton Exchange Membrane Fuel Cells and Growth of Anodic Oxide Films. Ph.D Thesis. Northeastern University, Boston. (2005).
- M Nachtegaal, M Marcus, J Sonke, J Vangronsveld, K Livi, D van Der Lelie, D Sparks. Effects of in situ Remediation on the Speciation and Bioavailability of Zinc in a Smelter Contaminated Soil. *Geochim. Cosmochim. Acta*. **69** (19), 4649-4664 (2005).
- J Roques, A Anderson, V Murthi, S Mukerjee. Potential Shift for OH(ads) Formation on the Pt Skin on Pt₃Co(111) Electrodes in Acid. *J. Electrochem. Soc.* **152**, E193 (2005).
- M Teliska, V Murthi, S Mukerjee, D Ramaker. Correlation of Water Activation, Surface Properties, and Oxygen Reduction Reactivity of Supported Pt-M/C Bimetallic Electrocatalysts Using XAS. *J. Electrochem. Soc.* **152**, A2159 (2005).

- M Teliska, W O'Grady, D Ramaker. Determination of O and OH Adsorption Sites in situ from Pt L23 X-ray Absorption Spectroscopy. *J. Phys. Chem. B.* **109** (16), 8076-8084 (2005).
- M Teliska, V Murthi, S Mukerjee, D Ramaker. In Situ Determination of O(H) Adsorption Sites on Pt Based Alloy Electrodes using X-ray Absorption Spectroscopy. *Fundamental Understanding of Electrode Processes in Memory of Professor Ernest B. Yeager*, Vol , p. 212-215, sponsored by The Electrochemical Society. (2005).
- A Voegelin, R Kretzschmar. Formation and Dissolution of Single and Mixed Zn and Ni Precipitates in Soil: Evidence From Column Experiments and Extended X-ray Absorption Fine Structure Spectroscopy. *Environ. Sci. Tech.* **39**, 5311-5318 (2005).
- A Voegelin, S Pfister, A Scheinost, M Marcus, R Kretzschmar. Changes in Zinc Speciation in Field Soil After Contamination with Zinc Oxide. *Environ. Sci. Tech.* **39**, 6616-6623 (2005).
- X Wang, J Spivey, H Lamb. NO Decomposition Over a Pd/MgO Catalyst Prepared from [Pd(acac)₂]. *Appl. Catal. B.* **56** (4), 261-268 (2005).
- Beamline X11B**
- D Ciuparu, P Haider, M Fernandez-Garcia, Y Chen, S Lim, G Haller, L Pfefferle. X-ray Absorption Spectroscopic Investigation of Partially Reduced Cobalt Species in Co-MCM-41 Catalysts During Synthesis of Single-Wall Carbon Nanotubes. *J. Phys. Chem. B.* **109**, 16332-16339 (2005).
- M Teliska, W O'Grady, D Ramaker. Determination of O and OH Adsorption Sites in situ from Pt L23 X-ray Absorption Spectroscopy. *J. Phys. Chem. B.* **109** (16), 8076-8084 (2005).
- Beamline X12A**
- G Carini, A Bolotnikov, G Camarda, G Wright, G De Geronimo, D Siddons, R James. Synchrotron Radiation Response Characterization of Coplanar Grid CZT Detectors. *Nuclear Science Symposium - Room Temperature Semiconductor Detector*, p. R2-5, sponsored by IEEE. (2005).
- G Carini, G Camarda, Z Zhong, D Siddons, A Bolotnikov, G Wright, B Barber, C Arnone, R James. High-Energy X-ray Diffraction and Topography Investigation of CdZnTe. *J. Electron. Mater.* **34** (6), 804-810 (2005).
- G Carini, G Camarda, Z Zhong, D Siddons, A Bolotnikov, G Wright, B Barber, C Arnone. High-Energy X-ray Diffraction and Topography Investigation of CdZnTe. *2004 U.S. Workshop on the Physics and Chemistry of II-VI Materials*, Vol , p. 804-810, sponsored by TMS, Air Force Res. Lab., Off. of Naval Res., U.S. Navy E-O Center Penn State Uni., U.S. Army SDMC. U.S. Army Res. Lab. U.S. Army RDECOM CERDEC Night Vision & Electronic Sensors Directorate. (2005).
- G Carini, A Bolotnikov, G Camarda, G De Geronimo, D Siddons, G Wright, R James. New Results from Testing of Coplanar-grid CdZnTe Detectors. *Hard X-ray and Gamma-Ray Detector Physics VII*, Vol , p. 59220M-1/6, sponsored by SPIE. (2005).
- Beamline X12B**
- R Agarwal, T Binz, S Swaminathan. Analysis of Active Site Residues of Botulinum Neurotoxin E by Mutational, Functional, and Structural Studies: Glu335Gln is an Apoenzyme. *Biochemistry.* **44**, 8291-8302 (2005).
- M Becker, J Bunikis, B Lade, J Dunn, A Barbour, C Lawson. Structural Investigation of *Borrelia burgdorferi* OspB, a Bactericidal Fab Target. *J. Biol. Chem.* **280** (17), 17363-17370 (2005).
- D Colleluori, R Reczkowski, F Emig, E Cama, J Cox, L Scolnick, K Compher, K Jude, S Han, et al. Probing the Role of the Hyper-Reactive Histidine Residue of Arginase. *Arch. Biochem. Biophys.* **444** (1), 15-26 (2005).
- L Di Costanzo, G Sabio, A Mora, P Rodriguez, A Ochoa, F Centeno, D Christianson. Crystal Structure of Human Arginase I at 1.29-Angstrom Resolution and Exploration of Inhibition in the Immune Response. *Proc Natl Acad Sci USA.* **102** (37), 13058-13063 (2005).
- G Georgiev, P Cebe, M Capel. Effects of Nematic Polymer Liquid Crystal on Crystallization and Structure of Pet/Vectra Blends. *J. Mater. Sci.* **40** (5), 1141-1152 (2005).
- B Grasberger, T Lu, C Schubert, D Parks, T Carver, H Koblish, M Cummings, L LaFrance, K Milkiewicz. Discovery and Cocrystal Structure of Benzodiazepinedione HDM2 Antagonists that Activate. *J. Med. Chem.* **48**, 909 (2005).
- G Hsu, X Huang, N Luneva, N Geacintov, L Beese. Structure of a High Fidelity DNA Polymerase Bound to a Benzo[A]Pyrene Adduct that Blocks Replication. *J. Biol. Chem.* **280**, 3764 (2005).
- D Huang, A Paydar, M Zhuang, M Waddell, J Holton, B Schulman. Structural Basis for Recruitment of Ubc12 by an E2 Binding Domain in NEDD8's E1. *Mol. Cell.* **17** (3), 341-350 (2005).
- W Li, S Kamtekar, Y Xiong, G Sarkis, N Grindley, T Steitz. Structure of a Synaptic gamma delta Resolvase Tetramer Covalently Linked to Two Cleaved DNAs. *Science.* **309**, 1210 (2005).
- F Perrino, S Harvey, S McMillin, T Hollis. The Human TREX2 3'-5' Exonuclease Structure Suggests a Mechanism for Efficient Nonprocessive DNA Catalysis. *J. Biol. Chem.* **280** (15), 15212-15218 (2005).
- D Shi, X Yu, L Roth, M Hiroki, Y Hathout, N Allewell, M Tuchman. Expression, Purification, Crystallization and Preliminary X-ray Crystallographic Studies of a Novel Acetylcitrulline deacetylase from *Xanthomonas Campestris*. *Acta Cryst. F.* **61**, 676-679 (2005).
- C Simmons, Q Hao, M Stipanuk. Preparation, Crystallization and X-ray Diffraction Analysis to 1.5 Å Resolution of Rat Cysteine Dioxygenase, a Mononuclear Iron Enzyme Responsible for Cysteine Thiol Oxidation. *Acta Cryst. F.* **F61**, 1013-1016 (2005).
- A Soares, Y Vehter. Experimental methods for measuring accurate high-amplitude phases and their importance in isomorphous replacement experiments. *Acta Cryst. D.* **D61**, 1521-1527 (2005).
- J Truglio, B Rhau, D Croteau, L Wang, M Skorvaga, E Karakas, M DellVecchia, H Wang, B Van Houten, C Kisker. Structural Insights Into the First Incision Reaction During Nucleotide Excision Repair. *EMBO J.* **24**, 885-894 (2005).
- A Varma, R Brown, G Birrane, J Ladias. Structural Basis for Cell Cycle Checkpoint Control by the BRCA1-CtIP Complex. *Biochemistry.* **44**, 10941-10946 (2005).
- L Vedula, D Cane, D Christianson. Role of Arginine-304 in the Diphosphate-Triggered Active Site Closure Mechanism of Trichodiene Synthase. *Biochemistry.* **44**, 12719 (2005).
- J Wang, K Stieglitz, E Kantrowitz. Metal Specificity is Correlated with Two Crucial Active Site Residues in *Escherichia coli* Alkaline Phosphatase. *Biochemistry.* **44**, 8378-8386 (2005).
- A Yamashita, S Singh, T Kawate, Y Jin, E Gouaux. Crystal Structure of a Bacterial Homologue of Na⁺/Cl⁻-Dependent Neurotransmitter Transporters. *Nature.* **437**, 215 (2005).
- Q Ye, I Imriskova-Sosova, B Hill, Z Jia. Identification of Disulfide Switch in BsSco, a Member of the Sco Family of Cytochrome c Oxidase Assembly Proteins. *Biochemistry.* **44**, 2934-2942 (2005).

Beamline X12C

- M Becker, J Bunikis, B Lade, J Dunn, A Barbour, C Lawson. Structural Investigation of *Borrelia burgdorferi* OspB, a Bactericidal Fab Target. *J. Biol. Chem.* **280** (17), 17363-17370 (2005).
- J Benach, W Edstrom, I Lee, K Das, B Copper, R Xiao, J Liu, B Rost, T Acton, et al.. The 2.35 Angstrom Structure of the TenA Homolog from *Pyrococcus furiosus* Supports an Enzymatic Function in Thiamine Metabolism. *Acta Cryst. D.* **61**, 589-598 (2005).
- J D'Aquino, J Tetenbaum-Novatt, A White, F Berkovitch, D Ringe. Mechanism of Metal Ion Activation of the Diphtheria Toxin Repressor DtxR. *Proc Natl Acad Sci USA.* **102** (51), 18408-18413 (2005).
- L Feng, S Zhou, L Gu, D Gell, J MacKay, M Weiss, A Gow, Y Shi. Structure of Oxidized Alpha-Haemoglobin Bound to AHSP Reveals a Protective Mechanism for HAEM. *Nature.* **435**, 697 (2005).
- Q Han, Y Gao, H Robinson, H Ding, S Wilson, J Li. Crystal Structures of *Aedes Aegypti* Kynurenine Aminotransferase. *FEBS Lett.* **272**, 2198 (2005).
- M Hu, P Li, L Song, P Jeffrey, T Chernova, K Wilkinson, R Cohen, Y Shi. Structure and Mechanisms of the Proteasome-associated Deubiquitinating Enzyme USP14. *EMBO J.* **24** (21), 3747 (2005).
- Q Huai, H Wang, Y Liu, H Kim, D Toft, H Ke. Structures of the N-Terminal and Middle Domains of *E. Coli* Hsp90 and Conformation Changes Upon ADP Binding. *Structure.* **13**, 579-590 (2005).
- M Huang, A Mazar, G Parry, A Higazi, A Kuo, D Cines. Crystallization of Soluble Urokinase Receptor (suPAR) in Complex with Urokinase Amino-Terminal Fragment (1-143). *Acta Cryst. D.* **61**, 697-700 (2005).
- L Jin, P Pandey, R Babine, J Gorga, K Seidl, E Gelfand, D weaver, S Abdel-Meguid, J Strickler. Crystal Structures of the FXIA Catalytic Domain in Complex with Ecotin Mutants Reveal Substrate-Like Interactions. *J. Biol. Chem.* **280**, 4704 (2005).
- L Jin, P Pandey, R Babine, D Weaver, S Abdel-Meguid, J Stricker. Mutation of Surface Residues to Promote Crystallization of Activated Factor XI as a Complex with Benzamidate: an Essential Step for the Iterative Structure-Based Design of Factor XI Inhibitors. *Acta Cryst. D.* **61**, 1418-1425 (2005).
- T Jonsson, M Murray, L Johnson, L Poole, W Lowther. Structural basis for the retroreduction of inactivated peroxiredoxins by human sulfiredoxin. *Biochemistry.* **44**, 8634-8642 (2005).
- C Kielkopf, S Luecke, M Green. U2AF-Homology-Motifs: Protein Recognition in the RRM World. *Genes Dev.* **18**, 1513-1526 (2005).
- D Kumaran, S Eswaramoorthy, F Studier, S Swaminathan. Structure and Mechanism of ADP-Ribose-1'-Monophosphatase (Appr-1' '-Pase), A Ubiquitous Cellular Processing Enzyme. *Protein Sci.* **14**, 719 (2005).
- A Moreno, M Rivera. Conceptions and First Results on the Electrocrystallization Behaviour of Ferritin. *Acta Cryst. D.* **61**, 1678-1681 (2005).
- H Nam, F Poy, H Saito, C Frederick. Structural Basis for the Function and Regulation of the Receptor Protein Tyrosine Phosphatase CD45. *J. Exp. Med.* **201**, 441 (2005).
- F Perrino, S Harvey, S McMillin, T Hollis. The Human TREX2 3'-5' Exonuclease Structure Suggests a Mechanism for Efficient Nonprocessive DNA Catalysis. *J. Biol. Chem.* **280** (15), 15212-15218 (2005).
- M Safo, Q Zhao, T Ko, F Musayev, H Robinson, N Scarsdale, A Wang, G Archer. Crystal Structures of the BLAI Repressor from *Staphylococcus aureus* and its Complex with DNA: Insights into Transcriptional Regulation of the BLA and MEC Operons. *J. Bacteriol.* **187**, 1833 (2005).
- J Schuermann, S Prewitt, C Davies, S Deutscher, J Tanner. Evidence for Structural Plasticity of Heavy Chain Complementarity-determining Region 3 in Antibody-ssDNA Recognition. *J. Mol. Biol.* **347**, 965 - 978 (2005).
- N Silvaggi, H Josephine, A Kuzin, R Nagarajan, R Pratt, J Kelly. Crystal Structures of Complexes Between the R61 DD-Peptidase and Peptidoglycan-Mimetic Beta-Lactams: A Non-Covalent Complex with a "Perfect Penicillin". *J. Mol. Biol.* **345**, 521-533 (2005).
- D Snyder, Y Chen, N Denissova, T Acton, J Aramini, M Ciano, R Karlin, J Liu, P Manor, et al.. Comparisons of NMR Spectral Quality and Success in Crystallization Demonstrate that NMR and X-ray Crystallography are Complementary Methods for Small Protein Structure Determination. *J. Am. Chem. Soc.* **127**, 16505-16511 (2005).
- A Stein, G Fuchs, C Fu, S Wolin, K Reinisch. Structural Insights into RNA Quality Control: The Ro Autoantigen Binds Misfolded RNAs Via its Central Cavity. *Cell.* **121** (4), 529-539 (2005).
- S Townson, J Samuelson, S Xu, A Aggarwal. Implications for Switching Restriction Enzyme Specificities from the Structure of BstYI Bound to a BglII DNA Sequence. *Structure.* **13** (5), 791-801 (2005).
- A Weichsel, E Maes, J Anderson, J Valenzuela, T Shokhireva, F Walker, W Montfort. Heme-Assisted S-Nitrosation of a Proximal Thiolate in a Nitric Oxide Transport Protein. *Proc Natl Acad Sci USA.* **102**, 594-599 (2005).
- C Wilson, T Kajander, L Regan. The Crystal Structure of NLPI. A Prokaryotic Tetratricopeptide Repeat Protein with a Globular Fold. *FEBS Lett.* **272**, 166 (2005).
- S Wright, V Rath, P Genereux, D Hageman, C Levy, L McClure, S McCoid, R McPherson, T Schelhorn, et al.. 5-Chloroindoloyl Glycine Amide Inhibitors of Glycogen Phosphorylase: Synthesis, In Vitro, In Vivo, and X-ray Crystallographic Characterization. *BioOrg. Med. Chem.* **15**, 459 (2005).
- Z Yang, J Horton, R Maunus, G Wilson, R Roberts, X Cheng. Structure of HinP1I Endonuclease Reveals a Striking Similarity to the Monomeric Restriction Enzyme MspI. *Nucleic Acids Res.* **33** (6), 1892-1901 (2005).
- Y Zuo, Y Wang, A Malhotra. Crystal Structure of *Escherichia coli* RNase D, an Exoribonuclease Involved in Structured RNA Processing. *Structure.* **13** (7), 973-984 (2005).

Beamline X14A

- E Akdgan, C Rawn, W Porter, E Payzant, A Safari. Size Effects in PbTiO3 nanocrystals: Effect of Particle Size on Spontaneous Polarization and Strains. *J. Appl. Phys.* **97**, 084305 (2005).
- K Kewalramani, G Evmenenko, C YU, K Kim, J Kmetko, P Dutta. Evidence of Surface Reconstruction During 'Bioinspired' Inorganic Nucleation at an Organic Template. *Surf. Sci. Lett.* **591**, L286-L291 (2005).
- J Li, S Moss, Y Zhang, A Mascarenhas, J Bai. X-ray Characterization of Atomic-Layer Superlattices. *J. Phys. D: Appl. Phys.* **38**, A147-A153 (2005).
- J Li, D Stokes, O Caha, S Ammu, J Bai, K Bassler, S Moss. Morphological Instability in InAs/GaSb Superlattices Due to Interfacial Bonds. *Phys. Rev. Lett.* **95**, 096104 (2005).
- E Ma. Alloys Created Between Immiscible Elements. *Prog. Mater. Sci.* **50**, 413-509 (2005).
- N Roberts, S Jaradat, L Hirst, Y Wang, S Wang, Z Liu, C Huang, J Bai, R Pinidak, H Gleeson. Biaxiality and Temperature Dependence of 3- and 4-layer Intermediate Smectic Phase

- Structures as Revealed by resonant X-ray Scattering. *Europhys. Lett.* **72** (6), 976-982 (2005).
- T Varga. Synthesis and Characterization of Some Low and Negative Thermal Expansion Materials. Ph.D. Thesis. Georgia Institute of Technology, Atlanta. (2005).
- P Williams, J Biernacki, C Rawn, L Walker, J Bai. Microanalytical and Computational Analysis of Class F Fly Ash. *ACI Mater. J.* **102**, 330-337 (2005).
- K Ye, D Patel. RNA Silencing Suppressor p21 of Beet Yellows Virus Forms an RNA binding Octameric Ring Structure. *Structure*. **13** (9), 1375-1384 (2005).
- Beamline X15A**
- D Connor, D Sayers, D Sumner, Z Zhong. Identification of Fatigue Damage in Cortical Bone by Diffraction Enhanced Imaging. *Nucl. Instrum. Meth. A.* **548** (1-2), 234-239 (2005).
- M Hasnah, C Parham, E Pisano, Z Zhong, O Oltulu, D Chapman. Mass Density Images from the Diffraction Enhanced Imaging Technique. *Phys. Med. Biol.* **32**, 549-552 (2005).
- X Lai, K Roberts, M Bedzyk, P Lyman, L Cardoso, J Sasaki. Structure of Habit-Modifying trivalent Transition Metal Cations (Mn³⁺, Cr³⁺) in Nearly Perfect Single Crystals of Potassium Dihydrogen Phosphate as Examined by X-ray Standing Waves, X-ray Absorption Spectroscopy, and Molecular Modeling. *Chem. Mater.* **17**, 4053-4061 (2005).
- J Li, J Williams, Z Zhong, K Kuettner, M Aurich, J Mollenhauer, C Muehleman. Reliability of Diffraction Enhanced Imaging for Assessment of Cartilage Lesions, Ex Vivo. *Osteoarthr. Cartilage*. **13**, 187-197 (2005).
- J Libera. In situ X-ray Structural Analysis of Polynucleotide Surface Adsorption and Metal-Phosphonate Self-Assembled Multilayers. Ph.D. Thesis. Northwestern University, Evanston. (2005).
- C Muehleman, J Li, K Kuettner, Z Zhong. Diffraction Enhanced X-ray Imaging of Musculoskeletal Lesions. *Osteoarthr. Cartilage*. **12**, s117-s117 (2005).
- M Teng. Use of Diffraction Enhanced Imaging to Determine the X-ray Refractive Indices of Various Tissues at Biologically-Relevant Energies. *The J. of Young Investigators*. **13**, 340 (2005).
- M Teng, Z Zhong. Use of Diffraction Enhanced Imaging to Determine the X-ray Refractive Indices of Various Tissues at Biologically-Relevant Energies. *The J. of Young Investigators*. **12**, online (2005).
- W Thomlinson, P Suortti, D Chapman. Recent Advances in Synchrotron Radiation Medical Research. *Nucl. Instrum. Meth. A.* **543** (1), 288-296 (2005).
- A Wagner, M Aurich, N Sieber, M Stoessel, W Wetzel, K Schmuck, M Lohmann, B Reime, J Metge, et al.. Options and Limitations of Joint cartilage Imaging: DEI in Comparison to MRI and Sonography. *Nucl. Instrum. Meth. A.* **548**, 47-53 (2005).
- M Wernick, L Chapman, O Oltulu, Z Zhong. Imaging Method Based on Attenuation, Refraction and Ultra-small-angle-scattering of X-rays. US Patent No. US 6,947,521 B2. (2005).
- M Wernick, J Brankov, D Chapman, Y Yang, E Pisano, C Parham, C Muehleman, Z Zhong, M Anastasio. Physical Model of Image formation in Multiple-Image Radiography. *SPIE: Developments in X-ray Tomography IV*, Vol 5535, p. 369-379, sponsored by SPIE. (2005).
- T Yuasa, H Sugiyama, Z Zhong, A Maksimenko, F Dilmanian, T Akatsuka, M Ando. High-Pass-Filtered Diffraction Microtomography by Coherent Hard X rays for Cell Imaging: Theoretical and Numerical Studies of the Imaging and Reconstruction Principles. *J. Opt. Soc. Am. A.* **22** (12), 2622-2634 (2005).
- Beamline X15B**
- F Alamgir, H Jain, D Williams, R Schwarz. Sub-Nanoscale Structural Origin of the Stability of the Pd-Ni-P Model Bulk Metallic Glass. *The Science of Complex Alloy Phases*, p. 163-182, TMS, Warrendale. (2005).
- Beamline X16A**
- S Ghose, I Robinson, P Bennett, F Himpfel. Structure of Double Row Quantum Wires in Au/Si(5 5 3). *Surf. Sci.* **581** (2-3), 199-206 (2005).
- S Ghose, P Bennett, I Robinson. Clustering of Au on the Faulted Half of the Si(111)- 7 x 7 Unit Cell. *Phys. Rev. B.* **71**, 073407 (2005).
- Beamline X16B**
- L Yang, M Fukuto. Modulated Phase of Phospholipids with a Two-Dimensional Square Lattice. *Phys. Rev. E.* **72**, 010901(R) (2005).
- Beamline X16C**
- A Frenkel, Y Feldman, V Lyahovitskaya, E Wachtel, I Lubomirsky. Microscopic Origin of Polarity in Quasiamorphous BaTiO₃. *Phys. Rev. B.* **71**, 1-1 (2005).
- A Frenkel, S Nemzer, I Pister, L Soussan, T Harris, Y Sun, M Rafailovich. Size-Controlled Synthesis and Characterization of Thiol-Stabilized Gold Nanoparticles. *J. Chem. Phys.* **123**, 1 (2005).
- M Pfeifer, O Robach, B Ocko, I Robinson. Thickness-Related Instability of Cu Thin Films on Ag(100). *Physica B.* **357**, 152-158 (2005).
- Beamline X17B1**
- K Bertagnolli, M Vail, J Qian, Y Zhao. High-Energy Synchrotron X-Ray Investigation of Residual Stress/Strain and Metal Distribution in Polycrystalline Diamond Compacts. *The First International Industrial Diamond Conference*, Vol , p. 5, sponsored by Element Six, UK, US Synthetic, USA. (2005).
- G Carini, G Camarda, Z Zhong, D Siddons, A Bolotnikov, G Wright, B Barber, C Arnone. High-Energy X-ray Diffraction and Topography Investigation of CdZnTe. *2004 U.S. Workshop on the Physics and Chemistry of II-VI Materials*, Vol , p. 804-810, sponsored by TMS, Air Force Res. Lab., Off. of Naval Res., U.S. Navy E-O Center Penn State Uni., U.S. Army SDMC. U.S. Army Res. Lab. U.S. Army RDECOM CERDEC Night Vision & Electronic Sensors Directorate. (2005).
- G Carini, G Camarda, Z Zhong, D Siddons, A Bolotnikov, G Wright, B Barber, C Arnone, R James. High-Energy X-ray Diffraction and Topography Investigation of CdZnTe. *J. Electron. Mater.* **34** (6), 804-810 (2005).
- M Croft, Z Zhong, N Jisrawi, I Zakharchenko, R Holtz, Y Gulak, J Skaritka, T Fast, K Sadananda, T Tsakalakos. Strain Profiling of Fatigue Crack Overload Effects Using Energy Dispersive X-Ray Diffraction. *Int. J. Fatigue*. **27**, 1408-1419 (2005).
- F Dilmanian, Y Qu, S Liu, C Cool, J Gilbert, J Hainfeld, C Kruse, J Laterra, D Lenihan, et al.. X-ray Microbeams: Tumor Therapy and Central Nervous System Research. *Nucl. Instrum. Meth. A.* **548** (1-2), 30-37 (2005).
- M Fernandez-Garcia, X Wang, C Berver, A Iglesias-Juez, J Hanson, J Rodriguez. Ca Doping of Nanosize Ce-Zr and Ce-Tb

- Solid Solutions: Structural and Electronic Effects. *Chem. Mater.* **17**, 4181-4193 (2005).
- M Hasnah, C Parham, E Pisano, Z Zhong, O Oltulu, D Chapman. Mass Density Images from the Diffraction Enhanced Imaging Technique. *Phys. Med. Biol.* **32**, 549-552 (2005).
- G Shirane, G Xu, P Gehring. Dynamics and Structure of PMN and PZN. *Ferroelectr.* **321**, 7-19 (2005).
- B Unks, R Bruni, H Eguchi, P Gorenstein, S Romaine. Long-term Stability and High Energy Reflectivity Measurements of Depth Graded Multilayer Coatings for X-ray Optics. American Astronomical Society, Washington. Prepared for American Astronomical Society Meeting 205. (2005).
- X Wang, J Rodriguez, J Hanson, D Gamarra, A Martinez-Arias, M Fernandez-Garcia. Unusual Physical and Chemical Properties of Cu in Ce_{1-x}Cu_xO₂ Oxides. *J. Phys. Chem. B.* **109**, 19595-19603 (2005).
- Beamline X17B2**
- B Li, J Zhang. Pressure and Temperature Dependence of Elastic Wave Velocity of MgSiO₃ Perovskite and the Composition of the Lower Mantle. *Phys. Earth Planet. Interiors.* **151** (1-2), 143-154 (2005).
- B Li, J Kung, T Uchida, Y Wang. Pressure Calibration to 20 GPa by use of Simultaneous Ultrasonic and X-ray Techniques. *J. Appl. Phys.* **98**, 13521 (2005).
- W Liu, J Kung, B Li. Elasticity of San Carlos olivine to 8 GPa and 1073 K. *Geophys. Res. Lett.* **32** (16), L16301 (2005).
- G Voronin, C Pantea, T Zerda, L Wang, Y Zhao. Thermal Equation-of-State of Osmium: A Synchrotron X-ray Diffraction Study. *J. Phys. Chem. Solids.* **66** (5), 705-710 (2005).
- J Zhang, Y Zhao, H Xu, M Zelinskas, L Wang, Y Wang, T Uchida. Pressure-Induced Amorphization and Phase Transformations in beta-LiAlSiO₄. *Chem. Mater.* **17**, 2817-2824 (2005).
- J Zhang, Y Zhao, C Pantea, J Qian, L Daemen, P Rigg, R Hixson, C Greeff, G Gray III, et al.. Experimental Constraints on the Phase Diagram of Elemental Zirconium. *J. Phys. Chem. Solids.* **66** (7), 1213-1219 (2005).
- Y Zhao, J Zhang, C Pantea, J Qian, L Daemen, P Rigg, R Hixson, G Gray, III, Y Yang, et al.. Thermal Equations of State of the alpha, beta, and omega Phases of Zirconium. *Phys. Rev. B.* **71**, 184119 (2005).
- Beamline X17B3**
- V Levitas, Y Ma, J Hashemi. Transformation-Induced Plasticity and Cascading Structural changes in Hexagonal Boron Nitride under High Pressure and Shear. *Appl. Phys. Lett.* **86**, 071912 (2005).
- Y Ma, M Somayazulu, G Shen, H Mao, J Shu, R Hemley. X-ray Diffraction Studies of Iron to Earth's Core Conditions. *New Developments in High-Pressure Minerals Physics and Applications to the Earth's Interior*, p. 455, Elsevier, Amsterdam. (2005).
- Beamline X17C**
- T Duffy. Synchrotron Facilities and the Study of Deep Planetary Interiors. *Rep. Prog. Phys.* **68**, 1811 (2005).
- Y Feng, M Somayazulu, R Jaramillo, T Rosenbaum, E Isaacs, J Hu, H Mao. Energy Dispersive X-ray Diffraction of Charge Density Waves Via Chemical Filtering. *Rev. Sci. Instrum.* **76** (6), 063913 (2005).
- R Hemley, H Mao, V Struzhkin. Synchrotron Radiation and High Pressure: New Light on Materials Under Extreme Conditions'. *J. Synch. Rad.* **12**, 135-154 (2005).
- B Kiefer, S Shieh, T Duffy, T Sekine. Strength, Elasticity, and Equation of State of Nanocrystalline Cubic Silicon Nitride (c-Si₃N₄) to 68 Gpa. *Phys. Rev. B.* **72**, 014102 (2005).
- V Levitas, Y Ma, J Hashemi. Transformation-Induced Plasticity and Cascading Structural changes in Hexagonal Boron Nitride under High Pressure and Shear. *Appl. Phys. Lett.* **86**, 071912 (2005).
- H Liu, J Tse, J Hu, Z Liu, L Wang, J Chen, D Weidner, Y Meng, D Hausermann, H Mao. Structural Refinement of the High-Pressure Phase of Aluminum Trihydroxide: In-Situ High-Pressure Angle Dispersive Synchrotron X-ray Diffraction and Theoretical Studies. *J. Phys. Chem. B.* **109**, 8857 (2005).
- H Liu, J Chen, J Hu, C Martin, D Weidner, D Hausermann, H Mao. Octahedral Tilting Evolution and Phase Transition in Orthorhombic NaMgF₃ Perovskite Under Pressure. *Geophys. Res. Lett.* **32** (4), L04304 (2005).
- Y Ma, M Somayazulu, G Shen, H Mao, J Shu, R Hemley. X-ray Diffraction Studies of Iron to Earth's Core Conditions. *New Developments in High-Pressure Minerals Physics and Applications to the Earth's Interior*, p. 455, Elsevier, Amsterdam. (2005).
- J Yang, W Bai, H Rong, Z Zhang, Z Xu, Q Fang, B Yan, T Li, Y Ren, S Chen. Na- and Zn- bearing (Mg,Fe)Al₂O₄ spinel exsolution from ilmenite and magnetite of eclogite in the main hole, CCSD. *2004 AGU meeting*, Vol , p. 85(4), sponsored by American Geologic Union. (2005).
- Beamline X18A**
- A Anderson, J Roques, S Mukerjee, V Murthi, N Markovic, V Stamenkovic. Activation Energies for Oxygen Reduction on Platinum Alloys: Theory and Experiment. *J. Phys. Chem. B.* **109**, 1198-1203 (2005).
- K Chung, W Yoon, H Lee, X Yang, J McBreen, B Deng, X Wang, M Yoshio, R Wang, et al.. Comparative Studies Between Oxygen Deficient LiMn₂O₄ and Al-doped LiMn₂O₄. *J. Power Sources.* **146**, 226 (2005).
- Y Ein-Eli, R Urian, W Wen, S Mukerjee. Low Temperature Performance of Copper/Nickel Modified LiMn₂O₄ Spinels. *Electrochim. Acta.* **50** (9), 1931-1937 (2005).
- C Jing, S Liu, X Meng. Arsenic Leachability and Speciation in Cement Immobilized Water Treatment Sludge. *Chemosphere.* **59** (9), 1241-1247 (2005).
- J Jones, E Slamovich, K Bowman. Product and Component Grain and Domain Textures in Ferroelectric Ceramics. *Mater. Sci. Forum.* **495-497** (2), 1401-1406 (2005).
- T Key, J Jones, W Shelley, B Iverson, H Li, E Slamovich, A King, K Bowman. Texture and Symmetry Relationships in Piezoelectric Materials. *Mater. Sci. Forum.* **495-497**, 13-22 (2005).
- T Key, J Jones, W Shelley, K Bowman. Quantifying Domain Textures in Lead Zirconate Titanate using 022 : 202 and 220 Diffraction Peaks. *Solid State Phenomena.* **105**, 379-384 (2005).
- Y Lee, E Elzinga, R Reeder. Cu(II) Adsorption at the Calcite- Water Interface in the Presence of Natural Organic Matter: Kinetic Studies and Molecular-Scale Characterization. *Geochim. Cosmochim. Acta.* **69**, 49-61 (2005).
- Z Zhu, T Andelman, M Yin, T Chen, S Ehrlich, S O'Brien, R Osgood, Jr.. Synchrotron X-ray Scattering of ZnO Nanorods: Periodic Ordering and Lattice Size. *J. Mater. Res.* **20** (4), 1033 (2005).
- Z Zhu, T Chen, Y Gu, J Warren, R Osgood, Jr.. Zinc Oxide Nanowires Grown by Vapor-Phase Transport using Selected Metal Catalysts: A Comparative Study. *Chem. Mater.* **17**, 4227-4234 (2005).

Beamline X18B

- A Abakumov, M Rozova, E Antipov, J Hadermann, G Van Tendeloo, M Lobanov, M Greenblatt, M Croft, E Tsiper, et al.. Synthesis, Cation Ordering, and Magnetic Properties of the $(\text{Sb}_{1-x}\text{Pb}_x)_2(\text{Mn}_{1-y}\text{Sb}_y)\text{O}_4$ Solid Solutions with the Sb_2MnO_4 -Type Structure. *Chem. Mater.* **17**, 1123-1134 (2005).
- O Alexeev, S Chin, M Engelhard, L Ortiz-Soto, M Amiridis. Effects of Reduction Temperature and Metal-Support Interactions on the Catalytic Activity of Pt/g- Al_2O_3 and Pt/ TiO_2 for the Oxidation of CO in the Presence and Absence of H_2 . *J. Phys. Chem. B.* **109** (49), 23430-23443 (2005).
- O Alexeev, F Li, M Amiridis, B Gates. Effects of Adsorbates on Supported Platinum and Iridium Clusters: Characterization in Reactive Atmospheres and During Alkene Hydrogenation Catalysis by X-ray Absorption Spectroscopy. *J. Phys. Chem. B.* **109** (6), 2338-2349 (2005).
- S Bare, S Kelly, W Sinkler, J Low, F Modica, S Valencia, A Corma, L Nemeth. Uniform Catalytic Site in Sn-beta Zeolite Determined using X-ray Absorption Fine Structure. *J. Am. Chem. Soc.* **127**, 12924-12932 (2005).
- V Bhirud, H Iddir, N Browning, B Gates. Intact and Fragmented Triosmium Clusters on MgO: Characterization by X-ray Absorption Spectroscopy and High-Resolution Transmission Electron Microscopy. *J. Phys. Chem. B.* **109**, 12738-12741 (2005).
- R Bindu, S Pandey, A Kumar, S Khalid, A Pimpale. Local Distortion of MnO_6 Octahedron in $\text{La}_{1-x}\text{Sr}_x\text{MnO}_{3+\Delta}$ ($x=0.1-0.9$): An EXAFS Study. *J. Phys.: Condens. Matter.* **17** (41), 6393-6404 (2005).
- S Bluskov, J Arocena, O Omotoso, J Young. Uptake, Distribution and Speciation of Chromium. *Int. J. Phytoremediation.* **7**, 153-165 (2005).
- T Chen, J Dutrizac, S Beauchemin. Characterization of Gold in the Anodes and Anode Slimes from a European Copper Refinery. *European Metalurgical Conference*, Vol 1, p. 165-182, sponsored by GDMB Gesellschaft für. (2005).
- E Chenu, G Jacobs, A Crawford, R Keogh, P Patterson, D Sparks, B Davis. Water-gas Shift: an Examination of Unpromoted and Pt Promoted MgO and Tetragonal and Monoclinic ZrO_2 by In-Situ DRIFTS. *Appl. Catal. B.* **59**, 45-56 (2005).
- J Dutrizac, T Chen, S Beauchemin. The Behavior of Thallium(III) During Jarosite Precipitation. *Hydrometallurgy.* **79**, 138-153 (2005).
- O Font, X Querol, F Huggins, J Chimenos, A Fernández, S Burgos, F Peña. Speciation of Major and Selected Trace Elements in IGCC Fly Ash. *Fuel.* **84**, 1364-1371 (2005).
- K Galbreath, R Schulz, D Toman, C Nyberg, F Huggins, G Huffman, E Zilliox. Nickel and Sulfur Speciation of Residual Oil Fly Ashes from Two Electric Utility Steam-Generating Units. *J. Air Waste Manage. Assoc.* **55**, 309-318 (2005).
- A Ganjoo, H Jain, S Khalid, C Pantano. Structural Modification of Ge-Se Amorphous Films with the Addition of Sb. *Philos. Mag. Lett.* **85** (10), 503-512 (2005).
- F Goodarzi, F Huggins. Speciation of Arsenic in Canadian Subbituminous and Bituminous Feed Coals and their Ash Byproducts. *Energ. Fuel.* **19**, 905-915 (2005).
- J Guzman, B Anderson, C Vinod, K Ramesh, J Niemantsverdriet, B Gates. Synthesis and Reactivity of Dimethyl Gold Complexes Supported on MgO: Characterized by Infrared and X-ray Absorption Spectroscopies. *Langmuir.* **21**, 3675-3683 (2005).
- J Guzman, S Carrettin, J Fierro-Gonzalez, Y Hao, B Gates, A Corma. CO oxidation Catalyzed by Supported Gold: Cooperation Between Gold and Nanocrystalline Rare-Earth Supports forms Reactive Surface Superoxide and Peroxide Species. *Angew. Chem. Int. Ed.* **44** (30), 4778-4781 (2005).
- G Jacobs, P Patterson, U Graham, A Crawford, A Dozier, B Davis. Catalytic Links Among the Water-Gas Shift, Water-Assisted Formic Acid Decomposition, and Methanol Steam Reforming Reactions over Pt Promoted Thoria. *J. Catal.* **235**, 79-91 (2005).
- G Jacobs, U Graham, E Chenu, P Patterson, A Dozier, B Davis. Low Temperature Water Gas Shift: Impact of Pt Promoter Loading on the Partial Reduction of Ceria and consequences for Catalyst Design. *J. Catal.* **229**, 499-512 (2005).
- G Jacobs, S Ricote, P Patterson, U Graham, A Dozier, S Khalid, E Rhodus, B Davis. Low Temperature Water-Gas Shift: Examining the Efficiency of Au as a Promoter for Ceria-Based Catalysts Prepared by CVD of a Au Precursor. *Appl. Catal. A.* **292**, 229-243 (2005).
- C Jing, X Meng, S Liu, S Baidas, R Patraju, C Christodoulatos, G Korfiatis. Surface Complexation of Organic Arsenic on Nanocrystalline Titanium Oxide. *J. Colloid Interface Sci.* **290** (1), 14-21 (2005).
- Y Lee, E Elzinga, R Reeder. Sorption Mechanisms of Zinc on Hydroxyapatite: Systematic Uptake Studies and EXAFS Spectroscopy Analysis. *Environ. Sci. Tech.* **39**, 4042-4048 (2005).
- A Liang, V Bhirud, J Ehresmann, P Kletnieks, J Haw, B Gates. A Site-Isolated Rhodium-Diethylene Complex Supported on Highly Dealuminated Y Zeolite: Synthesis and Characterization. *J. Phys. Chem. B.* **109**, 24236-24243 (2005).
- J Roques, A Anderson, V Murthi, S Mukerjee. Potential Shift for OH(ads) Formation on the Pt Skin on $\text{Pt}_3\text{Co}(111)$ Electrodes in Acid. *J. Electrochem. Soc.* **152**, E193 (2005).
- A Rouff, E Elzinga, R Reeder, N Fisher. The Influence of pH on the Kinetics, Reversibility and Mechanism of Pb(II) Sorption at the Calcite-Water Interface. *Geochim. Cosmochim. Acta.* **69** (22), 5173-5186 (2005).
- S Sen, B Aitken, S Khalid. Short-Range Structure and Chemical Order in in-Ge Sulfide and Selenide Glasses by X-ray Absorption Fine Structure Spectroscopy. *J. Non-Cryst. Solids.* **351** (19-20), 1710-1715 (2005).
- Y Shu, S Oyama. Synthesis, Characterization, and Hydrotreating Activity of Carbon-Supported Transition Metal Phosphides. *Carbon.* **43**, 7 (2005).
- M Teliska, V Murthi, S Mukerjee, D Ramaker. Correlation of Water Activation, Surface Properties, and Oxygen Reduction Reactivity of Supported Pt-M/C Bimetallic Electrocatalysts Using XAS. *J. Electrochem. Soc.* **152**, A2159 (2005).
- X Wang, J Rodriguez, J Hanson, M Perez, J Evans. In Situ Time-Resolved Characterization of Au-CeO₂ Catalysts During Water Gas Shift Reactions: presence of Au and O Vacancies in the Active Phase. *J. Chem. Phys.* **123**, 221101 (2005).
- S Wasson, W Linak, B Gullett, C King, A Touati, F Huggins, Y Chen, N Shah, G Huffman. Emissions of Chromium, Copper, Arsenic, and PCDDs/Fs from Open Burning of CCA-Treated Wood. *Environ. Sci. Tech.* **39** (22), 8865-8876 (2005).
- Y Xi, C Reed, Y Lee, S Oyama. Acetone Oxidation using Ozone on Manganese Oxide Catalysts. *J. Phys. Chem. B.* **109**, 17537-17596 (2005).
- W Yan, B Chen, S Mahurin, V Schwartz, D Mullins, A Lupini, S Pennycook, S Dai, S Overbury. Preparation and Comparison of Supported Gold Nanocatalysts on Anatase, Brookite, Rutile, and P25 Polymorphs of TiO_2 for Catalytic Oxidation of CO. *J. Phys. Chem. B.* **109**, 10676-10685 (2005).
- W Yoon, M Balasubramanian, K Chung, X Yang, J McBreen, C Grey, D Fischer. Investigation of the Charge Compensation Mechanism on the Electrochemically Li-Ion Deintercalated $\text{Li}_{1-x}\text{Co}_1/3\text{Ni}_1/3\text{Mn}_1/3\text{O}_2$ Electrode System by Combination of Soft and Hard X-ray Absorption Spectroscopy. *J. Am. Chem. Soc.* **127** (49), 17479-17487 (2005).

Beamline X19A

- A Abakumov, M Rozova, E Antipov, J Hadermann, G Van Tendeloo, M Lobanov, M Greenblatt, M Croft, E Tsiper, et al.. Synthesis, Cation Ordering, and Magnetic Properties of the $(\text{Sb}_{1-x}\text{Pb}_x)_2(\text{Mn}_{1-y}\text{Sb}_y)\text{O}_4$ Solid Solutions with the Sb_2MnO_4 -Type Structure. *Chem. Mater.* **17**, 1123-1134 (2005).
- B Bostick, K Theissen, R Dunbar, M Vairavamurthy. Record of Redox Status in Laminated Sediments from Lake Titicaca: A Sulfur K-Edge X-ray Absorption Near Edge Structure (XANES) Study. *Chem. Geol.* **219**, 163-174 (2005).
- O Font, X Querol, F Huggins, J Chimenos, A Fernández, S Burgos, F Peña. Speciation of Major and Selected Trace Elements in IGCC Fly Ash. *Fuel*. **84**, 1364-1371 (2005).
- F Goodarzi, F Huggins. Speciation of Chromium in Feed Coals and Ash Byproducts from Canadian Power Plants Burning Subbituminous and Bituminous Coals. *Energ. Fuel*. **19**, 2500-2508 (2005).
- C Jing, S Liu, M Patel, X Meng. Arsenic Leachability in Water Treatment Adsorbents. *Environ. Sci. Tech.* **39**, 5481-5487 (2005).
- C Jing, S Liu, X Meng. Arsenic Leachability and Speciation in Cement Immobilized Water Treatment Sludge. *Chemosphere*. **59** (9), 1241-1247 (2005).
- N Khare, D Hesterberg, J Martin. XANES Investigatin of Phosphate Sorption in Single and Binary Systems of Iron and Aluminum Oxide Minerals. *Environ. Sci. Tech.* **39**, 2152-2160 (2005).
- Q Lin, M Greenblatt, M Croft. Evolution of Structure and Magnetic Properties in Electron-Doped Double Perovskites, $\text{Sr}_{2-x}\text{La}_x\text{MnWO}_6$ ($0 < x < 2$). *Solid State Chem.* **178** (5), 1356-1366 (2005).
- J Majzlan, S Myneni. Speciation of Iron and Sulfate in Acid Waters: Aqueous Clusters to Mineral Precipitates. *Environ. Sci. Tech.* **39**, 188-194 (2005).
- S Pattanaik. X-ray Diffraction, XAFS and Scanning Electron Microscopy Study of Otolith of a Crevalle Jack Fish (caranx hippos). *Nucl. Instrum. Meth. B*. **229** (3-4), 367-374 (2005).
- S Sato, D Solomon, C Hyland, Q Ketterings, J Lehmann. Phosphorus Speciation in Manure and Manure-Amended Soils Using XANES Spectroscopy. *Environ. Sci. Tech.* **39** (19), 7485-7491 (2005).
- S Sayan, M Croft, N Nguyen, T Emge, E Gusev, H Kim, J Ehrstein, P McIntyre, E Garfunkel. Amorphous to Tetragonal Transition in Ultrathin Zirconia Films: Effect on the Electronic and Dielectric Properties. *Appl. Phys. Lett.* **86** (15), 152902 (2005).
- D Solomon, J Lehmann, I Lobe, C Martinez, S Tveitnes, C Du Preez, W Amelung. Sulphur Speciation and Biogeochemical Cycling in Long-Term Arable Cropping of Subtropical Soils: Evidence From Wet-Chemical Reduction and S K-Edge XANES Spectroscopy. *Eur. J. Soil Sci.*, 1-14 (2005).
- G Veith, M Greenblatt, M Croft, K Ramanujachary, J Hattrick-Simpers, S Lofland, I Nowik. Synthesis and Characterization of $\text{Sr}_3\text{FeMoO}_6.88$: An Oxygen-Deficient 2D Analogue of the Double Perovskite $\text{Sr}_2\text{FeMoO}_6$. *Chem. Mater.* **17**, 2562-2567 (2005).
- X Wang, J Hanson, J Rodriguez, C Belver, M Fernandez-Garcia. The Structural and Electronic Properties of Nanostructured $\text{Ce}_{(1-x-y)}\text{Zr}_x\text{Tb}_y\text{O}_2$ Ternary Oxides: Unusual Concentration of $\text{Tb}(3+)$ and Metal-Oxygen-Metal Interactions. *J. Chem. Phys.* **122** (15), 154711 (2005).
- R Wiltfong, S Mitra-Kirtley, O Mullins, B Andrews, G Fujisawa, J Larsen. Sulfur Speciation of Different Kerogens using XANES Spectroscopy. *Energ. Fuel*. **19** (5), 1971-76 (2005).
- S Yoon, L Diener, P Bloom, E Nater, W Bleam. X-ray Absorption

Studies of Ch_3Hg^+ -Binding Sites in Humic Substances. *Geochim. Cosmochim. Acta*. **69**, 1111-1121 (2005).

- F Zhao, J Lehmann, D Solomon, M Fox, S McGrath. Sulphur Speciation and Turnover in Soils: Evidence from Sulphur K-Edge XANES Spectroscopy and Isotope Dilution Studies. *Soil Biol. Biochem.* **38**, 1-8 (2005).

Beamline X19C

- J Bai, X Huang, M Dudley, B Wagner, R Davis, L Wu, Y Zhu. Intersecting Basal Plane and Prismatic Stacking Fault Structures and their Formation Mechanisms in GaN. *J. Appl. Phys.* **98**, 063510-1 - 063510-9 (2005).
- J Bai, M Dudley, L Chen, B Skromme, B Wagner, R Davis, U Chowdhury, R Dupuis. Structural Defects and Luminescence Features in Heteroepitaxial GaN Grown on On-Axis and Misoriented Substrates. *J. Appl. Phys.* **97**, 116101 (2005).
- J Bai, M Dudley, L Chen, B Skromme, P Hartlieb, E Michaels, J Kolis, B Wagner, R Davis, et al.. Relationship of Basal Plane and Prismatic Stacking Faults in GaN to Low Temperature Photoluminescence Peaks at $\sim 3.4\text{eV}$ and $\sim 3.2\text{eV}$. *2004 Materials Research Society Fall Meeting Proceedings*, Vol 81, p. E11.37, sponsored by Materials Research Society. (2005).
- G Dhanaraj, B Raghathamachar, J Bai, H Chung, M Dudley. Synchrotron X-ray Topographic Characterization of Defects in InP Bulk Crystals. *17th Indium Phosphide and Related Materials Conference*, Vol 8th, p. cd rom, (2005).
- M Hollingsworth, M Peterson, J Rush, M Brown, M Abel, A Black, M Dudley, B Raghathamachar, U Werner-Zwanziger, et al.. Memory and Perfection in Ferroelastic Inclusion Compounds. *Cryst. Growth Des.* **5**, 2100-2116 (2005).
- X Huang, J Bai, M Dudley, B Wagner, R Davis, Y Zhu. Step-Controlled Strain Relaxation in Vicinal Surface Epitaxy of Nitrides. *Phys. Rev. Lett.* **95**, 086101-1 - 086101-4 (2005).
- X Huang, J Bai, M Dudley, R Dupuis, U Chowdhury. Exptaxial Tilting of GaN Grown on Vicinal Surfaces of Sapphire. *Appl. Phys. Lett.* **86**, 211916 (2005).
- B Liu, J Edgar, B Raghathamachar, M Dudley, A Sarua, M Kuball, H Meyer, J Lin, H Jiang, et al.. Free Nucleation of Aluminum Nitride Single Crystals in HPBN Crucible by Sublimation. *Mater. Sci. Eng. B*. **117**, 99-104 (2005).
- S Malkova, F Long, R Stahelin, S Pingali, D Murray, W Cho, M Schlossman. X-ray Reflectivity Studies of cPLA?-C2 Domains Adsorbed onto Langmuir Monolayers of SOPC. *Biophys. J.* **89**, 1861 (2005).
- V Noveski, R Schlessler, B Raghathamachar, M Dudley, S Mahajan, S Beaudion, Z Sitar. Seeded Growth of Bulk AlN Crystals and Grain Evolution in Polycrystalline AlN Boules. *J. Cryst. Growth*. **279**, 13-19 (2005).
- S Pingali, T Takiue, G Luo, A Tikhonov, N Ideda, M Aratono, M Schlossman. X-ray Reflectivity and Interfacial Tension Study of the Structure and Phase Behavior of the Interface Between Water and Mixed Surfactant Solutions of $\text{CH}_3(\text{CH}_2)_{19}\text{OH}$ and $\text{CF}_3(\text{CF}_2)_7(\text{CH}_2)_2\text{OH}$ in Hexane. *J. Phys. Chem. B*. **109**, 1210-1225 (2005).
- M Schlossman. X-ray Scattering from Liquid-Liquid Interfaces. *Physica B*. **357** (1-2), 98-105 (2005).
- W Vetter, H Tsuchida, I Kamata, M Dudley. Simulation of Threading Dislocation Images in X-ray Topographs of Silicon Carbide Homo-Epilayers. *J. Appl. Cryst.* **38**, 442-447 (2005).
- Y Wang, G Ali, M Mikhov, V Vaidyanathan, B Skromme, B Raghathamachar, M Dudley. Correlation Between Morphological Defects, Electron Beam Induced Current Imaging, and the Electrical Properties of 4H-SiC Schottky Diodes. *J. Appl. Phys.* **97**, 013540-1 (2005).

Beamline X20A

- H Chen, Y Yao, J Kysar, I Noyan, Y Wang. Fourier Analysis of X-ray Micro-Diffraction Profiles to Characterize Laser Shock Peened Metals. *Int. J. Solids Struct.* **42** (11-12), 3471-3485 (2005).
- F Espinosa-Faller, R Howell, A Garcia-Adeva, S Conradson, A Ignatov, T Tyson, R Farrow, M Toney. Local Atomic Structure of Partially Ordered NiMn in NiMn/NiFe Exchange Coupled Layers: 1. XAFS Measurements and Structural Refinement. *J. Phys. Chem. B.* **109**, 10406-10418 (2005).
- S Kaldor, I Noyan. Flexural Loading of Rectangular Si Beams and Plates. *Mater. Sci. Eng. A.* **399** (1-2), 64-71 (2005).

Beamline X20B

- J Jordan-Sweet, C Detavernier, C Lavoie, P Mooney, M Toney. Applications of Synchrotron X-rays in Microelectronics Industry Research. *Nucl. Instrum. Meth. B.* **241** (1-4), 247-252 (2005).

Beamline X20C

- H Kim, C Detavernier, O van der Staten, S Rossnagel, A Kellock, D Park. Robust TaNx Diffusion Barrier for Cu-Interconnect Technology with Subnanometer Thickness by Metal-Organic Plasma-Enhanced Atomic Layer Deposition. *J. Appl. Phys.* **98**, 014308 (2005).
- S Raoux, C Rettner, J Jordan-Sweet, M Salinga, M Toney. Crystallization Behavior of Phase Change Nanostructures. *European Symposium on Phase Change and Ovonic Science*, Vol. , p. 14, sponsored by Plasmon. (2005).
- T Thomson, S Lee, M Toney, C Dewhurst, Y Ogrin, C Oates, S Sun. Agglomeration and Sintering in Annealed FePt Nanoparticle Assemblies Studied by Small Angle Neutron Scattering and X-ray Diffraction. *Phys. Rev. B.* **72**, 064441 (2005).

Beamline X21

- K Cavicchi, K Berthiaume, T Russell. Solvent Annealing Thin Films of Poly(isoprene-b-lactide). *Polymer.* **46** (25), 11635-11639 (2005).
- J Liao, L Yang, J Grashow, M Sacks. Molecular Orientation of Collagen in Intact Planar Connective Tissues Under Biaxial Stretch. *Acta Biomater.* **1** (1), 45-54 (2005).
- G Lynn, W Heller, A Mayusundari, K Minor, C Peterson. A Model for the Three-Dimensional Structure of Human Plasma Vitronectin from Small-angle Scattering Measurements. *Biochemistry.* **44** (2), 565-574 (2005).
- G Ozaydin, A Ozcan, Y Wang, K Ludwig, H Zhou, R Headrick, D Siddons. Real-Time X-ray Studies of Mo-Seeded Self-Organized Si Nanodot Formation During Low Energy Ar⁺ Ion Bombardment. *Appl. Phys. Lett.* **87**, 163104 (2005).
- Q Qian, T Tyson, W Caliebe, C Kao. High-Efficiency High-energy-Resolution Spectrometer for Inelastic X-ray Scattering. *J. Phys. Chem. Solids.* **66** (12), 2295 (2005).
- A Sehgal, Y Lalatonne, J Berret, M Morvan. Precipitation-Redispersion of Cerium Oxide Nanoparticles with Poly(acrylic acid): Toward Stable Dispersions. *Langmuir.* **21**, 9359-9364 (2005).
- H Yang, M Ling, T Shin, C Ryu, Z Bao. Universal Effects of Solubility and Thermal Annealing for Structure Formation in Regioregular Poly(3-alkyl thiophene) Series. *American Chemical Society National Meeting*, Vol 92, p. 295, sponsored by American Chemical Society. (2005).
- H Yang, T Shin, Z Bao, K Cho, C Ryu. Volatile Solvent Solubility

and Thermal Annealing Effects on Regio-regular P3HT Thin Film Structure and Its Correlation with TFT Charge Mobility. *American Chemical Society National Meeting*, Vol 92, p. 604, sponsored by American Chemical Society. (2005).

- H Yang, T Shin, M Ling, K Cho, C Ryu, Z Bao. Conducting AFM and 2D GIXD Studies on Pentacene Thin Films. *J. Am. Chem. Soc.* **127**, 11542-11543 (2005).
- L Yang, M Fukuto. Modulated Phase of Phospholipids with a Two-Dimensional Square Lattice. *Phys. Rev. E.* **72**, 010901(R) (2005).
- H Yang, T Shin, L Yang, K Cho, C Ryu, Z Bao. Effect of Mesoscale Crystalline Structure on the Field-Effect Mobility of Regioregular Poly(3-hexyl thiophene) in Thin-Film Transistors. *Adv. Func. Mater.* **15** (4), 671-676 (2005).

Beamline X22A

- J Fossum, E Gudding, M Fonseca, Y Meheust, E DiMasi, T Gog, C Venkataraman. Observations of Orientational Ordering in Aqueous Suspensions of a Nano-Layered Silicate. *Energy.* **30** (6), 873-883 (2005).
- O Gang, K Alvine, M Fukuto, P Pershan, C Black, B Ocko. Liquids on Topologically Nano-Patterned Surfaces. *Phys. Rev. Lett.* **95**, 217801 (2005).
- F He, B Wells, S Shapiro. Strain Phase Diagram and Domain Orientation in SrTiO₃ Thin Films. *Phys. Rev. Lett.* **94** (17), 176101 (2005).
- F He. Phase Transitions and Properties of Epitaxial Perovskite Films. Ph.D. Thesis. University of Connecticut, Storrs. (2005).
- S Kwak, E DiMasi, Y Han, J Aizenberg, I Kuzmenko. Orientation and Mg Incorporation of Calcite Grown on Functionalized Self-Assembled Monolayers: A Synchrotron X-ray Study. *Cryst. Growth Des.* **5** (6), 2139-2145 (2005).
- M Nelson, N Cain, B Ocko, D Gin, S Hammond, D Schwartz. Periodic Arrays of Interfacial Cylindrical reverse Micelles. *Langmuir.* **21**, 9799-9802 (2005).
- G Shirane, G Xu, P Gehring. Dynamics and Structure of PMN and PZN. *Ferroelectr.* **321**, 7-19 (2005).
- B Smarsly, A Gibaud, W Ruland, D Sturmayer, C Brinker. Quantitative SAXS Analysis of Oriented 2D Hexagonal Cylindrical Silica Mesostructures in Thin Films Obtained from Nonionic Surfactants. *Langmuir.* **21**, 3858-3866 (2005).
- R Turgeman, O Gershevit, M Deutsch, B Ocko, A Gedanken, C Sukenik. Crystallization of Highly Oriented ZnO Microrods on Carboxylic Acid-Terminated SAMs. *Chem. Mater.* **17**, 5048-5056 (2005).
- J Wang, I Robinson, B Ocko, R Adzic. Adsorbate-Geometry Specific Subsurface Relaxation in the CO/Pt(111) System. *J. Phys. Chem. B.* **109** (1), 24 (2005).
- G Xu, H Hiraka, G Shirane, J Li, J Wang, D Viehland. Low Symmetry Phase in (001) BiFeO₃ Epitaxial Constrained Thin Films. *Appl. Phys. Lett.* **86**, 182905 (2005).
- T Xu, M Misner, S Kim, J Sievert, O Gang, B Ocko, T Russell. Selective Solvent Induced Reversible Surface Reconstruction of Diblock Copolymer Thin Films. *New Polymeric Materials*, p. 158-170, Oxford University Press, New York. (2005).

Beamline X22B

- K Cavicchi, K Berthiaume, T Russell. Solvent Annealing Thin Films of Poly(isoprene-b-lactide). *Polymer.* **46** (25), 11635-11639 (2005).
- B Discher, D Noy, J Strzalka, S Ye, C Moser, J Lear, K Blasie, L Dutton. Design of Amphiphilic Protein Maquettes: Controlling

- Assembly, Membrane Insertion, and Cofactor Interactions. *Biochemistry*. **44** (37), 12329-12343 (2005).
- S Dourdain, J Bardeau, M Colas, B Smarsly, A Mehdi, B Ocko, A Gibaud. Determination by X-ray Reflectivity and Small Angle X-ray Scattering of the Porous Properties of Mesoporous Silica Thin Films. *Appl. Phys. Lett.* **86**, 113108 (2005).
- S Dourdain, A Rezaire, A Mehdi, B Ocko, A Gibaud. Real time GISAXS study of Micelle hydration in CTAB templated silica thin films. *Physica B*. **357** (1-2), 180-184 (2005).
- A Grigoriev, O Shpyrko, C Steimer, P Pershan, B Ocko, M Deutsch, B Lin, M Meron, T Graber, J Gebhardt. Surface Oxidation of Liquid Sn. *Surf. Sci.* **575** (3), 223-232 (2005).
- M Henderson, A Gibaud, J Bardeau, A Rennie, J White. A Zirconium Oxide Film Self-Assembled at the Air-Water Interface. *Physica B*. **357** (1-2), 27-33 (2005).
- B Ocko, H Kraack, P Pershan, E Sloutskin, L Tamam, M Deutsch. Crystalline Phases of Alkyl-Thiol Monolayers on Liquid Mercury. *Phys. Rev. Lett.* **94**, 017802 (2005).
- E Sloutskin, C Bain, B Ocko, M Deutsch. Surface Freezing of Chain Molecules at the Liquid-Liquid and Liquid-Air Interfaces. *Faraday Discuss.* **129**, 339-352 (2005).
- E Sloutskin, B Ocko, L Tamam, I Kuzmenko, T Gog, M Deutsch. Surface Layering in Ionic Liquids: An X-ray Reflectivity Study. *J. Am. Chem. Soc.* **127**, 7796-7804 (2005).
- L Tamam, H Kraack, E Sloutskin, B Ocko, P Pershan, A Ulman, M Deutsch. Structure of Mercaptobiphenyl Monolayers on Mercury. *J. Phys. Chem.* **109**, 12534-12543 (2005).
- T Xu, M Misner, S Kim, J Sievert, O Gang, B Ocko, T Russell. Selective Solvent Induced Reversible Surface Reconstruction of Diblock Copolymer Thin Films. *New Polymeric Materials*, p. 158-170, Oxford University Press, New York. (2005).
- S Ye, B Discher, J Strzalka, T Xu, S Wu, D Noy, I Kuzmenko, T Gog, K Blasie, et al.. Amphiphilic Four-Helix Bundle Peptides Designed for Light-Induced Electron Transfer Across a Soft Interface. *Nano Lett.* **5** (9), 1658-1667 (2005).
- Beamline X22C**
- M Castro-Colin, W Donner, S Moss, Z Islam, S Sinha, R Nemanich, H Metzger, P Bosecke, T Shulli. Synchrotron X-ray Studies of Vitreous SiO₂ Over Si(001). I. Anisotropic Glass Contribution. *Phys. Rev. B*. **71**, 045310 (2005).
- F He. Phase Transitions and Properties of Epitaxial Perovskite Films. Ph.D. Thesis. University of Connecticut, Storrs. (2005).
- M Hucker, Y Kim, G Gu, J Tranquada, B Gaulin, J Lynn. Neutron Scattering Study on La_{1.9}Ca_{1.1}Cu₂O₆+ δ and La_{1.85}Sr_{0.15}Ca Cu₂O₆+ δ . *Phys. Rev. B*. **71**, 094510 (2005).
- P Lyman, V Shneerson, R Fung, R Harder, E Lu, S Parihar, D Saldin. Atomic-Scale Visualization of Surfaces with X rays. *Phys. Rev. B: Condens. Matter*. **71** (8), 081402-1-4 (2005).
- Beamline X23A2**
- J Ablett, J Woicik, C Kao. New Correction Procedure For X-ray Spectroscopic Fluorescence Data: Simulations and Experiment. *Adv. X-Ray Anal.* **48**, 266-273 (2005).
- F Alamgir, H Jain, D Williams, R Schwarz. Sub-Nanoscale Structural Origin of the Stability of the Pd-Ni-P Model Bulk Metallic Glass. *The Science of Complex Alloy Phases*, p. 163-182, TMS, Warrendale. (2005).
- P Amama, S Lim, D Ciuparu, Y Yang, L Pfefferle, G Haller. Synthesis, Characterization, and Stability of Fe-MCM-41 for Production of Carbon Nanotubes by Acetylene Pyrolysis. *J. Phys. Chem. B*. **109**, 2645-2656 (2005).
- D Ciuparu, P Haider, M Fernandez-Garcia, Y Chen, S Lim, G Haller, L Pfefferle. X-ray Absorption Spectroscopic Investigation of Partially Reduced Cobalt Species in Co-MCM-41 Catalysts During Synthesis of Single-Wall Carbon Nanotubes. *J. Phys. Chem. B*. **109**, 16332-16339 (2005).
- P Haider, Y Chen, S Lim, G Haller, L Pfefferle, D Ciuparu. Application of the Generalized 2D Correlation Analysis to Dynamic Near-Edge X-ray Absorption Spectroscopy Data. *J. Am. Chem. Soc.* **127**, 1906-1912 (2005).
- S Lim, D Ciuparu, Y Chen, Y Yang, L Pfefferle, G Haller. Pore Curvature Effect on the Stability of Co-MCM-41 and the Formation of Size-Controllable Subnanometer Co Clusters. *J. Phys. Chem. B*. **109**, 2285-2294 (2005).
- E Ma. Alloys Created Between Immiscible Elements. *Prog. Mater. Sci.* **50**, 413-509 (2005).
- D McKeown, H Gan, I Pegg. Silver Valence and Local Environments in Borosilicate and Calcium Aluminoborate Waste Glasses as determined from X-ray Absorption Spectroscopy. *J. Non-Cryst. Solids*. **351**, 3826-3833 (2005).
- A Rouff, E Elzinga, R Reeder, N Fisher. The Influence of pH on the Kinetics, Reversibility and Mechanism of Pb(II) Sorption at the Calcite-Water Interface. *Geochim. Cosmochim. Acta*. **69** (22), 5173-5186 (2005).
- M Sahiner, D Downey, S Novak, J Woicik, D Arena. The Local Structural Characterization of the Inactive Clusters in B, Bf₂ and B23 Implanted Si Wafers using X-ray Techniques. *Microelectr. J.* **36**, 522-526 (2005).
- Beamline X23B**
- S Calvin, E Carpenter, V Cestone, L Kurihara, V Harris, E Brown. Automated System for X-Ray Absorption Spectroscopy of Nanoparticle Nucleation and Growth. *Rev. Sci. Instrum.* **76** (1), 016103-1 - 016103-3 (2005).
- Q Huang, G Evmenenko, P Dutta, p Lee, N Armstrong, T Marks. Covalently Bound Hole-Injecting Nanostructures. Systematics of Molecular Architecture, Thickness, Saturation, and Electron-Blocking Characteristics on Organic Light-Emitting Diode Luminance, Turn-on Voltage, and Quantum Efficiency. *J. Am. Chem. Soc.* **127**, 10227-10242 (2005).
- S Morrison, C Cahill, E Carpenter, S Calvin, V Harris. Atomic Engineering of Mixed Ferrite and Core-Shell Nanoparticles. *J. Nanosci. Nanotechnol.* **5** (9), 1323-1344 (2005).
- Q Qian, T Tyson, W Caliebe, C Kao. High-Efficiency High-energy-Resolution Spectrometer for Inelastic X-ray Scattering. *J. Phys. Chem. Solids*. **66** (12), 2295 (2005).
- M Teliska, V Murthi, S Mukerjee, D Ramaker. In Situ Determination of O(H) Adsorption Sites on Pt Based Alloy Electrodes using X-ray Absorption Spectroscopy. *Fundamental Understanding of Electrode Processes in Memory of Professor Ernest B. Yeager*, Vol , p. 212-215, sponsored by The Electrochemical Society. (2005).
- H Yan, P Lee, N Armstrong, A Graham, G Evmenenko, P Dutta, T Marks. High-Performance Hole-Transport Layers for Polymer Light-Emitting Diodes. Implementation of Organosiloxane Cross-Linking Chemistry in Polymeric Electroluminescent Devices. *J. Am. Chem. Soc.* **127**, 3172-3183 (2005).
- A Yang, Z Chen, X Zuo, D Arena, J Kirkland, C Vittoria, V Harris. Cation-Disorder-Enhanced Magnetization in Pulsed-Laser-Deposited CuFe₂O₄ Films. *Appl. Phys. Lett.* **86**, 252510 (2005).
- A Yang, X Zuo, I Chen, Z Chen, C Vittoria, V Harris. Magnetic and Structural Properties of Pulsed Laser Deposited CuFe₂O₄ Films. *J. Appl. Phys.* **97**, 10G107 (2005).
- T Zubkov, A Lucassen, D Freeman, Y Feldman, S Cohen,

- G Evmenenko, P Dutta, M van der Boom. Photoinduced Deprotection and ZnO Patterning of Hydroxyl-Terminated Siloxane-Based Monolayers. *J. Phys. Chem. B.* **109**, 14144-14153 (2005).
- X Zuo, A Yang, S Yoon, J Christodoulides, V G. Harris, C Vittoria. Large Induced Magnetic Anisotropy in Manganese Spinel Ferrite Films. *Appl. Phys. Lett.* **87**, 152505 (2005).
- X Zuo, A Yang, S Yoon, I Christodoulides, V Harris, C Vittoria. Magnetic Properties of Manganese Ferrite Films Grown at Atomic Scale. *J. Appl. Phys.* **97**, 10G103 (2005).
- ### Beamline X24A
- J Woicik. Site-Specific X-ray Photoelectron Spectroscopy using X-ray Standing Waves. *Nucl. Instrum. Meth. A.* **547** (1), 227-234 (2005).
- ### Beamline X24C
- J Seely, B Kjornrattanawanich, G Holland, R Korde. Response of a SiC Photodiode to Extreme Ultraviolet through Visible Radiation. *Opt. Lett.* **30** (23), 3120 (2005).
- J Seely, U Feldman, G Holland, J Weaver, A Mostovych, S Obenschain, A Schmitt, R Lehmborg, B Kjornrattanawanich, C Back. Absolutely Calibrated Vacuum Ultraviolet Spectra in the 150-250-Nm Range from Plasmas Generated by the Nike Krf Laser. *Phys. Plasmas*. **12** (6), 062701 (2005).
- J Weaver, M Busquet, D Colombant, A Mostovych, U Feldman, M Klapisch, J Seely, C Brown, G Holland. Experimental Benchmark for an Improved Simulation of Absolute Soft-X-ray Emission from Polystyrene Targets Irradiated with the Nike Laser. *Phys. Rev. Lett.* **94**, 045002 (2005).
- D Windt, J Seely, B Kjornrattanawanich, Y Uspenskii. Terbium-Based Extreme Ultraviolet Multilayers. *Opt. Lett.* **30** (23), 3186 (2005).
- ### Beamline X25
- R Agarwal, T Binz, S Swaminathan. Analysis of Active Site Residues of Botulinum Neurotoxin E by Mutational, Functional, and Structural Studies: Glu335Gln is an Apoenzyme. *Biochemistry*. **44**, 8291-8302 (2005).
- J Avalos, K Bever, C Wolberger. Mechanism of Sirtuin Inhibition by Nicotinamide: Altering the NAD⁺ Cosubstrate Specificity of a Sir2 Enzyme. *Mol. Cell*. **17** (6), 855-868 (2005).
- T Bai, M Becker, A Gupta, P Strike, V Murphy, R Anders, A Batchelor. Structure of AMA1 from Plasmodium falciparum Reveals A Clustering of Polymorphisms that Surround a Conserved Hydrophobic Pocket. *Proc Natl Acad Sci USA*. **102** (36), 12736-12741 (2005).
- T Biswas, H Aihara, M Radman-Livaja, D Filman, A Landy, T Ellenberger. A Structural Basis for Allosteric Control of DNA Recombination by λ Integrase. *Nature*. **435**, 1059 (2005).
- S Bouyain, P Longo, S Li, K Ferguson, D Leahy. The Extracellular Region of ErbB4 Adopts a Tethered Conformation in the Absence of Ligand. *Proc Natl Acad Sci USA*. **102**, 15024-15029 (2005).
- E Campbell, O Pavlova, N Zenkin, F Leon, H Irschik, R Jansen, K Severinov, S Darst. Structural, Functional, and Genetic Analysis of Sorangicin Inhibition of Bacterial RNA Polymerase. *EMBO J.* **24**, 674 (2005).
- S Cho, C Swaminathan, J Yang, M Kerzic, R Guan, M Kieke, D Kranz, R Mariuzza, E Sundberg. Structural Basis of Affinity Maturation and Intramolecular Cooperativity in a Protein-Protein Interaction. *Structure*. **13** (12), 1775-1787 (2005).
- D Colletuori, R Reczkowski, F Emig, E Cama, J Cox, L Scolnick, K Compher, K Jude, S Han, et al. Probing the Role of the Hyper-Reactive Histidine Residue of Arginase. *Arch. Biochem. Biophys.* **444** (1), 15-26 (2005).
- G Dong, A Hutagalung, C Fu, P Novick, K Reinisch. The Structures of Exocyst Subunit Exo70p and the Exo84p C-terminal Domains Reveal a Common Motif. *Nat. Struct. Mol. Biol.* **12** (12), 1094 (2005).
- D Duda, H Walden, J Sfondouris, B Schulman. Structural Analysis of Escherichia Coli ThiF. *J. Mol. Biol.* **349** (4), 774-786 (2005).
- S Eathiraj, X Pan, C Ritacco, D Lambright. Structural Basis of Family-Wide Rab GTPase Recognition by Rabenosyn-5. *Nature*. **436**, 415 (2005).
- L Feng, D Gell, S Zhou, L Gu, Y Kong, J Li, M Hu, N Yan, C Lee, et al.. Molecular Mechanism of AHSP-Mediated Stabilization of Alpha-Hemoglobin. *Cell*. **119**, 629 (2005).
- L Feng, S Zhou, L Gu, D Gell, J MacKay, M Weiss, A Gow, Y Shi. Structure of Oxidized Alpha-Haemoglobin Bound to AHSP Reveals a Protective Mechanism for HAEM. *Nature*. **435**, 697 (2005).
- G Golan, D Zharkov, H Feinberg, A Fernandes, E Zaika, J Kycia, A Grollman, G Shoham, et al.. Structure of the Uncomplexed DNA Repair Enzyme Interdomain Flexibility. *Nucleic Acids Res.* **33**, 5006 (2005).
- A Gupta, T Bai, V Murphy, P Strike, R Anders, A Batchelor. Refolding, Purification, and Crystallization of Apical Membrane Antigen 1 from Plasmodium. *Protein Expr. Purif.* **41** (1), 186-198 (2005).
- L Higgins, F Yan, P Liu, H Liu, C Drennan. Structural Insight into Antibiotic Fosfomycin Biosynthesis by a Mononuclear Iron Enzyme. *Nature*. **437**, 838-844 (2005).
- c Hobartner, R Rieder, C Kreutz, B Puffer, K Lang, A Polonskaia, A Serganov, R Micura. Synthesis of RNAs with up to 100 Nucleotides Containing Site-Specific 2'-methylseleno Labels for use in X-ray Crystallography. *J. Am. Chem. Soc.* **127** (34), 12035-12045 (2005).
- M Hu, P Li, L Song, P Jeffrey, T Chernova, K Wilkinson, R Cohen, Y Shi. Structure and Mechanisms of the Proteasome-associated Deubiquitinating Enzyme USP14. *EMBO J.* **24** (21), 3747 (2005).
- Q Huai, H Wang, Y Liu, H Kim, D Toft, H Ke. Structures of the N-Terminal and Middle Domains of E. Coli Hsp90 and Conformation Changes Upon ADP Binding. *Structure*. **13**, 579-590 (2005).
- D Huang, A Paydar, M Zhuang, M Waddell, J Holton, B Schulman. Structural Basis for Recruitment of Ubc12 by an E2 Binding Domain in NEDD8's E1. *Mol. Cell*. **17** (3), 341-350 (2005).
- A Iffland, D Kohls, S Low, J Luan, Y Zhang, M Kothe, Q Cao, A Kamath, Y Ding, T Ellenberger. Structural Determinants for Inhibitor Specificity and Selectivity in PDE2A using the Wheat Germ In Vitro Translation System. *Biochemistry*. **44**, 8312-8325 (2005).
- Y Im, S Raychaudhuri, W Prinz, J Hurley. Structural Mechanism for Sterol Sensing and Transport by OSBP-Related Proteins. *Nature*. **437**, 154-158 (2005).
- S Jayaraman, S Eswaramoorthy, S Ahmed, L Smith, S Swaminathan. N-Terminal Helix Reorients in Recombinant C-Fragment of Clostridium Botulinum Type B. *Biochem. Biophys. Res. Commun.* **330** (1), 29 (2005).
- S Kamtekar, A Berman, J Wang, J Lazaro, M de Vega, L Blanco, M Salas, T Steitz. Insights into Strand Displacement and Processivity from the Crystal Structure of the Protein-primed DNA Polymerase of Bacteriophage phi29. *Mol. Cell*. **16**, 609-618 (2005).
- S Kang, B Crane. Effects of Interface Mutations on Association Modes and Electron-Transfer Rates Between Proteins. *Proc Natl Acad Sci USA*. **102** (43), 15465-15470 (2005).

- C Kielkopf, S Luecke, M Green. U2AF-Homology-Motifs: Protein Recognition in the RRM World. *Genes Dev.* **18**, 1513-1526 (2005).
- S Lahr, D Engel, S Stayrook, O Maglio, B North, S Geremia, A Lombardi, W DeGrado. Analysis and Design of Turns in alpha-Helical Hairpins. *J. Mol. Biol.* **346** (5), 1441-1454 (2005).
- S Lee, A Lee, J Chen, R MacKinnon, W Chin. Structure of the KvAP voltage-dependent K⁺ channel and its dependence on the lipid membrane. *Proc Natl Acad Sci USA*. **102** (43), 15441-15446 (2005).
- B Lepore, F Ruzicka, P Frey, D Ringe. The X-ray Crystal Structure of lysine-2,3-aminomutase from Clostridium Subterminale. *Proc Natl Acad Sci USA*. **102** (39), 13819-13824 (2005).
- K Li, K Zhao, B Ossareh-Nazari, G Da, C Dargemont, R Marmorstein. Structural Basis for Interaction Between the UBP3 Deubiquitinating Enzyme and Its BRE5 Cofactor. *J. Biol. Chem.* **280**, 29176 (2005).
- W Li, S Kamtekar, Y Xiong, G Sarkis, N Grindley, T Steitz. Structure of a Synaptic gamma delta Resolvase Tetramer Covalently Linked to Two Cleaved DNAs. *Science*. **309**, 1210 (2005).
- S Li, R Depetris, D Barford, J Chernoff, S Hubbard. Crystal Structure of a Complex Between Protein Tyrosine Phosphatase 1B and the Insulin Receptor Tyrosine Kinase. *Structure*. **13** (11), 1643-1651 (2005).
- H Li, S van Vranken, Y Zhao, Z Li, Y Guo, L Eisele, Y Li. Crystal Structures of T Cell Receptor (Beta) Chains Related to Rheumatoid Arthritis. *Protein Sci.* **14**, 3025 (2005).
- A Liinas, N Ahmed, M Cordaro, A Laws, J Frere, M Delmarcelle, N Silvaggi, J Kelly, M Page. Inactivation of Bacterial DD-Peptidase by Beta-Sultams. *Biochemistry*. **44**, 7738-7746 (2005).
- S Long, E Campbell, R MacKinnon. Voltage Sensor of Kv1.2: Structural Basis of Electromechanical Coupling. *Science*. **309**, 903 (2005).
- S Long, E Campbell, R MacKinnon. Crystal Structure of a Mammalian Voltage-Dependent Shaker Family K⁺ Channel. *Science*. **309**, 897 (2005).
- G Miller, M Wilson, P Majerus, J Hurley. Specificity Determinants in Inositol Polyphosphate Synthesis: Crystal Structure of Inositol 1,3,4-Trisphosphate 5/6-Kinase. *Mol. Cell*. **18** (2), 201-212 (2005).
- M Neiditch, M Federle, S Miller, B Bassler, F Hughson. Regulation of LuxPQ Receptor Activity by the Quorum-Sensing Signal Autoinducer-2. *Mol. Cell*. **18** (5), 507-518 (2005).
- K Pant, B Crane. Structure of a Loose Dimer: an Intermediate in Nitric Oxide Synthase Assembly. *J. Mol. Biol.* **352** (4), 932-940 (2005).
- E Rangarajan, Y Li, P Iannuzzi, M Cygler, A Matte. Crystal Structure of Escherichia coli Crotonobetianyl-CoA: Carnitine CoA-Transferase (CaiB) and Its Complexes with CoA and Carnitiny-CoA. *Biochemistry*. **44**, 5728-5738 (2005).
- S Riedl, W Li, Y Chao, R Schwarzenbacher, Y Shi. Structure of the Apoptotic Protease-Activating Factor 1 Bound to ADP. *Nature*. **434**, 926 (2005).
- T Schmeing, K Huang, S Strobel, T Steitz. An Induced-fit Mechanism to Promote Peptidyl Bond Formation and Exclude Hydrolysis of Peptidyl-tRNA. *Nature*. **438**, 520-524 (2005).
- T Schmeing, K Huang, D Kitchen, S Strobel, T Steitz. Structural Insights into the Mechanism of the Peptidyl Transferase Reaction Suggest Oxyanion Transition State Stabilization by Water and a Substrate Proton Shuttle. *Mol. Cell*. **20**, 437-448 (2005).
- A Serganov, S Keiper, L Malinina, V Tereshko, E Skripkin, C Hobartnet, A Polonskaia, Z Dauter, A Jaschke, D Patel. Structural basis for Diels-Alder ribozyme-catalyzed carbon-carbon bond formation. *Nat. Struct. Mol. Biol.* **12** (3), 218-224 (2005).
- K Shi, C Brown, Z Gu, B Kozlowski, G Dunny, D Ohlendorf, C Earhart. Structure of Peptide Sex Pheromone Receptor PrgX and PrgX/Pheromone Complexes and Regulation of Conjugation in Enterococcus faecalis. *Proc Natl Acad Sci USA*. **102** (51), 18596-18601 (2005).
- E Sickmier, D Brekasis, S Paranawithana, J Bonanno, M Paget, S Burley, C Kielkopf. X-ray Structure of a Rex-Family Repressor/ NADH Complex Insights into the Mechanism of Redox Sensing. *Structure*. **13**, 43-54 (2005).
- X Siebert, B Eipper, R Mains, S Prigge, N Blackburn, L Amzel. The Catalytic Copper of Peptidylglycine alpha-Hydroxylating Monooxygenase also Plays a Critical Structural Role. *Biophys. J.* **89** (5), 3312-3319 (2005).
- X Siebert. Structural Probes into the Mechanism of PAM, a Peptide-Amidating Enzyme. Ph. D. Thesis. Johns Hopkins School of Medicine, Baltimore. (2005).
- M Stahley, S Strobel. Structural Evidence for a Two-Metal-ion Mechanism of Group I Intron Splicing. *Science*. **309**, 1587 (2005).
- B Staker, M Feese, M Cushman, Y Pommier, D Zembower, L Stewart, A Burgin. Structures of Three Classes of Anticancer Agents Bound to the Human Topoisomerase I-DNA Covalent Complex. *J. Med. Chem.* **48** (7), 2336-2345 (2005).
- A Stein, G Fuchs, C Fu, S Wolin, K Reinisch. Structural Insights into RNA Quality Control: The Ro Autoantigen Binds Misfolded RNAs Via its Central Cavity. *Cell*. **121** (4), 529-539 (2005).
- A Tocilj, J Schrag, Y Li, B Schneider, L Reitzer, A Matte, M Cygler. Crystal Structure of N-succinylarginine Dihydrolase AstB, Bound to Substrate and Product, an Enzyme from the Arginine Catabolic Pathway of Escherichia Coli. *J. Biol. Chem.* **280** (16), 15800-15808 (2005).
- N Tolia, E Enemark, B Sim, L Joshua-Tor. Structural Basis for the EBA-175 Erythrocyte Invasion Pathway of the Malaria Parasite Plasmodium Falciparum. *Cell*. **122**, 183-193 (2005).
- D Tu, G Blaha, P Moore, T Steitz. Structures of MLSBK Antibiotics Bound to Mutated Large Ribosomal Subunits Provide a Structural Explanation for Resistance. *Cell*. **121** (2), 257-270 (2005).
- S Tuske, S Sarafianos, X Wang, B Hudson, E Sineva, J Mukhopadhyay, J Birktoft, O Leroy, S Ismail, et al.. Inhibition of Bacterial RNA Polymerase by Streptolydigin: Stabilization of a Straight-Bridge-Helix Active-Center Conformation. *Cell*. **122** (4), 541-552 (2005).
- H Wei, A Ruthenburg, S Bechis, G Verdine. Nucleotide-dependent Domain Movement in the ATPase Domain of a Human Type IIA DNA Topoisomerase. *J. Biol. Chem.* **280** (44), 37041-37047 (2005).
- N Yan, J Chai, E Lee, L Gu, Q Liu, J He, J Wu, D Kokel, H Li, et al.. Structure of the CED-4-CED-9 Complex Provides Insights into Programmed Cell Death in Caenorhabditis elegans. *Nature*. **437**, 831 (2005).

Beamline X26A

- C Andrade, T Preharaj, H Jamieson, D Fortin. The potential for geochemical and microbial remobilization of arsenic from sediments in Yellowknife Bay, Great Slave Lake: Progress. Geological Sciences, Queen's University, Kingston. Prepared for Indian and Northern Affairs Canada. (2005).
- T Biswas, H Aihara, M Radman-Livaja, D Filman, A Landy, T Ellenberger. A Structural Basis for Allosteric Control of DNA Recombination by lamda Integrase. *Nature*. **435**, 1059 (2005).
- L Briebe, R Kokoska, K Bebenek, T Kunkel, T Ellenberger. A Lysine Residue in the Fingers Subdomain of T7 DNA Polymerase Modulates the Miscoding Potential of 8-Oxo-7,8-

- Dihydroguanosine. *Structure*. **13** (11), 1653-1659 (2005).
- M Cheng, M Levy, D Schulze, D Huber. Mn Transition States During Infection and Early Pathogenesis in Rice Blast Relative to Resistance and Susceptibility. *J. Phytopathology*. **95**, S19 (2005).
- J Flinn, D Hunter, D Linkous, A Lanzirrotti, L Smith, J Brightwell, B Jones. Enhanced Zinc Consumption Causes Memory Deficits and Increased Brain Levels of Zinc. *Physiol. Behav.* **83**, 793-803 (2005).
- V Fthenakis, M Fuhrmann, J Heiser, A Lanzirrotti, J Fitts, W Wang. Emissions and Encapsulation of Cadmium in CdTe PV Modules During Fires. *Prog. Photovolt.* **13** (8), 713-723 (2005).
- M Fuhrmann, A Lanzirrotti. 241Am, 137Cs, Sr and Pb Uptake by Tobacco as Influenced by Application of Fe Chelators to Soil. *J. Environ. Radioact.* **82** (1), 33-50 (2005).
- M Ginder-Vogel, T Borch, M Mayes, P Jardine, S Fendorf. Chromate Reduction and Retention Processes within Arid Subsurface Environments. *Environ. Sci. Tech.* **39** (20), 7833-7839 (2005).
- B Jackson, P Williams, A Lanzirrotti, P Bertsch. Evidence for Biogenic Pyromorphite Formation by the Nematode *Caenorhabditis Elegans*. *Environ. Sci. Tech.* **39** (15), 5620-5625 (2005).
- K Jones, H Feng, A Lanzirrotti, D Mahajan. Mapping Metal Catalysts using Synchrotron Computed Microtomography (CMT) and Micro-X-ray Fluorescence (μ XRF). *Top. Catal.* **32** (3-4), 263-272 (2005).
- K Jones, H Feng, A Lanzirrotti, D Mahajan. Synchrotron X-ray Microprobe and Computed Microtomography for Characterization of Nanocatalysts. *Nucl. Instrum. Meth. B*. **241**, 331-334 (2005).
- G Miller, M Wilson, P Majerus, J Hurley. Specificity Determinants in Inositol Polyphosphate Synthesis: Crystal Structure of Inositol 1,3,4-Trisphosphate 5/6-Kinase. *Mol. Cell*. **18** (2), 201-212 (2005).
- L Miller, M Ruppel, C Ott, R Smith, A Lanzirrotti. Development and Applications of an Epifluorescence Module for Synchrotron X-ray Fluorescence Imaging. *Rev. Sci. Instrum.* **76**, 066107 (2005).
- C Negra, D Ross, A Lanzirrotti. Oxidizing Behavior of Soil Manganese: Interactions among Abundance, Oxidation State, and pH. *Soil Sci. Soc. Am. J.* **69** (1), 87-95 (2005).
- C Negra, D Ross, A Lanzirrotti. Soil Manganese Oxides and Trace Metals: Competitive Sorption and Microfocused Synchrotron X-ray Fluorescence Mapping. *Soil Sci. Soc. Am. J.* **69** (2), 353-361 (2005).
- T Punshon, B Jackson, A Lanzirrotti, W Hopkins, P Bertsch, J Burger. Application of Synchrotron X-ray Microbeam Spectroscopy to the Determination of Metal Distribution and Speciation in Biological Tissues. *Spectrosc. Lett.* **38**, 343-363 (2005).
- T Punshon, A Lanzirrotti, S Harper, P Bertsch, J Burger. Distribution and Speciation of Metals in Annual Rings of Black Willow. *J. Environ. Qual.* **34** (4), 1165-1173 (2005).
- M Ruppel. Development and Applications of an Epifluorescence Module for Synchrotron X-ray Fluorescence Imaging. Masters Thesis. Stony Brook University, Stony Brook. (2005).
- T Schuler, D Ederer, S Itza-Ortiz, G Woods, T Callcott, J Woicik. Character of the Insulating State in NiO: a Mixture of Charge-Transfer and Mott-Hubbard Character. *Phys. Rev. B*. **71**, 115113 (2005).
- B Staker, M Feese, M Cushman, Y Pommier, D Zembower, L Stewart, A Burgin. Structures of Three Classes of Anticancer Agents Bound to the Human Topoisomerase I-DNA Covalent Complex. *J. Med. Chem.* **48** (7), 2336-2345 (2005).
- T Telivala, L Miller. Effect of Metal Ions on the Secondary Structure of Amyloid beta (Ab) in Alzheimer's disease. Masters Thesis. SUNY at Stony Brook, Stony Brook. (2005).
- I Thompson, D Huber, C Guest, D Schulze. Fungal Manganese Oxidation in a Reduced Soil. *Environ. Microbiol.* **7** (9), 1480-1487 (2005).
- T Tokunaga, J Wan, J Pena, E Brodie, M Firestone, T Hazen, S Sutton, A Lanzirrotti, M Newville. Uranium Reduction in Sediments under Diffusion-Limited Transport of Organic Carbon. *Environ. Sci. Tech.* **39** (18), 7077-7083 (2005).
- D Vantelon, A Lanzirrotti, A Scheinost, R Kretzschmar. Spatial Distribution and Speciation of Lead around Corroding Bullets in a Shooting Range Soil Studied by Micro-X-ray Fluorescence and Absorption Spectroscopy. *Environ. Sci. Tech.* **39** (13), 4808-4815 (2005).
- S Walker, H Jamieson, A Lanzirrotti, C Andrade, G Hall. The Speciation of Arsenic in Iron Oxides in Mine Wastes from the Giant Gold Mine, N.W.T.: Application of Synchrotron Micro-XRD and Micro-XANES at the Grain Scale. *Can. Mineral.* **43** (4), 1205-1224 (2005).
- Q Wang, A Kretlow, M Beekes, D Naumann, L Miller. In Situ Characterization of Prion Protein Structure and Metal Accumulation in Scrapie-Infected Cells by Synchrotron Infrared and X-ray Imaging. *Vib. Spectrosc.* **38**, 61-69 (2005).

Beamline X26C

- J Amor, J Swails, X Zhu, C Roy, H Nagai, A Ingmundson, X Cheng, R Kahn. The Structure of RalF, an ADP-Ribosylation Factor Guanine Nucleotide Exchange Factor from *Legionella pneumophila*, Reveals the Presence of a Cap over the Active Site. *J. Biol. Chem.* **280** (2), 1392-1400 (2005).
- P Cherepanov, A Ambrosio, S Rahman, T Ellenberger, A Engelman. Structural Basis for the Recognition Between HIV-1 Integrase and Transcriptional Coactivator p75. *Proc Natl Acad Sci USA*. **102** (48), 17308-17313 (2005).
- P Davison, H Schubert, J Reid, C Iorg, A Heroux, C Hill, C Hunter. Structural and Biochemical Characterization of Gun4 Suggests a Mechanism for Its Role in Chlorophyll Biosynthesis. *Biochemistry*. **44** (21), 7603-7612 (2005).
- B Ford, K Skowronek, S Boykevisch, D Bar-Sagi, N Nassar. Structure of the G60A mutant of Ras: Implications for the Dominant Negative Effect. *J. Biol. Chem.* **280** (27), 25697-25705 (2005).
- B Gao, A Bertrand, W Boles, H Ellis, T Mallett. Crystallization and Preliminary X-ray Crystallographic Studies of the Alkanesulfonate FMN Reductase from *Escherichia coli*. *Acta Cryst. F*. **61**, 837-840 (2005).
- J Horton, K Sawada, M Nishibori, X Cheng. Structural Basis for Inhibition of Histamine N-Methyltransferase by Diverse Drugs. *J. Mol. Biol.* **353** (2), 334-344 (2005).
- H Hsu, B Stillman, R Xu. Structural Basis for Origin Recognition Complex 1 Protein-Silence Information Regulator 1 Protein Interaction in Epigenetic Silencing. *Proc Natl Acad Sci USA*. **102**, 8519-8524 (2005).
- E Karakas, H Wilson, T Graf, S Xiang, S Jaramillo-Busquets, K Rajagopalan, C Kisker. Structural Insights into Sulfite Oxidase Deficiency. *J. Biol. Chem.* **280** (39), 33506-15 (2005).
- I Loftin, S Franke, S Roberts, A Weichsel, A Heroux, W Montfort, C Rensing, M McEvoy. A Novel Copper-Binding Fold for the Periplasmic Copper Resistance Protein CusF. *Biochemistry*. **44**, 10533-10540 (2005).
- J Ma, Y Yuan, G Meister, Y Pei, T Tuschi, D Patel. Structural Basis for 5' -end-specific Recognition of Guide RNA by the A. fulgidu Piwi Protein. *Nature*. **434**, 666 (2005).
- P Paaventhan, C Kong, J Joseph, M Chung, P Kolatkar. Structure

- of Rhodocetin Reveals Noncovalently Bound Heterodimer Interface. *Protein Sci.* **14**, 169 (2005).
- F Rivas, N Tolia, J Song, J Aragon, J Liu, G Hannon, L Joshua-Tor. Purified Argonaute2 and an siRNA form Recombinant Human RISC. *Nat. Struct. Mol. Biol.* **12** (4), 340-349 (2005).
- D Shi, X Yu, L Roth, M Hiroki, Y Hathout, N Allewell, M Tuchman. Expression, Purification, Crystallization and Preliminary X-ray Crystallographic Studies of a Novel Acetylchitinase from *Xanthomonas Campestris*. *Acta Cryst. F.* **61**, 676-679 (2005).
- X Siebert, B Eipper, R Mains, S Prigge, N Blackburn, L Amzel. The Catalytic Copper of Peptidylglycine alpha-Hydroxylating Monooxygenase also Plays a Critical Structural Role. *Biophys. J.* **89** (5), 3312-3319 (2005).
- X Siebert. Structural Probes into the Mechanism of PAM, a Peptide-Amidating Enzyme. Ph. D. Thesis. Johns Hopkins School of Medicine, Baltimore. (2005).
- A Soares, Y Vechter. Experimental methods for measuring accurate high-amplitude phases and their importance in isomorphous replacement experiments. *Acta Cryst. D.* **D61**, 1521-1527 (2005).
- J Suryadi, E Tran, E Maxwell, B Brown, II. The Crystal Structure of the Methanocaldococcus jannaschii Multifunctional L7Ae RNA-Binding Protein Reveals an Induced-Fit Interaction with the Box C/D RNAs. *Biochemistry.* **44**, 9657-9672 (2005).
- Y Tie, P Boross, Y Wang, L Gaddis, f Liu, X Chen, J Tozser, R Harrison, I Weber. Molecular Basis for Substrate Recognition and Drug Resistance from 1.1 to 1.6 Angstrom Resolution Crystal Structures of HIV-1 Protease Mutants with Substrate Analogs. *FEBS J.* **272** (20), 5265 (2005).
- N Tolia, E Enemark, B Sim, L Joshua-Tor. Structural Basis for the EBA-175 Erythrocyte Invasion Pathway of the Malaria Parasite Plasmodium Falciparum. *Cell.* **122**, 183-193 (2005).
- J Truglio, B Rhau, D Croteau, L Wang, M Skorvaga, E Karakas, M DellVecchia, H Wang, B Van Houten, C Kisker. Structural Insights Into the First Incision Reaction During Nucleotide Excision Repair. *EMBO J.* **24**, 885-894 (2005).
- J Wang, K Stieglitz, E Kantrowitz. Metal Specificity is Correlated with Two Crucial Active Site Residues in Escherichia coli Alkaline Phosphatase. *Biochemistry.* **44**, 8378-8386 (2005).
- Beamline X27A**
- J Ablett. High-Brightness Hard X-ray Scanning Nano-Probes at NSLS II. *Nucl. Instrum. Meth. B.* **241**, 238-241 (2005).
- K Jones, H Feng, A Lanzirrotti, D Mahajan. Mapping Metal Catalysts using Synchrotron Computed Microtomography (CMT) and Micro-X-ray Fluorescence (μ XRF). *Top. Catal.* **32** (3-4), 263-272 (2005).
- Beamline X27B**
- E Kossel. NMR-Untersuchungen zum mikroskopischen Fluss in Perkolationsmodellobjekten. Ph.D. Thesis. Universtaet Ulm, Ulm. (2005).
- Beamline X27C**
- C Avila-Orta, C Burger, R Somani, L Yang, G Marom, F Medellin-Rodriguez, B Hsiao. Shear Induced Crystallization in Isotactic Polypropylene within the Oriented Scaffold of Non-crystalline Ultra High Molecular Weight Polyethylene. *Polymer.* **46**, 8859-8871 (2005).
- J Celli, B Gregor, B Turner, N Afdhal, R Bansil, S Erramilli. Viscoelastic Properties and Dynamics of Porcine Gastric Mucin. *Biomacromolecules.* **6**, 1329 (2005).
- X Chen, C Burger, X Wang, W He, K Yoon, R Somani, D Fang, I Sics, L Rong, et al.. In-Situ X-Ray Scattering Studies of Fluorinated Multi-Wall Carbon Nanotube (FMWNT)/Fluorinated Ethylene Propylene (FEP) Composite Fiber during Stretching. *ACS, PMSE Preprints*, Vol 93, p. 751-752, sponsored by ACS. (2005).
- J Chen, C Burger, C Krishnan, B Chu. Morphogenesis of Highly Ordered Mixed-Valent Mesoporous Molybdenum Oxides. *J. Am. Chem. Soc.* **127**, 14140-14141 (2005).
- X Chen, K Yoon, C Burger, I Sics, D Fang, B Hsiao, B Chu. In-Situ X-ray Scattering Studies of a Unique Toughening Mechanism in Surface-Modified Carbon Nanofiber/UHMWPE Nanocomposite Films. *Macromolecules.* **38**, 3883-3893 (2005).
- L Cui, J Miao, L Zhu, I Sics, B Hsiao. Confined Discotic Liquid Crystalline Self-assembly in a Novel Coil-coil-disk Triblock Oligomer. *ACS, PMSE Preprints*, Vol 93, p. 286-287, sponsored by ACS. (2005).
- L Cui, S Dahmane, X Tong, L Zhu, Y Zhao. Using Self-Assembly to Prepare Multifunctional Diblock Copolymers Containing Azopyridine Moiety. *Macromolecules.* **38**, 2076-2084 (2005).
- L Cui, J Miao, L Zhu, I Sics, B Hsiao. Confined Discotic Liquid Crystalline Self-Assembly in a Novel Coil-Coil-Disk Triblock Oligomer. *Macromolecules.* **38**, 3386-3394 (2005).
- D Dikovsky, G Marom, C Avila-orta, R Somani, B Hsiao. Shear-Induced Crystallization in Isotactic Polypropylene Containing Ultra-High Molecular Weight Polyethylene Oriented Precursor Domains. *Polymer.* **45**, 3096-3104 (2005).
- D Dikovsky, G Marom, C Avila-Orta, R Somani, B Hsiao. Shear-Induced Crystallization in Isotactic Polypropylene Containing Ultra-High Molecular Weight Polyethylene Oriented Precursor Domains. *Polymer.* **46** (9), 3096-3104 (2005).
- L Drummy, D Phillips, M Stone, B Farmer, R Naik. Thermally Induced Alpha-Helix to Beta-Sheet Transition in Regenerated Silk Fibers and Films. *Biomacromolecules.* **6** (6), 3328-3333 (2005).
- Z Espinosa, F Medellin-Rodriguez, N Stribeck, A Almendarez-Camarillo, B Hsiao, S Vega-diaz. Complex Isothermal Crystallization and Melting Behavior of Nylon 6 Nanoclay-Hybrids. *Macromolecules.* **38** (10), 4246-4253 (2005).
- H Fong, S Dickins, G Flaim. Evaluation of Dental Restorative Composites Containing Polyhedral Oligomeric Silsesquioxane Methacrylate. *Dent. Mater.* **21** (6), 520-529 (2005).
- K Fukukawa, L Zhu, P Gopalan, M Ueda, S Yang. Synthesis and Characterization of Silicon-containing Block Copolymers from Nitroxide-mediated Living Free Radical Polymerization. *Macromolecules.* **28** (2), 263-270 (2005).
- M Gelfer, C Burger, B Chu, B Hsiao, A Drozdov, M Si, M Rafailovich, B Sauer, J Gilman. Relationships Between Structure and Rheology in Model Nanocomposites of Ethylene-Vinyl-Based Copolymers and Organoclays. *Macromolecules.* **38**, 3765-3775 (2005).
- M Gelfer, C Burger, G Panek, G Jeschke, A Fadeev, M Si, M Rafailovich, P Nawani, J Gilman, et al.. Investigation of Thermally Induced Phase Transitions and Degradation of Organoclays Based on Synthetic Somasif Clays using in-situ X-ray Scattering. *ACS, PMSE Preprints*, , Vol 92, p. 441-442, sponsored by ACS. (2005).
- G Georgiev. Effects of Nematic Polymer Liquid Crystal on Crystallization and Structure of PET/Vectra Blends. *J. Mater. Sci.* **40**, 1140 (2005).
- G Georgiev, P Cebe, M Capel. Effects of Nematic Polymer Liquid Crystal on Crystallization and Structure of Pet/Vectra Blends. *J. Mater. Sci.* **40** (5), 1141-1152 (2005).
- H Heinz, H Koerner, K Anderson, R Vaia, B Farmer. Force Field

- for Mica-Type Silicates and Dynamics of Octadecylammonium Chains Grafted to Montmorillonite. *Chem. Mater.* **17**, 5658 (2005).
- R Ho, T Chung, J Tsai, J Kuo, B Hsiao, I Sics. Crystallization of Poly(styrene)-b-syndiotactic Poly(propylene) Block Copolymers from Confinement to Breakout. *Macromol. Rapid Commun.* **26**, 107-111 (2005).
- R Ho, T Lin, M Jhong, T Chung, B Ko, Y Chen. Phase Transformation in Self-Assembly of the Gold(Poly(4-vinylpyridine)-b-poly(ϵ -caprolactone) Hybrid System. *Macromolecules*. **38** (21), 8607 (2005).
- R Ho, Y Chiang, C Lin, B Huang. Crystallization and Melting Behavior of Poly(ϵ -caprolactone) Under Physical Confinement. *Macromolecules*. **38**, 4769-4779 (2005).
- B Hsiao, M Gelfer. Synchrotron X-ray Techniques for the Study of Clay-Based Polymer Nanocomposites. *American Chemical Society Rubber Division Preprint*, Vol , p. 66, sponsored by American Chemical Society Rubber Division . (2005).
- B Hsiao, L Yang, R Somani, C Avila-Orta, L Zhu. Unexpected Shish-Kebab Structure in a Sheared Polyethylene Melt. *Phys. Rev. Lett.* **94**, 117802 (2005).
- P Huang, S Chen, R Van Horn, Y Guo, R Quirk, B Lotz, E Thomas, B Hsiao, C Avila-Orta, I Sics. PEO Crystal Orientation Changes within an Inverted Cylindrical Morphology Constructed by a PEO-b-PS Block Copolymer. *ACS, PMSE Preprints*, Vol 93, p. 284-285, sponsored by ACS. (2005).
- A Kelarakis, K Yoon, I Sics, R Somani, B Hsiao, B Chu. Uniaxial Deformation of an Elastomer Nanocomposite Containing Modified Carbon Nanofibers by in situ Synchrotron X-ray Diffraction. *Polymer*. **46** (14), 5103-5117 (2005).
- J Keum, C Burger, F Zuo, I Sics, B Hsiao, T Sun, A Lustiger. Synchrotron X-ray Diffraction/Scattering Studies on the Nucleation and Growth Habits of Flow-induced shish-kebab structure in Linear Polyethylene (HDPE) Melts. *ACS, PMSE Preprints*, Vol 93, p. 759-760, sponsored by ACS. (2005).
- J Keum, C Burger, B Hsiao, R Somani, L Yang, R Kolb, H Chen, C Lue. Synchrotron X-ray Scattering Studies of the Nature of Shear-Induced Shish-kebab Structure in Polyethylene Melt. *Prog. Coll. Pol. Sci. S.* **130**, 114-126 (2005).
- J Keum, R Somani, F Zuo, C Burger, I Sics, B Hsiao, H Chen, R Kolb, C Lue. Probing Flow-Induced Precursor Structures in Blown Polyethylene Films by Synchrotron X-rays During Constrained Melting. *Macromolecules*. **38**, 5128-5136 (2005).
- H Koerner, W Liu, M Alexander, P Mirau, H Dowty, R Vaia. Deformation-Morphology Correlations in Electrically Conductive Carbon Nanotube-Thermoplastic Polyurethane Nanocomposites. *Polymer*. **46** (12), 4405-4420 (2005).
- H Koerner, E Hampton, D Dean, Z Turgut, L Drummy, P Mirau, R Vaia. Generating Triaxial Reinforced Epoxy/Montmorillonite Nanocomposites with Uniaxial Magnetic Fields. *Chem. Mater.* **17**, 1990-1996 (2005).
- H Koerner, G Price, N Pearce, M Alexander, R Vaia. Remotely Actuated Polymer Nanocomposites-Stress-Recovery of Carbon-Nanotube-Filled Thermoplastic Elastomers. *Nat. Mater.* **3**, 115-120 (2005).
- S Kohjiya, M Tosaka, S Poompradub, A Kato, J Shimanuki, Y Ikeda, S Toki, B Hsiao. Nano-structural Elucidation in Carbon Black Loaded NR Vulcanizate by 3D-TEM and in situ WAXD Measurements. *American Chemical Society Rubber Division Preprint*, Vol , p. 33, sponsored by American Chemical Society Rubber Division . (2005).
- B Larin, G Marom, C Avila-Orta, R Somani, B Hsiao. Orientated Crystallization in Discontinuous Aramid Fiber/isotactic Polypropylene Composites under Shear Flow Conditions. *J. Appl. Polym. Sci.* **98**, 1113 (2005).
- H Lee, L Zhu, R Weiss. Formation of Nanoparticles during Melt mixing a Thermotropic Liquid Crystalline Polyester and Sulfonated Polystyrene Ionomers: Morphology and Origin of Formation. *Polymer*. **46**, 10841 (2005).
- Y Loo, K Eakabayashi, Y Huang, R Register, B Hsiao. Thin Crystal Melting Produces the Low-Temperature Endotherm in Ethylene/Methacrylic Acid Ionomers. *Polymer*. **46** (14), 5118-5124 (2005).
- J Miao, G Xu, L Zhu, L Tian, K Uhrich, C Avila-Orta, B Hsiao, M Utz. Chain-folding and Overall Molecular Conformation in a Novel Amphiphilic Starlike Macromolecule. *Macromolecules*. **38**, 7074-7082 (2005).
- C Mitchell, R Krishnamoorti. Non-isothermal Crystallization of in situ Polymerized Poly(ϵ -caprolactone) Functionalized-SWNT Nanocomposites. *Polymer*. **46** (20), 8796-8804 (2005).
- P Nawani, M Gelfer, B Hsiao. Investigations of Morphology and Thermal Behavior of Transition Metal Ions Modified Clays using in-situ X-ray Scattering. *ACS, PMSE Preprints*, Vol 93, p. 757-758, sponsored by ACS. (2005).
- K Page, K Cable, R Moore. Molecular Origins of the Thermal Transitions and Dynamic Mechanical Relaxations in Perfluorosulfonate Ionomers. *Macromolecules*. **38**, 6472-6484 (2005).
- B Pate, E Thomas, R Pytel. Processing the Right Actuator: The Relationship Between Nanostructure and Materials Properties of Higher-Order Pyrroles. *229th ACS National Meeting*, Vol , p. ORGN-238, sponsored by American Chemical Society. (2005).
- B Pate, T Baker, K Lai, E Thomas. Synthesis and Dispersion of tin(IV) Sulfide Nano- and Microparticulate Fillers. *230th ACS National Meeting*, Vol , p. INOR-399, sponsored by American Chemical Society. (2005).
- H Shin, W Lindquist, D Sahagian, S Song. Analysis of the Vesicular Structure of Basalts. *Comput. Geosci.* **31** (4), 473-487 (2005).
- I Sics, L Rong, B Hsiao, B Chu. Advanced Polymers Beamline (X27C) at National Synchrotron Light Source, BNL. *ACS, PMSE Preprints*, Vol 93, p. 120, sponsored by ACS. (2005).
- R Somani, L Yang, L Zhu, B Hsiao. Flow-Induced Shish Kebab Precursor Structures in Entangled Polymer Melts. *Polymer*. **46**, 8587-8623 (2005).
- L Sun, E Ertel, L Zhu, B Hsiao, C Avila-Orta, I Sics. Reversible De-Intercalation and Intercalation Induced by Polymer Crystallization and Melting in a Poly(ethylene oxide)/Organoclay Nanocomposite. *Langmuir*. **21**, 5672-5676 (2005).
- K Tenneti, X Chen, C Li, X Wan, Q Zhou, I Sics, B Hsiao. Asymmetric Liquid Crystalline Rod Coil Block Copolymer System. *American Chemical Society*, Vol , p. TECH-100, sponsored by American Chemical Society. (2005).
- K Tenneti, X Chen, C Li, X Wan, Q Zhou, I Sics, B Hsiao. Asymmetric Liquid Crystalline Rod-Coil Block Copolymer System. *ACS, PMSE Preprints*, Vol 93, p. 364-365, sponsored by ACS. (2005).
- K Tenneti, C Li, Y Tu, X Wan, Q Zhou, C Avila-Orta, B Hsiao. On the Influence of Temperature and Volume Fraction on Liquid Crystalline Block Copolymer Nanoscale Architectures. *APS National Meeting*, Vol , p. LACC 505, sponsored by APS. (2005).
- K Tenneti, X Chen, C Li, Y Tu, X Wan, Q Zhou, I Sics, B Hsiao. Perforated Layer Structures in Liquid Crystalline Rod-coil Block Copolymers. *J. Am. Chem. Soc.* **127** (44), 15481-15490 (2005).
- S Toki, B Hsiao, S Kohjiya, M Tosaka, A Tsou, S Datta. Synchrotron X-Ray Studies of Vulcanized Rubbers and Thermoplastic Elastomers. *American Chemical Society Rubber Division Preprint*, Vol , p. 32, sponsored by American Chemical Society Rubber Division . (2005).

- S Toki, I Sics, B Hsiao, M Tosaka, S Poompradub, Y Ikeda, S Kohjiya. Probing the Nature of Stain-Induced Crystallization in Polyisoprene Rubber by Combined Thermomechanical and In Situ X-ray Diffraction Techniques. *Macromolecules*. **38**, 7064-7073 (2005).
- R Vaia, H Koerner, B Hsiao, I Sics. Morphology -- Deformation Correlations in Nanocomposite Elastomers. *American Chemical Society Rubber Division Preprint*, Vol , p. 63, sponsored by American Chemical Society Rubber Division . (2005).
- Z Wang, H Wang, K Shimizu, J Dong, B Hsiao, C Han. Structural and Morphological Development in Poly(ethylene-co-hexene) and Poly(ethylene-co-butylene) Blends Due to the Competition between Liquid-Liquid Phase Separation and Crystallization. *Polymer*. **46** (8), 2675-2684 (2005).
- J Xu, B Guo, J Zhou, L Li, J Wu, M Kowalczyk. Observation of Banded Spherulites in Pure poly(L-lactide) and its Miscible Blends with Amorphous Polymers. *Polymer*. **46**, 9176 (2005).
- H Xu. Transitions from Solid to Liquid in Isotactic Polystyrene Studied by Thermal Analysis and X-ray Scattering. *Polymer*. **46**, 8734 (2005).
- J Zhang, J Wu. Crystallinity and orientation development in poly(L-lactic acid) fibers during annealing and drawing. *Annual Technical Conference - Society of Plastics Engineers* , Vol , p. 1747, sponsored by Annual Technical Conference - Society of Plastics Engineers . (2005).
- H Zhou, C Burger, J Chen, B Hsiao, B Chu, L Graham, M Glimcher. Interpretation of 2D Small-Angle X-Ray Diffraction Patterns from Mineralized Collagen Fibrils in Fish Bone. *ACS, PMSE Preprints*, Vol 93, p. 755-756, sponsored by ACS. (2005).
- L Zhu, L Sun, J Miao, L Cui, Q Ge, R Quirk, C Xue, S Cheng, B Hsiao, C Avila-Orta. Epitaxial Phase Transformation between Cylindrical and Double Gyroid Mesophases. *Materials Research Society Meeting*, Vol 856E, p. BB2.3.1-BB2.3.6, sponsored by MRS. (2005).
- F Zou, H Chen, J Li, R Wevers, G Meyers, J Keum, X Chen, B Hsiao. In-situ Synchrotron SAXS/WAXD Studies on Stretching of Isotactic Polypropylene. *ACS, PMSE Preprints*, , Vol 93, p. 761-762, sponsored by ACS. (2005).
- Beamline X28C**
- T Adilakshmi, P Ramaswamy, S Woodson. Protein-Independent Folding Pathway of the 16 S rRNA 5' Domain. *J. Mol. Biol.* **351** (3), 508-519 (2005).
- M Brenowitz, D Erie, M Chance. Catching RNA Polymerase in the act of Binding: Intermediates in Transcription Illuminated by Synchrotron Footprinting. *Proc Natl Acad Sci USA*. **102**, 4659-4660 (2005).
- J Guan, K Takamoto, S Almo, E Reisler, M Chance. Structure and Dynamics of the Actin Filament. *Biochemistry*. **44**, 3166-3175 (2005).
- S Gupta, W Mangel, M Sullivan, K Takamoto, M Chance. Synchrotron Footprinting Provides Insight into Adenovirus Protease-DNA Interactions. *Synch. Rad. News*. **18**, 25-33 (2005).
- P Rangan. Folding of the Azoarcus Intron. Ph.D. Thesis. John Hopkins University, Baltimore. (2005).
- K Takamoto, M Chance. A New Approach for Nucleic Acid Footprinting Data Analysis. *BioTech. J.* **5**, 194-197 (2005).
- S Woodson. Metal Ions and RNA Folding: A Highly Charged Topic with a Dynamic Future. *Curr Opin Chem Biol*. **9**, 104-109 (2005).
- G Xu, J Kiselar, Q He, M Chance. Secondary Reactions and Strategies to Improve Quantitative Protein Footprinting. *Anal. Chem.* **77**, 3029-3037 (2005).
- G Xu, M Chance. Radiolytic Modification of Sulfur Containing Acidic Amino Residues in Model Peptides: Fundamental Studies for Protein Footprinting. *Anal. Chem.* **77**, 2437-2449 (2005).
- Beamline X29A**
- R Agarwal, T Binz, S Swaminathan. Structural Analysis of Botulinum Neurotoxin Serotype F Light Chain: Implications on Substrate Binding and Inhibitor Design. *Biochemistry*. **44**, 11758-11765 (2005).
- E Bitto, C Bingman, H Robinson, S Allard, G Wesenberg, G Phillips, Jr.. The Crystal Structure at 2.5 Angstrom Resolution of Human Basophilic Leukemia-Expressed Protein BLES03. *Acta Cryst. F*. **61**, 812 (2005).
- J Brown, Z Zhou, L Reshetnikova, H Robinson, R Yammani, L Tobacman, C Cohen. Structure of the Mid-Region Tropomyosin: Bending and Binding Sites for Actin. *Proc Natl Acad Sci USA*. **102** (52), 18878-18883 (2005).
- L Deng, C Velikovskiy, C Swaminathan , S Cho, R Mariuzza. Structural Basis for Recognition of the T Cell Adaptor Protein SLP-76 by the SH3 Domain of Phospholipase CGAMMA1. *J. Mol. Biol.* **352**, 1 (2005).
- M DiMattia, L Govindasamy, H Levy, B Whitaker-Gurda, E Kohlbrenner, J Chiorini, R McKenna, N Muzyczka, S Zolotukhin, M Agbandje-McKenna. Production, Purification, Crystallization and Preliminary X-ray Structural Studies of Adeno-Associated Virus Serotype 5. *Acta Cryst. F*. **F61**, 917-921 (2005).
- G Dong, A Hutagalung, C Fu, P Novick, K Reinisch. The Structures of Exocyst Subunit Exo70p and the Exo84p C-terminal Domains Reveal a Common Motif. *Nat. Struct. Mol. Biol.* **12** (12), 1094 (2005).
- A Forster, E Masters, F Whitby, H Robinson, C Hill. The 1.9 Angstrom Structure of a Proteasome-11S Activator Complex and Implications for the Proteasome-Pan/PA700 Interactions. *Mol. Cell. Bio.* **18**, 589 (2005).
- J Gorman, L Shapiro. Crystal Structures of the Tryptophan Repressor binding Protein WrbA and complexes with Flavin Mononucleotide. *Protein Sci.* **14**, 3004-3012 (2005).
- M Hahn, M Nicholson, J Pyrdol, K Wucherpfennig. Unconventional Topology of Self Peptide-Major Histocompatibility Complex Binding by a Human Autoimmune T Cell Receptor. *Nat. Immunol.* **6**, 490-496 (2005).
- Y Im, S Raychaudhuri, W Prinz, J Hurley. Structural Mechanism for Sterol Sensing and Transport by OSBP-Related Proteins. *Nature*. **437**, 154-158 (2005).
- S Long, E Campbell, R MacKinnon. Crystal Structure of a Mammalian Voltage-Dependent Shaker Family K⁺ Channel. *Science*. **309**, 897 (2005).
- S Long, E Campbell, R MacKinnon. Voltage Sensor of Kv1.2: Structural Basis of Electromechanical Coupling. *Science*. **309**, 903 (2005).
- I Mirza, I Nazi, M Korczynska, G Wright, A Berghuis. Crystal Structure of Homoserine Transacetylase from *Haemophilus influenzae* Reveals a New Family of alpha/beta-Hydrolases. *Biochemistry*. **44**, 15768-15773 (2005).
- M Nicholson, M Hahn, K Wucherpfennig. Unusual features of Self-Peptide/MHC Binding by Autoimmune T Cell Receptors. *Immunity*. **23** (4), 351-360 (2005).
- J Wang, K Stieglitz, J Cardia, E Kantrowitz. Structural Basis for Ordered Substrate Binding and Cooperativity in Aspartate Transcarbamoylase. *Proc Natl Acad Sci USA*. **102**, 8881-8886 (2005).
- H Wang, Y Liu, Y Chen, H Robinson, H Ke. Multiple Elements Jointly Determine Inhibitor Selectivity of Cyclic Nucleotide Phosphodiesterases 4 and 7. *J. Biol. Chem.* **280**, 30949 (2005).

C Zhan, E Fedorov, W Shi, U Ramagopal, R Thirumuruhan, B Manjasetty, S Almo, A Fiser, M Chance, A Fedorov. The ybeY Protein from Escherichia coli is a Metalloprotein. *Acta Cryst. F.* **61** (11), 959-963 (2005).

NLSL Staff

- J Ablett. High-Brightness Hard X-ray Scanning Nano-Probes at NLSL II. *Nucl. Instrum. Meth. B.* **241**, 238-241 (2005).
- T Beetz, M Howells, C Kao, J Kirz, E Lima, T Menten, H Miao, C Sanchez-Hanke, D Sayre, D Shapiro. Apparatus for X-ray Diffraction Microscopy and Tomography of Cryo Specimens. *Nucl. Instrum. Meth. A.* **545** (1-2), 459-468 (2005).
- J Bengtsson. Control of Dynamic Aperture for Synchrotron Light Sources. *Proceedings of the 2005 Particle Accelerator Conference, Knoxville Tennessee*, Vol , p. 1670-1672, sponsored by IEEE. (2005).
- R Bindu, S Pandey, A Kumar, S Khalid, A Pimpale. Local Distortion of MnO₆ Octahedron in La_{1-x}Sr_xMnO_{3+Δ} (X=0.1-0.9): An Exafs Study. *J. Phys.: Condens. Matter.* **17** (41), 6393-6404 (2005).
- A Blednykh, S Krinsky, B Podobedov, J Rose, N Towne. Harmonic Cavity Performance for NLSL-II. *Particle Accelerator 2005*, p. 2544-2546, (2005).
- Y Cai, H Mao, P Chow, J Tse, Y Ma, S Patchkovskii, J Shu, V Struzhkin, R Hemley, et al.. Ordering of Hydrogen Bonds in High-Pressure Low-Temperature H₂O. *Phys. Rev. Lett.* **94**, 025502 (2005).
- A Cavaliere, D Fritz, S Lee, P Bucksbaum, D Reis, J Rudati, D Mills, P Fuoss, G Stephenson, et al.. Clocking Femtosecond X-rays. *Phys. Rev. Lett.* **94**, 114801 (2005).
- S Chakraborty, B Sahoo, I Teraoka, L Miller, R Gross. Enzyme-Catalyzed Regioselective Modification of Starch Nanoparticles. *Macromolecules.* **38** (1), 61-68 (2005).
- K Chalut, V Litvinenko, I Pinayev, S Khalid, A Pimpale. Method of Phase-Space Tomography of Rapidly Evolving E Beams. *Phys. Rev. ST AB.* **8** (10), 102802 (2005).
- O Chmaissem, B Dabrowski, S Kolesnik, J Mais, J Jorgenson, S Short, C Botez, P Stephens. Effects of A-Site Ordering on the Structures and Properties of La_{1-x}Ba_xMnO₃(X~0.5). *Phys. Rev. B.* **72**, 104426 (2005).
- M Croft, Z Zhong, N Jisrawi, I Zakharchenko, R Holtz, Y Gulak, J Skaritka, T Fast, K Sadananda, T Tsakalakos. Strain Profiling of Fatigue Crack Overload Effects Using Energy Dispersive X-Ray Diffraction. *Int. J. Fatigue.* **27**, 1408-1419 (2005).
- C Foerster, J Hu, E Haas. Results of Vacuum Pump Oil Testing to Minimize Oil Waste at the NLSL. *American Vacuum Society Symposium*, Vol , p. 1, sponsored by NLSL. (2005).
- D Fong, C Cionca, Y Yacoby, G Stephenson, J Eastman, P Fuoss, S Streiffer, C Thompson, R Clarke, et al.. Direct Structural Determination in Ultrathin Ferroelectric Films by Analysis of Synchrotron X-ray Scattering Measurements. *Phys. Rev. B.* **71**, 144112 (2005).
- K Gaffney, A Lindenberg, J Larsson, K Sokolowski-Tinten, C Blome, O Synnergren, J Sheppard, C Coleman, A MacPhee, et al.. Observation of Structural Anisotropy and the Onset of Liquidlike Motion During the Nonothermal Melting of InSb. *Phys. Rev. Lett.* **95**, 125701 (2005).
- A Ganjoo, H Jain, S Khalid, C Pantano. Structural Modification of Ge-Se Amorphous Films with the Addition of Sb. *Philos. Mag. Lett.* **85** (10), 503-512 (2005).
- P Glans, T Learmonth, K Smith, T Valla, P Johnson, S Hulbert, W McCarroll, M Greenblatt. Charge-Density-Wave Gap in the Quasi-Two-Dimensional Conductor Na_{0.9}Mo₆O₁₇ Measured by Angle-Resolved Photoemission Spectroscopy. *Phys. Rev. B.* **72**, 035115 (2005).
- Y Guan, Z Dios, D Arena, L Cheng, W Bailey. Transmission-Mode X-ray Magnetic Circular Dichroism Characterization of Moment Alignment in Tb-Doped Ni₈₁Fe₁₉. *J. Appl. Phys.* **97**, 10A719 (2005).
- E Haas, R Scheuerer, E Losee. Vortex Tube Machining Improves Safety While Reducing Environmental Waste. *Mod. Mach. Shop.* **78** (4), 54 (2005).
- M Hasnah, C Parham, E Pisano, Z Zhong, O Oltulu, D Chapman. Mass Density Images from the Diffraction Enhanced Imaging Technique. *Med. Phys.* **32**, 549 (2005).
- M Hasnah, C Parham, E Pisano, Z Zhong, O Oltulu, D Chapman. Mass Density Images from the Diffraction Enhanced Imaging Technique. *Phys. Med. Biol.* **32**, 549-552 (2005).
- G Jacobs, S Ricote, P Patterson, U Graham, A Dozier, S Khalid, E Rhodus, B Davis. Low Temperature Water-Gas Shift: Examining the Efficiency of Au as a Promoter for Ceria-Based Catalysts Prepared by CVD of a Au Precursor. *Appl. Catal. A.* **292**, 229-243 (2005).
- T Kajander, A Cortajarena, E Main, S Mochrie, L Regan. A New Folding Paradigm for Repeat Proteins. *J. Am. Chem. Soc.* **127**, 10188-10190 (2005).
- H Kim, C Detavernier, O van der Statten, S Rosnagel, A Kellock, D Park. Robust Ta_{Nx} Diffusion Barrier for Cu-Interconnect Technology with Subnanometer Thickness by Metal-Organic Plasma-Enhanced Atomic Layer Deposition. *J. Appl. Phys.* **98**, 014308 (2005).
- S Kramer, J Bengtsson. Dynamic Aperture Optimization for Low Emittance Light Sources. *Proceedings of the 2005 Particle Accelerator Conference, Knoxville Tennessee*, Vol , p. 3378-3380, sponsored by IEEE. (2005).
- S Krinsky. Transverse Impedance of a Smooth Flat Taper. *Phys. Rev. ST AB.* **8**, 124403 (2005).
- S Kwak, E DiMasi, Y Han, J Aizenberg, I Kuzmenko. Orientation and Mg Incorporation of Calcite Grown on Functionalized Self-Assembled Monolayers: A Synchrotron X-ray Study. *Cryst. Growth Des.* **5** (6), 2139-2145 (2005).
- J Li, J Williams, Z Zhong, K Kuettner, M Aurich, J Mollenhauer, C Muehleman. Reliability of Diffraction Enhanced Imaging for Assessment of Cartilage Lesions, Ex Vivo. *Osteoarthr. Cartilage.* **13**, 187-197 (2005).
- A Lindenberg, J Larsson, K Sokolowski-Tinten, K Gaffney, G MacPhee, D Weinstein, D Lowney, T Allison, T Matthews, et al.. Atomic-Scale Visualization of Inertial Dynamics. *Science.* **308**, 392 (2005).
- R Lobo, J LaVeigne, D Reitze, D Tanner, Z Barber, E Jacques, P Bosland, M Burns, G Carr. Photoinduced Time-Resolved Electrodynamics of Superconducting Metals and Alloys. *Phys. Rev. B.* **72**, 024510 (2005).
- J Lu, G Rozgonyi, A Schonecker, A Gutjahr, Z Liu. Impact of Oxygen on Carbon Precipitation in Polycrystalline Ribbon Silicon. *J. Appl. Phys.* **97**, 033509 (2005).
- C Marrows, P Steadman, A Hampson, L Michez, B Hickey, N Telling, D Arena, J Dvorak, S Langridge. Probing Magnetic Ordering in Multilayers using Soft X-ray Resonant Magnetic Scattering. *Phys. Rev. B: Condens. Matter.* **72**, 024421 (2005).
- L Michez, C Marrows, P Steadman, B Hickey, D Arena, J Dvorak, H Zhang, D Bucknall, S Langridge. Resonant X-ray Scattering from a Magnetic Multilayer Reflection Grating. *Appl. Phys. Lett.* **86**, 112502 (2005).
- L Miller, R Smith. Synchrotrons Versus Globars, Point-Detectors Versus Focal Plane Arrays: Selecting the Best Source and Detector for Specific Infrared Microspectroscopy and Imaging

- Applications. *Vib. Spectrosc.* **38** (1-2), 237-240 (2005).
- L Miller, M Ruppel, C Ott, R Smith, A Lanzirrotti. Development and Applications of an Epifluorescence Module for Synchrotron -ray Fluorescence Imaging. *Rev. Sci. Instrum.* **76**, 066107 (2005).
- L Miller. National Synchrotron Light Source Activity Report 2004. Government Printing Office, Washington. Prepared for BNL-NSLS. (2005).
- C Muehleman, J Li, K Kuettner, Z Zhong. Diffraction Enhanced X-ray Imaging of Musculoskeletal Lesions. *Osteoarthr. Cartilage*. **12**, s117-s117 (2005).
- G Ozaydin, A Ozcan, Y Wang, K Ludwig, H Zhou, R Headrick, D Siddons. Real-Time X-ray Studies of Mo-Seeded Self-Organized Si Nanodot Formation During Low Energy Ar⁺ Ion Bombardment. *Appl. Phys. Lett.* **87**, 163104 (2005).
- N Roberts, S Jaradat, L Hirst, Y Wang, S Wang, Z Liu, C Huang, J Bai, R Pinidak, H Gleeson. Biaxiality and Temperature Dependence of 3- and 4-layer Intermediate Smectic Phase Structures as Revealed by resonant X-ray Scattering. *Europhys. Lett.* **72** (6), 976-982 (2005).
- F Sakamoto, H Iijima, K Dobashi, T Imai, T Ueda, T Watanabe, M Uesaka. Emittance and Energy Measurements of Low-Energy Electron Beam Using Optical Transition Radiation Techniques. *Jpn. J. Appl. Phys., Part 1*. **44** (3), 1485-1491 (2005).
- A Serganov, S Keiper, L Malinina, V Tereshko, E Skripkin, C Hobartnet, A Polonskaia, Z Dauter, A Jaschke, D Patel. Structural basis for Diels-Alder ribozyme-catalyzed carbon-carbon bond formation. *Nat. Struct. Mol. Biol.* **12** (3), 218-224 (2005).
- T Shin, M Ree. In Situ Infrared Spectroscopy Study on Imidization Reaction and Imidization-Induced Refractive Index and Thickness Variations in Microscale Thin Films of a Poly(amic ester). *Langmuir*. **21**, 6081-6085 (2005).
- P Smith, I Koch, R Gordon, D Mandoli, B Chapman, K Reimer. X-ray Absorption Near-Edge Structure Analysis of Arsenic Species for Application to Biological Environmental Samples. *Environ. Sci. Tech.* **39**, 248-254 (2005).
- S Stadler, D Minott, D Harley, J Craig, M Khan, I Dubenko, N Ali, K Story, J Dvorak, et al.. Element-Specific Magnetic Properties of Co₂MnSi Thin Films. *J. Appl. Phys.* **97**, 10C302 (2005).
- M Teng, Z Zhong. Use of Diffraction Enhanced Imaging to Determine the X-ray Refractive Indices of Various Tissues at Biologically-Relevant Energies. *The J. of Young Investigators*. **12**, online (2005).
- A Vahedi-Faridi, V Stojanoff, J Yeh. The Effects of Flash-Annealing on Glycerol Kinase Crystals. *Acta Cryst. D*. **61** (7), 982-989 (2005).
- E Vescovo, H Kim, J Ablett, S Chambers. Spin-polarized Conduction in Localized Ferromagnetic Materials: The Case of Fe₃O₄ on MgO(100). *J. Appl. Phys.* **98**, 084507 (2005).
- A Wagner, M Aurich, N Sieber, M Stoessel, W Wetzler, K Schmuck, M Lohmann, B Reime, J Metge, et al.. Options and Limitations of Joint cartilage Imaging: DEI in Comparison to MRI and Sonography. *Nucl. Instrum. Meth. A*. **548**, 47-53 (2005).
- Q Wang, A Kretlow, M Beekes, D Naumann, L Miller. In Situ Characterization of Prion Protein Structure and Metal Accumulation in Scrapie-Infected Cells by Synchrotron Infrared and X-ray Imaging. *Vib. Spectrosc.* **38**, 61-69 (2005).
- Q Wang, W Sanad, L Miller, A Voigt, K Klingel, R Kandolf, K Stangl, G Baumann. Infrared Imaging of Compositional Changes in Inflammatory Cardiomyopathy. *Vib. Spectrosc.* **38**, 217-222 (2005).
- M Wernick, L Chapman, O Oltulu, Z Zhong. Imaging Method Based on Attenuation, Refraction and Ultra-small-angle-scattering of X-rays. US Patent No. US 6,947,521 B2. (2005).
- M Wernick, J Brankov, D Chapman, Y Yang, E Pisano, C Parham, C Muehleman, Z Zhong, M Anastasio. Physical Model of Image formation in Multiple-Image Radiography. *SPIE: Developments in X-ray Tomography IV*, Vol 5535, p. 369-379, sponsored by SPIE. (2005).
- B Wood, K Bamberg, L Miller, M Quinn, L Chiriboga, M Diem, D McNaughton. Infrared Imaging of Normal and Diseased Cervical Tissue Sections. *Biomedical Applications of Micro- and Nanoengineering II*, Vol 5651, p. 78-84, sponsored by SPIE--The International Society for Optical Engineering. (2005).
- H Yang, T Shin, L Yang, K Cho, C Ryu, Z Bao. Effect of Mesoscale Crystalline Structure on the Field-Effect Mobility of Regioregular Poly(3-hexyl thiophene) in Thin-Film Transistors. *Adv. Func. Mater.* **15** (4), 671-676 (2005).
- L Yang, M Fukuto. Modulated Phase of Phospholipids with a Two-Dimensional Square Lattice. *Phys. Rev. E*. **72**, 010901(R) (2005).
- H Yang, T Shin, M Ling, K Cho, C Ryu, Z Bao. Conducting AFM and 2D GIXD Studies on Pentacene Thin Films. *J. Am. Chem. Soc.* **127**, 11542-11543 (2005).
- A Yang, Z Chen, X Zuo, D Arena, J Kirkland, C Vittoria, V Harris. Cation-Disorder-Enhanced Magnetization in Pulsed-Laser-Deposited CuFe₂O₄ Films. *Appl. Phys. Lett.* **86**, 252510 (2005).
- T Yuasa, H Sugiyama, Z Zhong, A Maksimenko, F Dilmanian, T Akatsuka, M Ando. High-Pass-Filtered Diffraction Microtomography by Coherent Hard X rays for Cell Imaging: Theoretical and Numerical Studies of the Imaging and Reconstruction Principles. *J. Opt. Soc. Am. A*. **22** (12), 2622-2634 (2005).
- I Zegkinoglou, J Stempfer, C Nelson, P Hill, J Chakhalian, C Bernhard, J Lang, G Srajer, H Fukazawa, et al.. Orbital Ordering Transition in Ca₂Ru₄ Observed with Resonant X-ray Diffraction. *Phys. Rev. Lett.* **95**, 136401 (2005).
- Z Zhu, T Andelman, M Yin, T Chen, S Ehrlich, S O'Brien, R Osgood, Jr.. Synchrotron X-ray Scattering of ZnO Nanorods: Periodic Ordering and Lattice Size. *J. Mater. Res.* **20** (4), 1033 (2005).